Abstract: ATP dependent chromatin re-modeling factors have previously been shown to play a pivotal role in the regulation of gene expression in several model organisms, including yeast, fruit fly and human. When encountered with a nutrient depleted environment Dictyostelium discoideum enter a process of multicellular development which requires the correct temporal and spatial expression of a large subset of genes. Here it is shown that two of these ATP dependent chromatin re-modelling factors, INO80 and CHDC, are required for the correct expression of developmental genes of Dictyostelium discoideum and subsequent multicellular morphogenesis. These factors are identified as having a key role in the earlier stage of aggregation and cellular chemotaxis towards the developmental chemoattractant cAMP. Genetic disruption of genes encoding major subunits of these complexes, arp8 and chdC, both result in a decreased ability to form correct fruiting bodies, also showing a marked decrease in chemotactic ability. In each case, these defects are seen to occur through different mechanisms, indicating the role of multiple pathways in the regulation of Dictyostelium chemotaxis. Interestingly, both mutant cell lines are also responsive to the neuropsychiatric treatment drug lithium and are shown to affect elements of the inositol signaling pathway.

# ATP-dependent chromatin re-modeling factors regulate expression of genes involved in Dictyostelium discoideum development and chemotaxis

Benjamin James Rogers

Cardiff University

2010

UMI Number: U516651

# All rights reserved

#### INFORMATION TO ALL USERS

The quality of this reproduction is dependent upon the quality of the copy submitted.

In the unlikely event that the author did not send a complete manuscript and there are missing pages, these will be noted. Also, if material had to be removed, a note will indicate the deletion.



#### UMI U516651

Published by ProQuest LLC 2013. Copyright in the Dissertation held by the Author.

Microform Edition © ProQuest LLC.

All rights reserved. This work is protected against unauthorized copying under Title 17, United States Code.



ProQuest LLC 789 East Eisenhower Parkway P.O. Box 1346 Ann Arbor, MI 48106-1346

# Acknowledgments

There are a great many people that have been an immense help and inspiration over the last four years whilst I have been at Cardiff University. First and foremost my supervisors Professor Adrian Harwood and Dr Nick Kent must be thanked for the advice and guidance that they have provided during the time of my PhD, this would have been a much more difficult time without their help. Secondly I would like to thank my colleagues in the Harwood, Dale, Kent and Watson labs. Particular thanks should be given to Jo Forde, Emma Dalton, Regina Teo and Pete Watson who have offered limitless help and backing both in the lab and out. Beyond the University a number of my friends have been particularly supportive over my time in Cardiff. Arthur and Tasmin Parkinson, Tom Beardshaw and Felicity Rudge all provided me with a spare room or sofa whilst I was attempting to write up and both Zoe Walters and Holly Callaghan lent a sympathetic ear and advice when it was required. Finally I would like to thank my family, in particular my grandparents who have been a huge inspiration and I would like to dedicate my work to the memory of my grandparents Cyril and Morfydd Rogers.

# **Contents**

Chapter 1 – Introduction title page	. 11
1.1 The history of the therapeutic use of lithium and mood disorders	. 12
1.2 Inositol phosphate biosynthesis and the inositol depletion hypothesis	. 16
1.3 Dictyostelium as a model organism	. 18
1.4 An introduction to cell movement by chemotaxis	. 23
1.5 cAMP signaling in Dictyostelium	. 28
1.6 Previous work on this project	. 32
1.7 The basics of chromatin structure: How is DNA packaged inside the nucleus?	33
1.8 Accessing the DNA: An introduction to chromatin re-modeling	. 34
1.9 There are four classes of chromatin re-modelers	. 38
1.10 The INO80 complex and Actin related proteins	. 41
1.11 The CHD family of chromatin re-modelers	. 45
1.12 Regulation and specificity of chromatin re-modelers	. 49
1.13 Summary and aims of project	. 50
Chapter 2 – Materials & Methods title page	. 51
2.1 Bioinformatics	. 52
2.2 Dictyostelium cell culture	. 52
2.3 Cell lines used in these studies	53
2.4 RNA extraction and cDNA synthesis	. 54
2.5 RT-PCR analysis of expression	. 55
2.6 Extraction of genomic DNA	. 57
2.7 Dictyostelium transformation	. 57
2.8 Western blotting	. 58
2.9 Analysis of cell movement (Chemotaxis assay)	. 58

2.10 Immunofluorescence	59
2.11 Dictyostelium development assay	60
2.12 Dictyostelium cAMP pulse assay	60
2.13 Dictyostelium affinity purification	61
2.14 RNA-seq and data analysis	62
2.15 Chromatin Immuno-precipitation (ChIP)	69
2.16 Picogreen assay	70
2.17 ChIP-seq and data analysis	71
Chapter 3 – Arp8 and the INO80 complex are involved in regulating genes	involved
with starvation induced development in Dictyostelium discoideum	73
3.1 Arp8 expression	74
3.2 Arp8 null mutants show a delay in the onset of development	76
3.3 arp8 null cells exhibit a defect in cAMP signaling	79
3.4 Null cells exhibit a delayed expression of the cAMP signalling genes	
during development	81
3.5 Mixing the cell population can rescue the delay phenotype	83
3.6 Stimulating the null cells with cAMP rescues the expression of the	
cAMP signalling genes	85
3.7 RNA-seq data reveals the genes which are affected by Arp8 during	
vegetative growth	87
3.8 RNA-seq data reveals the genes which are affected by Arp8 during	
early Dictyostelium development	94
3.9 Summary	98
Chapter 4 – Arp8 and the INO80 complex regulate <i>Dictyostelium</i> chemotaxis.	99
4.1 Chemotaxis is impaired in a cAMP concentration dependent manner	100

4.2 Impaired chemotaxis could be due to a build up of PiP3 on the membrane103
4.3 Transcription of PiP3 regulating genes ino1 and impA1 is attenuated in arp8
null cells
4.4 ChIP verifies that INO80 acts directly on the ino1 and impA1 promotors108
4.5 Treating null cells with Lithium improves chemotaxis
4.6 Analysis of RNA-seq data reveals a number of genes affected that are involved
in chemotaxis113
4.7 Summary
Chapter 5 – The mutant LisG encodes a CHD ortholog involved in maintaining
correct Dictyostelium development
5.1 Introduction to CHDC (LisG null)
5.2 CHDC null mutants exhibit severe developmental arrest which can be rescued by
mixing with wild-type populations
5.3 Expression of CHDC increases during the period leading up to aggregation 124
5.4 CHDC nulls show decreased expression of pre-spore and pre-stalk genes 126
5.5 CHDC null cells show a deficiency in cAMP signaling during aggregation 128
5.6 RNA-seq reveals more insight into the changes in gene expression brought
about by CHDC during development
5.7 RNA-seq data reveals the genes which are affected by CHDC at the loose
mound stage during Dictyostelium development
5.8 ChIP-seq data reveals the pattern of re-modeler binding throughout
development
5.9 Summary
Chapter 6 – CHDC affects lithium sensitivity

6.1 The LisG REMI exhibits an improved chemotaxis which provides it with	
litium resistance	
6.2 The CHDC null mutant shows an opposite responses to both chemoattractant	
and lithium treatment	
6.3 The chemotactic response to lithium is possibly controlled, at least in part	
by the relative expression of the inositol biosynthetic genes inol and impA1 157	
6.4 Genes involved in chemotaxis identified by RNA-sequencing	
6.5 Summary	
Chapter 7 – Discussion	
7.1 The INO80 complex is involved in regulating <i>Dictyostelium</i> development 167	
7.2 Chemotaxing cells respond across a large order of magnitude and alter	
signaling mechanisms accordingly	
7.3 The Dictyostelium CHD8 homolog CHDC plays a significant role	
during starvation induced development	
7.4 The two CHDC mutants respond oppositely to cAMP gradients and	
to lithium treatment	
7.5 Final conclusions	
Appendix A – Gene Ontology (GO) data	
Appendix B – Published Papers	
References	
Figures & Tables	
Figure 1.1 Metabolism of soluble inositol phosphates	
Figure 1.2 The developmental life cycle of Dictyostelium discoideum	
Figure 1.3 Internal and external signaling relating to cAMP	
synthesis and chemotaxis	

Figure 1.4 Methods of action of chromatin re-modeling factors	37
Figure 1.5 There are 4 classes of ATP dependent chromatin re-modelers	40
Figure 1.6 The INO80 complex	44
Figure 1.7 The CHD family	48
Figure 2.1A The initial steps of Illumina sequencing	67
Figure 2.1B The final steps of Illumina sequencing	68
Figure 3.1 Arp8 expression patterns	61
Figure 3.2 Arp8 null cells have a delayed development phenotype	78
Figure 3.3 Arp8 null cells have delayed production of cAMP pulses	80
Figure 3.4 Expression profiles of genes involved in cAMP signalling	82
Figure 3.5 Mixing the null cells with wild-type forms chimeras capable	
of developing normally	84
Figure 3.6 Stimulating null cells with cAMP returns the expression of	
the cAMP signaling genes	86
Fig 3.7 Arp8 knock out affects a greater number of genes 8 hours	
into starvation	91
Table 3.1 Summary of genes affected by arp8 knock out	. 92
Table 3.2 Genes up-regulated during vegetative growth	92
Table 3.3 Genes down-regulated during vegetative growth	93
Table 3.4 Genes up-regulated involved in development	96
Table 3.5 Genes down-regulated involved in development	97
Figure 4.1 arp8 nulls also show decreased chemotaxis	02
Figure 4.2 arp8 null cells show an increased build up of PIP3	
on the membrane10	05

Figure 4.3 Inositol biosynthetic genes are directly regulated by the INO80
complex
Figure 4.4 Treatment with Lithium also improves null cell chemotaxis
Table 4.1 Genes up-regulated involved in chemotaxis
Table 4.2 Genes down-regulated involved in chemotaxis
Figure 5.1 LisG is a member of the CHD family of chromatin re-modelers 119
Figure 5.2 CHDC cells show a severe developmental defect
Figure 5.3 CHDC expression increases with cell density
Figure 5.4 Expression profiles of genes marking pre-stalk and pre-spore cells127
Figure 5.5 There are distinct deficiencies in CHDC null cell cAMP signaling 129
Fig 5.6 CHDC knock out affects a greater number of genes following 12 hours
of starvation
Table 5.1 Summary of genes affected by chdC knock out
Table 5.2 Genes up-regulated during vegetative growth
Table 5.3 Genes down-regulated during vegetative growth
Table 5.4 development associated genes down-regulated 12 hours into starvation. 140
Table 5.5 development associated genes up-regulated 12 hours into starvation 141
Figure 5.7 A large portion of genes are consistently bound throughout
development
Figure 5.8 A large percentage of the genes down-regulated during vegetative
growth are bound by the CHDC re-modeler
Figure 5.9 A large percentage of the genes up-regulated during vegetative
growth are bound by the CHDC re-modeler
Figure 5.10 A large percentage of the genes down-regulated after
12 hours of starvation are also bound by the CHDC re-modeler

Figure 5.11 A much lower percentage of the genes up-regulated after
12 hours of starvation are also bound by the CHDC re-modeler 149
Figure 6.1 LisG REMI mutant is protected against the effects
of lithium
Figure 6.2 CHDC null mutant shows greatly impaired chemotaxis that is
rescued by lithium treatment
Figure 6.3 Both inol and impAl show different expression patterns in the CHDC
null cells
Table 6.1 Genes down-regulated involved in chemotaxis
Table 6.2 Genes up-regulated involved in chemotaxis

# **Chapter 1:**

# Introduction

Summary: The primary aims of this project were to investigate the roles of ATP dependent re-modeling factors during the starvation response of the social amoeba *Dictyostelium discoideum*. We investigated the roles of these complexes, to gain a better understanding of how they work, the pathways affected during this process and provide some insight into the roles that they play in the cells response to the mood stabilizing drug lithium.

Two specific chromatin re-modelers became the focus of this project; INO80 and CHDC. Both have been shown to be highly important in other organisms, with INO80 being involved in regulating inositol biosynthesis in yeast and the CHDC proteins being implicated in a number of human developmental disorders. This research was designed to investigate whether these complexes affect *Dictyostelium* in a similar manner and whether they could be further characterized in a simpler developmental system. We also set out to identify any new roles of these re-modelers, if any, in this organism.

#### 1.1 The history of the therapeutic use of lithium and mood disorders

Bipolar disorder, or manic depression, is an extremely prevalent neuropsychiatric mood disorder with severe symptoms that can often have devastating effects on quality of life [1]. This disease can become life threatening in conjunction with other psychiatric conditions. Patients swing erratically between a deep depression and an overblown mania with no control over which phase they will be in at any one time. If untreated, there is a 25% chance of suicide, with an estimation of one million deaths worldwide per year [1,2]. Bipolar disorder has been well classified with behavioral models however, the underlying molecular biological systems controlling these symptoms remains unclear. Traditional research models for this disease have involved patient and rodent behavioral studies, however recently there has been an increase in simpler biological systems such as the social amoeba *Dictyostelium discoideum*.

The study of the mechanism of action of several mood stabilising drugs on this disease has long been an ongoing research interest, with the goal of improving these treatments. Lithium, along with valproic acid (VPA) and carbamazepine (CBZ) are the most commonly prescribed mood stabilising drugs in the treatment of a number of these disorders [2]. These treatments are all non-curative and require long term usage with extremely poor response rates in many cases. In all of these cases the therapeutic mechanism is not understood, yet establishing the molecular targets of these drugs will hopefully lead to a better appreciation of the principles governing the symptoms of bipolar disorder and the development of new and improved therapies.

Lithium was initially used as an anti-manic agent in the 19<sup>th</sup> Century. However, its use diminished before being re-introduced in 1949 by John Cade [3]. Since then it has been widely used as the best available treatment for both long and

short-term phases of bi-polar disorder. Whilst still being one of the most commonly used drugs it does still have several drawbacks. These include a large number of patients being unresponsive to treatment and an increasing intolerance to side effects, which include tremors, nausea and diarrohea [4]. This is likely to be due to lithium having several direct biological targets.

Several direct biological targets of lithium have been identified; Inositol monophosphatase (IMPase), Inositol polyphosphate 1-phosphatase (IPPase), glycogen synthase kinase-3 (GSK3), Fructose-1, 6-bisphosphate phosphatase (FBPase), Bisphosphate nucleotidase (BPNase) and Phosphoglucomutase (PGM). IMPase and IPPase are both involved in the inositol biosynthetic pathway and are rate limiting enzymes involved in the recycling and *de novo* synthesis of free inositol and are inhibited non-competitively by lithium [5]. Recycling of inositol phosphates (IP's) and phosphotidylinositides (PI's) are essential to maintain intracellular PI mediated cell signaling in response to external signals. The regulation of IP's and PI's have been implicated in the causes of bipolar disorder in the inositol depletion hypothesis and are discussed in the next section.

GSK3 is a serine-threonine kinase and a key regulating factor of several signaling pathways including the Wnt pathway and the PI-3 kinase pathway [6], affecting a diverse range of cellular processes. One of the most relevant to bipolar disorder is the inhibition of GSK3's pro-apoptotic effects. This occurs through activation of several transcription factors, including the β-catenin destruction complex [7]. When GSK3 becomes inhibited by lithium, this leads to inhibition of the apoptotic pathway.

FBPase and PGM are the least studied of the direct targets of lithium and considered less likely to be the therapeutic target of lithium. FBPase removes the 1-

phosphate from fructose, 6-bisphosphate to produce fructose 6-phosphate. Bisphosphate nucleotidase (BPNase) removes the 3'-phosphate from 3'-phosphoadenosine 5'-phosphate (PAP) to form adenosine 5'-phosphate (AMP). Phosphoglucomutase (PGM) is involved in the processes of glycogenolysis and glycogenesis and catalyzes glucose 1-phosphate from glucose 6-phosphate. All are inhibited by lithium within the therapeutic range [2].

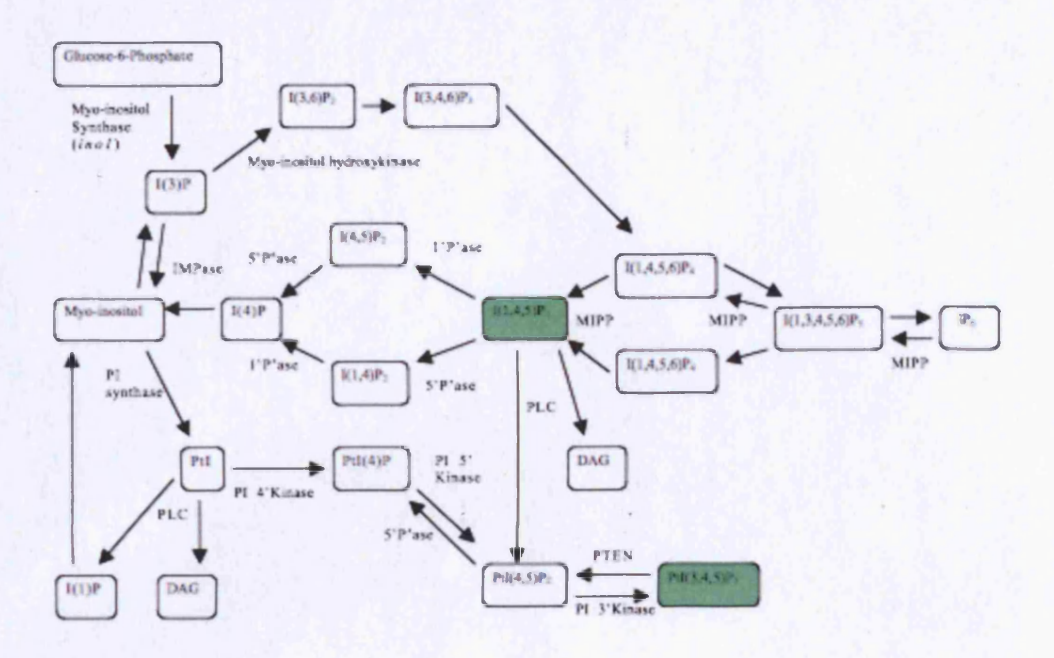


Fig. 1.1 Metabolism of soluble inositol phosphates

The above diagram indicates the metabolic pathways linking the soluble inositol phosphates found in *Dictyostelium discoideum*.

Abbreviations found in the diagram; I - Inositol, P - phosphate, DAG - Diacylglycerol, PtI - Phosphotidylinositol, P'ase - phosphatase, PLC - phospholipase C, MIPP - Multiple inositol polyphosphate phosphatase.

## 1.2 Inositol phosphate biosynthesis and the inositol depletion hypothesis

Inositol phosphate and the membrane lipid phosphatidylinositol are wide ranging, highly regulated second messenger signaling molecules (summarized in Fig. 1.1). Through phosphorylation of the six hydroxyl moieties on the core inositol carbon ring a great diversity of signaling molecules are synthesized affecting a large number of cellular processes. Inositol phosphate signaling has been implicated as being one of the possible molecular mechanisms of bipolar disorder [12].

Myo-inositol is produced in several ways; *de novo* synthesis occurs from glucose-6-phosphate, catalysed by myo-inositol-phosphate synthase (encoded by the gene *ino1*) [8], recycling of the higher order inositol phosphates and finally by uptake from the extra-cellular media by specific myo-inositol transport channels [9].

In the inositol signaling pathway, free myo-inositol is first converted to PtI by the enzyme phosphatidylinositol synthase and further phosphorylated to PtI(4)P and PtI(4,5)P<sub>2</sub> by the PI4' kinase and PI5' kinase respectively. PtI(4,5)P<sub>2</sub> is a significant pool of cellular inositol phosphate and is the substrate for both Phospholipase C (PLC) and the PI3' kinase in response to external stimuli. PLC hydrolyses PtI(4,5)P<sub>2</sub> to the signaling molecules I(1,4,5)P<sub>3</sub> and diacylglycerol (DAG), both of which are involved in a number of cellular responses including release of Ca<sup>2+</sup> from intracellular stores and the production of higher order inositol phosphates [10].

The inositol depletion hypothesis was the first proposed mechanism for a bipolar disorder treatment. Described nearly 20 years ago by Berridge et al [11] it attempted to explain the biological mechanism behind the treatment of manic depression with lithium. The hyposthesis suggested that second messenger signaling could be reduced by lithium's affect on the free pool of inositol in the brain. This was proposed to occur via the inhibition of IMPase and IPPase, reducing the levels of free

inositol by breaking the inositol signaling pathway (Fig. 1.1). However conclusive clinical evidence either for or against this theory has been difficult to establish.

Early evidence linking lithium to this theory came in 1971 with Allison and Stewarts [12] work on the rat cerebral cortex indicating a 30% decrease in myoinositol concentration in this region following lithium treatment. Further work by the same group later coupled this decrease with a build up of IP<sub>1</sub>, the substrate for IMPase [13]. More recently, post-mortem clinical investigations have also revealed a decrease in the inositol levels in the fontal cortex of bipolar patients [14]. Treatment of Dictyostelium with lithium, or VPA, leads to a reduced cellular concentration of I(1,4,5)P<sub>3</sub>. This is taken as an indication of the reduction of intracellular inositol phosphate based signaling [15]. Investigations into dorsal root ganglion (DRG) neuronal growth cone movement have shown that the retardation of growth seen with lithium and VPA treatment can be rescued with the administration of myo-inositol to the DRGs [16].

However, there is some inconclusive evidence that is not in concurrence with what we would expect if the inositol depletion hypothesis were true. It has been observed that not only myo-inositol (the biologically active isomer) but also epinositol can inhibit observed lithium pillocarbine induced seizures in rats [17]. Also knocking out both *impal* and *impa2*, encoding IMPase, in yeast does not lead to a depletion of inositol levels, as would be have been expected [18], arguing against an inhibition of IMPase leading to inositol depletion.

#### 1.3 Dictyostelium as a model organism

Dictyostelium discoideum, commonly known as a social amoeba, is a soil dwelling eukaryote native to North America, discovered in the 1930's by Kenneth Raper [19]. In 2000 Dictyostelium was included in an NIH list of 10 non-mammalian model organisms cementing its place in current biomedical research. The organism is well placed for this role, being more complex than some lower organisms such as the two yeast species, yet being simpler and more genetically malleable than higher organisms such as round worm and fruit fly.

Dictyostelium can be subjected to high levels of genetic manipulation and coupled with the recent sequencing of the genome has produced an incredibly versatile tool for studying cellular processes in a modern research environment. The genome consists of 6 chromosomes plus an extra chromosomal palindromic element comprised of ribosomal RNA. The highly AT rich genome is known to encode ~12,500 genes with a total size of 34Mb [20]. Dictyostelium occurs along a branch towards the base of metazoan evolution and when compared to yeast, shares a greater number of genes homologous to higher organisms, making them a very good genetic model. The haploid genome of this organism provides an ability to easily manipulate the genetic material producing knock out and epitope tagging knock-in cell lines by homologous recombination and ectopic over-expresser strains by transformation with extra-chromosomal plasmids among other current biochemical techniques.

The organism displays a number of unique characteristics that make it suitable for the study of a number of biological processes. When there is an ample supply of bacterial food, or supplemented media, in their environment these free-living organisms grow and feed as individuals and divide by binary fission. However, when the food supply is diminished a change occurs. The cells begin aggregating, by a

process of chemotaxis. Chemotaxis is the movement of the organism towards a chemical attractant. They then undergo a strict regime of differentiation and development. This produces a multi-cellular organism, of about 10<sup>5</sup> cells, going through several developmental stages (outlined in Fig. 1.2). The final structure consists of a single spore laden head, a stalk and a basal disc anchoring it to the substratum. This fruiting body will then stay in this form until conditions become favorable again, whereupon the spore cells will germinate to form new amoebae. This switch between uni- and multi-cellular organism reflects many of the characteristics observed during differentiation and development in higher organisms. This provides a unique opportunity to study development and cellular differentiation in a genetically simpler system. This is extremely relevant to this thesis as ATP dependent chromatin remodeling has been suggested to have evolved to accommodate the changes inherent in a switch from uni- to multi-cellularity [21].

Complex cellular processes described in higher metazoans have also been observed in *Dictyostelium*. These include cell movement, chemotaxis, phagocytosis, pattern formation and signal transduction pathways, which all play roles in *Dictyostelium* development [22, 23]. In fact *Dictyostelium* has proven to be the most widely investigated model organism for cellular chemotaxis, providing many insights into other systems such as neutrophils and leukocytes. Particularly relevant to this project *Dictyostelium* cells are shown to be responsive to lithium in a chemotactically detrimental manner [1]. Treatment of cells with therapeutic levels of lithium greatly reduces the directionality and speed of *Dictyostelium* migration and also affects the chemotactic index to a lesser degree (lithium treatment also reduces the ability of the cells to form full fruiting bodies with increasing concentrations) [24].

Due to the organisms haploid genome, the production of mutants is relatively less difficult than with some other model organisms. There are several methods for producing mutants, one of which is restiriction enzyme-mediated integration (REMI). This is a powerful tool for producing a large mutant library which can then be screened to identify genes involved in specific biological processes. Originally developed in yeast this process was first utilized in Dictyostelium to identify developmentally regulated genes [103]. Mutants are produced by first creating insertion sites in the genome by digestion with the restriction enzyme DpnII. Following this wild-type cells are transformed by electroporation with a plasmid containing complimentary (BamH1) sites and an insertional antibiotic resistance cassette, allowing for selection of mutants. Once the library is created by growing transformants in the presence of the selective antibiotic, the mutants found to contain an insert are then screened for a particular biological trait. The affected genes can subsequently be identified by IPCR. Sequences flanking the resistance cassette are identified by plasmid rescue and then subsequently used to search the genome database [104]. Subsequent replication of each mutant is usually created by homolgous recombination.

This process of creating gene deletion mutants by homologous recombination was used to produce both the *arp8* null mutant and the final cell line used in this study: the *chdC* null. As the *Dictyostelium* genome is haploid homologous recombination is an extremely effective method for producing gene deletions. This technique was developed and first utilized by De Lozanne & Spudich in 1987 [105] to investigate the role of myosin in cell motility and during development. The process once again utilizes the insertion of an antibiotic resistance cassette into the genome. A linearized plasmid is created containing the resistance cassette, flanked by two

homologous regions to the gene of interest. This is then transformed to the background strain, in both of these cases AX2, and selected for by growth in the presence of the appropriate antibiotic.

The easy accessibility of the cells genetic, biochemical and cell biology coupled with high levels of genetic manipulation, robust system of development and chemotaxis, easy cell culture and control in the laboratory make *Dictyostelium* a particularly good model organism for studying the affects of ATP dependent chromatin remodeling factors on cellular development.

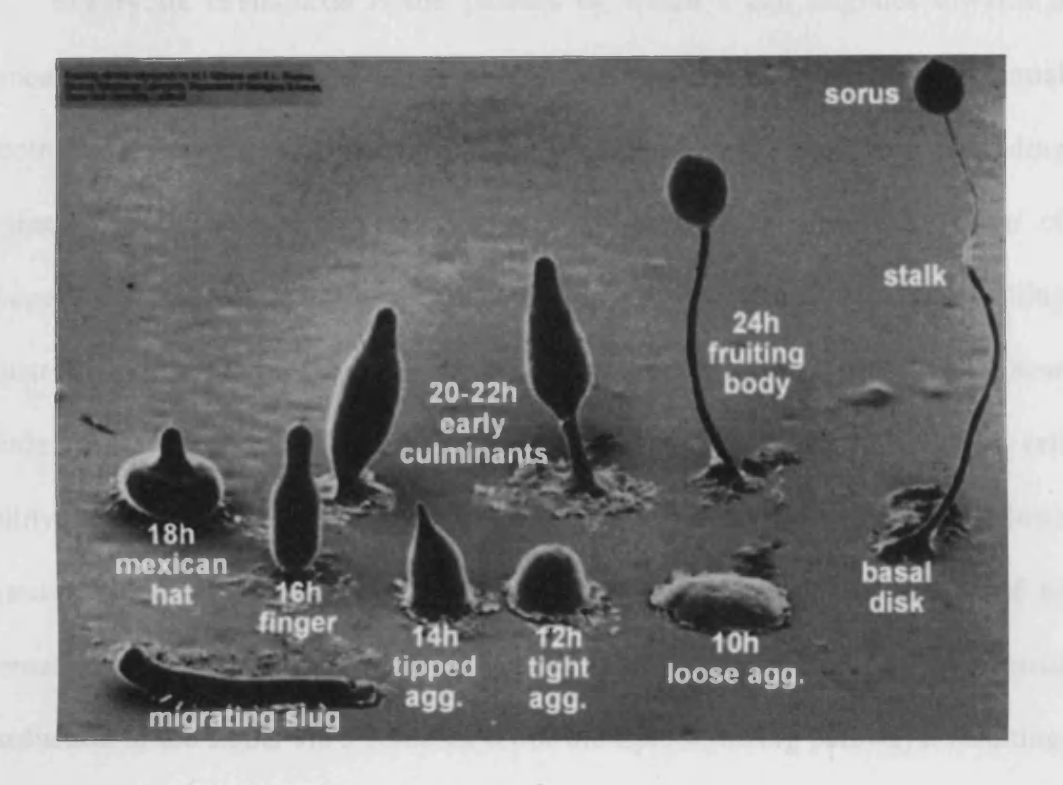


Fig. 1.2 The developmental life cycle of Dictyostelium discoideum

Electron microscope images, originally produced by MGrimson and Blanton, copyright M.J. Grimson and R.L. Blanton, Biological Sciences Electron Microscopy Laboratory, Texas Tech University. The morphological stages are all clearly demonstrated in this image. The process of starvation induced cellular differentiation and development can be seen through early aggregation to form the loose mound and following aggregate structures resulting in first the slug and finally the fully culminated fruiting body.

#### 1.4 An introduction to cell movement by chemotaxis.

Eukaryotic chemotaxis is the process by which a cell migrates towards a chemoattractant source along a diffusible chemical gradient. It is seen to be essential in both lower and higher organisms for such basic cellular processes as finding nutrients, cell division, embryogenesis, wound healing and the break down of pathogens by neutrophils. Accurate detection of these gradients and the resulting cellular migratory response requires several key aspects of current cell biology. These include internal and external signal detection and transduction, functions of cell motility, cell polarity and substrate adhesion. This biological process usually follows a similar molecular pathway in most organisms, beginning with the binding of an external signaling molecule to a cell surface receptor. This is followed by the internal transduction of the signal via a complex set of multiple signaling pathways, resulting, in the re-organisation of the cell cytoskeleton components and the formation of new pseudopods through the generation of a gradient of cellular components.

In *Dictyostelium*, there are two chemoattractants that have been widely studied; the movement in vegetative cells towards a folate source secreted by bacteria in vegetative cells and the chemotaxis towards cAMP as a response to a lack of nutrients within the cells' environment. In the absence of a chemical stimulus, the cells produce pseudopods randomly over their surface and move about the environment in a meandering fashion, searching for a chemical attractant to follow. Upon encountering a chemical signal the cells have to determine the direction of the source and are remarkably well adapted to this in that they are able to sense differences in chemo-attractant concentration of as little as 2% across the length of the cell [25]. This process requires a highly fine tuned system of detection of external signaling and localization of internal cellular response.

One of the early key pieces of work in the field of Dictyostelium chemotaxis indicated PIP<sub>3</sub> as a major signaling molecule. It was observed that PIP<sub>3</sub>-specific pleckstrin homology (PH) domain of the cytosolic regulator of adenylyl cyclase (CRAC) protein localized to the membrane in response to a directed extracellular cAMP stimulus [25]. This set up a whole series of further research describing a Dictyostelium theoretical "biological compass" which was required to direct the cells towards the cAMP source. These experiments supported PIP<sub>3</sub> as the major signaling molecule in chemotaxis, with PI3-kinase synthesizing PIP<sub>3</sub> at the leading edge and PTEN converting it back to PIP<sub>2</sub> at the rear of the cell [26]. Cells also have a rapid ability to re-orientate the localization of PIP<sub>3</sub>, in response to cAMP, coinciding with a change in cellular orientation. PIP<sub>3</sub> has recently been shown to be the major signaling target for the affects of lithium on chemotaxis in Dictyostelium [1]. However, recent experimental evidence has started to dispute this theory. A study where all five of the Dictyostelium PI-3 kinases were genetically disrupted simultaneously showed that although these mutants did not show any PIP, localisation, they still retained the ability to chemotax towards a cAMP gradient with only marginal difference to wildtype [27]. This suggests that PIP<sub>3</sub> is not the sole signaling mechanism responsible for the chemotactic response. Chemo-attractant gradients are usually set-up using one of two standard methods, these being a microinjector or a zigmond chamber (fully described in materials and methods chapter) [28].

It is now apparent that there are several key signaling pathways involved in mediating chemotaxis and that each may come into play during different stages of the process. Phospho-lipase A2 (PLA2) has been implicated in a study where the gene encoding PLA2 was either knocked out or chemically inhibited in the PI3-kinase mutants. These cells show a greater level of disruption to chemotaxis, but yet were not

fully inhibited [29]. Further experiments on these pathways have investigated the steepness of the gradient on cells lacking the PI-3 kinase and PLA2 pathways coupled with a number of inhibitory drugs. The resulting data has suggested that either pathway can give rise to normal chemotaxis in a steep gradient, however when the gradient is shallow loss of either pathway results in a reduction of chemotactic ability [30]. Further research that has suggested that cells respond differently to differing gradients has shown that the PIP<sub>3</sub> localisation to the leading edge is only seen with steeper gradients and additionally is distributed in a more even pattern around the cell membrane in shallower gradients [31, 32].

Another pathway implicated in the control of gradient sensing in *Dictyostelium* and linked to PIP<sub>3</sub> signaling, is the target of rapamycin complex 2 (TORC2), via an interaction with PI3K. Individual genetic disruption of several key subunits of this complex leads to chemotactic defects in *Dictyostelium*. This complex is activated upon stimulation of the cell by cAMP whereupon it induces the phosphorylation of two PKB isoforms; PKBA and PKBR1 (PKBG). PKBA is normally found in the cytosol, but upon stimulation translocates to the membrane and is phosphorylated in a PI3K dependent manner, whereas PKBR1 is always found at the membrane [33].

Further research by van Haastert and co-workers has suggested that there are in fact four individual signaling pathways involved in mediating chemotaxis in *Dictyostelium* [34]. They suggest that the PIP<sub>3</sub> and PLA2 pathways are involved in early chemotaxis, up to 5 hours after starvation, with these pathways becoming redundant towards 7 hours. They go on to show the involvement of cGMP in chemotaxis as cGMP null cells can no longer chemotax at 7H in the presence of both PI3-kinase and PLA2 pharmacological inhibitors. It is worth noting that these cells

can chemotax if only one or the other inhibitor is administered suggesting that the PI3-kinase and PLA2 pathways can still mediate chemotaxis at this point but are not essential. The fourth pathway mentioned was initially identified by Roelofs and van Haastert [35] with the deletion of two genes encoding soluble guanylyl cyclases (sGCs) GCA gca and sgc. Knocking out these genes once again significantly affects chemotaxis in the presence of both PI3-kinase and PLA2 inhibitors, 7 hours into starvation.

All the evidence suggests that there are several different signaling mechanisms involved in *Dictyostelium* chemotaxis and that they each become involved at different points during starvation in accordance with increasing extracellular concentrations of cAMP that occur as the cells aggregate into a tighter mound structure (Fig. 1.2)

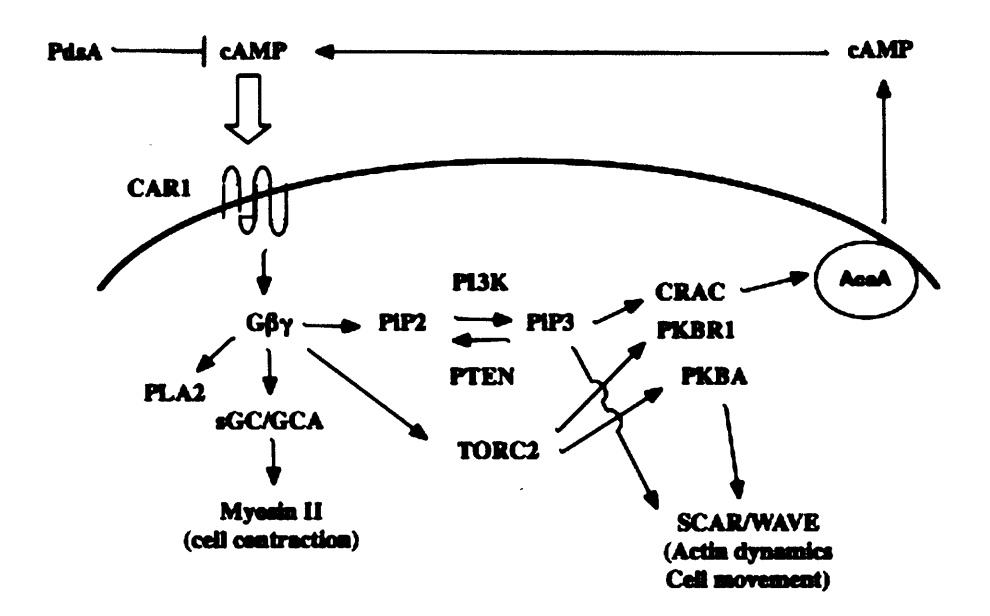


Fig. 1.3 Internal and external signaling relating to cAMP synthesis and chemotaxis

The productions of rhythmical cAMP pulses is produced via a complex intra- and extra-cellular signaling relay. The process is triggered by an external cAMP stimulus which in turn triggers the production of intra-cellular cAMP through ACA stimulation. This occurs through the activation of Ras proteins which in turn activate PI3K resulting in an increase in PIP3 levels at the membrane. PIP3 recruits the PH-domain containing proteins; CRAC and PKBA which activate ACA. A second function of stimulation id to activate the TOR pathway which will lead to the further activation of ACA and the SCAR/WAVE complex, involved in cell movement through actin dynamics.

## 1.5 cAMP signaling in Dictyostelium

The aggregation and subsequent differentiation and development of *Dictyostelium* had been noticed for some time before the chemo-attractant that controlled this process was identified. This chemical was identified to be cAMP in 1967 following an investigation by Konijin et al [36]. Following this a successive number of papers described the role of cAMP in bninding cell surface receptors, its effect on cellular differentiation and the positive feedback increasing its own synthesis in the stimulated cell, reviewed in [37].

Under starvation conditions *Dictyostelium* form spontaneous signaling centers that start to synthesise and secrete cAMP. Neighboring cells sense this signal and start to chemotax towards the source whilst themselves synthesising and secreting their own cAMP relay signal to be passed back through the population. This sets up a pattern of coherent travel in response to periodic waves of cAMP release. These waves of chemical transmitter release can take the form of the Belousov-Zhabotiniski (BZ) reaction in the shape of spiraling waves traveling through the population [38]. Alternatively they may take the form of concentric circles emanating from the signaling center. The periodicity of these pulses of cAMP is ~6mins during the initiation of development and chemotaxis but decreases as the cells approach the mound stage to provide a more continuous stimulus required for cell sorting.

The signal is detected by a series of cAMP receptors. These are all members of a family of 7-transmembrane domain receptors coupled to heterotrimeric G-proteins. Termed CAR1-4 each has a varying affinity for cAMP corresponding to its distinct temporal and spatial expression pattern during the development process [39, 40, 41, 42]. CAR1 has the highest affinity, followed by CAR3 and finally CAR2 and CAR4 having the lowest affinity. These decreasing affinities reflect the increasing

external concentration of cAMP during development. A study on the receptors ability to rescue mutations in the early receptors CAR1 and CAR3 discovered that all of the receptors can mediate the aggregation response in place of CAR1 suggesting a similar regulatory and activation mechanism for all [43]. CAR1 is also transcriptionally responsive to differing concentrations of cAMP by being under the control of two promoters. The first has a higher affinity for cAMP and is expressed earlyier during aggregation. The second has a lower affinity for the chemo attractant and is expressed later in development in response to higher external cAMP [44]. CAR2 has been implicated in the correct patterning of cells during mound stage differentiation. Expression is found exclusively in the prestalk A cells and removal of this receptor results in the arrest of development at the mound stage [40].

Adenylyl cyclase A (ACA) is the enzyme responsible for the production of the majority of the *Dictyostelium* cells cAMP. It is a 12 transmembrane domain protein with two cyclase domains sharing homology with the mammalian ACA [45]. Expression of the gene encoding ACA, *acaA*, is high during the early stages of development. The activation of ACA quickly follows stimulation of the cells CAR1 receptor with extracellular cAMP and is rapidly saturated and adapts to a constant stimulus. Activation occurs through the dissociation of the βγ dimer from the heterotrimeric G-protein G2 which then binds and activates PI3-kinase which catalyses the phosphorylation of PIP<sub>2</sub> to PIP<sub>3</sub>. PIP<sub>3</sub> then recruits CRAC through the previously mentioned affinity for the PH domain. Cells lacking the PI3-kinases are deficient for signal relay and synthesis of cAMP [46]. Once at the membrane CRAC interacts with ACA, although the exact mechanism for this interaction is currently unclear. CRAC was the first gene to be discovered that was related to cAMP

production. A genetic screen identified a mutant, synag7 that could not synthesise cAMP and could only aggregate when mixed with wild-type cells [47].

There are two further adenylyl cyclases in *Dictyostelium*: ACB and ACG. Both follow differing expression patterns to ACA, with ACB transcription increasing after 4H of starvation and remaining constant till culmination, whereas ACG expression is limited to fully developed fruiting bodies and is involved in germination [48]. ACB is thought to be involved in terminal differentiation as ACB nulls show normal development to the slug stage, following which they fail to produce normal fruiting bodies, showing unstable spore heads and elongated stalks [49]. ACG null cells are able to develop to produce normal fruiting bodies but display abnormalities in germination, with cells germinating spontaneously even under unfavorable conditions of high osmolarity [50].

The mechanisms for the cyclical hydrolysis of cAMP are equally important in such a dynamic signaling system as exists to regulate Dictyostelium chemotaxis and this role falls to the phosphodiesterases. There are 5 phosphodiesterases identified in Dictyostelium: PdsA hydrolyses both cAMP and cGMP, whereas Pde3 and PdeD are cGMP specific, RegA is cAMP specific and PdeE hydrolyses cAMP at a six-fold higher rate than cGMP [51]. The principal phosphodiesterase to be involved in early development and chemotaxis is PdsA, being expressed early in starving cells and found in both secreted and extracellular membrane bound forms. PdsA activity is regulated by a similarly secreted inhibitor; PDI which binds only the soluble form, reducing the  $K_{\rm M}$  for cAMP [52]. When extracellular levels of cAMP are high PdsA expression is enhanced, whereas when levels are low expression of PDI is promoted. The expression of PdsA is also highly regulated with the gene being controlled by three promoters, each becoming active during different stages of development, one

being active during growth, the second for aggregation and the third during multicellular development [53].

A body of work, by Cox et al [54] investigating the action of these phosphodiesterases has suggested that they play a key role in setting up the pattern of cAMP release throughout the population. Their hypothesis suggests that cells start signaling weakly with the cAMP emanating from a signaling center in a concentric circle. These patterns of release do not allow for a refractory period between pulses and need the cells at the aggregation center to keep emitting the pulses to maintain the signaling. However, if the pulses of cAMP meet other pulses spreading throughout the population they become disrupted and start to produce spiral waves. This disruption allows time for the action of the phosphodiesterases to reduce cAMP levels and allow the cells to recover and become responsive to cAMP once again. This enables the cells to maintain a pattern of release and stimulation without the need for pacemaker cells at the center of the aggregation territory.

The cell density factor (CMF) is also involved in regulating cAMP signaling in *Dictyostelium* development through activating transcription of the slow dissociating form of the CAR1 receptor and by promoting the loss of ligand binding. Cells lacking CMF have been shown to be unable activate the CAR1 receptors even in high cAMP concentrations suggesting that binding of CMF will not itself elicit a response but it will allow for cAMP binding and induction of the second messenger responses leading to chemotaxis and development [55]

#### 1.6 Previous work on this project.

Melanie Keim-Reder, a previous student of the Harwood lab, carried out a restriction enzyme mediated mutagenesis (REMI) screen looking for lithium insensitive mutants and identified several candidates for analysis. REMI involves the random insertion of an antibiotic resistance cassette throughout the genome and then screening for mutants which are selective for specific criteria (a full description of this technique is covered in materials & methods section 2.3). In this case the mutants were screened for lithium resistance. Two of those discovered in this screen were termed LisA and LisG. Both of these mutants showed an ability to aggregate in the presence of 10mM lithium. Initial findings showed that LisA increased inol gene expression in a similar way to that of a prolyl oligopeptidase (PO) inhibitor, which was dependent on the absence of the LisG mutation [Melanie-Keim Reder PhD Thesis]. Inverse PCR on LisG showed that the mutant possessed a 182bp fragment cloned into the LisG gene. It was found in the intron between the first and second of four open reading frames. Whilst being resistant to lithium affects on aggregation, RT-PCR data has shown that the original LisG mutant still expressed the LisG gene [56]. Preliminary analysis of LisG's sequence revealed a conserved split Snf2 ATPase domain and two downstream chromodomains suggesting that LisG could be an ATP dependent chromatin remodeling factor. The presence of the chromodomains identified LisG as being most likely to be part of the CHD family of chromatin remodelers. A literature search for other possible chromatin remodeling factors that may be involved in regulating Dictyostelium development and play a role in inositol biosynthesis identified the INO80 complex. This complex is another ATP dependent chromatin re-modeler and has a role in yeast as a modulator of inol, also being under regulation by higher order inositol phosphates [57].

#### 1.7 The basics of chromatin structure: How is DNA packaged inside the nucleus?

The most important question when addressing the issue of chromatin dynamics is how the cell manages to pack 2 meters of genetic material into a nucleus that is only micrometers in diameter. The most basic unit of this process is the formation of the nucleosome. DNA in eukaryotic cells is packaged into a compact chromatin fiber formed of regularly spaced repeating units known as nucleosomes and results in the DNA being compacted about sevenfold. Each nucleosome consists of DNA, bound to a histone complex, forming the nucleosome. Each histone complex consists of four different histone molecules, H2A, H2B, H3 and H4, arranged into two dimers of H2B-H2B and a stable H3-H4 tetramer. There are also a large number of histone variants that confer a range of different properties to the nucleosome and build specific chromatin structures [58]. The DNA is wrapped around the histone molecule in 1.65 super-helical turns consisting of 147 base pairs reviewed by Luger and Hansen [59]. However, this level of folding is still too low to accommodate the full length of the DNA within the nucleus. The chromatin structure is then subject to much higher levels of folding resulting in undefined highly compact structures.

The packaging of DNA into chromatin provides a definite barrier to the processes of transcription, replication, repair and recombination in cells. A highly specified and regulated system is required to allow these processes to proceed with correct gene expression at the right time.

#### 1.8 Accessing the DNA: An introduction to chromatin re-modeling.

The next question that arises within the scope of chromatin dynamics is how can this tightly packaged chromatin be accessed during key cellular operations such as transcription, replication or repair? The answer to this question is inherent to the answer to the previous question of how is chromatin packaged within the cell. When the DNA is held within nucleosomes and compact higher order structures, only a very small fraction of it is available for transcription. This is the standard structure during times of cell division, however, when the cell is required to execute various processes such as growth, DNA replication, DNA repair or recombination the correct spatial and temporal exposure of genes is required and this occurs through direct re-modeling of the chromatin.

The question of how chromatin is remodeled is answered by three processes that work in parallel to restructure the basic nucleosomal subunits of chromatin. Working together these form a dynamic system that allow the packaging and unpackaging of the DNA elements that allow transcription. The three processes are DNA methylation, covalent modification of the histones or replacement with a histone variant and the direct remodeling of the nucleosome spacing by ATP dependent chromatin re-modelers.

DNA methylation is linked to several aspects of chromatin dynamics and epigenetics, having been seen to be involved in genetic silencing, chromatin organization and differentiation. The process involves the methylation of cytosine residues in the context of CG dinucleotides and has been typically observed in mammals during embryogenesis where methylation patterns are maintained unchanged in somatic cells [60]. It was initially thought that *Dictyostelium* did not possess a DNA methyltransferase; however, recent studies have identified a candidate

and a number of genes possessing methylated cytosines. A drop in these levels of methylation have been identified in strains lacking the suggested *Dictyostelium* DNA methyltransferase and a number of developmental defects are observed [61].

The histones themselves are capable of being post-translationally covalently modified directly on several positions of their histone tails. This establishes correct nucleosomal spacing and confers epigenetically maintained developmental phenotypes. There are 3 types of post-translational modification (PTM) that can affect the histones. These are intrinsic, which affect the nucleosome directly, extrinsic, which affect the chromatin structure and effector-mediated, relating to changes brought about by interaction between PTMs and non-PTM chromatin effecting elements [58]. One function of effector mediated covalent modifications is the recruitment of ATP dependent chromatin re-modelers through a specific binding domain. These include PHD and CHROMO domains that are targeted to specific methylated lysine residues and BROMO domains that recognize acetylated histone tails. In Dictyostelium the inhibition of a histone deacetylase (HDAC) results in histone hyperacteylation and a delay in development with affected expression of a number of cAMP dependent genes [62]. It is apparent that histone modifications result in altered biological outputs yet their exact affect on cellular processes has yet to be fully appreciated.

The final group of chromatin modifying enzymes are the ATP dependent chromatin re-modelers. This group was initially discovered in yeast with the SWI/SNF complex which was initially classed as both a regulator of mating type switching (SWI) or for growth on no sucrose containing media (SNF, sucrose non-fermenter) [63]. There are now four recognized classes of ATP dependent re-modelers which are all characterized by a highly conserved ATPase domain that utilises energy

derived from ATP hydrolysis to alter the histone DNA interactions in a multitude of ways. These core members of the family exist in a large number of different complexes in most eukaryotic organisms resulting in a great range of specificity for various targets. This allows organisms to regulate a large number of cellular processes from this core family of ATPases conferring both environment and developmental stage specific gene expression [64].

It is seen that not only does chromatin provide a method of compacting DNA into the nucleus but it also provides a highly regulated system for controlling gene expression through a varied series of remodeling processes.

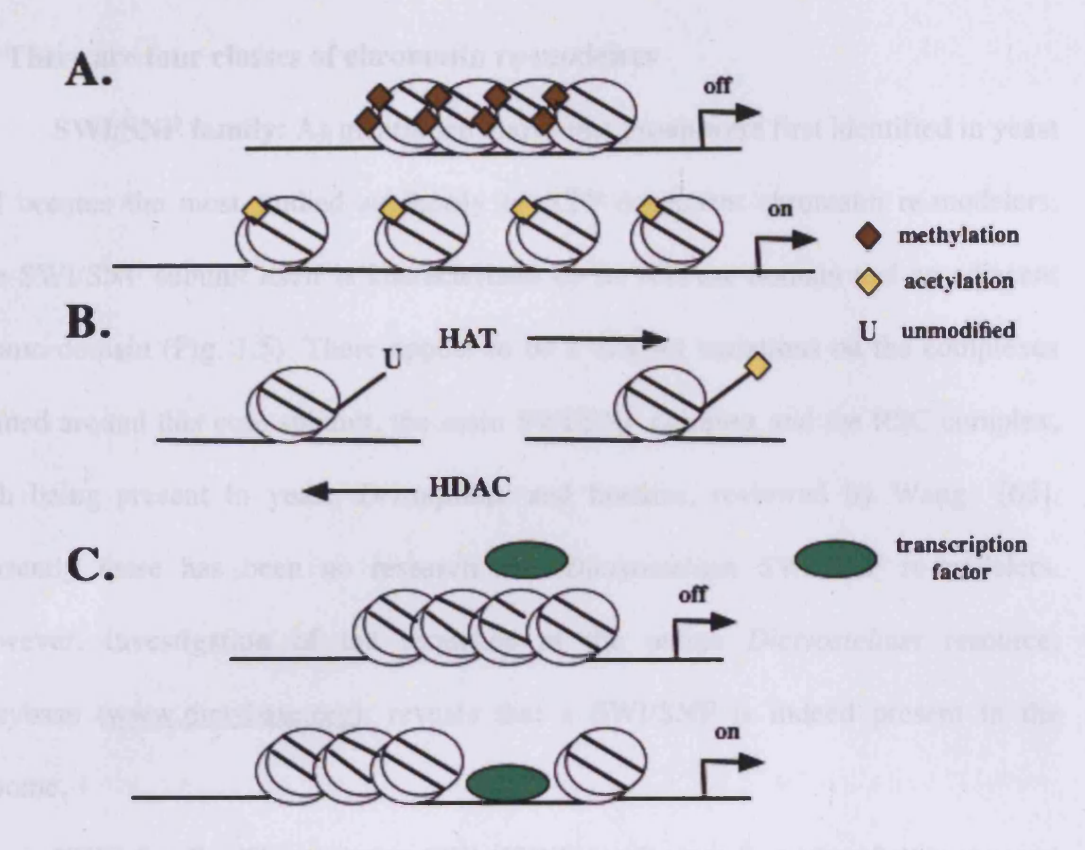


Fig 1.4 Methods of action of chromatin remodelling factors.

A.) DNA methyltransferases methylate cysteines on nucleosomal DNA providing a form of transcriptional repression. Removing this methylations allows for nucleosomal remodeling and transcription. B.) Modification of histone tails are yet another key element in regulating transcription. Here a Histone acetyl transferase (HAT) is shown to acetylate the histone tail, whereas a histone deacetyltransferase (HDAC) is seen to remove it. C.) ATP dependent chromatin remdelling factors use energy derived from ATP to reposition nucleosomes allowing the access of transcription factors and transcriptional activation or repression.

#### 1.9 There are four classes of chromatin re-modelers

SWI/SNF family: As mentioned above this group were first identified in yeast and became the most studied subfamily of ATP dependent chromatin re-modelers. The SWI/SNF subunit itself is characterized by its ATPase domain and an adjacent Bromo domain (Fig. 1.5). There appear to be 2 distinct variations on the complexes formed around this core subunit, the main SWI/SNF complex and the RSC complex, both being present in yeast, *Drosophila*, and humans, reviewed by Wang [65]. Currently there has been no research into *Dictyostelium* SWI/SNF re-modelers. However, investigation of the sequence at the online *Dictyostelium* resource; dictybase (www.dictybase.org), reveals that a SWI/SNF is indeed present in the genome.

ISWI family: The imitation SWI (ISWI) family was first identified by several in vitro re-modeling experiments in Drosophila. These investigations identified a single ISWI as the core subunit of three re-modeling complexes: NURF, ACF and CHRAC. Subsequent analysis has identified a second ISWI, ISW2 in other model organisms. The ISWI protein is characterized by the ATPase domain alongside SANT and SLIDE domains which have been shown to be DNA and nucleosome binding domains also found in many other chromatin binding proteins. The ISWIs are also characterized by a lack of any domains that recognize a direct covalent histone modification such as methylation or acetylation. The ISWI complex works by sliding nucleosomes along the strand of DNA allowing an ordered spacing between the nucleosomes, or restructuring the nucleosome pattern. ISWI also appears to have a function in establishing higher order chromatin structures being required to correctly incorporate the linker histone protein H1, reviewed by Corona and Tamkun [66]. At

present there has been no published research into the role of ISWI in *Dictyostelium*, although, there is an ISWI identified in the genome.

CHD family: Members of the Chromodomain helicase DNA binding protein subfamily are characterized by the SWI/SNF like ATPase domain and also by the presence of two N-terminal CHROMO domains. This is a large family consisting of 9 members, divided into 3 sub-groups: CHD1-2 in the first both containing a C-terminal DNA binding domain, CHD3-4 in the second both containing paired PHD zinc finger domains and CHD6-9 in the final group are defined by a paired BRK (Brahma and Kismet) domain, reviewed by Marfella and Imbalzano [67]. The first CHD protein to be identified in *Dictyostelium* was the LisG mutant; DDB\_G0293012, mentioned in Chapter 1.4. Further sequence analysis has identified two other CHD family proteins in the genome, one falling into the CHD1-2 subfamily; DDB\_G0284171 and the other also falling within the CHD6-9 group; DDB\_G0280705. The *Dictyostelium* genome does not contain any members of the CHD3-4 subfamily.

INO80 family: The INO80 subfamily consists of two very large multi-subunit complexes involved in transcriptional activation and repair, the INO80 complex and the SWR1 complex, with *Dictyostelium* only possessing the INO80 complex. Both the INO80 and SWR1 subunits are characterized by a split ATPase domain and their binding to two Ruv-B like proteins termed Rvb1 and Rvb2. INO80 complexes have been identified and characterized in yeast, fruit fly, and human, reviewed by Bao and Shen [68].

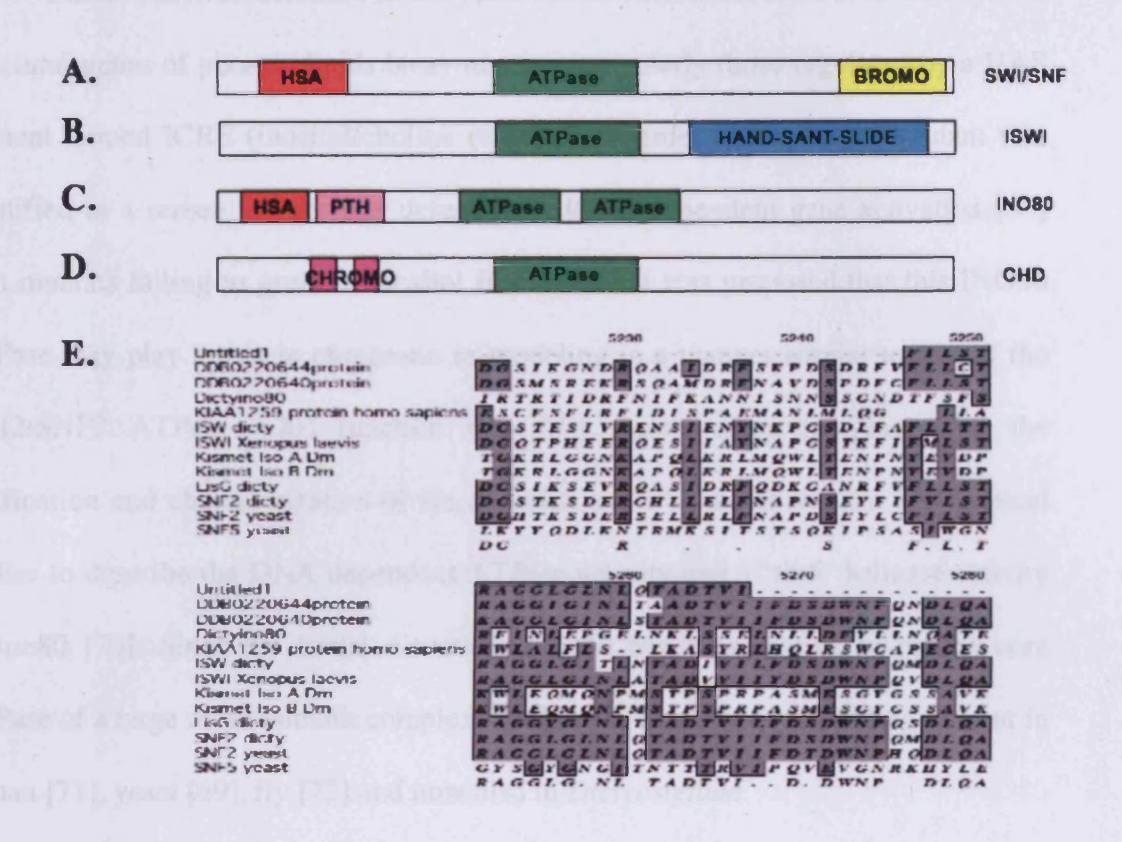


Fig. 1.5 There are 4 classes of ATP dependent chromatin remodelling factors.

A.)The domains conserved across the SWI/SNF family are the N-terminal HSA domain which binds ARPs and the C-terminal BROMO domain, recognising acetylated lysines on histone tails. B.) The ISWI family is classified by its HAND-SANT-SLIDE domain which is found in the c-terminus. SANT binds unmodified histone tails, whereas SLIDE binds nucleosomal DNA. C.) The INO80 complex is characterised by a split ATPase domain and a HSA and PTH domain, both binding other complex proteins described later. D.) The CHD family is distinguished by the CHROMO domains which target methylated lysines, typically marking areas of activated chromatin. E.) Alignment of the ATPase domain from several factors in several organisms.

NB: Untitled 1 = Dicty CHDC

# 1.10 The INO80 complex and Actin related proteins

Ino80 was first identified in the yeast *Saccaromyces cerevisiae*, in a study into structural genes of phospholipids biosynthesis, particularly those regulated by a UAS element termed ICRE (inositol/choline responsive element). The *ino80*- mutant was identified in a screen for mutants defective in ICRE dependent gene activation [69] with mutants failing to grow in inositol free media. It was proposed that this INO80 ATPase may play a role in chromatin re-modeling in a manner similar to that of the SWI2/SNF2 ATPase. This function was first shown again in yeast with the purification and characterization of the complex and a series of *in vitro* biochemical studies to describe the DNA dependent ATPase activity and 3' to 5' helicase activity of Ino80 [70]. Since the initial discovery INO80 has been shown to be the core ATPase of a large multi-subunit complex involved in chromatin remodeling present in human [71], yeast [69], fly [72] and now also in *Dictyostelium*.

Co-immuno-precipitation of the INO80 protein revealed the other subunits involved in the remodeling of chromatin [70] (outlined in Fig. 1.6). Two of the most conserved subunits found across all species are the actin related proteins Arp5 and Arp8. Bioinformatic analysis reveals that these proteins are also present and highly conserved in the Dictyostelid family [73].

Conventional Actin and the actin related proteins are members of a large, evolutionarily ancient and highly conserved family of proteins. The family is characterized by a common tertiary structure centered around an actin fold which contains a nucleotide binding pocket known to bind ATP. The actin related proteins were originally classified along their similarity to conventional actin and were termed Arp1 through to Arp11 with Arp1 being the most similar [74]. Arps 1-3 and 10-11 are all cytoplasmic and are involved in structural roles in the cytoskeleton, with the

Arp2/3 complex playing a role in cytoskeleton restructuring through interactions with the SCAR/WAVE complex in *Dictyostelium* [75]. The remainder of the Arps, are involved with various chromatin remodeling complexes, being found to interact with SWI/SNF, INO80 and SWR1 but not with ISWI or CHD complexes. Interaction with these complexes has been shown to occur through a specific helicase-SANT (HAS) domain [76]. Arps 1-6, 8 and 10 have all been identified in the *Dictyostelium* and other members of the Dictyostelid family's genomes [73].

It is currently not fully understood whether the Arps are providing regulation of the catalytic activity of the ATP dependent chromatin re-modelers or if they are involved in maintaining the structure of the complexes, evidence exists for both cases. Arp5 and Arp8 are the two actin related proteins that were identified as members of the INO80 complex in yeast immuno precipitation experiments [70]. Arp5 and Arp8 have been shown to have a requirement in preserving the integrity of the INO80 complex with deletion strains having severe affects on complex assembly. Null strains of Arp5 and Arp8 both phenocopy the deletion of the INO80 subunit in yeast and both show similar changes in *pho5* gene expression to an INO80 deletion [77].

The Rvb AAA<sup>+</sup> ATPases, Rvb1 and Rvb2, are another highly conserved group of proteins that are found consistently to be part of both the INO80 and SWR1 complex in all organisms investigated [78]. They have both been shown to be directly related to the bacterial RuvB ATPase which is involved in the resolution of holliday junctions that occur during homologous recombination [79]. Both are shown to be essential for complex function in yeast as null strains appear to lose binding of Arp5, which has been shown to exist in a separate regulatory complex with both Rvbs [78].

The most well documented effects of the yeast INO80 complex on transcription have been on the *ino1* and *pho5* promotors. PHO5 encodes a

phosphatase required for the uptake of extracellular phosphates when the internal pools have become exhausted. Under normal conditions four nucleosomes are found to sit across the *pho5* promotor blocking transcription. However when cells are grown in phosphate free media a transcription factor, Pho4p, binds a part of the promotor and recruits INO80 and SWI/SNF which both act to re-position the nucleosomes allowing access to the promoter for the cells transcriptional machinery, reviewed by Conway [79]. Re-modeling of the yeast *ino1* promotor occurs in a similar way involving the recruitment of both INO80 and SWI/SNF. Recent ChIP studies have indicated that a transcription factor, Ino2p/Ino4p, binds the upstream *cis*-acting promoter element UAS<sub>INO</sub> which is inhibited in repressing conditions by the regulatory Opi1p. Upon stimulation, due to a decrease in cellular inositol, Opi1p dissociates from the Ino2p/Ino4p complex stimulating the activation of INO80 and SWI/SNF at the *ino1* promotor resulting in the movement of nucleosomes to allow transcription [80].

This complex has also been shown to be involved in both activation and repression of genes involved in several signaling pathways beyond inositol phosphate signaling. Microarray data investigating the role of INO80 complex from *Arabidopsis thaliana* and yeast has indicated transcriptional regulation of up to 20% of all genes [79]. There has also been strong evidence to link the action of the INO80 complex with the repair of double strand breaks (DSBs) through histone H2A phosphorylation. This action of histone phosphorylation by ATM/ATR-like checkpoint kinases is one of the first actions that correlates with the repair response to DSBs [81]. Yeast strains lacking either INO80, ARP5 or ARP8 are all hypersensitive to DNA damaging agents and have been shown to recruit to sites of DSBs by ChIP [82].

A.

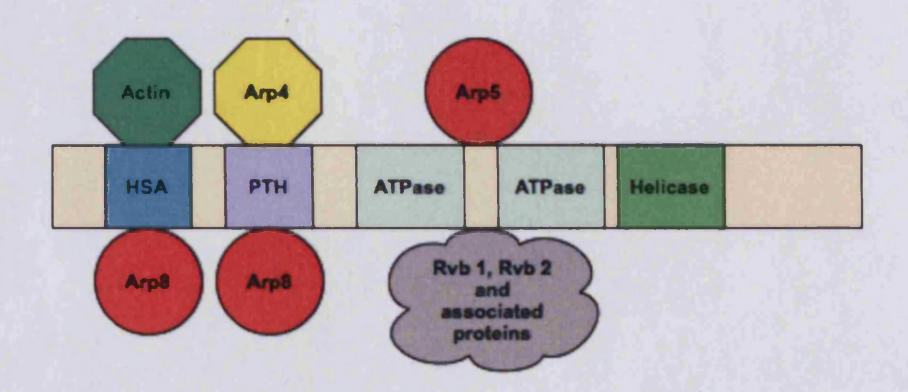


Fig. 1.6 The INO80 complex

**A.**) A diagram of the binding of INO80 to its subunits as determined in Saccharomyces cerevisiae adapted from a review by Conaway and Conaway [79].

# 1.11 The CHD family of chromatin re-modelers

The CHROMO domain was first identified in the epigenetic repressors Polycomb (Pc) and Heterochromatin protein 1 (HP1) of *Drosophilla* [83] and subsequently the first CHD protein was characterized in mice during a search for regulators of immunoglobin regulators [84]. Following on from this initial characterization; 9 CHD proteins have been identified across a large number of eukaryotic organisms, including protists, plants, insects and mammals. They have been shown to be involved in many processes through interaction with a large number of binding partners providing either transcriptional activation or repression. All members of the CHD family are extremely high molecular weight, ranging from ~220kDa up to 300kDa all sharing large amounts of sequence homology.

In those early experiments the chromodomain was shown to be an ~35 amino acid sequence that has subsequently been expanded to encompass ~60 amino acids and been indicated to be highly conserved amongst family members. In recent structural studies, the highly conserved region has been reduced further to a conserved core of ~21 amino acids termed the chromobox [85]. The double chromodomain structure has been shown to have a specific binding recognition for a direct covalent tri-methylation of the lysine at position 4 of histone H3 [86] (H3K4me) a recognized hallmark of transcriptionally active chromatin in eukaryotes. This binding can result in both the formation of heterochromatin and the regulation of developmentally regulated homeotic genes. In the case of the CHD proteins, unlike Pc and HP1, the chromodomains interact to bind the modified histone tail. The functional significance of the DNA binding domain of the CHD proteins has yet to be elucidated, however it is currently understood that the mouse chromodomain preferentially binds the minor groove of DNA in vitro with a long A-T rich sequence preference [87].

Of the three CHD proteins we have identified in *Dictyostelium*, two fall in the third class and share the highest sequence similarity to CHD7 and CHD8. The most commonly studied member of the CHD7 subfamily is the *Drosophilla* gene *kismet*, which has been identified to be involved in the maintenance of spatially restricted patterns of homeotic gene expression in the developing larvae [88]. This group is characterized by its BRK domains found at the N-terminus, a 41 amino acid structure that has also been observed to be associated with other transcription and chromatin associated proteins [88], yet the exact function of these domains is currently unknown.

There is also still very little information on the binding partners of this final subfamily of CHD proteins. CHD6 has been suggested to associate with RNApolII and has been seen to co-localise to sites of transcription in human cells [89]. Neither CHD7, or the *Drosophilla* isoform *kismet* have been shown to have any binding partners at present. In mice, CHD8 has been identified as binding the chromatin insulator protein CTCF [90] which has been implicated in the definition of distinctly regulated regions of neighboring chromatin and acting as a boundary to block the affect of nearby enhancers.

It was not until recently that the CHD proteins were implicated in any developmental processes. However the whole spectrum of ATP-dependent remodelers have now been characterized as playing a role in the development of higher organisms [91]. Specifically CHD7 has been shown to be involved in the development of several organs in human systems, including the gut [92], lip and palate [93] and also plays a role in human developmental disease. CHD7 has been implicated in the human CHARGE syndrome [94]. This disease is associated with multiple congenital abnormalities including; coloboma, heart malformation, choanal

atresia, retardation of growth and development often specifically ear and genital abnormalities [95]. CHD8 has also been implicated recently as a possible molecular cause in another human multi abnormality disorder associated with developmental defects and cognitive impairment [96]. Along with implications in disease models CHD8 has been highlighted in regulating many diverse roles within the cell, including the regulation of androgen responsive transcription [97], efficient RNApol III transcription [98] and the suppression of p53 mediated apoptosis during early embryogenesis [99].

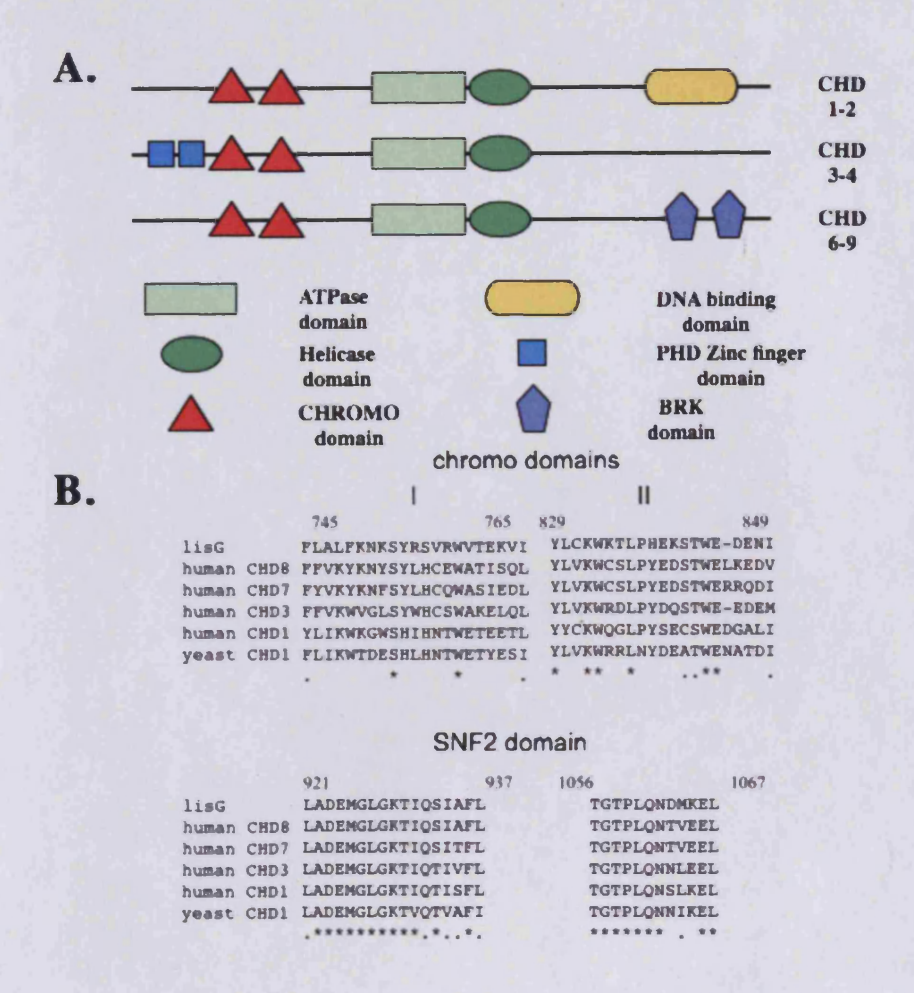


Fig. 1.7 The CHD family

**A.**) Schematic diagram indicating the key domains that distinguish each of the three subfamilies of CHD proteins. **B.**) Alignment of the CHROMO box domain of the CHD subfamilies in Dictyostelium, Human and Yeast. Alignments were performed using the clustly algorithm in the MACvector software.

# 1.12 Regulation and specificity of chromatin re-modelers

To accurately regulate chromatin dynamics, in a temporally specific way, so as to provide the right changes in chromatin structure during the correct developmental stages, some form of regulation of the complexes themselves must occur. In chapter 1.8 the regulation of the binding and activation of INO80 and SWI/SNF at the *ino1* and *pho5* promotors by transcription factors has already been described, but what other mechanisms have been discovered? There are several other possible modes of regulation for these complexes. These include post-translational modification of the ATPase subunit itself, or one of the other subunits that form these large complexes, by histone modification or histone variants (mentioned in chapter 1.6) or by interaction with a secondary messenger signaling molecules [100].

It is the final one of these processes that seems to be the most interesting in terms of the inositol phosphate signaling pathway and this project. Recent investigations into the roles of inositol phosphates as regulatory secondary messengers have suggested an involvement of higher IPs that may modulate the activation and inhibition of the INO80 complex [57]. Using an *in vitro* assay to assess the movement of reconstituted mono-nucleosomes along a strand of DNA containing the *ino1* promotor they showed that IP<sub>4</sub> and IP<sub>5</sub> positively regulate SWI/SNF mediated transcription from the *ino1* promotor whereas IP<sub>6</sub> negatively regulates the INO80 complex to inhibit transcription. In a similar manner recent evidence has suggested a role for IP<sub>7</sub> in the negative regulation of a series of transcription factors and kinases involved in recruiting INO80 and SWI/SNF to the *pho5* promotor [101].

# 1.13 Summary and aims of project.

The developmental roles of ATP-dependent chromatin remodeling factors are beginning to become clear in several model organisms and it is becoming apparent that they are responsible for the correct expression and patterning of gene expression in many cell types. Failure to regulate these complexes correctly is likely to result in aberrant gene expression and the incorrect development and differentiation of cell types.

The aims of this project were to use current and up to date molecular biological techniques to characterize the effects of genetically ablating the genes *chdc* and *arp8* in the model organism *Dictyostelium discoideum*. The study will focus particularly on starvation induced development and the chemotactic process by which cells aggregate in the early stages. The study will also look at the role of lithium on these complexes and in these processes to try to further elucidate the mechanism of action of this important treatment in the control of bipolar disorder.

# **Chapter 2:**

# **Materials and methods**

#### 2.1 Bioinformatics

Identification of *Dictyostelium* homologue of Arp8 and identification of CHDC (previously LisG) was performed using the Dictybase website (www.Dictybase.org) [102]. The actin related proteins had previously been identified in *Dictyostelium* and the sequences were readily available on Dictybase.

CHDC had previously been identified in the thesis of Melanie Keim-Reder and the sequence was available to me. Further analysis utilizing the whole protein sequences identified a further 2 CHD family proteins in the *Dictyostelium* genome which we have termed CHDA and CHDB. Further analysis identified highly conserved CHROMO domains in all family members which showed significant homology to CHROMO domains in other species. Dictybase reference codes are given for all *Dictyostelium* genes. Alignments were constructed using the Clustal algorithm as part of the MacVector 7.2 software suite (Accelerys).

#### 2.2 Dictyostelium cell culture

Dictyostelium cells were grown axenically in HL-5 medium (14 g/L proteose peptone, 7 g/L yeast extract, 13.5 g/L glucose, 0.5 g/L Na<sub>2</sub>HPO<sub>4</sub>, 0.5 g/L KH<sub>2</sub>PO<sub>4</sub>,pH 6.4.) for normal culture and all antibiotic selections. Cells were also grown and allowed to develop on SM agar plates (10 g/L proteose peptone, 1 g/L yeast extract, 10 g/L glucose, 1.9 g/L KH<sub>2</sub>PO<sub>4</sub>, 1.3 g/L K<sub>2</sub>HPO<sub>4</sub>.3H<sub>2</sub>O, 0.49 g/L MgSO<sub>4</sub>, 17 g/L agar) on a lawn of *Klebsiella aerogenes* by standard methods. The *arp8* null and LisG-REMI and CHDC null strains were all grown in the presence of 10μg ml<sup>-1</sup> Blasticidin. Cell lines transformed with the *ecmA*-gal, *ecmB*-gal and *pspA*-gal were grown in the presence of 40 μg ml<sup>-1</sup> Geneticin (G418). In all cases, except where

otherwise stated, the AX2 strain was used as wild-type and is the parent of all mutants. When required, cells were pelleted by centrifugation at 700g for 2 minutes.

Cells were washed in KK2 buffer (16.5 mM KH<sub>2</sub>PO<sub>4</sub>, 3.8 mM K<sub>2</sub>HPO<sub>4</sub> pH 6.2) before all starvation experiments. Then  $2x10^7$  cells were collected and resuspended in 1ml KK2 before being applied to a black whatman nitrocellulose filter placed on top of 2 whatman filter pads soaked in KK2. The cells were left for 5 mins for the excess to filter through and this was then aspirated off and the cells left in a humid environment to develop. After the desired development time, the cells were washed off the filter, pelleted and the pellets frozen for future use.

#### 2.3 Cell lines used in these studies

Several cell lines were used in the investigations into the roles of the two ATP dependent chromatin re-modelers. Three different lines were used in the experiments relating to the INO80 complex. These were the *arp8* null line, the Arp8-GFP line and the IMPase-GFP (*arp8* null) line. The first two cell lines were produced in the laboratory of Annette Muller-Taubenberger at Ludwig-Maximilian Universitat in Munich. The null cell was produced by homologous recombination (process described in Chapter 1.3) whereas the tagged cell line was produced by transforming wild-type AX2 cells with an extrachromosomal plasmid expressing the *arp8* gene with a GFP tag at the C-terminus. The final cell line used in relation to the first part of the project was produced by transforming an IMPase-GFP expressing plasmid into the *arp8* null cell line by electroporation (procedure described in Chapter 2.7). The plasmid was produced by Dr. Jason King and expresses the *impA1* gene with an N-terminus GFP tag. The plasmid is fully described in King et al, 2010 [24].

A further two cell lines were used in the research into the CHDC re-modeler. These were the REMI mutant LisG (lithium sensitive mutant G) and the null cell line *chdc* null. The LisG mutant was produced by Dr Melanie Keim-Reder during her PhD and was made by restriction enzyme-mediated integration (REMI), which is fully described in Chapter 1.3. The mutant was identified in a screen for lithium sensitive mutants and more detail on its production is found in Chapter 5. The final mutant strain *chdC* null was produced by a technician in the Harwood lab; David Proctor who used homolgous recombination to knock out regions coding key domains in the *chdC* gene. More detail on this mutant is also found in Chapter 5.

#### 2.4 RNA extraction and cDNA synthesis

Following development, total RNA was extracted using a GE kit. RNA quality was then checked by running 1µl on a 1% formaldehyde/agarose/ethidium bromide gel. Any samples lacking two clear ribosomal bands or any sign of genomic contamination were discarded. RNA was then quantified by measuring absorbance at 260 and 280nm using a nanodrop spectrophotometer. Reverse transcription was done using 1µg total RNA using Qiagen's Quantitect reverse transcription kit as per the manufacturers instructions. In all cases random primers were used. Once the reaction was complete all samples were diluted 1:10 to a final volume of 200µl. For all samples a no RT reaction was also performed and analyzed using a set of primers for PKBA1 to check for genomic contamination.

# 2.5 RT-PCR analysis of expression

To check for expression of each gene, cDNA was analysed by RT-PCR. For each gene the following primer pairs were used to generate a 200-300bp specific product for each gene:

Ig7 Fw = TCCAAGAGGAAGAGGAGAACTGC

*Ig7* Rv = CGCTACCTTAGGACCGTCATAGTTAC

*impk1* Fw = GCAGGTTCAACACCATTCAAAAAATC

*impk1* Rv = TCCAACACTATCCATTCCTTACCATC

impk2 Fw = TGGTAGTTTTTTGAGTGTCAGCCC

*impk2* Rv = TGATGATGTTGTTGTTGTTGTAGTG

arp8 Fw = CCTTCTGAAGCAGTTGGCACTACCACA

arp8 Rv = ATGGTTGTGGCACATAGGGTGGTA

acaA Fw = CATTCTAGAGGCGGTATTGGC

acaA Rv = GGAGAAAATGTCTGATTTCGCTT

carA Fw = CCAGCCAATGAAACATCATTG

carA Rv = AGGGAAACCACCATTGACAG

pdsA Fw = CCATTGGGTACAACTGGTGGA

pdsA Rv = AACTGCCCATGATGGATAGGT

inol Fw = GACACCGTCGTCGTTATGTGGT

inol Rv = GCAATCATATCATCGACAACATTTG

*impal* Fw = GATCAAGAGGAACCAATTAAGGTTTC

*impal* Rv = CCTTTTGAGTAATCTAATTGTTGTTT

ecmB Fw = GCCAACGTTGAAAAAGCTGAA

ecmB Rv = ACAGTTTACTGGGGTGTGAGA

ecmA Fw = GTACAATCACCAACAGTACCG

ecmA Rv = GAGACCACCAATTAAACCAGAG

cotB Fw = GATTGCGATGGTTTATCAAAAGATC

cotB Rv = AGCAAGACAATCGTTACTATCTCT

pspA Fw = ACATTGGCCAATCAAAATCCAGT

pspA Rv = TTGGTGCGGGTGTGGCAG

chdC Fw = AGTACTACTGCATCAACGACAACAAG

chdC Rv = TGGTGGTCTTTTTGATGTTGCTAT

PCR conditions used were 34 cycles of 95° x 30s, 56.5° x 30s and 68° x 15s. The reaction mix contained iQ SYBR green supermix (Bio-Rad), 100nM of each primer and 5μl cDNA was used as template in all reactions. Data was collected using an Opticon 2 instrument (MJ Research). Each reaction was then subjected to melting curve analysis, to verify product quality. All samples were run in triplicate, and in at least 2 independent experiments. Expression analysis was carried out using the Biogazelle qbase software [106, 107]. This piece of software utilizes a modified version of the original delta-deltal Ct method [108] to allow for multiple reference genes and therefore a more accurate normalization and calculation of calibrated data. The reference genes used in all cases were *rnlA* (Ig7), *ipmkA* and *ipmkB* (DDB 0203614 and DDB 0218526) which have all been shown previously to have unchanging expression during development.

#### 2.6 Extraction of genomic DNA

For use as a control PCR template.  $10^7$  cells were pelleted and washed once in KK2 before being dissolved in 1ml DNAzol reagent (Invitrogen). Cell debris was then removed by centrifugation at 15,000 x g, and DNA precipitated from the supernatant by the addition of 0.5 ml 100% ethanol. This was left for 5 minutes at room temperature before centrifugation at 15,000 x g for 5 minutes. The DNA pellet was then washed once in 70% ethanol and finally dissolved in 100µl 8mM NaOH. The pH was then adjusted to 7.0 using 3.2µl 1M HEPES buffer.

# 2.7 Dictyostelium transformation

Cells were transformed by electroporation as previously described [109]. Briefly, 10<sup>7</sup> cells, growing in log-phase were washed once in ice-cold electroporation buffer (50 mM sucrose in KK2) before being resuspended in a final volume of 800µl in an electroporation cuvette. For integrating plasmids, 20µg and for episomal plasmids 10µg DNA was then added and incubated on ice for 10 minutes. Cells were then electroporated at 1kV before a further 10 minute incubation on ice. The cells were then transferred into a 10cm petri dish and 8µl of salt solution (0.1 M MgCl<sub>2</sub>, 0.1 M CaCl<sub>2</sub>) added. After 20 more minutes the cells were then finally resuspended in 10 ml HL-5 medium.

After 24 hours, transformations of knockout vectors were cloned into 6 x 96 well plates in the presence of 10  $\mu$ g/ml blasticidin S. After approximately 2 weeks, multiple clones were seen and transferred into individual wells of a 24 well plate for screening. Transformations with episomal expression vectors were simply expanded in 10cm dishes and selection started 24 hours post-transformation with 20  $\mu$ g/ml G418. Due to the extrachromosomal nature of these vectors, all clones should have

the same copy number and have no positional affects. Therefore, sub cloning is unnecessary and all colonies produced were pooled. This technique was used to transform the IMPase-GFP over expressing plasmid into the *arp8* null cells.

# 2.8 Western blotting

For western blotting, cells were lysed in Laemelli buffer (50 mM Tris-HCL pH 6.8, 100 mM dithiothreitol, 2% SDS, 0.1% bromophenol blue, 10% glycerol) and boiled for 5 minutes to denature proteins before running on either a 10% polyacrylamide gel or a 12-3% Tris-Acetate gel for larger proteins. The protein from  $2 \times 10^5$  cells was loaded per lane. Western blotting was then carried out using standard methods, and probed with either a rabbit  $\alpha$ -Arp5 antibody (Gift from A Mueller Taubenberger) or a  $\alpha$ -CHDC antibody (developed by Open Biosystems) both used at 1:1,000 dilution. This was followed by a secondary horse-radish peroxidase (HRP)-conjugated  $\alpha$ -rabbit antibody (Sigma), used at 1:10,000 dilution. In all cases Pierce ECL reagent was used as HRP substrate.

#### 2.9 Analysis of cell movement (Chemotaxis assay)

For analysis of random cell movement, 24 hours prior to analysis, cells were seeded at 3 x 10<sup>5</sup> /ml in FM minimal medium. On the day of the experiment, the cells were re-suspended and 40 µl transferred to a glass-bottomed chamber slide (Lab-Tek) containing 2 ml medium. Cells were then left for 30 minutes to attach and recover before the medium was aspirated and replaced with KK2 containing either sodium or lithium chloride. They were then left for 1 hour before analysis.

For chemotaxis assays, growing cells were washed once and resuspended at 5 x 10<sup>6</sup> cells /ml in KK2. Cells were then shaken for 5 hours and subjected to 100 nM

cAMP pulses at 6 minute intervals. LiCl treatment was included for the final hour only. After 5 hours a small number of cells was then allowed to adhere to a glass slide before being exposed to a cAMP gradient using a Zigmond chamber [110]. The chamber was set up with 1µM cAMP (in KK2) on one site and KK2 on the other and left for 15 minutes before analysis.

In all experiments DIC images were taken using an Olympus IX71 inverted microscope with a 20x objective (NA 0.45). As our microscope is equipped with a motorized stage, 8 fields of view were taken simultaneously for each sample. Images were captured every 10 seconds for 10 minutes. DIAS 3.4.1 software (Soll Technologies Inc.) was then used to analysis the images. In this analysis, for each frame of the movie each cell was automatically outlined and cell paths determined. At this stage any cell that contacts another was disregarded. The average speed, persistence, acceleration, direction change, roundness and chemotactic index over the 10 minute period was calculated for each cell and in every case a minimum of 50 cells were measured and averaged. All experiments were repeated at least 4 times and, normalized to a NaCl control value as indicated. In all cases statistical analysis was done using an unpaired 2-tailed T-test.

# 2.10 Immunofluorescence

For immunofluorescence imaging, cells were seeded onto poly-L-lysine coated coverslips, and allowed to adhere for 30 minutes. Coverslips were then washed twice in PBS and fixed in 3% paraformaldehyde (in PBS) for 20 minutes. They were then washed three times more and permeabilised by two incubations of 15 minutes in 1% gelatin/ 0.2% saponin. Cells were then stained with 1µg/ml 4',6-Diamidino-2-phenylindole dihydrochloride (DAPI). Coverslips were then washed and mounted on

slides using Vectorshield mounting medium (Vector Labs). Images were then taken using a 40x oil immersion objective on a Leica TCS SP2 confocal microscope.

# 2.11 Dictyostelium development assay

Cells were cultured to 80% confluency before being washed in KK2 and resuspended in fresh KK2 at a density of 10<sup>6</sup> cells/ml. 6-well plates were prepared containing 1ml non-nutirent KK2 agar in each well. 1ml of cells was seeded into each well and allowed to adhere for 30 minutes before excess liquid was aspirated off. Timelapse images of cells were taken every 5 minutes, under brightfield conditions using Olympus IX71 inverted microscope with a 4x objective and the simplepci image capture software. The availability of an automatic stage made it possible to take multiple fields of view and as such 9 images, creating a 3 by 3 grid, were taken for each sample. Images were processed using ImageJ to create a 'montage movie' consisting of all 9 fields of view.

# 2.12 Dictyostelium cAMP pulse assay.

Cells were cultured to 80% confluency before being washed in KK2 and resuspended in fresh KK2 at a density of 10<sup>6</sup> cells/ml. 6-well plates were prepared containing 1ml of non-nutrient KK2 agar in each well. 5ml of cells was seeded into each well and allowed to adhere for 30 minutes before excess liquid was aspirated off. Timelapse images of cells were taken every 30 seconds, under dark-field conditions using an Olympus IX71 inverted microscope with a 4x objective and the simplepci image capture software. The availability of an automatic stage made it possible to take multiple fields of view and as such 9 images, creating a 3 by 3 grid, were taken for each sample. Images were processed using ImageJ to create a 'montage movie'

consisting of all 9 fields of view. Following the creation of the montage the movies are subject to several rounds of processing to better visualise the cAMP pulses. The most important feature of this processing is the image subtraction whereby for each frame in the movie it is subtracted from the successive frame. This produces a movie whereby the subtle movement in shape that the cells exhibit between frames is more pronounced and visible as the characteristic waves. To highlight these waves the movies are further subjected to rounds of Gaussian blurring to further visually enhance the movement of the waves.

The biology behind this technique is that as the cells move in response to the cAMP pulses they change morphology to a more streamlined structure through reorganization of the actin cytoskeleton. It is this change in shape between responsive, moving and refractive that is observable using this technique. The change in structure results in a change in the light reflection pattern visible, depending on the state of the cell.

#### 2.13 Dictyostelium affinity purification.

Arp8-GFP cells (a gift from A Mueller Taubenberger) were harvested and washed in KK2 before being resuspended in fresh KK2 and allowed to develop on black nitrocellulose filters for 8 Hours, as described in section 2.2, to achieve maximum expression of Arp5. Cells were washed off the filters, pelleted, resuspended in 5ml 1% Paraformaldahyde (in water) and incubated for 10 minutes. Cross-linking was quenched by the addition of glycine (to a final concentration of 1.25mM) and a further incubation of 5 minutes. Samples were then pelleted and washed twice in KK2 before being lysed in 1ml lysis buffer (150mM NaCl, 50mM Tris, 0.1% NP-40 and 10% glycerol supplemented with a Roche complete inhibitor

tablet). Samples were incubated on ice for 20 minutes, centrifuged at 16,000rpm and passed through a 0.2μM filter. 50μl of a GFP-Trap coupled to agarose beads (Chromotek) were added to each supernatant, these were incubated at 4°C for 1 hour. Beads were pelleted at 500g and washed 3 times with wash buffer (150mM NaCl, 50mM Tris, 10% glycerol supplemented with a Roche complete inhibitor tablet) before being resuspended in 50μl NuPage buffer. Samples were boiled at 95° for 5 minutes (reversing the cross-linking) and loaded onto a 4-12% Bis-Tris (Invitrogen), which was then subject to analysis by western blot using the αArp5 antibody.

# 2.14 RNA-seq and data analysis.

Recent developments in next generation, or deep, sequencing technologies have allowed for a more complete view of an organisms transcriptome. Studies utililising these techniques have increasingly changed the views of researchers as to the complexity of the eukaryotic transcriptome by allowing a far more detailed measurement of transcripts than previous techniques such as microarrays and previous sequencing technologies.

The technique works by harvesting poly(A)+ RNA from the cell population and converting this to a cDNA library. Specific adaptors are ligated to the ends of this cDNA library and then a short sequence read of 30bp is obtained from the sequences using next generation sequencing technology. This technique can be applied to a number of systems including Roche 454 and ABI SOLID systems however the Illumina platform was opted for in this study. The Illumina machine system consists of a flow cell with an optically clear surface to which the adaptor ligated DNAfragments are attached. The fragments are then extended and amplified by bridge PCR resulting in a high density surface with many millions of copies of the

template. These template copies are the sequenced using a four colour sequencing by synthesis system producing many millions of sequence reads in the ouput (process outlined in Fig 2.1A). Advantages over previous transcriptomic analysis include; not being limited to identifying sequences corresoponding to exisiting genomic sequences and also a greater reduction in the background signal produced as there is no hybridization efficiency or cross-hybridization to take into account and no saturation of signal. All of which are problems with microarray technologies.

For the experiments RNA was isolated using the technique outlined in section 2.3.  $1\mu g$  was taken and applied to the Illumina RNA-seq sample preparation kit (Illumina). The protocol was followed as supplied and the samples were checked using an Agilent Bioanalyzer for RNA integrity. An RNA integrity number of 8 was taken as the minimum accepted value. Once the cDNA libraries were prepared the samples were run on an Illumina genome analyzer II system. The resulting data was run through the Illumina pipeline following sequencing to remove any reads resulting from annealed adaptors or adaptor primers and then output in the Fastq file format for analysis.

One of the problems that has been associated with the RNA-seq technique is data analysis and in particular how to go about analyzing such large amounts of data in a meaningful and significant way. The objectives and ideas on the table are similar to those of microarray analysis, however the particulars are incredibly different. The first step required is the mapping of the reads to a reference genome and then from there upwards the data takes on increasingly more complex patterns with increasingly abstract layers of information. To analyze these data a piece of software from DNAstar called Arraystar (<a href="http://www.dnastar.com/t-products-arraystar.aspx">http://www.dnastar.com/t-products-arraystar.aspx</a>) was

used. This piece of software has algorithms both for analyzing microarray and RNAseq data with the possibility of comparing the two sets of data if needs be.

Before analysis with Arraystar quality control of the data was performed using an algorithm found on the online resource for next-gen sequencing; Galaxy (<a href="http://usegalaxy.org">http://usegalaxy.org</a>). This website provides a number of online tools for the manipulation and validation of sequencing data and has particularly good resources for assessing the quality of sequencing reads.

Once the quality control has been performed the data is now input to the Arraystar software. Each run file is imported individually along with the reference genome for your organism, in this case the *Dictyostelium discoideum* AX4 genome downloaded from the NCBI website. Consultion was held with the group responsible for sequencing and annotating both the AX2 and AX4 sequences for *Dictyostelium discoideum* as concern was raised that our wild-type strains used were the AX2 yet this reference was not yet available for download. The suggestions were to allow for a number of mismatches when performing the alignments as the differences between the two strains are mainly scattered single base changes and this should allow for these (personnal communication from Gareth Bloomfield, garethb@mrc-lmb.cam.ac.uk).

After the data is imported into Arraystar the reads need to be aligned to the reference genome using the qseq algorithm. There are a number of alignment options that allow the tailoring of the analysis to the quality of the data etc. For my analysis the minimum mer length was set to 27 as this was just below my read length and my reads were of a sufficient quality to not need trimming. For mismatches a minimum of 90% matches was set to allow for approx 3 mismatched bases in the reads, this would hopefully compensate for using the AX4 reference genome over AX2. Reads that

occurred more than 100 times and also reads that mapped to more than 25 places were occluded to reduce the read counts identified in any regions of high homology arising from conserved domains found in paralogous gene families and repeat regions as well as placing an upward cap on the read counts of extremely highly expressed genes. Once the sequences are mapped to the genome a lower limit of read counts was determined by looking at the read counts of several genes all known to have no expression in wild-type during vegetative growth. The average read count for all genes looked at in this group was 6 so this was taken to be the number of reads associated with an untranscribed gene and therefore would be our baseline for all future analysis, with all genes with a read count below 6 being occluded.

Initial representation of the data is through another DNAstar product; GenVision (<a href="http://www.dnastar.com/t-products-genvision.aspx">http://www.dnastar.com/t-products-genvision.aspx</a>) which allows the visual representation of the reads against the reference sequence. Whilst showing the coverage of the genome this representation does not yield much meaningful data. To really get an idea of what is going on in these systems the data needs to be compared between cell types and time points. Arraystar allows the fold change comparison between 2 data sets and also allows you to put several constraints on this comparison such as minimum number of reads (taken here to be our baseline of 6) and a minimum fold change in gene expression. Once this has been performed the genes that fit the criteria, exhibiting a suitable fold change in expression, are exported to a separate table for Gene onotology (GO) analysis.

Gene ontology relates to a defined set of terms that describe gene product characteristics and annotations in an attempt to standardize the way in which genes, products and attributes are referred to across all species. A large number of organisms have had their genomes annotated in relation to the terms defined by the gene

ontology consortium (http://www.geneontology.org/) and this includes Dictyostelium. The GO annotations are imported to Arraystar and the genes exported in the foldchange comparison are subject to GO analysis where they are grouped depending on their annotations. The groupings are scored on their significance by a p-value which is defined as the probability that the number of genes occurring in the grouping has occurred by chance. Therefore a low p-value is a more significant grouping. The data is also scored by a z-value that represents the number of standard deviations away from the expected number of genes the actual value is. Using these tools it is easy to see which biological processes contain the largest number of genes showing a fold change above the threshold dictated earlier in the process. It is also possible to pick out individual processes and identify which genes show a difference between the two samples or time points. It is therefore possible, using this analysis pipeline, to identify the changes in gene expression in specific biological processes in which you are interested between 2 samples using data sets collected based on total RNA levels within a cell type or at a specific time point. Data representation from this point on is then up to the user.

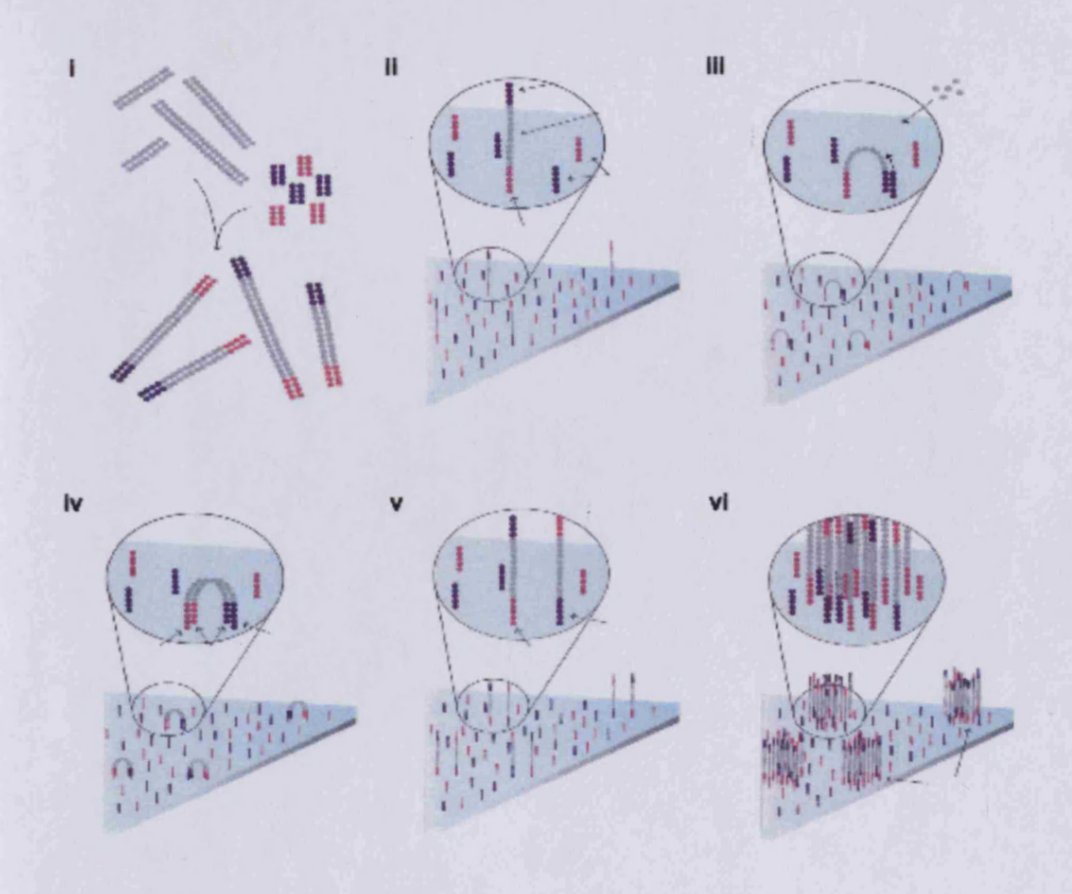


Fig. 2.1A The initial steps of Illumina sequencing.

i.) Preparing the sample, unique adaptor sequences are ligated to the ends of the fragmented DNA. ii.) Attaching the DNA fragments randomly to the flow cell surface. iii.) Initiate bridge amplification of sequences. iv.) Double stranded DNA bridges are formed enzymatically. v.) The Double stranded DNA is denatured to leave two single stranded templates on the flow cell surface. vi.) Amplification produces several million clusters of template in the flow cell.

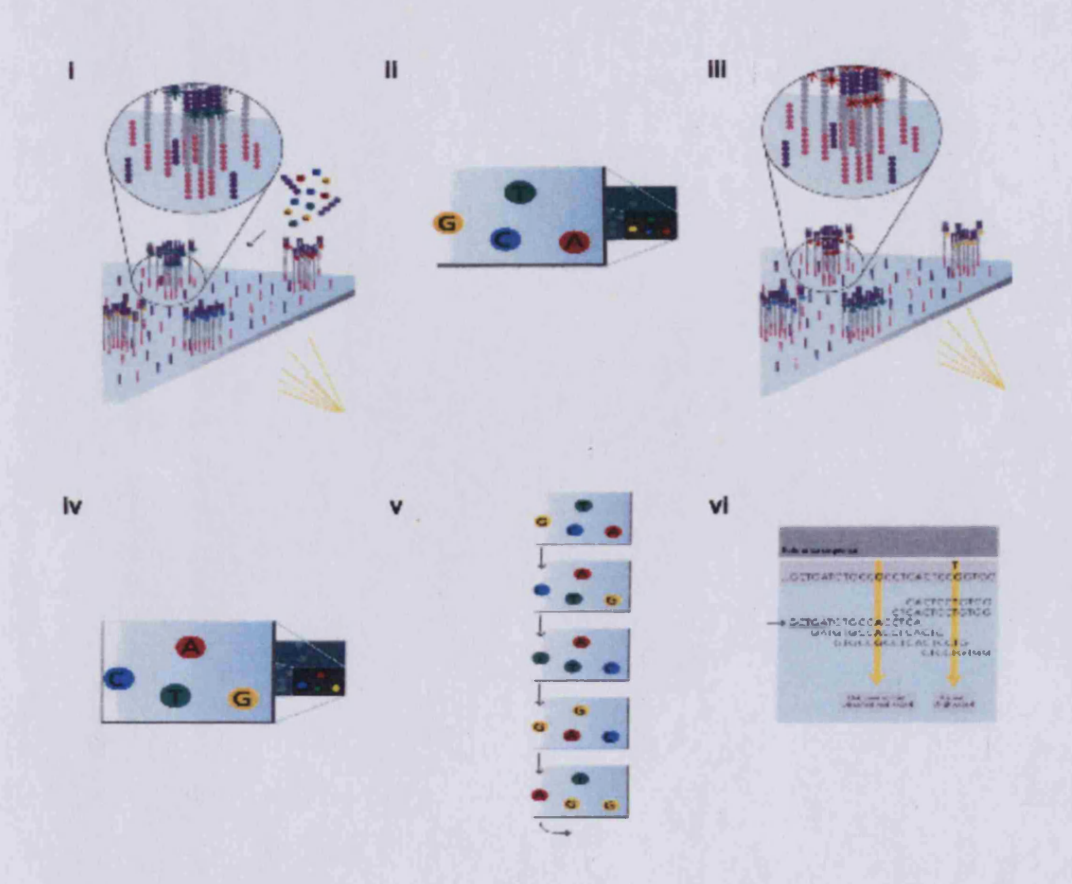


Fig. 2.1B The final steps of Illumina sequencing.

i.) Initiation of the first sequencing cycle; 4 labelled reversible terminators are added alongside primers and polymerase. ii.) Laser excitation and capture of emitted signal identifies the first base in the sequence. iii.) The first step is repeated iv.) The second step is repeated, identifying the second base in the sequence. v.) The process is repeated until the full sequence is identified. vi.) Reads are aligned to a reference genome and the sequences are identified.

# 2.15 Chromatin Immuno-precipitation (ChIP)

ChIP utilizes a specific antibody and fixation techniques to immunoprecipitate proteins/complexes bound to DNA and subsequently identify the regions of DNA to which the protein/complex of interested is bound.

1x10<sup>8</sup> Cells were allowed to develop on multiple black nitrocellulose filters as described in 2.2 and harvested every 4 hours by washing off using a micro pipette. Cells were pooled and then washed twice in KK2 and then fixed by the addition of 10ml 1% paraformladehyde for 10 mins. The fixing reaction was quenched with the addition of 2M Glycine to a final concentration of 1.25M. The pellets were washed twice with KK2 and then snap frozen on dry ice and stored at -80C.

ChIP was performed using the MAGnify ChIP kit (Invitrogen) following the manufacturers instructions. Particulars variations include; sonications were carried out on a Soniprep 150 sonicator, with an amplitude of 20 microns, in a 1ml volume. 6 x 10s pulses on ice were required to shear down to ~1000bp chromatin fragments and 15 10s pulses to shear down to ~300-400bp fragments.  $10\mu$ l was kept to assay the shearing of the sample by reversing cross linking over night at  $65^{\circ}$ C and run on a 1% agarose gel, plus checked for concentration by nanodrop.  $10\mu$ l of unsheared DNA was also kept before sonication for the input sample. Positive control IP was performed using a ChIP verified RNApolII antibody (Invitrogen), whilst a beads alone IP was performed along with an IP the null background as negative controls.

Analysis of ChIP DNA was performed using RT-PCR for the *ino1* promotor.

Primers used were:

ino1 Fw = GACACCGTCGTCGTTATGTGGT

ino1 Rv = GCAATCATATCATCGACAACATTTG

PCR conditions used were 40 cycles of 95° x 30s, 56.5° x 30s and 68° x 15s. The reaction mix contained iQ SYBR green supermix (Bio-Rad), 100nM of each primer and  $5\mu$ l ChIP'ed DNA was used as template in all reactions. Data was collected using an Opticon 2 instrument (MJ Research). Each reaction was then subjected to melting curve analysis, to verify product quality. Products were also run on a 1% agarose gel for a final analysis.

# 2.16 Picogreen assay

The quantities of DNA purified by the ChIP reaction are often too small to be measured reliably using a spectrophotometer and so a picogreen assay was utilized. The kit used was the Quant-iT DS DNA assay (Invitrogen) all reactions were performed as per the manufacturers instructions. Standards used were  $0\mu$ l,  $0.5\mu$ l,  $1\mu$ l,  $2\mu$ l,  $3\mu$ l, and  $4\mu$ l then each sample was run in triplicate. Reads were made on a Fluostar Optima fluorimeter and all read data exported to excel. Standard curves were made and the concentration of unknowns calculated from these.

# 2.17 ChIP-seq and data analysis

The results from the RNA-seq show the genome wide changes in transcription between two samples. However, there is no way of knowing if, in the case of my research, the effects are directly due to knocking out the chromatin re-modeler or if they are a secondary affect caused by another transcriptional change that was initially due to the removal of the re-modeler. ChIP-sequencing (ChIP-seq) provides a method of identifying the specific DNA binding sites of these complexes utilizing DNA precipitated by the ChIP method described in 2.15. This gives the ability to identify changes in promoter binding between developmental time points, when combined with RNA-seq data this should provide a comprehensive view of the roles of these complexes during development.

The ChIP'ed DNA needs to be sonicated down to approximately 300-400bp before IP, then once the DNA is eluted it is ligated to adaptors in a similar process to that used to create the cDNA libraries for the RNA-seq experiments (Fig 2.1A). Samples were prepared for use on the Illumina genome analyzer using the Illumina ChIP-seq adaptor ligation kit (Illumina). All reactions were carried out with 10ng ChIP purified DNA starting material and following the manufacturers instructions. Once prepared, the samples were checked using an Agilent Bioanalyzer for fragment size and DNA purity. Following quality control the samples were run on an Illumina genome analyzer II system. As with the RNA-seq experiment, the resulting data was run through the Illumina pipeline following sequencing to remove any reads resulting from annealed adaptors or adaptor primers and then output in the Fastq file format for analysis.

Data analysis is once again very similar to RNA-seq analysis in the initial stages. Once the reads have been mapped a two sided analysis needs to be performed to account for the background that is inherent in ChIP-seq data. A control sample is needed for this and is usually a no antibody IP or, as in this case, performing the IP on the null cell line. This analysis was performed using the analysis software CLC genomics workbench, provided by CLCbio.

### **Chapter 3:**

# Arp8 and the INO80 complex are involved in regulating genes involved with starvation induced development in *Dictyostelium discoideum*.

Summary: Starvation induced development in *Dictyostelium discoideum* relies on the cells ability to accurately detect and relay the cAMP signal throughout the population. This involves detecting the abundance of nutrients in the environment, the size of the population and the correct temporal expression of the cAMP producing, detecting and regulatory machinery. Here the mutation in the actin related protein Arp8 is seen to have an affect on the correct timing of development. This is seen to occur through an affect on the expression of specific genes involved in the production and propagation of the cAMP signal. Next generation sequencing data provides further evidence to suggest that the null cells are delayed in their ability to enter development through the mis-regulation of several genes involved in initiating this process.

#### 3.1 Arp8 expression

To investigate the role of the INO80 complex in *Dictyostelium discoideum* we targeted the subunit Arp8. Arp8 had previously been shown to be a key member of the complex in yeast and knocking out this protein phenocopied the knock out of the INO80 ATPase subunit [73].

Arp8, being a member of the chromatin binding complex INO80 should be expected to localize to the nucleus. To test for this localization, a strain of AX2 was produced expressing a GFP tagged Arp8 (a gift from the laboratory of Annette Mueller Taubenberger, situated in the Institute for cell biology, Faculty of medicine, Ludwig-Maximilian universitat in Munich) and fluorescence microscopy was used to image the GFP fluorescence. The GFP tag is situated at the C-terminus of the Arp8 protein. This was coupled with DAPI staining of the nucleus and the two are shown to co-localize in the cell (Fig. 3.1B-C). This indicates that, just as expected the Arp8 protein expression is situated mainly, but not exclusively, in the nucleus of the cell.

Developmental timing is a key aspect of the starvation process in Dictyostelium. If the INO80 complex were to be involved in regulating this process it is possible that the expression of the complex components themselves could be developmentally regulated, including arp8. This idea was assessed using qRT-PCR on cells isolated every 4 hours following the initiation of starvation. Fig. 3.1A shows that the expression of arp8 increases gradually during the first 12 hours of development, decreasing again for the final 12 hours. These data are in agreement with RNA-seq data published online at the dictyexpress website (www.ailab.si/dictyexpress). This expression pattern seen here suggests a role for arp8 in modulation of genes involved in early development and aggregation leading us to primarily investigate these stages.

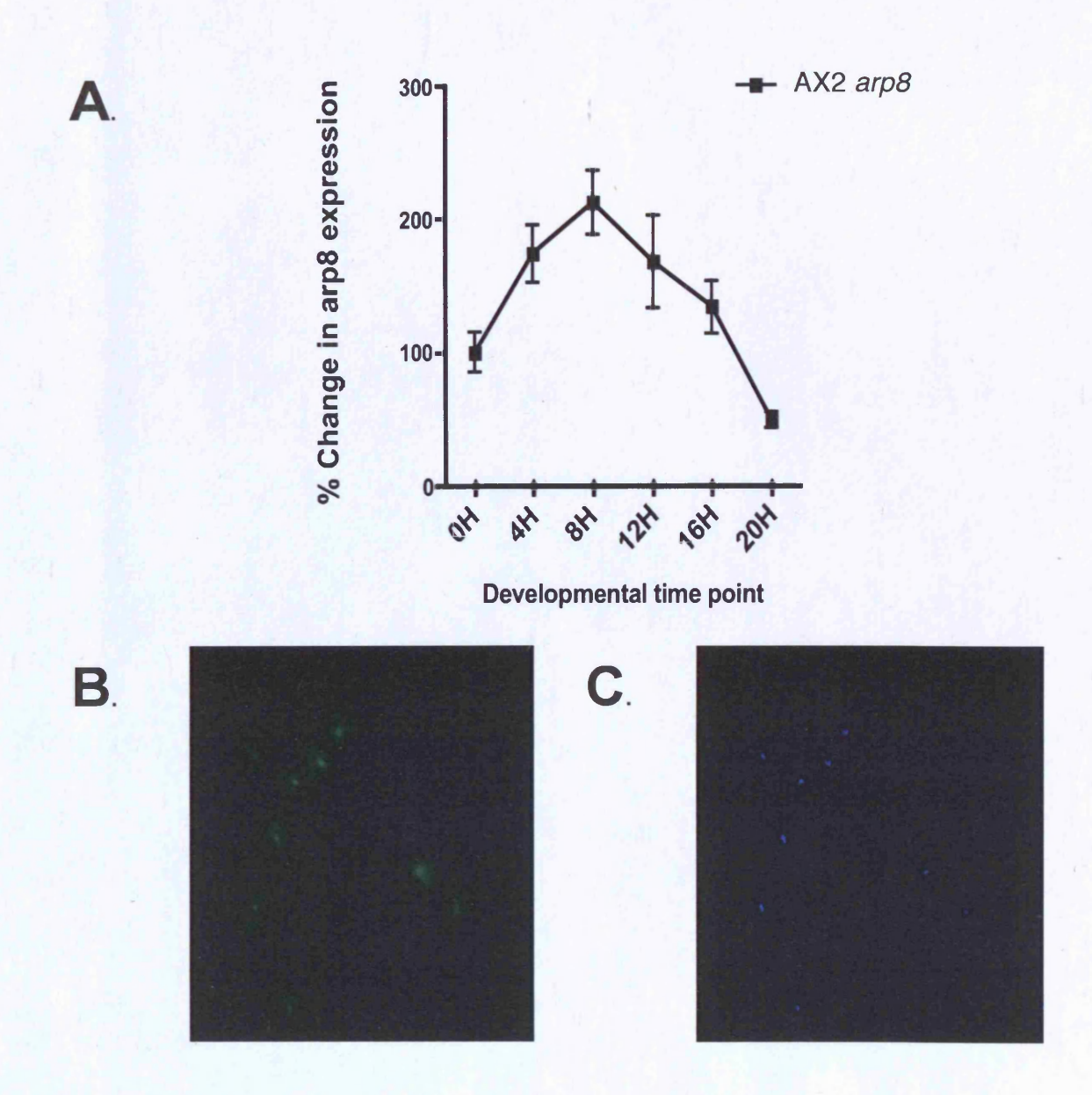


Fig. 3.1 Arp8 expression patters.

**A.**) Expression of *arp8* in wild-type cells is seen to increase over the first 12 hours of development, decreasing for the latter 12 hours. Total mRNA was analysed by RT-PCR and normalised to Ig7, IPMK1 and IPMK2. **B.**) Arp8-GFP expression is seen to co-localise with **C.**) nuclear staining with DAPI. Images were taken at 40X magnification.

#### 3.2 Arp8 null mutants show a delay in the onset of development

To further investigate the role of arp8 in Dictyostelium discoideum we also received an arp8 null cell line, a further gift from the laboratory of Annette Mueller Taubenberger, situated in the Institute for cell biology, Faculty of medicine, Ludwig-Maximilian universitat in Munich. The deletion was created by inserting a blasticidin resistance cassette, by homologous recombination, into the coding region for the arp8 gene. This resistance was then used to screen for clones that contained the deletion, which were then subsequently screened by PCR.

When starved of nutrients, wild-type Dictyostelium undergo a process of development, culminating in a multi-cellular organism capable of surviving periods of low nutrients. During this process a number of distinct morphological states are observed and occur under a common timing (Fig. 3.2A). Using brightfield time-lapse microscopy these stages become clearly visible. Any defects in the timing of development, or the structure of the fruiting bodies produced becomes apparent. After around 8 hours the cells can be observed to have aggregated to form a loose mound of around 10<sup>5</sup> cells. Continuing on from this stage, from between 10 and 12 hours the cells have started to push up away from the surface forming what is colloquially known as the "mexican hat" structure. Over the next four hours this "mexican hat" has toppled over and a slug like structure is formed, capable of phototaxing towards a light source. As 20 hours after starvation approaches the slug ceases its movement, draws in its tail and starts to rise once again from the surface finally culminating in a head of living spores supported by a stalk of dead cells after approximately 22-24 hours. The data presented in Fig. 3.2A indicate that the control wild-type cells follow this specific developmental pattern.

The arp8 null mutants exhibit a distinct delay in this developmental process that ranges from around 5 hours onwards. Not all cells enter development at the same time, some taking as long as 15-20 hours to initiate. These data describe cells showing a 5-6 hour delay in starting aggregation. Each morphological structure following this, loose mound, slug and full culminant, all show a similarly timed delay in formation. This suggests that the process does not accommodate and catch up once it has started and that the delay is persistent. It is notable that there is also a greatly reduced, number and size of, aggregation territories for the arp8 null mutant and a large number of cells are left outside this area. However, these cells then start to rearrange and organize themselves into later rounds of aggregation and development. This possibly leads to the varied delay in the development of the cells. When at full culmination the fruiting bodies show little morphological difference to wild-type with the major observation being a slightly decreased size of spore head. It is worth noting that whilst there is a significant phenotype in developing arp8 mutants, there was no observed phenotype during vegetative growth.

The fact that the developmental delay is not uniform across the population suggests that the delay is not due to a fixed factor missing from the cells as this would be likely to produce a universally timed delay. One likely suggestion is the lack, or low abundance, of an external signaling molecule that needs to build up to a significant threshold before being responsible for initiating the development process. There are a number of likely candidates including cAMP and the conditioned mediating factor (CMF) which is responsible for sensing cell density [55] and involved in the initiation of cAMP signaling. Our second possible hypothesis is that the signal recognition machinery may be defective and the cells simply cannot tell that the signal is there until a threshold has been reached.

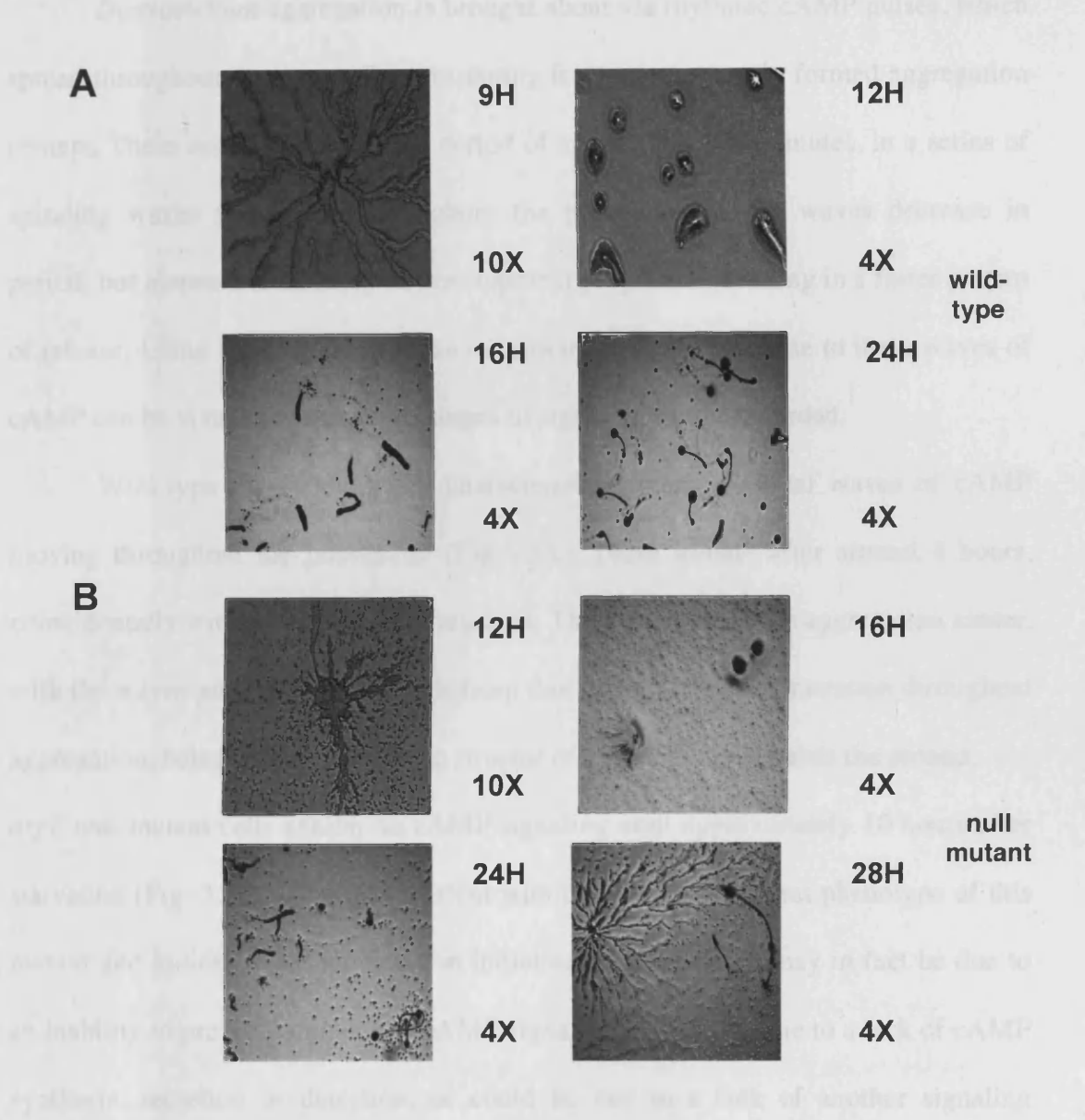


Fig. 3.2 Arp8 null cells have a delayed development phenotype

Development of cells on non nutrient agar. A.) Over the course of 24H the wild-type cells aggregate and differentiate to form multi-cellular fruiting bodies seen in the final image. B.) arp8 null cells take a minimum of 5H longer to initiate aggregation, having fewer and smaller aggregation territories. Once it has begun development follows a normal timeline and with no noticeable other phenotype. Both experiments were repeated at least three times.

#### 3.3 arp8 null cells exhibit a defect in cAMP signalling

Dictyostelium aggregation is brought about via rhythmic cAMP pulses, which spread throughout the population, emanating from spontaneously formed aggregation centers. These occur with an initial period of approximately 6 minutes, in a series of spiraling waves that spread throughout the population. These waves decrease in period, but increase in intensity as development progresses resulting in a faster pattern of release. Using darkfield time-lapse microscopy cellular response to these waves of cAMP can be visualized and any changes in signaling can be recorded.

Wild-type cells exhibit the characteristic pattern of spiral waves of cAMP moving throughout the population (Fig.3.3A). These initiate after around 4 hours, coincidentally with the onset of aggregation. They originate at the aggregation center, with the waves propagating outwards from this point. The pulses maintain throughout aggregation, being directed down the streams of cells moving towards the mound. arp8 null mutant cells exhibit no cAMP signaling until approximately 10 hours after starvation (Fig. 3.3B). This is consistent with the late development phenotype of this mutant and indicates that the delay in initiation of aggregation may in fact be due to an inability to properly initiate the cAMP signal. This could be due to a lack of cAMP synthesis, secretion or detection, or could be due to a lack of another signaling molecule. When the cells eventually start to signal, the waves take the form of concentric circles as opposed to spirals, a condition that has previously been attributed to a lack of PDI an inhibitor of the secreted phosphodiesterase [54]. Cells lacking PDI can only produce concentric circle patterns as an increase in the inhibition of PDEs will increase cAMP levels and reduce the cells ability to recover from stimulation. This suggests that the delay in initiation of cAMP signals could be due to a defect in expression of the cAMP signaling genes in early development.

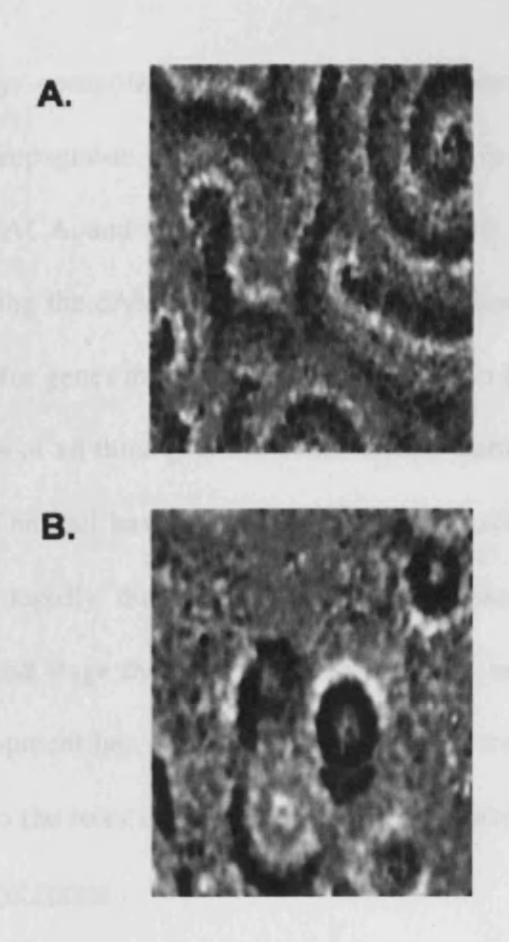


Fig. 3.3 Arp8 null cells have delayed production of cAMP pulses

Single frame still images extracted from supplementary movies ax2cAMPpulse.avi and arp8nullcAMPpulse.avi. **A.**) Wild-type cells show the characteristic spiral pattern of cAMP pulses moving through the population. These pulses initiate after approx 4H. **B.**) *arp8* null cells do not show this characteristic pulsing pattern once signalling has initiated, approx 5 hours after wild-type. The pattern seen is more erratic and produces a concentric circle pattern. Both experiments were repeated at least three times.

### 3.4 Null cells exhibit a delayed expression of the cAMP signalling genes during development

Three key components of the cellular machinery responsible for the production and propagation of the cAMP signal are the cAMP receptor CAR1, the adenylyl cyclase, ACA, and the phosphodiesterase PDE. Having all been shown to be essential for sensing the cAMP signal and efficient chemotaxis, these represent good initial candidates for genes that may be mis-regulated in the *arp8* null cells [51, 111].

Expression of all three genes shows a similar pattern to each other in wild-type cells (Fig. 3.4). They all have a relatively low expression during vegetative growth which increases rapidly during the aggregation phase towards 12 hours. Upon reaching the mound stage the expression starts to fall once again as their role in the process of development has been played. These data are in agreement with previous investigations into the roles of these genes and also currently available RNA-seq data <a href="https://www.ailab.si/dictyexpress">www.ailab.si/dictyexpress</a>.

The null cells also all show a similar pattern of expression for carA, acaA, and pdsA (Fig 3.4). However, this pattern is one of a severe delay and a retardation of the levels of transcription of these genes, with the peak occurring much later at approximately 16 hours after the onset of starvation. This delayed expression correlates with the observed delayed development phenotype and the delayed production of cAMP signals previously observed. It is now apparent that the delay is most likely due to an inability to signal to one another that starvation has begun and the process of aggregation needs to begin. However, this does no show whether this mis-regulation of these genes is down to a direct affect of the loss of arp8 or as an artifact of the loss on another external factor.

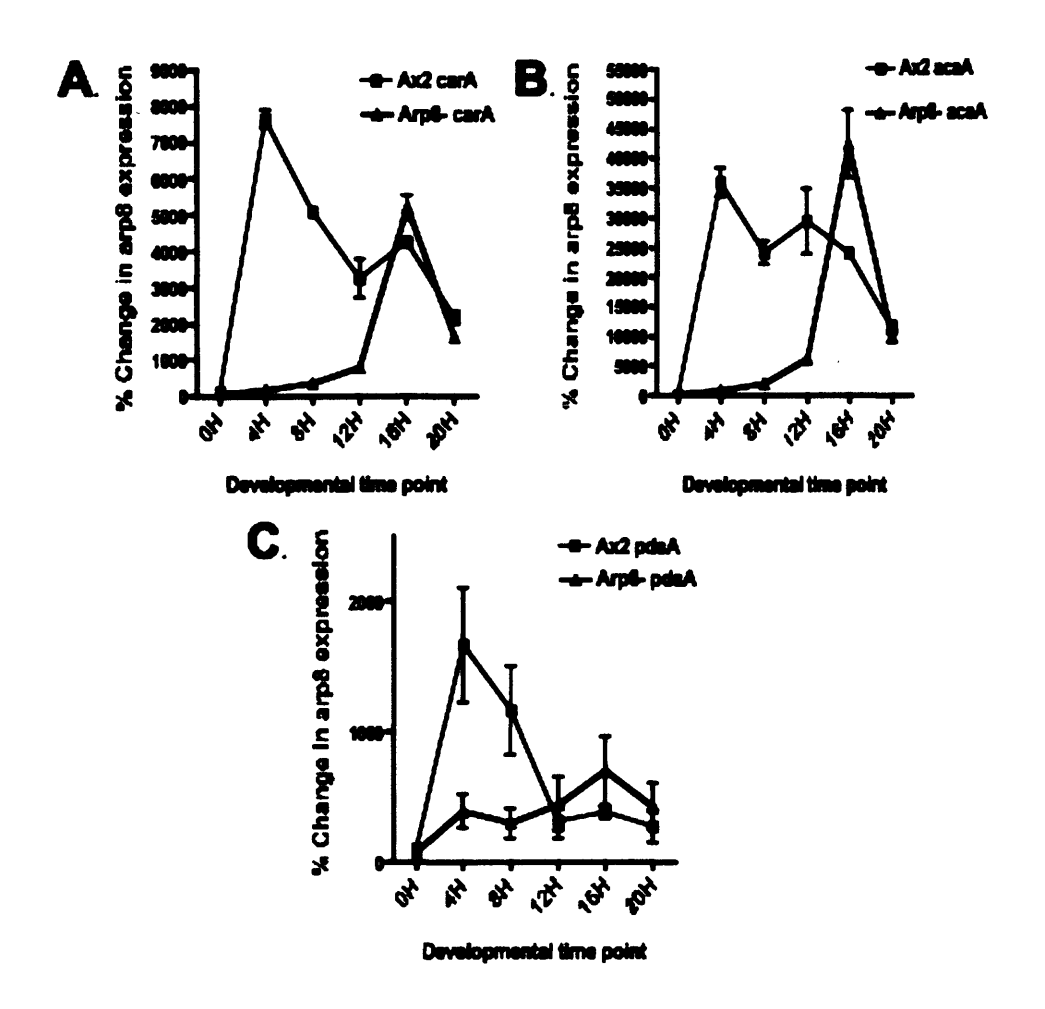


Fig. 3.4 Expression profiles of genes involved in cAMP signaling.

Analysis of the mRNA levels present in wild type or *arp8* null cells by QRT-PCR. All expression is normalized to AX2 0H which is given a 100% expression value. All genes analyzed show a similar expression pattern in wild-type cells, with an increase over the first 4 hours. *arp8* null cells also follow a similar pattern across all genes examined, with a delayed and reduced peak of transcription.

#### 3.5 Mixing the cell population can rescue the delay phenotype

To test the theory that the delay in aggregation and cAMP pulsing is due to an external signaling factor; arp8 null cells were mixed with decreasing amounts of wild type cells. If this delay is indeed due to the null mutants lacking an extra-cellular signaling molecule, mixing the cells with wild-type should return this molecule to the environment and rescue the phenotype. If it is down to the affect of the INO80 complex on the genes responsible for producing the signal it should not.

Mixing as few as 1% wild-type cells with *arp8* null cells and allowing them to develop on nitrocellulose filters rescues the delay in development (Fig. 3.5A). The combined population develop along a similar developmental time frame as the wild-type cells alone. They produce chimeric fruiting bodies indistinguishable from wild-type alone. This does suggests that the phenotype may well be due to the loss of another external signaling molecule, rather than a direct affect on cAMP producing genes and an inability to produce, or detect, the signal.

In a similar experiment, the cells were again allowed to develop, this time on KK2 agar and were imaged using darkfield time-lapse microscopy to identify any rescue of cAMP signalling. These cells showed an almost wild-type timing of the initiation of cAMP pulsing (Fig. 3.5B). However, the pattern of the pulses produced was still that of a concentric circle rather than the spiral patterns observed in wild-type. It could be, in this case, that the cAMP producing genes have been rescued in their expression yet others responsible for cAMP degradation, i.e the phosphodiesterases, have not.

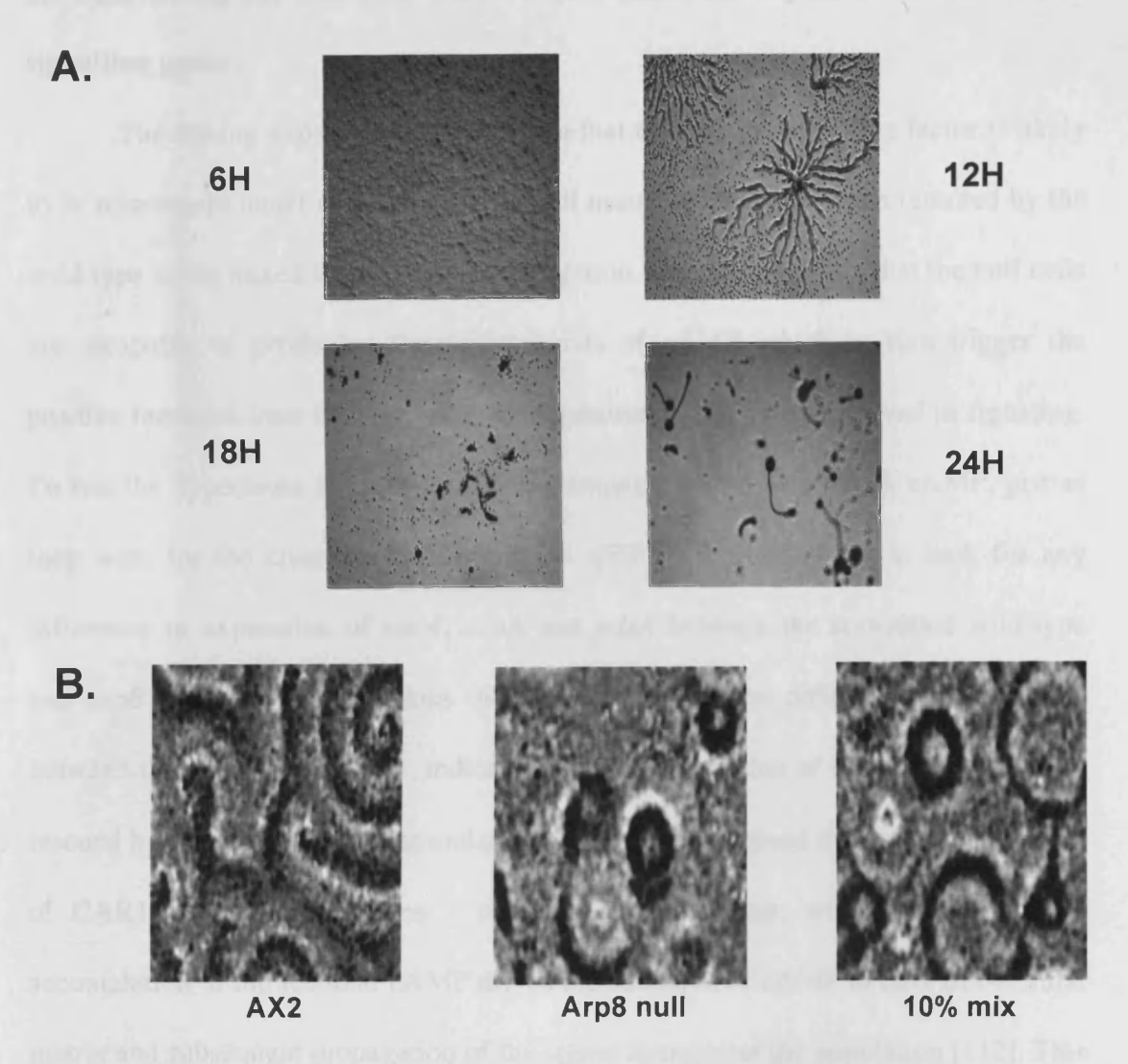


Fig. 3.5 Mixing null cells with wild-type forms chimeras that are capable of developing normally.

A.) Development of mutant *arp8* null cells mixed with 10% wild-type cells on nitrocellulose filters. The cells develop under the normal time frame of 24 hours. All image are at 4X magnification. B.) Still frame images taken from the supplementary movies; 10%mixcAMPpulse.avi, ax2cAMPpulse.avi and arp8nullcAMPpulse.avi. The third image depicts the correct temporal production of cAMP pulses, however, the patterns are still concentric circles, not spirals.

### 3.6 Stimulating the null cells with cAMP rescues the expression of the cAMP signalling genes

The mixing experiments have shown that an external signalling factor is likely to be missing, or under expressed, in the null mutants, which has been returned by the wild-type strain mixed throughout the population. One possibility is that the null cells are incapable of producing the initial bursts of cAMP which in turn trigger the positive feedback loop leading to the up-regulation of the genes involved in signaling. To test the hypothesis the null cells were stimulated for 5 hours with cAMP, just as they were for the chemotaxis experiments. qRT-PCR was utilized to look for any difference in expression of carA, acaA and pdsA between the stimulated wild-type and arp8 null cells. Observations indicate that there is no difference in expression between these two populations, indicating that the expression of these genes has been rescued by addition of cAMP stimulation. It has been proposed that initial stimulation of CAR1 by cAMP regulates a positive feedback loop, whereby the transient accumulation of intracellular cAMP drives the secretion of cAMP to the extra-cellular matrix and subsequent propagation of the signal throughout the population [112]. This occurs through the increased expression of the CAR1 receptor at the membrane, driven by an increase in extra-cellular cAMP signal coupled with an increase in CMF expression as a result of increased cell density [42, 55]. This strongly indicates that a lack of initial extra cellular cAMP signalling in the arp8 null cells could be responsible for the lack of gene expression, subsequently leading to a loss of cAMP secretion and the delay in aggregation.

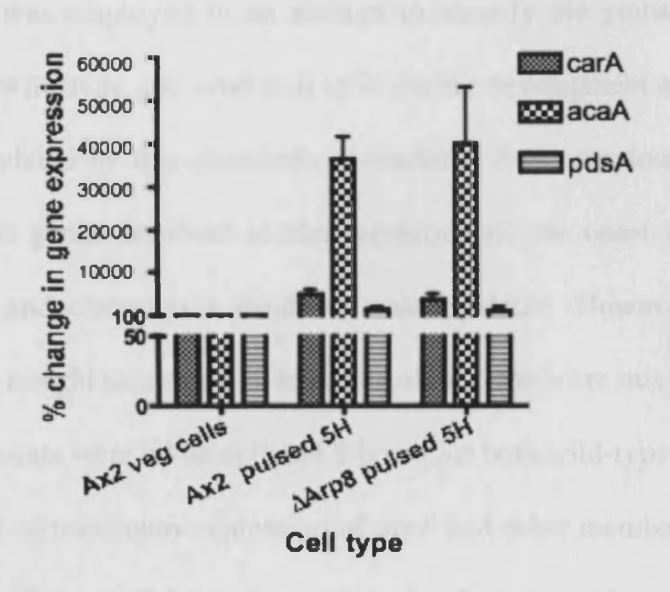


Fig. 3.6 Supplying null cells with cAMP returns the expression of cAMP synthetic genes.

All cells were pulsed for 5 hours with 1uM cAMP and total mRNA was extracted. Total mRNA levels present in wild type or *arp8* null cells was analyzed by QRT-PCR. All expression is normalized to AX2 0H which is given a 100% expression value. There is no difference between expression levels for any of the cAMP synthetic genes analyzed.

### 3.7 RNA-seq data reveals the genes which are affected by Arp8 during vegetative growth.

RNA-seq was employed in an attempt to identify the global transcriptional changes between wild-type and *arp8* null cells during development and thus indicate the processes regulated by this chromatin re-modeler. From previous experiments it was expected that genes involved in the regulation of the onset of development, cAMP signaling and chemotaxis would be mis-regulated. However, this analysis would provide an insight into other biological systems which are mis-expressed in the null cells. Time points were taken at 0 and 8 hours for both wild-type and null cells. 8 hours is the point of maximum expression of *arp8* and other members of the INO80 complex and therefore would be expected to be the point of greatest impact on transcription.

Quality control scores, from the Galaxy resource website, were extremely good for all data sets with none of the samples requiring any trimming. The data provided was then aligned to the *Dictyostelium* Ax4 reference genome sequence using the DNAstar Arraystar Qseq algorithms (full description in materials & methods). Following the alignment of the reads, the fold difference between samples was calculated using the Arraystar software. To gain the best understanding of what processes are affected when the *arp8* gene is knocked out comparisons were drawn between the wild-type and null cells between time points; i.e. comparing AX2 0H to *arp8*null 0H and AX2 8 to *arp8*null 8H. This would give a comprehensive view of the genes influenced by the INO80 complex at each time-point. For each time point the data was normalized to the base level of 6 read counts, through the Arraystars inbuilt filters. This base level was previously decided to be the level for un-expressed genes (see chapter 2).

To make sure that we are looking at real changes in gene expression a base limit of 2-fold change in gene expression was taken either way. Any changes below this were discarded through Arraystars filtering system. Looking at the total numbers of genes affected it is immediately apparent that there are far less affected by the knock out of *arp8* during vegetative growth than later on in development (Fig. 3.7A and B). A total of 3163 genes are affected after 8H of starvation compared to a total of 921 during vegetative growth. There are a larger number of genes that are down-regulated by the knock out of *arp8* at both time points, with nearly twice as many genes showing a decrease in expression (Table 1). To analyze such a large amount of data initially proved daunting. However, a decision was made to initially scan the data looking for genes that were known, from the literature, to be involved in development before following this up with a comprehensive gene ontology analysis (to be described later).

At 0H the first noticeable genes to be negatively affected are several of the Discoidin encoding genes;  $dscC\ 1+2$ ,  $dscD\ 1+2$ ,  $dscA\ 1+2$  and the discoidin 2 gene dscE (Table 2). Discoidin is one of the most studied families in Dictyostelium biology and is involved in the initiation of the starvation response, initially being expressed when cell density increases and continues to be expressed through early development [113]. Observing these genes down-regulated with such a delayed development phenotype as is seen in the arp8 null cells stands to reason as Discoidin is involved in the progression of this process and considered one of the main biological markers of development within the field.

Two other notable genes are found within the group of genes which exhibit the largest drop in expression. These are; lmcA and smlA. The first of these is also known as V4, a gene involved in the transition from growth to development [114]. The protein

is normally expressed during vegetative growth and is found to deactivate upon the onset of development. Similarly to *arp8* null cells, cells deficient in V4 fail to aggregate and are incapable of initiating the cAMP response, lacking the receptor and phosphodiesterase. *smlA* encodes a protein responsible for the regulation or processing of a secreted factor involved in regulating size of aggregates; countin [115, 116]. Countin is the major subunit of the counting factor (CF) complex that is involved in regulating the size of aggregates. The *smlA* gene is expressed normally during vegetative growth and early development, with *smlA*- cells exhibiting a reduced aggregation size and territory phenotype. The fact that *smlA* expression is reduced in *arp8* nulls could account for the reduced aggregation territories observed (Fig. 3.2).

A second gene is seen near the top of the list of over-expressed genes and this is the gene *ctnB* which encodes the protein countin2 a homologue to the countin discussed above [117]. Mixing experiments have shown that both countin proteins are required for normal aggregation sizes, with *ctnB*- strains forming smaller aggregates but *ctnA*-/*ctnB*- chimeras developing normally. Over expression of *ctnB* could be a response to the reduced expression of *smlA* which would cause an over-repression of the countin 1 protein.

The final genes identified in the list are both only down regulated a much smaller amount but are both instrumental in the growth – development transition. They are in fact two of the growth development transition genes; gdt1 and gdt2. These genes were identified as repressing the function of discoidin [118, 119] and all containing a putative protein kinase domain. gdt1 lacks a catalytic domain and so therefore may not function as the kinase it has been predicted to. It is once again found mainly in vegetative cells and rapidly disappears upon the onset of

development. A lack of gdt1 and or gdt2 leads to a rapid onset of development, which would not happen in this case due to the absence of discoidin.

Following on and looking at those genes which are up-regulated during vegetative growth identifies a number of genes that are known to be involved in influencing development. The most notable of the group include; lmcB, 3B-1+2 and cinC.

Interestingly one of the most over-expressed genes found in this group is lmcB the homolog to lmcA one of the most highly under-expressed genes in the arp8 null cells. My only explanation for this is that they are both regulated by different control mechanisms and that the expression of lmcB increases to compensate for the drop in lmcA.

Both of the homologs of the prespore specific protein 3B are seen to be over-expressed in this gene set. This gene is normally expressed later in development [120] and so goes against the general theory we are building here that Arp8 and INO80 control early developmental gene expression. However, it does serve to show that these factors are incredibly diverse and play a large number of cellular roles, activating and repressing different genes at all stages of development.

Another interesting gene that appears to be up-regulated in these cells is *cinC*. This is the *Dictyostelium* homolog of elongation factor 2 EF-2 and is normally only found in vegetative cells [121]. The fact that it appears at 8 hours into development lends further evidence to the suggestion that these cells are experiencing a delay in the onset of the developmental process.

The genes identified here all suggest that the arp8 null cells would exhibit a delay in the onset of starvation induced development (barring 3B-1+2), the phenotype which they do indeed exhibit.

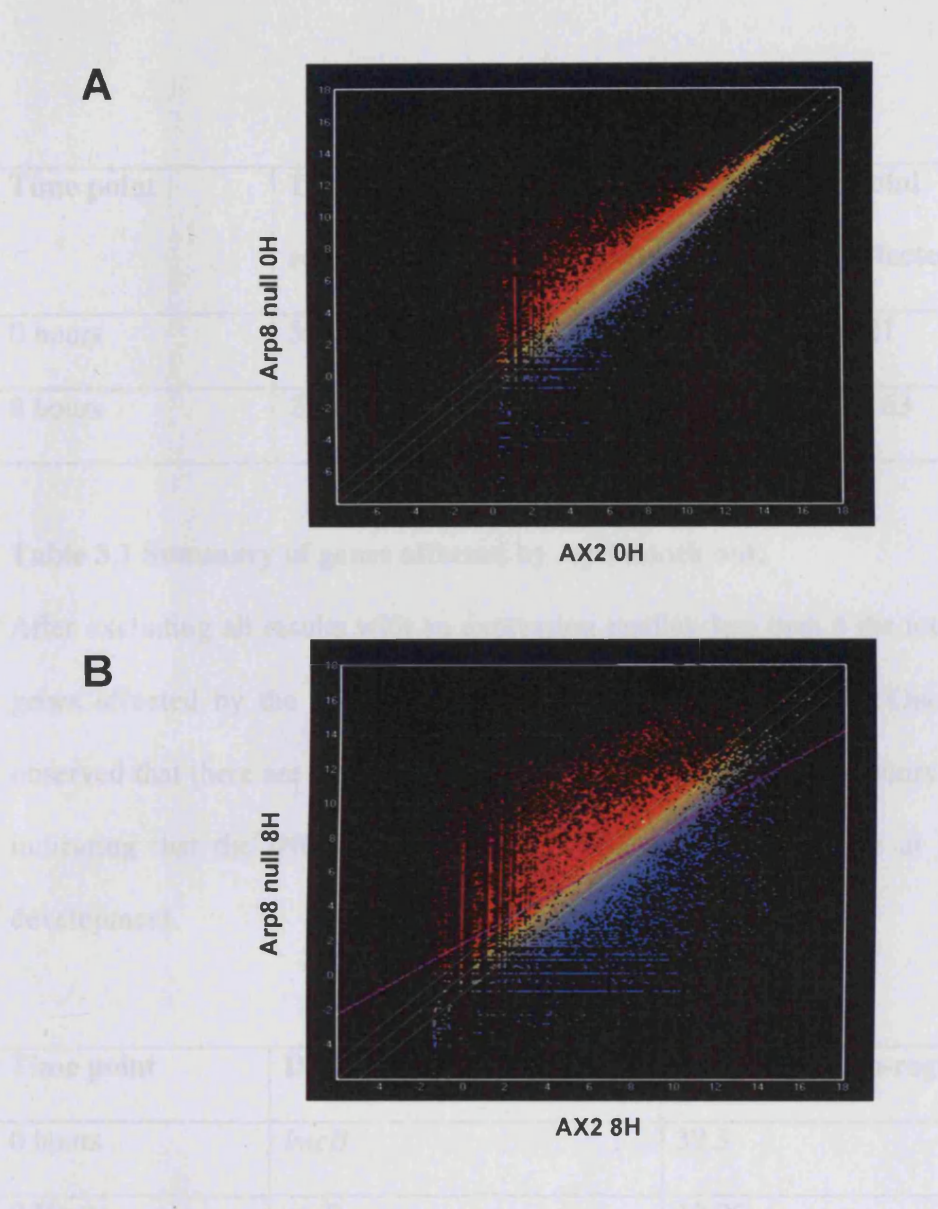


Fig. 3.7 Arp8 knock out affects a greater number of genes 8 hours into starvation.

Scatter plots indicating the fold change in gene expression comparing A.) Wild-type and null cells during vegetative growth and B.) wild-type and null cells after 8 hours of starvation. Points above the line represent an increase in expression, those below exhibit a decrease. A much larger number of genes, both up and down regulated, is seen on the 8 hour plot, suggesting that the INO90 complex plays a greater role at this time point.

Time point	Total genes down-	Total genes up-	Total genes
	regulated	regulated	affected
0 hours	593	328	921
8 hours	2221	942	3163

Table 3.1 Summary of genes affected by arp8 knock out.

After excluding all results with an expression reading less than 6 the total number of genes affected by the knock out of *arp8* are summarized above. Once again it is observed that there are almost 3 times more genes affected after 8 hours of starvation indicating that the INO80 complex plays a more significant role at this point of development.

Time point	Dictybase ID/gene name	Fold change up-regulated
0 hours	lmcB	39.3
0 Hours	ctnB	10.96
0 Hours	3B-1 (and 3B-2)	6.98
0 Hours	cinC	7.75

Table 3.2 Genes up-regulated during vegetative growth.

A small subset of the genes up-regulated in the *arp8* null cells compared to wild-type during vegetative growth. These genes are all possible candidates for contributing to the delayed phenotype observed in the null cells.

Dictybase ID/gene name	Fold change down-regulated
dscC	44.18
dscD	39.85
dscA	35.13
dscE	11.43
smlA	8.73
lmcA	64.02
gdt2	2.40
gdt1	2.39
	dscC  dscD  dscA  dscE  smlA  lmcA  gdt2

Table 3.3 Genes down-regulated during vegetative growth.

A small number of the genes that are seen to be down-regulated in the *arp8* null cells compared to wild-type during vegetative growth. All of these genes could be potentially responsible for the delayed phenotype observed in the null cells, either working individually or in concert.

### 3.8 RNA-seq data reveals the genes which are affected by Arp8 during early Dictyostelium development.

Moving on to look at the 8 hour time point, as mentioned earlier, there are a much larger number of genes that have been affected by the knockout, with a total of 2221 genes exhibiting a 2-fold or more decrease in expression and 942 showing an increase of 2-fold or more. These data indicate that the INO80 complex is more heavily involved in the activation of genes but also does play a repressive role too. The largest group of genes that stand out of the list of 2-fold down regulated genes, that also exhibit the largest decrease in expression are those of the growth factor; prespore cell inducing factor (PsiA). Four members of this gene family exhibit a larger than 250-fold drop in expression in the arp8 null cells. PsiA is a secreted glycoprotein that is involved in controlling the differentiation of both prestalk and prespore genes in developing populations [122] and is maximally expressed at the loose mound stage which explains why there is a such a large difference in expression as these cells are approaching this point at 8 hours into development. Looking for other genes also known to be involved in the control of prespore and prestalk differentiation several other key genes are seen to be down regulated. This includes the prestalk specific marker genes ecmA and ecmB plus the key prespore specific marker genes pspA and cotB [123, 124, 125]. All of these genes are down-regulated by several hundred fold in some cases showing a further clear delay in a set of genes involved in later development. Another major group of genes down-regulated in this mutant, which have already been validated in this thesis by rt-pcr, are those involved in cAMP production. All three of acaA, carA and pdsA exhibit a reduction in transcription as do pdeE and carB, another phosphodiesterase and cAMP receptor respectively, that are involved in the production of the chemotactic signal and initiation of development.

When analyzing the up-regulated genes with a 2-fold change in expression or higher the gene with the largest change is a histactophillin, hatA, a gene which's actin binding product is a membrane anchoring protein, tethering actin to the membrane [126], with mutants having a defect in spore fruition. A second histactophillin, hatA, is also highly up-regulated suggesting a later role for the INO80 complex in regulating genes involved in spore viability during fruiting.

The next pair of genes noticeable in the list are the conditioned mediating factor (CMF) receptor genes *cmfA* and *cmfB*. These genes products are involved in the initiation of development by activating transcription of the slow dissociating isoform of the CAR1 receptor [55]. At this point the null cells are beginning to enter development and so will be starting to secrete CMF in response to this, which will in turn activate the full cAMP signaling cascade (described in chapter 1). Several of the Discoidin genes are also up-regulated at this point in the null cells. These genes, as mentioned above, are expressed in response to the initiation of starvation and the secretion of CMF. So as CMF is expressed at this point in the null cells, so also is Discoidin, which is leading the cells into the full development cycle.

The final large group of genes that is apparent from the gene list is a large selection of the ribosomal proteins. The fact that these genes are still being expressed so highly suggests that there is still a high level of translation occurring which would be synonymous with cells that are growing vegetatively, lending more genetic evidence to the idea that the null cells are developmentally delayed. All of the evidence from these genes identified by RNA-seq lends further evidence to the idea that the INO80 complex is involved in regulating early starvation induced development in *Dictyostelium discoidin*.

Time point	Dictybase ID/gene name	Fold change up-regulated
8 hours	hatA	231.88
8 hours	cmfB	98.39
8 hours	hatB	90.03
8 hours	dscA	20.65
8 hours	dscC	8.45
8 hours	cmfA	7.54
8 hours	dscD	6.96
8 hours	rps12	121.63
8 hours	rpl15	102.46
8 hours	rpl13	91.35
8 hours	rpl88	91.33
8 hours	rpl26	86.85
8 hours	rpl4	80.55
8 hours	rpl21	69.81
8 hours	rpl12	69.87

Table 3.4 Genes up-regulated involved in development

This selection of up-regulated genes represents those that were immediately obvious as potential effectors of the delayed development phenotype, or changes that have occurred as a result of this after 12 hours of starvation.

Time point	Dictybase ID/gene name	Fold change down-regulated
8 hours	expl8	3458.8
8 hours	psiA	2319.5
8 hours	cotC	1871.7
8 hours	pspA	674.4
8 hours	psiM	592.2
8 hours	cotB	525.0
8 hours	ecmD	522.3
8 hours	psiC	431.1
8 hours	ecmA	351.8
8 hours	psiS	257.0
8 hours	pspB	228.0
8 hours	pspD	184.0
8 hours	cotA	122.0
8 hours	acaA	100.0
8 hours	cotD	70.0
8 hours	carB	69.9
8 hours	pdeE	49.0
8 hours	carA	19.0
8 hours	ecmB	10.0

Table 3.5 Genes down-regulated involved in development

A selection of genes down-regulated 8 hours into development that are likely to be associated with the delayed development phenotype, either possibly contributing to or being a direct result of the phenotype.

### 3.9 Summary

- Arp8 is a member of the INO80 chromatin re-modeling complex.
- In yeast INO80 is involved in regulating inositol biosynthesis by controlling expression of *ino1*.
- arp8 null cells exhibit a delay in the onset of development.
- This delay is due to an initial inability to produce correct cAMP signaling.
- The genes responsible for producing this signaling are delayed in their expression, starting to be expressed approximately 12 hours late.
- Expression of these genes can be rescued by pulsing the cells with cAMP and the developmental delay phenotype can be rescued by mixing the cells with wild type.
- RNA-seq data reveals a large number of other genes involved in regulating development which are mis-expressed in arp8 null cells.

### **Chapter 4:**

## Arp8 and the INO80 complex regulate *Dictyostelium* chemotaxis

Sumary: One of the key fundamental characteristics of *Dictyostelium* development is the ability of the cells to respond to concentrations of chemoattractant over several orders of magnitude. Here a mutation in a member of the large multi-subunit ATP dependent INO80 chromatin remodeling complex is identified. *arp8* null mutants reduce the concentration range under which the cells are able to chemotax. PIP<sub>3</sub> is a key signaling molecule in this process, having been show to translocate to the site of chemoattractant stimulation in steep gradients. Here it is shown that Arp8 is involved in maintaining the correct levels of PIP<sub>3</sub> production via suppression of 2 genes involved in inositol biosynthesis, *ino1* and *impa1*.

### 4.1 Chemotaxis is impaired in a cAMP concentration dependent manner

Starving Dictyostelium amoeba aggregate by chemotaxis towards a cAMP source. Cells response to cAMP is adaptable to the concentration of the chemoattractant experienced at different developmental stages. During the onset of chemotaxis the cells are subjected to very low concentrations in the nanoMolar range, rising up to those greater than 1µM later on in the mound. The ways in which cells respond to varying steepness of gradient in this process can be investigated in a zigmond chamber [28]. This chamber sets up a shallow gradient of cAMP upon which cells are allowed to chemotax. This process is recorded using time lapse microscopy. Cells pulsed with 1µM cAMP for 5 hours are in a chemotactically competent state and wild type cells in this condition are capable of migrating up a shallow cAMP gradient in a zygmond chamber ranging from 10nM to 1µM (Fig. 4.1A). The cells were all able to chemotax with a high chemotactic index (CI), however, in lower concentrations (10nM) of cAMP, at the source of the zigmond chamber, both the speed and directionality of the cells were reduced. These data suggest that cells are able to chemotax in extremely low and high gradients of cAMP switching from high to low sensitivity with a preference for more persistant movement when a stronger gradient is encountered. This system would enable the cells to preferentially move towards larger aggregation centers, directing the cells towards the mound. In early chemotaxis this switch from high to low sensitivity may be regulated by the switch between the two carA promoters. The early promoter producing a more sensitive receptor than the late [44].

arp8 null cells have a severe defect in their ability to chemotax and respond over a much smaller range of cAMP concentrations. In steeper gradients, where there is a much greater concentration in the source of the chamber to that in the sink, the

majority of the null cells freeze and round up, not displaying any chemotaxis at all. In fact when arp8 null cells are conditioned by pulsing and placed in a zigmond chamber, with a  $1\mu$ M source, only 44% of cells respond to the stimulus. Those that do respond, do so with severely diminished CI, directionality and speed (Fig. 4.1B). However, leaving the null cells for longer in the cAMP gradient sees a greater number of cells start to respond to the stimulus. After 1 hour 71% of cells have started to respond to the gradient with a CI, directionality and speed comparable to that of wild-type (Table 1). This is an interesting and previously unreported phenotype and could have a number of explanations. It is possible that the cells may be over producing a signal which decreases with time, or alternatively it is possible that the breakdown of cAMP in the chamber is rapid enough to create a shallower gradient which the cells are then able to sense.

Investigating these hypothesis the experiments are repeated using sequentially shallower gradients of cAMP, with cAMP sources once again ranging from 10nM up to  $1\mu$ M. If the cells start to respond due to a breakdown of extra-cellular cAMP then they should start to exhibit a greater response with an increasingly shallower gradient. This is seen to be the case. As cAMP concentration at the source is decreased the ability of the cells to sense the gradient was increased, with a higher percentage of cells responding. The cells that regained their ability to sense the gradient did so with an increasingly better CI, directionality and speed (Table 1). These data suggest that the Arp8 null mutants are capable of responding to a much smaller range of cAMP concentrations than wild-type a phenomenon suggested but not described before. These data show that *Dictyostelium* cells respond to a cAMP over a large order of magnitude which is controlled at least in part by the action of the INO80 complex and Arp8 as arp8 null cells can not respond over the same concentration range.

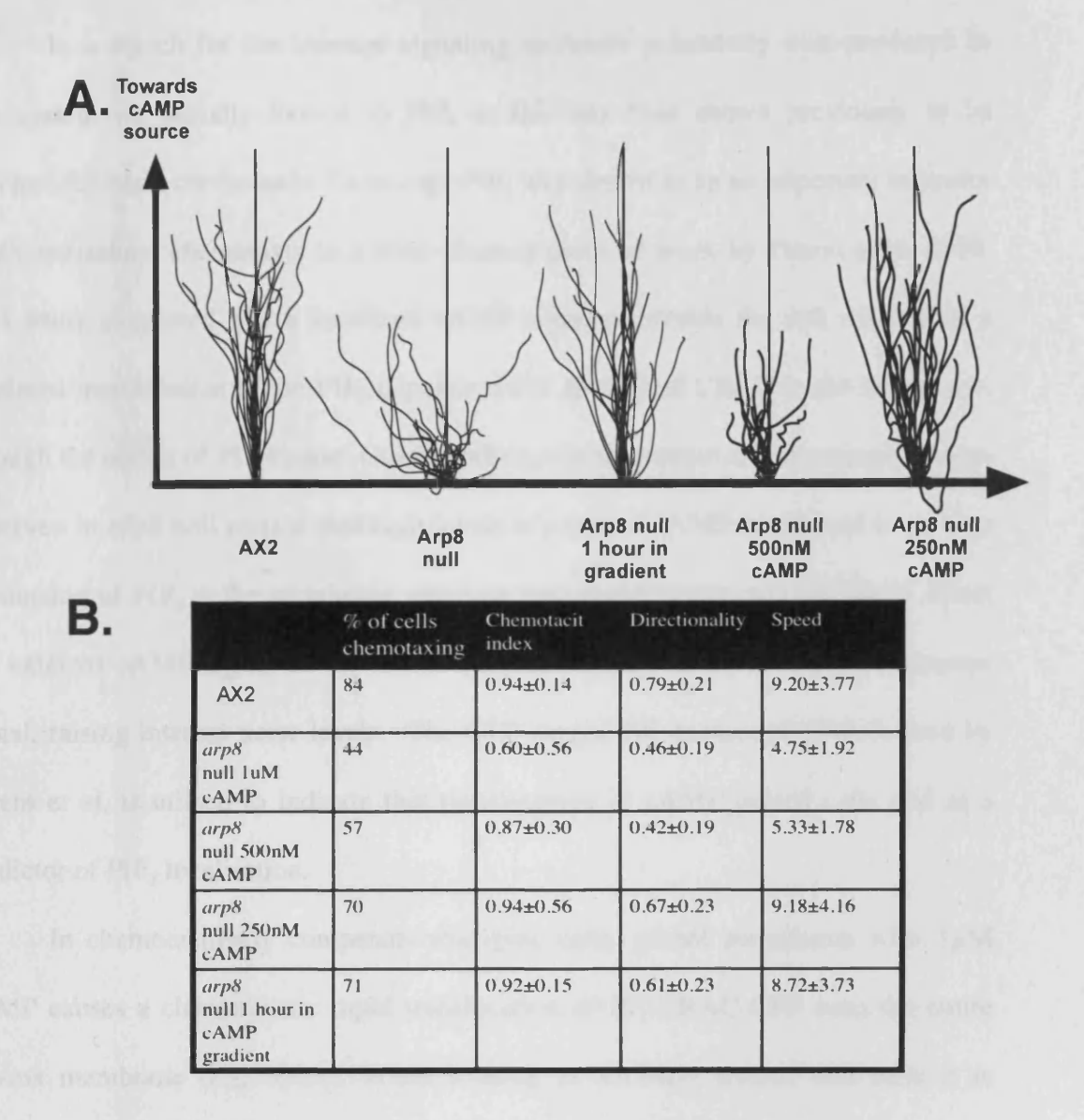


Fig. 4.1 arp8 nulls also show decreased chemotaxis.

**A.**) Traces taken from 3D-DIAS software that outline the movement of 20 randomly selected cells taken from a pool collected over 3 days. *arp8* nulls display decreased ability to chemotax which can be rescued by lowering the cAMP concentration at the sink, or by leaving the cells longer in the gradient. **B.**) The values for CI, directionality and speed as calculated by 3D-DIAS.

#### 4.2 Impaired chemotaxis could be due to a build up of PiP3 on the membrane

In a search for the internal signaling molecule potentially over-produced in this system we initially looked to PIP<sub>3</sub> as this has been shown previously to be required for early chemotaxis. To re-cap, PIP<sub>3</sub> was shown to be an important indicator of *Dictyostelium* chemotaxis in a field-shaping piece of work by Parent et al, 1998. This study suggested that a localized cAMP stimulus outside the cell resulted in a localized translocation of the PIP<sub>3</sub> dependent PH domain of CRAC to the membrane, through the action of PI3-kinase. Our hypothesis for the stalled chemotaxis phenotype observed in *arp8* null cells is that high levels of external cAMP could lead to an over production of PIP<sub>3</sub> at the membrane which in turn could lead to an inability to detect the external cAMP signal as the whole system has become flooded by the internal signal, raising internal noise levels. The GFP tagged PH domain of CRAC, used by Parent et al, is utilsed to indicate this translocation in cAMP pulsed cells and as a predictor of PIP<sub>3</sub> localisation.

In chemotactically competent wild-type cells, global stimulation with  $1\mu$ M cAMP causes a characteristic rapid translocation of PH-CRAC-GFP onto the entire plasma membrane (Fig. 4.2A). When looking at similarly treated null cells it is apparent immediately that there is a significant difference as PH-CRAC-GFP is already situated on the plasma membrane even before stimulation with cAMP. Once the cells have been stimulated no further translocation takes place. These data would be in agreement with the notion of too much PIP<sub>3</sub> on the membrane resulting in a loss of sensitivity to cAMP. These cells would appear to be sensing a cAMP gradient in all directions resulting in an increased signal to noise ratio and therefore it is unsurprising that they round up and do not move as a stimulus in all directions is as bad as no stimulus at all for directional chemotaxis.

To corroborate this evidence we also looked at the phosphorylation of a protein kinase B (PKB) homologue PkbA. PkbA only becomes active when it is phosphorylated at the membrane in a PI3 kinase dependent manner. This translocation to the membrane has previously been shown to be dependent on a PH domain which binds membrane associated PIP<sub>3</sub> [33]. In the wild-type cells the phosphorylated form of PkbA (p-PkbA) was seen to increase after 10s, peaked at 20s and then decreased over the remainder of the observed minute (Fig. 4.2B). The null cells exhibit a basal level of p-PkbA prior to stimulation with cAMP which then rises to peak much higher than the wild-type level after 20s and takes longer than the observed minute to diminish (Fig. 4.2B). These data also suggest that pulsing the cells with cAMP places the cells in a state whereby they have higher basal levels of PIP<sub>3</sub> at the membrane that then prevents them from properly sensing a steep gradient of cAMP and therefore from chemotaxing.

In summary an excess of PIP<sub>3</sub> on the membrane of *arp8* null cells may lead to an increase in noise in the internal signaling system which would result in cells being unable to respond to higher concentrations of cAMP as the receptors would become completely saturated all around the membrane much quicker due to the excess in the signal resulting in a higher signal to noise ratio through which the signal would not be detected.

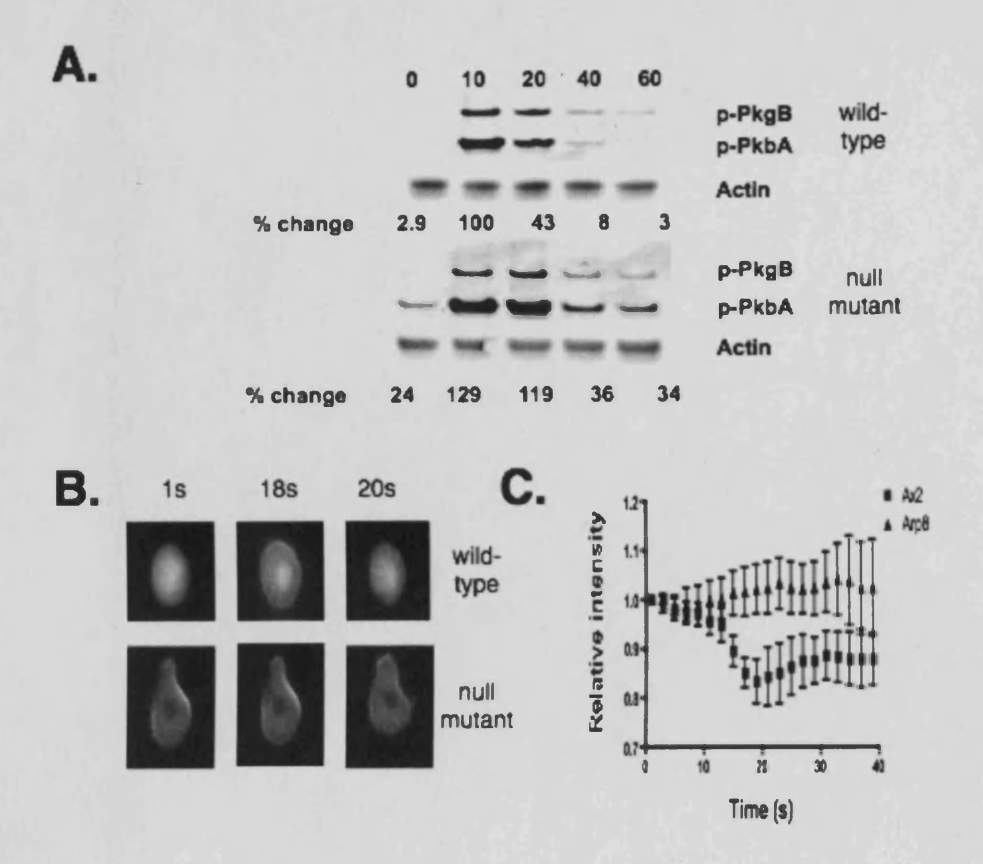


Fig. 4.2 arp8 null cells show an increased build up of PIP3 on the membrane.

**A.**) Western blot analysis of the phosphorylation of PKBA and PKBG in both wild-type and mutant cell lines following stimulation with 1uM cAMP. The percentage change was calculated by normalising all samples to the highest wild-type peak at 10s and taking this value as 100%. Actin was used as a loading control. **B.**) Translocation of the PIP3 specific marker; PH-CRAC-GFP to the plasma membrane following stimulation with 1uM cAMP. Images were taken at 60X magnification on a Olympus IX71 inverted microscope. **C.**) Graphical representation of the intensity of the translocation calculated by measuring the ratio between cytosolic and extra-cellular fluorescence over time.

### 4.3 Transcription of PiP3 regulating genes *ino1* and *impA1* is attenuated in *arp8* null cells.

The genes *impa1* and *ino1* are involved in the bio-synthesis of inositol phosphates within the cell. *ino1* encodes the gene myo-inositol synthase, involved in de-novo inositol monophosphate synthesis, whereas *impA1* encodes inositol monophosphate a gene involved in the recycling of inositol phosphates by hydrolising inositol monphosphate to free inositol. *ino1* expression has been shown to be affected by the knock out of *arp8* in yeast [77] and *impa1* has been implicated in the regulation of PIP<sub>3</sub> signaling as it regulates the levels of free inositol. If the expression of either of these genes were to be regulated by Arp8 in *Dictyostelium* then this could lead to a change in PIP<sub>3</sub> signaling though an increase in synthesized PIP<sub>2</sub> levels.

Looking at the expression of both of these genes by qRT-PCR, we observe an increase in expression in cells undergoing vegetative growth. This increase is maintained over the first half of development with there being approximately a 20% increase consistently throughout the first 12 hours (Fig. 4.3A). These data suggest that the INO80 complex and Arp8 are involved in repression of these inositol biosynthetic genes and in keeping the levels of PIP<sub>2</sub> production low during early aggregation. The over-production of these genes, in the case of the null cells, results in a higher level of de novo synthesis of inositol with an ensuing increase in PIP<sub>2</sub> levels leading to higher levels of PIP<sub>3</sub> produced by the PI3 kinases.

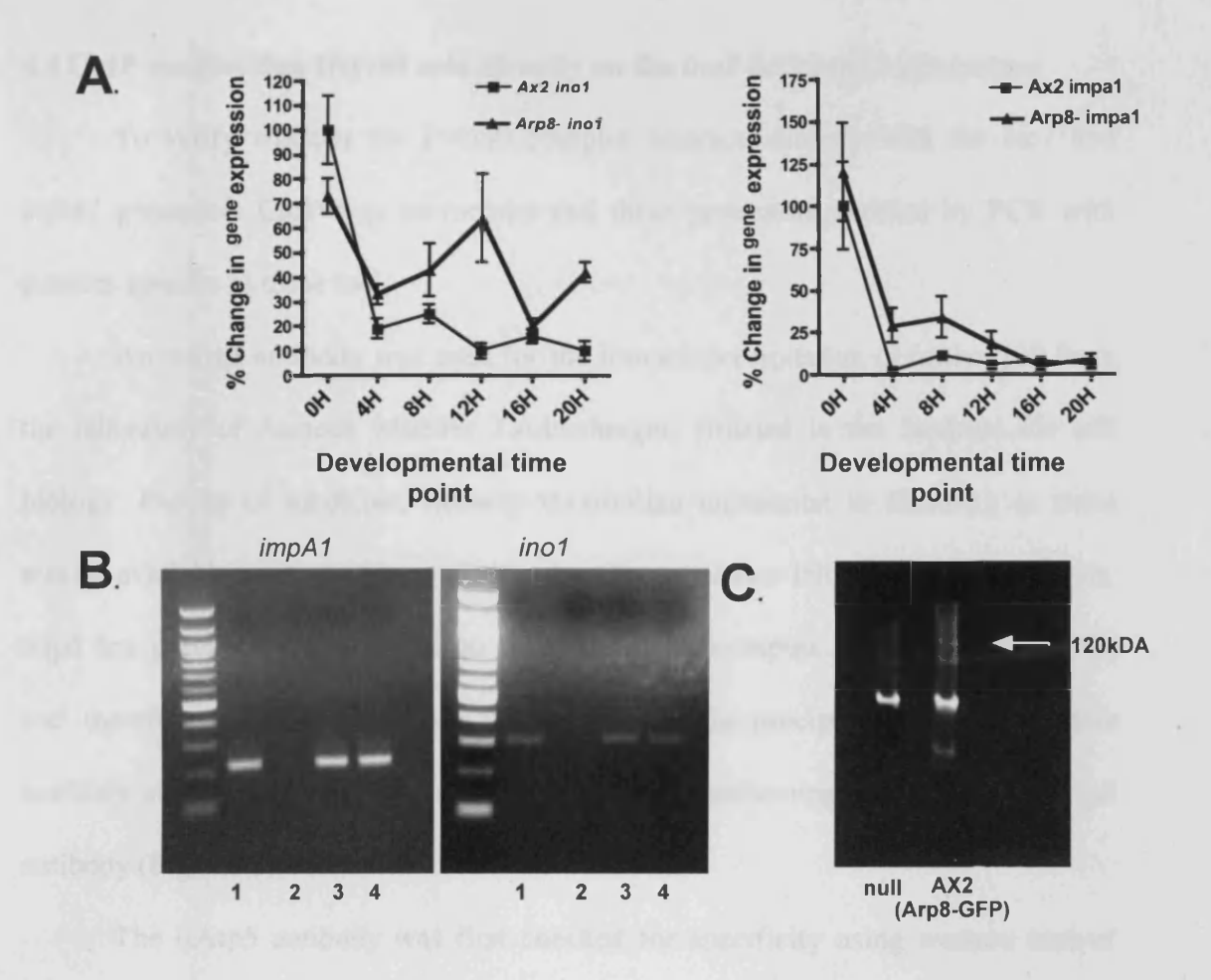


**Fig. 4.3 Inositol biosynthetic genes are directly regulated by the INO80 complex A.)** Analysis of the mRNA levels present in wild type or *arp8* null cells by QRT-PCR.

All expression is normalized to AX2 0H which is given a 100% expression value.

Both genes analyzed show a similar expression pattern in wild-type cells, dropping off over the early stages of development. Null cell expression remains consistently higher than wild-type throughout development. **B.)** ChIP with the ARP5 antibody shows that the INO80 complex interacts directly with the *ino1* and *impA1* promotors.

1- anti Arp5, 2 - just beads, 3 - anti RNApolII 4 - Genomic DNA control. **C.)** Western blot of Arp8-GFP expressing wild type and *arp8* null extracts Immuno-precipitated with the ARP5 antibody and probed with a GFP antibody. An approximately 120kDa band indicates that Arp8-GFP co-IP's with Arp5

### 4.4 ChIP verifies that INO80 acts directly on the ino1 and impA1 promotors

To verify whether the INO80 complex interacts directly with the *ino1* and *impA1* promotors ChIP was performed and these promotors verified by PCR with primers specific to these loci.

An  $\alpha$ Arp5 antibody was used for the immunoprecipitation (a further gift from the laboratory of Annette Mueller Taubenberger, situated in the Institute for cell biology, Faculty of medicine, Ludwig-Maximilian universitat in Munich), as there was no available antibody to any of the other *Dictyostelium* INO80 complex subunits. Arp5 has previously been shown to be essential for complex function in yeast [77] and therefore an assumption was made that immunoprecipitating (IP) with this antibody should also target the same promoters as performing the IP with an Arp8 antibody (Fig. 4.3C).

The αArp5 antibody was first checked for specificity using western blot of wild-type cells developed to 8H. 8H is the time of maximum expression of *arp8* (Chapter 3, Fig. 3.1) and also has been seen to be the point of maximum expression for INO80 in previous RNA-seq experiments (Dictyexpress). There are 3 bands picked up by the antibody (Fig. 4.3C). The 79 kDa band is Arp5 and the lowest band is extremely likely to be actin, with the final band possibly representing one of the other Actin related proteins. To control for the lack of specificity and that one of the other proteins observed may be binding the promoters of interest ChIP was also performed on chromatin isolated from *arp8* null cells. Any positive hits that occur in both samples should then be either resulting from one of the other proteins pulled down by the antibody or background from non-specific binding to the beads used.

Before continuing it was necessary to validate the above assumption that performing an IP with the Arp5 antibody will identify Arp8 bound proteins and DNA.

An IP of the GFP tagged Arp8 strain was performed at 8 hours into starvation, with the Arp5 antibody. This was subsequently then western blotted and probed with the GFP antibody to show that an IP with Arp5 will also immunoprecipitate Arp8. Two bands were seen on the blot, with the 98 kDa band being Arp8-GFP and the other lower band likely to be degradation product (Fig. 4.3C).

For these ChIP experiments chromatin was sonicated down to ~1000bp and analysis of the ChIP isolated DNA was by PCR using primers specific to 100-200bp regions of the genes *ino1* and *impA1* (sequences in chapter 2). Specific bands are observed for both *ino1* and *impa1* in the wild-type samples (Fig. 4.3B), but not in the null cells indicating a direct interaction between the INO80 complex and both of these promoters. These bands are lost in the null mutants indicating that Arp8 is essential for binding to these promoters. Control samples of RNApolII isolated DNA and genomic DNA confirm the bands are not due to primer dimers.

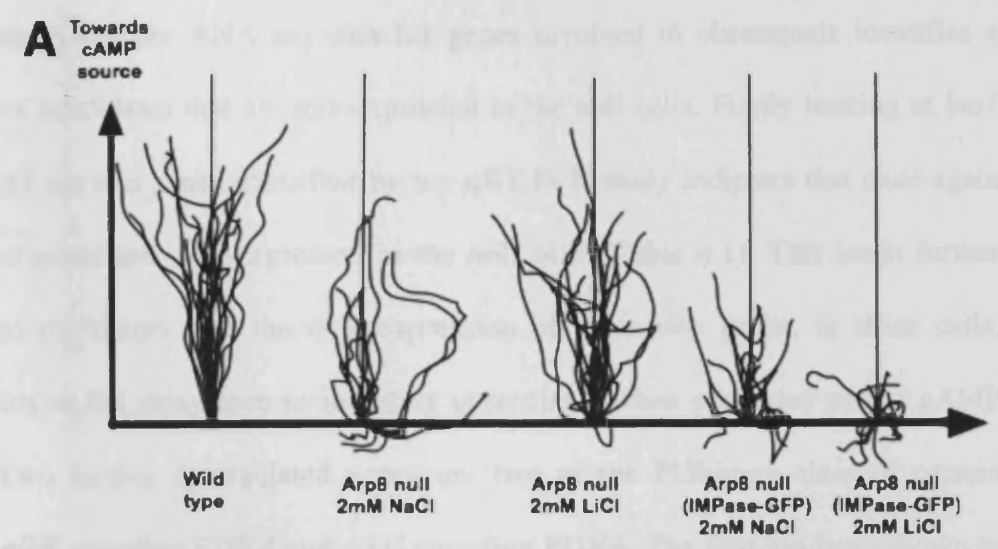
### 4.5 Treating null cells with Lithium improves chemotaxis

Lithium has been shown to have an inhibitory role on the enzyme IMPase [2]. It has been indicated as having a therapeutic role in the management of bipolar disorder in humans [3], with the inositol depletion hypothesis suggesting that this may modulate the levels of inositol in the brain [12]. Previous work investigating the effects of lithium treatment on *Dictyostelium* show that it produces an inhibitory affect on chemotaxis [1]. This is suggested to occur by reducing the pool of PIP<sub>2</sub> available for PIP<sub>3</sub> signaling. If the *arp8* null cell chemotactic phenotype that has been observed in this study were due to the increased expression of *impa1* and subsequent increase in PIP<sub>3</sub>, treatment with lithium should inhibit the enzymatic activity of IMPase resulting in the restoration of the cells chemotactic ability.

75% of cells treated with 2mM LiCl respond to the cAMP gradient compared to the 44% of cells that were untreated. These cells do this with an improved CI, directionality and speed (Fig. 4.4). These data indicate that treatment with low concentrations of LiCl will sufficiently inhibit IMPase enough that the PIP<sub>2</sub> levels decrease to a point where the cells' can detect the cAMP gradient. Higher concentrations of lithium begin to reduce the cells ability to chemotax again. This could be due to higher concentration affecting one of the other targets of lithium in the cell which can have an affect on chemotaxis, such as GSK3 [2].

To further test this theory a plasmid that over-expresses IMPase was transformed into the *arp8* null cells, using the electroporation method outlined in the materials and methods. These cells would be expected to produce sufficiently large amounts of IMPase to raise the levels of PIP<sub>3</sub> to an extent where lithium rescue will not be possible. Untreated *arp8*null (IMPase-GFP) cells have even worse chemotactic ability than null cells alone, with only 31% of cells sensing the gradient at all. When

with 2mM Lithium there is no effect on the cells and if anything they behave worse than the untreated cells. These data indicate that it is indeed likely to be an elevation of IMPase that results in the *arp8* null chemotactic phenotype. Having its effect through elevated PIP<sub>3</sub> signaling, resulting in an inability to sense the cAMP gradient.



	% of cells chemotaxing	Chemotactic index	Directionality	Speed
Wild-type	84	0.94±0.14	0.79±0.21	9.20±3.77
arp8 null 2mM NaCl	44	0.60±0.56	0.46±0.19	4.75±1.92
arp8 null 2mM LiCl	74	0.87±0.34	0.68±0.25	8.78=3.98
arp8 null (Impase-GFP) 2mM NaCl	31	0.67±0.54	0.39±0.17	4.84±1.72
arp8 null (IMPase-GFP)	29	0.57±0.77	0.27±0.09	3.34±0.89

Fig. 4.4 Treatment with Lithium also improves null cell chemotaxis.

**A.**) Traces taken from 3D-DIAS software that outline the movement of 20 randomly selected cells taken from a pool collected over 3 days. Treatment with low doses of LiCl, within therapeutic levels, leads to an improvement in chemotactic ability. Raising the internal levels of PIP2 through over-expression of IMPase works to counter the effects of LiCl and removes the ability to rescue the cells. **B.**) The values for CI, directionality and speed as calculated by 3D-DIAS.

### 4.6 Analysis of RNA-seq data reveals a number of genes affected that are involved in chemotaxis.

Inspecting the RNA-seq data for genes involved in chemotaxis identifies a number of candidates that are mis-expressed in the null cells. Firstly looking at inol and impA1 the two genes identified by my qRT-PCR study indicates that once again these two genes are over-expressed in the null cells (Table 4.1). This lends further weight to the theory that the over-expression of these two genes, in these cells, contributes to the delay seen in initiating chemotaxis when presented with a cAMP signal. Two further up-regulated genes are two of the PI3kinase class of protein kinases pikF encoding PI3K4 and pikH encoding PI3K6. The first has been shown to be one of the PI3kinases involved in phosphorylating PIP<sub>2</sub> to PIP<sub>3</sub> in response to cAMP stimulation. The second, PI3K6, is unlikely to be involved in chemotaxis as it has been shown to not localize to the cell cortex upon cAMP stimulation [127]. An over production of this PI3K may also lead to an increase in the unstimulated levels of PIP<sub>3</sub> at the membrane. Conversely to this, when looking for chemotaxis associated genes that have been down-regulated in the arp8 null cells it is seen that a further two of the PI3kinases have reduced expression compared to wild-type. Both pikB and pikD show a reduction in expression. This could be the cells making an attempt to internally regulate the over production of PIP<sub>3</sub> and reduce the levels.

pldA encodes a phospholipaseD which has been shown to be essential for actin relocalisation in both endocytosis and motility, as inhibition of this molecule reduces both. Also the production of PIP<sub>2</sub> by the PI(4,5)kinase has been shown to be regulated by the synthesis of the PLD product phosphatic acid (PtdOH). The reduction in expression of pldA could also contribute to both the chemotactic and developmental defects observed in the arp8 null cells.

The enzyme prolyl-oligopeptidase (PO) has previously been implicated in Dictyostelium chemotaxis by work from our lab [24], with PO being identified as a modulator of the sensitivity of cells to lithium treatment and a negative regulator of IP<sub>3</sub> synthesis. The gene encoding PO, dpoA, is seen to be downregulated in the null cells after 8 hours of starvation. This suggests a possible further attempt by the cells to reduce over-produced PIP<sub>3</sub> levels by limiting the amount of IP<sub>3</sub> entering the system and thereby reducing the amount of substrate for IMPase. Another gene that has reduced expression in the null cells after 8 hours is dd5P1, one of the 5'phosphatases also involved in the recycling of the inositol phosphates. A decrease in this enzyme would also be limiting in the cells ability to turn around the inositol phosphates and could result in a reduction of PIP<sub>2</sub> levels.

The RNA-seq data has provided more evidence to suggest that a number of genes are mis-expressed in the *arp8* null cells resulting in the over-production of the signaling molecule PIP<sub>3</sub> resulting in an increase in the noise in the system which has decreased the cells ability to sense the direction from which a cAMP signal has emanated.

Dictybase ID/gene name	Fold change up-regulated
ino l	54.21
impA1	14.97
pikF	7.36
pikH	6.247
	ino l impA1 pikF

Table 4.1 Genes up-regulated involved in chemotaxis

Several genes known to be involved in *Dictyostelium* chemotaxis are observed to be up-regulated in the *arp8* null cells, which could result in the over-production of PIP<sub>2</sub> and subsequently PIP<sub>3</sub> at the membrane, increasing noise in the system and reducing the cells ability to detect a cAMP signal.

Time point	Dictybase ID/gene name	Fold change down-regulated
8 hours	pldA	10.6
8 hours	dpoA	5.7
8 hours	dd5P1	2.7
8 hours	pikB	2.65
8 hours	pikD	2.3

Table 4.2 Genes down-regulated involved in chemotaxis

A number of genes previously shown to be involved in *Dictyostelium* chemotaxis are seen to be down-regulated in the *arp8* null cells. In two of the cases this could contribute to the over-production of PIP<sub>2</sub> and subsequently PIP<sub>3</sub> at the membrane. However the others may be an attempt by the cell to return these levels to normal and resume chemotaxis.

#### 4.7 Summary

- Chemotaxis is the process by which Dictyostelium aggregate under starvation conditions. The signaling molecule is cAMP.
- Onset of chemotaxis is delayed in arp8 null cells.
- This delay is rescued either by allowing time for the cAMP concentration to decrease, starting with a lower concentration of signal or treatment with lithium.
- These data go to show that Dictyostelium cells are able respond to a cAMP over a large order of magnitude. This adaptive response is controlled in part by the INO80 complex.
- The delay is caused by an over exaggerated response to cAMP resulting in the over-production of the signaling molecule PIP<sub>3</sub> at the membrane. This increases the noise in the system reducing the cells ability to detect the external signal.
- Treatment with lithium decreases this noise by inhibiting the enzyme IMPase and breaking the cycle of PIP<sub>2</sub> synthesis, therefore reducing PIP<sub>3</sub> signalling.
- RNA-seq data also indicates a number of other genes involved in the chemotactic process that are disrupted by the knock out of *arp8*.

### **Chapter 5:**

# The mutant LisG encodes a CHD ortholog involved in maintaining correct *Dictyostelium* development

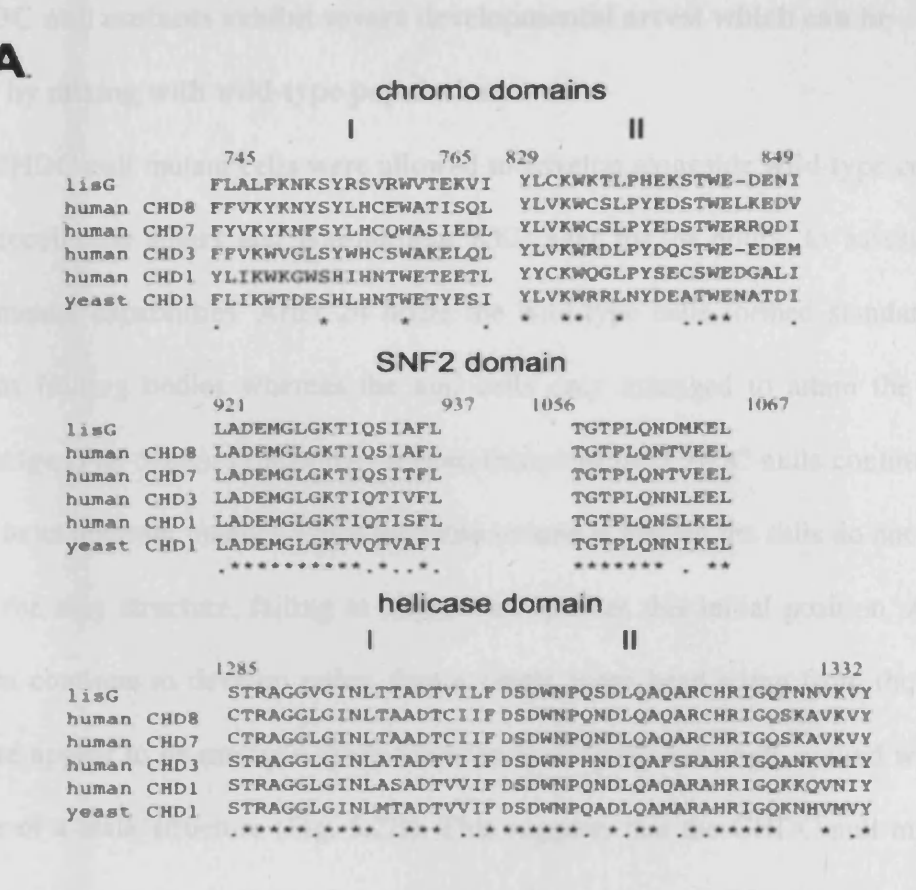
Summary: The mutant LisG was previously identified in a screen for lithium sensitivity. It was shown to encode a CHROMO helicase domain containing protein that we have designated CHDC. Null mutants of CHDC exhibit a severe developmental delay with full developmental arrest occurring at the loose mound stage. Expression of several genes; involved in the correct differentiation of both prestalk and pre-spore genes are down-regulated. The CHDC null cells also show a complete lack of ability to signal with cAMP throughout the population, which could lead to the deficiency in development. Next generation sequencing reveals a number of genes regulated by the CHDC re-modeler.

#### 5.1 Introduction to CHDC (LisG null)

Initial identification of the LisG REMI mutant came from a lithium sensitivity screen where it was characterized as being able to develop in the presence of 10mM LiCl. Inverse PCR was performed to obtain the entire open reading frame and Dictybase searches identified a gene of ~3000aa [Keim-Reder, PhD thesis. 2006], the dictybase ID being DDB\_G0293012. Initial Genbank searches identified a SNF2 like ATPase domain of the kind found in ATP dependent chromatin re-modelers with a 60-70% similarity between the characteristic helicase specific peptide sequences. The search also identified 2 CHROMO domains and a DNA binding domain, which classified the protein as a member of the CHD family of chromatin modifiers.

Following on from this research, further searches on the Dictybase database have identified 2 additional CHROMO domain containing proteins which we propose here to also be members of the CHD family. These can be found at Dictybase ID DDB\_G0284171 and DDB\_G0280705 Both of these protein sequences also contain double CHROMO domains, a SNF2 like ATPase domain and DNA binding domain (Fig. 5.1B). We have termed the CHD proteins CHDA through to C, with LisG being CHDC as it shares greatest homology to the third sub-group of higher organism CHD proteins particularly CHD7 and CHD8.

Whilst having a lithium resistant phenotype, earlier RT-PCR analysis of LisG gene expression indicated that there was still transcription of at least part of the gene in the REMI mutant and so further efforts were taken to knock out the whole message. A CHDC null mutant was created by a previous technician in the Harwood lab, Dave Proctor. Homologous recombination was used to insert a blasticidin resistance cassette into the gene, removing the majority of the functional domains. The clones were screened for blasticidin resistance, and the was insertion confirmed by PCR.



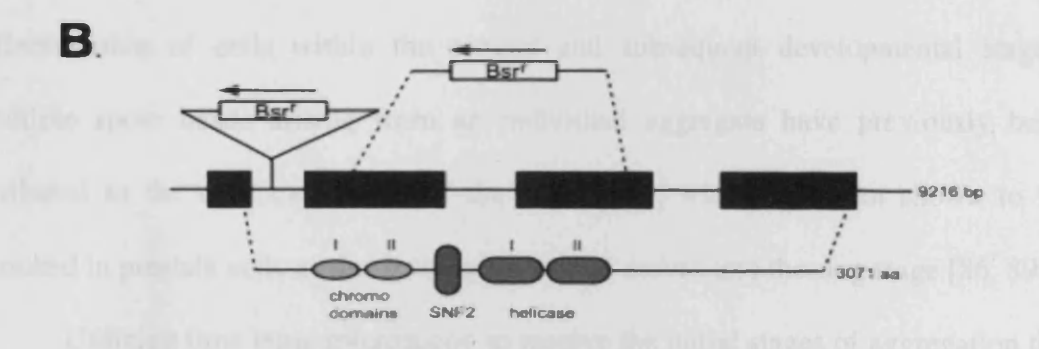


Fig. 5.1 LisG is a member of the CHD family of chromatin remodelers.

A.) An alignment of the CHROMO, SNF2 and helicase domians of LisG, several human CHDs and the yeast CHD1. All alignments were performed with the CLUSTLW algorithm B.) Diagram indicating the regions that have been affected in each of the mutant strains LisG REMI and CHDC null. The first Bsr resistance cassette belongs to the REMI mutant and the second indicates the insert in the CHDC null strain.

## 5.2 CHDC null mutants exhibit severe developmental arrest which can be rescued by mixing with wild-type populations.

CHDC null mutant cells were allowed to develop alongside wild-type cells on both nitrocellulose filters and non-nutrient KK2 agar for 24 hours, to assess their developmental capabilities. After 24 hours the wild-type cells formed standard full culminant fruiting bodies whereas the null cells only managed to attain the loose mound stage (Fig. 5.2A). Following on from this point the CHDC nulls continued to develop in an aberrant manner. Once the loose mound is formed the cells do not go on to form the slug structure, failing to migrate away from this initial position. As the structures continue to develop rather than a single spore head rising from the basal disk there appear to be multiple spore heads emanating from a single mound with no evidence of a stalk structure (Fig. 5.2B). This suggests that the CHDC null mutants are missing either an individual, or several, factors responsible for the correct differentiation of cells within the mound and subsequent developmental stages. Multiple spore heads arising from an individual aggregate have previously been attributed to the over expression of the *rasD* gene, which has been shown to be enriched in prestalk cells as the developing mound moves into the slug stage [86, 89].

Utilizing time lapse microscopy to resolve the initial stages of aggregation the cells do not stream but rather they tend to move around in a random pattern (supplementary movie; CHDCnull.avi), until they start to stick together to form rather clumpy aggregates (Fig. 5.2C). This is unlike the Arp8 null cells where there was a delay in the onset of fairly normal aggregation, producing normal looking fruiting bodies. This suggests a different cause behind these developmental defects observed in the CHDC nulls.

However, similarly to the *arp8* null cell line the CHDC null developmental defect can also be rescued by mixing the population with as little as 5% wild-type cells. This mixture of cell types then develops, forming a chimeric fruiting body. Varying ratios of wild-type to CHDC null cells were tried ranging from 90% down to 1%. It appears that 5% wild-type is the lower limit for the chimeras to take on any morphological resemblance of a normal wild-type culminant (Fig. 5.2D). At a 5% chimeric cell mix the fruiting bodies do take longer than wild-type alone to develop, needing over 35 hours plus to reach a fully developed fruiting body and do appear morphologically smaller than wild-type alone. The fact that they manage to form mature fruiting bodies with as little as 5% wild-type cells suggests that the cells are not simply sorting themselves into wild-type and mutant mounds and the wild-type develop as there are too few in the population for this to occur. As the number of wild-type cells in the population increases fewer of the morphological defects are seen and the fruiting bodies look distinctly more like the wild-type alone and the time for the cells to develop also decreases.

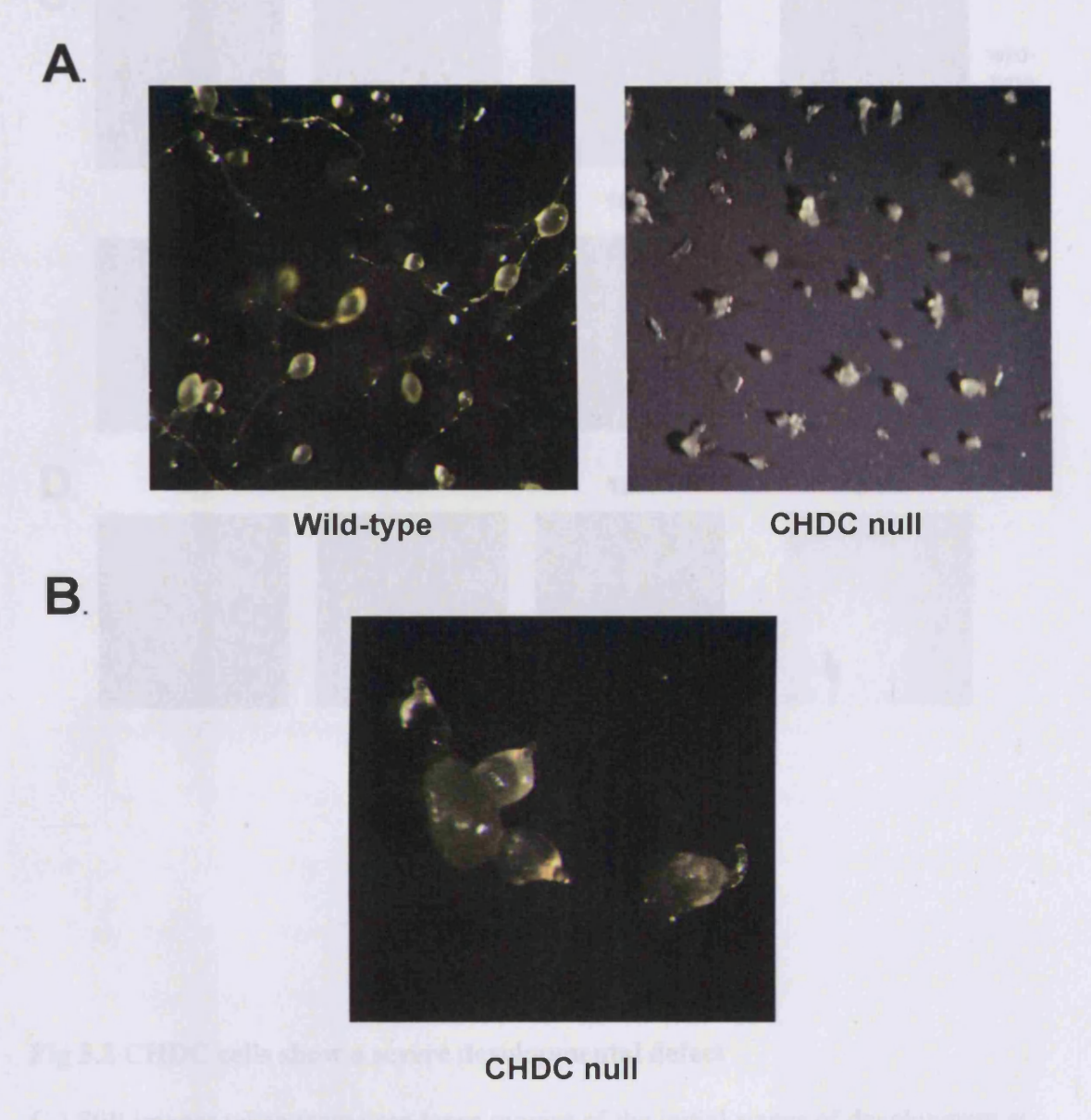


Fig. 5.2 CHDC cells show a severe developmental defect

**A.**) Wild-type and CHDC null cells were allowed to develop for 24 hours on nitrocellulose filters. Whilst the wild-type aggregates have reached full culmination, the null cells have arrested at the mound stage. **B.**) When allowed to develop beyond 24 hours the CHDC nulls start to develop aberrant spore heads, often with several emanating from a single mound.

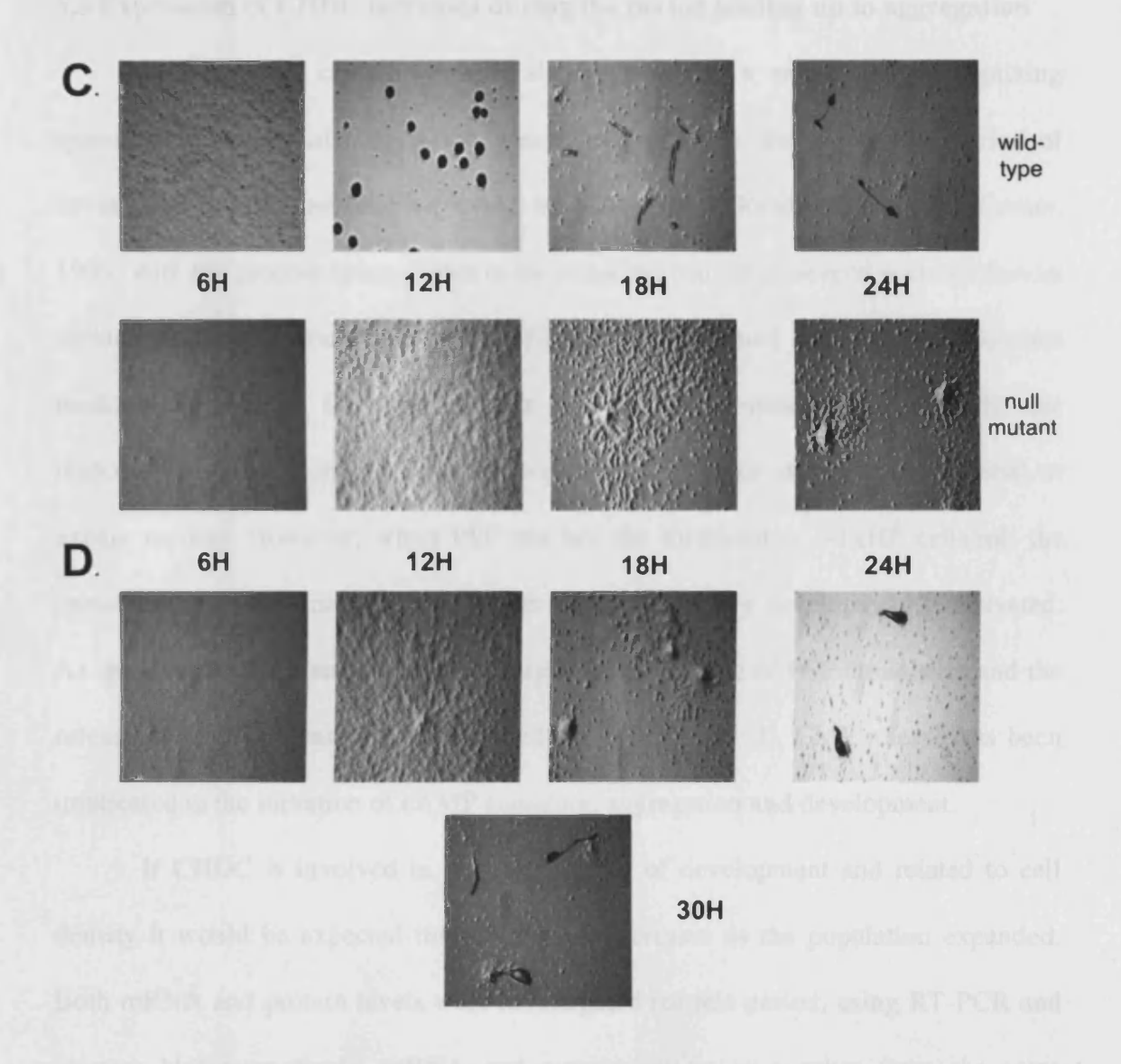


Fig 5.2 CHDC cells show a severe developmental defect

C.) Still images taken from time-lapse movies of the initial stages of development at 4X magnification. No aggregation streams are observed, with the cells seeming to move randomly, slowly aggregating to form loose mounds. D.) Chimeric developments arising from 10% wild-type mixed into the CHDC population.

#### 5.3 Expression of CHDC increases during the period leading up to aggregation

Dictyostelium cells have been shown to utilize a cell density recognizing system during the initial starvation period leading up to the aggregation period of development. This has been reviewed by Clarke and Gomer (Clarke and Gomer, 1995) with the process being shown to be under the control of several secreted factors including the pre-starvation factor (PSF) and as mentioned earlier the conditioned media factor (CMF). During vegetative growth cells continuously secrete PSF the response to which is inhibited by the presence of a source of nutrients (bacterial or axenic media). However, when PSF reaches the threshold of ~1x10<sup>6</sup> cells/ml; the transcriptional initiation of several genes required for early development is activated. As the bacterial food supply becomes depleted, the release of PSF diminishes and the release of CMF increases. As mentioned earlier (Chapter 3), CMF release has been implicated in the initiation of cAMP signaling, aggregation and development.

If CHDC is involved in the early stages of development and related to cell density it would be expected that expression increases as the population expanded. Both mRNA and protein levels were investigated for this period, using RT-PCR and western blot respectively. mRNA and protein extract were taken from the same cultures prepared from axenically growing wild-type cells of increasing cell density, ranging from  $5 \times 10^5$  to  $5 \times 10^6$ . A 150% increase in mRNA expression is seen between  $5 \times 10^5$  and  $1 \times 10^6$  cells/ml (Fig. 5.3A) which stabilizes from this point onwards. Probing protein extracts with an anti-CHDC antibody also sees a similar increase in induction during the same time-period (Fig. 5.3B). These data suggest that CHDC induction is coincidental with the initiation of starvation induced development, in response to an increased population and decreased food source.

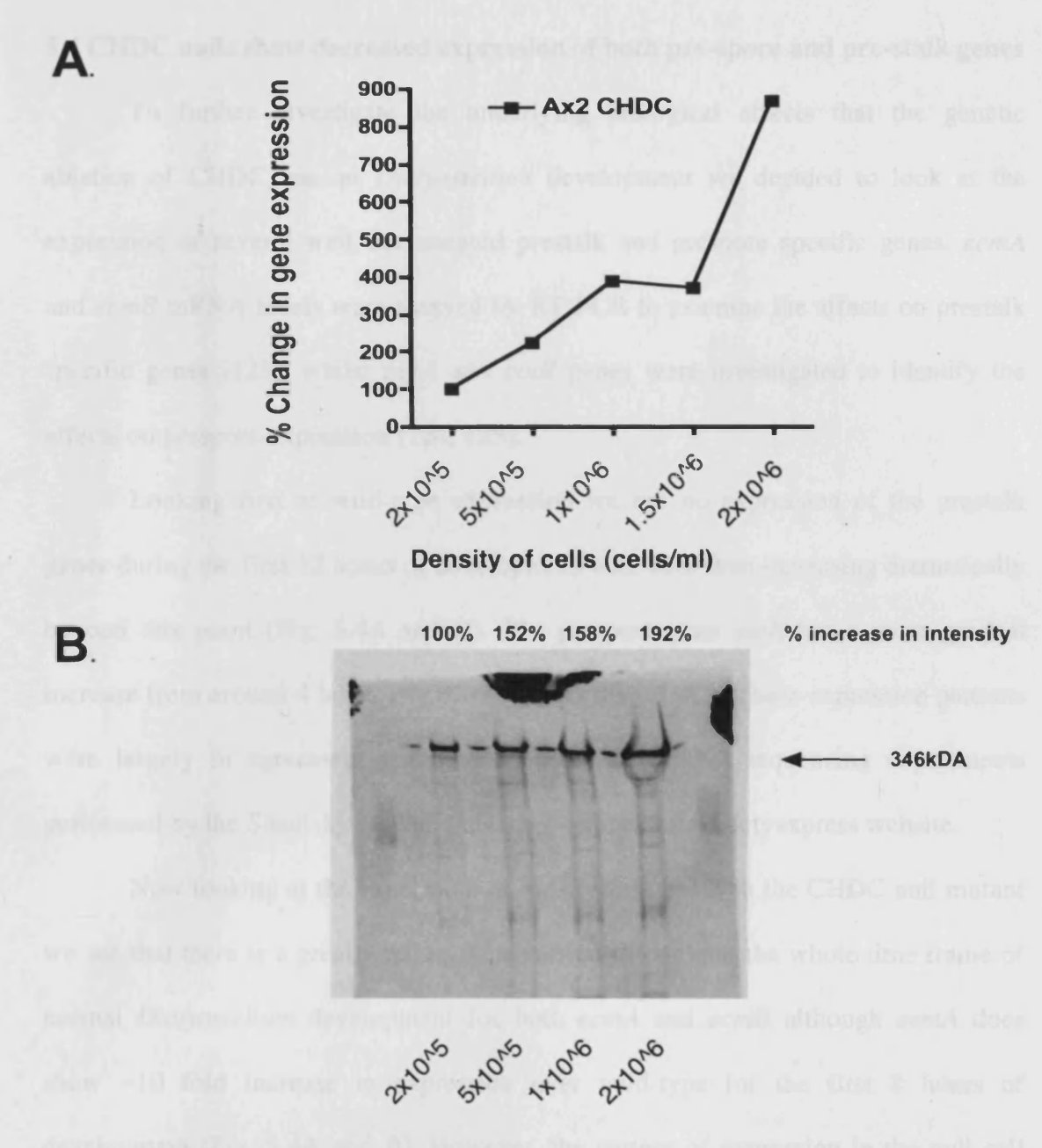


Fig. 5.3 CHDC expression increases with cell density.

A.) qRT-PCR data indicating the increase in CHDC mRNA as cell density increases.

**B.**) Expression of CHDC protein also increases with cell density. Intensity values were calculated using imagej and normalised against the background on the gel. The top band of 346kDA is CHDC the lower bands represent protein degradation, whereas the smaller bands between wells are spill over due to the large volume needed to be loaded.

#### 5.4 CHDC nulls show decreased expression of both pre-spore and pre-stalk genes

To further investigate the underlying biological affects that the genetic ablation of CHDC has on *Dictyostelium* development we decided to look at the expression of several well documented prestalk and prespore specific genes. *ecmA* and *ecmB* mRNA levels were assayed by RT-PCR to examine the affects on prestalk specific genes [123], whilst *pspA* and *cotB* genes were investigated to identify the affects on prespore expression [124, 125].

Looking first at wild-type expression we see no expression of the prestalk genes during the first 12 hours of development with both then increasing dramatically beyond this point (Fig. 5.4A and B). The prespore gene *cotB* has a more gradual increase from around 4 hours into development (Fig. 5.4C). These expression patterns were largely in agreement with those observed in RNA-sequencing experiments performed by the Shaulsky lab and published online at the Dictyexpress website.

Now looking at the expression of the prestalk genes in the CHDC null mutant we see that there is a greatly reduced expression throughout the whole time frame of normal Dictyostelium development for both ecmA and ecmB although ecmA does show ~10 fold increase in expression over wild-type for the first 8 hours of development (Fig. 5.4A and B). However, the pattern of expression in the null cell line follows that of the wild-type cells, yet on a scale several orders of magnitude less, ranging from ~5 fold to ~25 fold less. Similarly, the expression patterns of the prespore genes pspA and cotB are both similarly decreased, once again also following similar developmental expression pattern (Fig. 5.4C). Judging from these data it can be decided that CHDC plays an important role in the regulation of both prespore and prestalk genes during normal Dictyostelium development in wild-type cells, whether this role is direct or not can not be elucidated from this experiment.

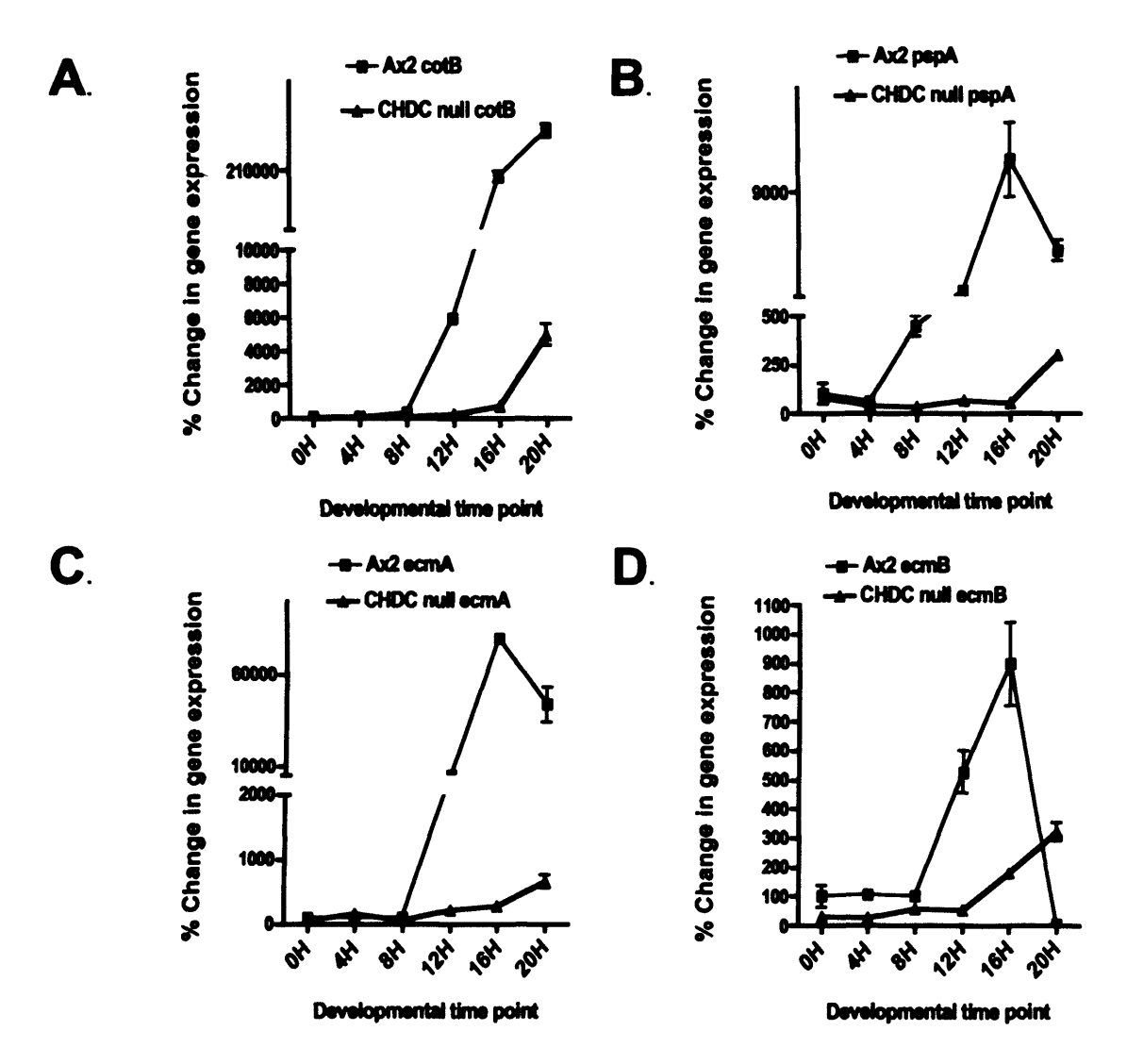


Fig. 5.4 Expression profiles of genes marking pre-stalk and pre-spore cells

Analysis of the mRNA levels present in wild type or *chdC* null cells by QRT-PCR.

All expression is normalized to AX2 0H which is given a 100% expression value. All genes analyzed show a similar expression pattern with there being a large decrease in transcription in both pre-spore and pre-stalk genes.

#### 5.5 CHDC null cells show a deficiency in cAMP signaling during aggregation

The dark-field time lapse microscopy technique was utilised once again to visualize the cAMP signaling throughout the population of cells. To recap, as the cells move through the population towards the cAMP source they change morphology which creates a change in the light reflective pattern visible through the microscope appearing as spiral waves and concentric circles of movement through the population. The CHDC null cells do not appear to produce any manner of consistent cAMP movement patterns through the population. There do appear to be random bursts that appear sporadically and do serve to partially direct the cells towards an aggregation center (Fig. 5.5). Once the cells have managed to aggregate into a loose mound there do appear to be intense pulses of cAMP throughout the structure. However, this does not appear to be satisfactory to progress beyond this structure.

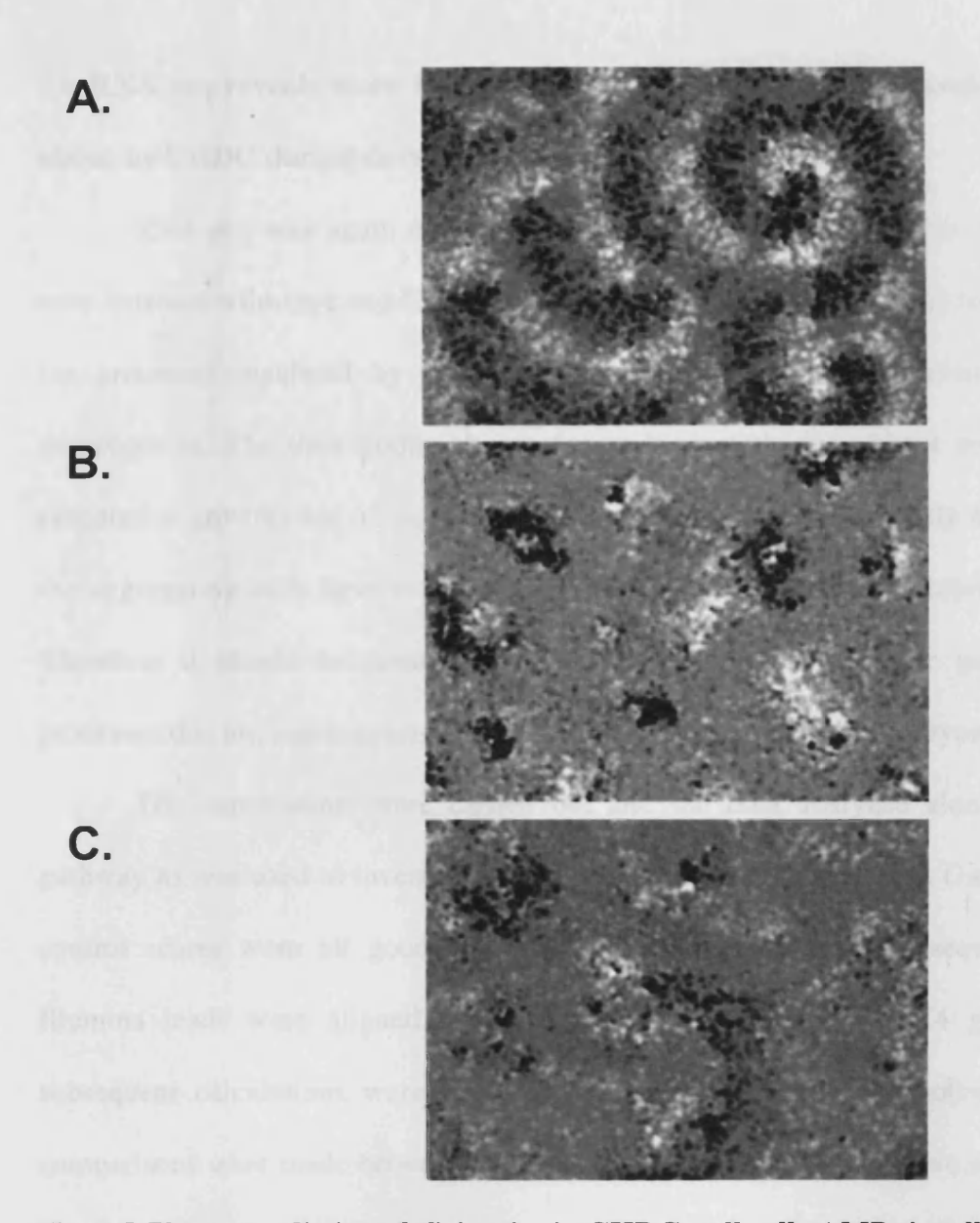


Fig. 5.5 There are distinct deficiencies in CHDC null cell cAMP signalling.

Single frame still images extracted from supplementary movies ax2cAMPpulse.avi, CHDCcAMPpulse.avi, and 10%mixCHDCcAMPpulse.avi A.) Wild-type cells show the characteristic spiral pattern of cAMP pulses moving through the population. These pulses initiate after approx 4H. B.) *chdC* null cells do not show this any characteristic pulsing patterns once signaling has initiated. Signaling appears to be constrained within the confines of the lose mound and not beyond. C.) When the population of null cells is mixed with as little as 10% wild-type cells then some cAMP signaling does return. An arm of a spiral is visible in the center of the image

## 5.6 RNA-seq reveals more insight into the changes in gene expression brought about by CHDC during development

RNA-seq was again employed to assess the global changes in transcription seen between wild-type and CHDC null cells. This will give a better understanding of the processes regulated by this chromatin re-modeler during starvation induced development. The time points chosen for analysis with this mutant were 0 hours (vegetative growth) and 12 hours into development as this was roughly the time that the aggregating cells have reached the loose mound stage and development arrests. Therefore it should be possible to elucidate at least some of the genes and or processes that are mis-expressed and involved in producing this phenotype.

The experiments were carried out and the data analyzed along the same pathway as was used to investigate the *arp8* null mutant in chapter 3. Galaxy quality control scores were all good and indicated no need to trim the sequences. The Illumina reads were aligned to the *Dictyostelium discoideum* AX4 genome and subsequent calculations were all carried out using the Arraystar software. Direct comparisons were made between AX2 and *chdC* null at both vegetative stage and 12 hours into development to give the most complete view of the changes in expression between the mutant and wild-type. For each time point the data was normalized to the base level of 6 read counts, through the Arraystars inbuilt filters. This base level was previously decided to be the level for un-expressed genes (see chapter 2). To ensure that we are looking at real changes in gene expression a base limit of 2-fold change in gene expression was taken either up or down. Changes below this were discarded through Arraystars filtering system. When addressing the total numbers of genes affected, it is observed that there are many less affected by the knock out of *chdC* during vegetative growth than later on in development (Fig. 5.6 plus Table 5.1).

Looking through the data for notable genes that are up-regulated in *chdC* null at 0H identifies a small number which may be at least in part responsible, or involved in, the developmental arrest phenotype observed.

gmsA encodes the gamete and mating specific protein. This is one of several proteins involved in sexual cell fusion and the recognition of different mating types. Knock outs of gmsA have been shown to be incapable of undergoing sexual development [128]. Expression of this gene could be increased to encourage sexual development in these cells as they cannot develop normally. This is could occur if this re-modeler worked to inhibit the expression of sexual development genes but is more likely an indirect affect of knocking out chdc.

Conversely to what is seen with the *arp8* null, the gene *dscA*, encoding discoidin, is seen to be up-regulated. Discoidin is expressed during early development and is involved in the initiation of the starvation response [113]. This would make you expect the cells to enter development early if anything yet they develop along a normal time frame to wild-type cells during the aggregation phase, suggests that this process is not under the control of discoidin alone.

3B-1 (and 3B-2) is a prespore specific gene, once again normally expressed later in development [120]. Expression of this gene was also seen to be higher in the arp8 null cells where it was in opposition to the general pattern of developmental gene expression.

Looking for genes that are down-regulated in the *chdC* null during vegetative growth yields some extremely interesting results. One of the genes with the largest difference in expression between wild-type and mutant cells is *yelA*. This gene encodes an elongation initiation factor; eIF-4, involved in the regulation of terminal differentiation. Knocking out this gene has been shown to give a phenotype almost

identical to that of the arrested development phenotype of the chdC null mutant. This is that they produce loose yellow colored mounds, where development arrests and they also have been shown to produce aberrant cAMP wave patterns [129]. It is highly likely that the developmental phenotype observed in the null cells is directly due to the down-regulation of this elongation initiation factor. However, there may also be other factors involved in producing this phenotype and also other affects of the knock out of chdC on the cells that are less strikingly apparent.

A number of factors associated with the countin complex were also seen to be down-regulated in these cells. The countin complex is involved in sensing and regulating the size of aggregates. cf60, cf45, cfaA and cfaB are all decreased in expression suggesting these cells may have a decreased ability to create normal sized aggregations and therefore produce incorrect mound sizes [115]. This does in fact occur with chdC null mounds appearing highly varied in size.

Similarly to the *arp8* null cells *gdt1* is again seen to be down-regulated in the *chdC* null strain. The growth development transition factor 1 expression is down three fold in these mutants. This protein is responsible for regulating the entry into the developmental cycle and is seen to directly repress the function of discoidin [118].

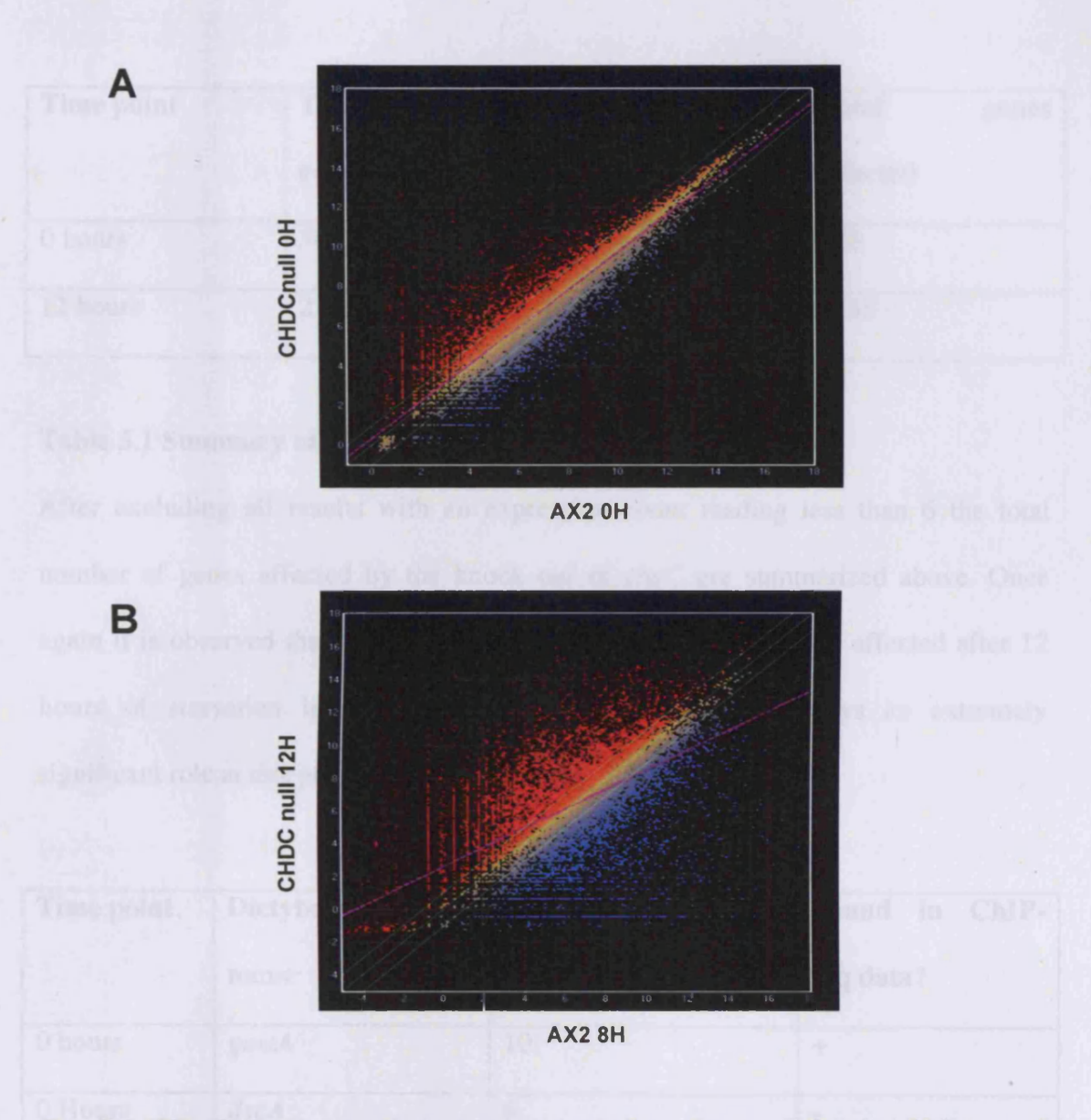


Fig. 5.6 CHDC knock out affects a greater number of genes following 12 hours of starvation.

Scatter plots indicating the fold change in gene expression comparing A.) Wild-type and null cells during vegetative growth and B.) wild-type and null cells after 12 hours of starvation. Points above the line represent an increase in expression, those below exhibit a decrease. A much larger number of genes, both up and down regulated, is seen on the 12 hour plot, suggesting that the CHDC re-modeler plays a more significant role through development

Time point	Total genes down-	Total genes up-	Total genes
	regulated	regulated	affected
0 hours	562	264	826
12 hours	2140	995	3135

Table 5.1 Summary of genes affected by chdC knock out.

After excluding all results with an expression count reading less than 6 the total number of genes affected by the knock out of *chdC* are summarized above. Once again it is observed that there are nearly four times as many genes affected after 12 hours of starvation indicating that the CHDC re-modeler plays an extremely significant role at this point of development.

Time point	Dictybase ID/gene	Fold change up-	Found in ChIP-
	name	regulated	seq data?
0 hours	gmsA	10	+
0 Hours	dscA	6	-
0 Hours	3B-1 (and 3B-2)	5	+

Table 5.2 Genes up-regulated during vegetative growth.

A small subset of the genes up-regulated in the *chdC* null cells compared to wild-type during vegetative growth. These genes are all possible candidates for contributing early to the arrested development phenotype observed.

Time point	Dictybase ID/gene	Fold change down-	Found in ChIP-seq
	name	regulated	data?
0 hours	yelA	8	+
0 hours	cf60	4	+
0 hours	cf45	4	+
0 hours	cfaA	3	+
0 hours	cfaB	3	+
0 hours	gdt1	3	+

Table 5.3 Genes down-regulated during vegetative growth.

A small number of the genes that are seen to be down-regulated in the *chdC* null cells compared to wild-type during vegetative growth. All of these genes could be potentially responsible for contributing to the arrested development phenotype observed in the null cells.

## 5.7 RNA-seq data reveals the genes which are affected by CHDC at the loose mound stage during *Dictyostelium* development.

Similarly to the *arp8* null mutant there are a much larger number of genes affected by knocking out *chdC* later in development. 12 hours after starvation both wild-type and the mutant have reached a loose mound stage and this is where development arrests for the null cells. Looking at the total number of gene affected by the knock out nearly four times as many genes are mis-expressed, being either up- or down-regulated in the null cells at 12 hours compared to those affected during vegetative growth.

The gene encoding the eIF-4 initiation factor is still seen to be down-regulated by 8 fold suggesting that this decrease in expression is consistent through development. As the change in expression of this gene is identified as a likely candidate for causing the developmental arrest and disrupted cAMP signaling patterns, this lends further weight to this hypothesis.

There are also a large number of down-regulated genes involved in the differentiation of pre-spore and pre-stalk cells which is unsurprising as these cells arrest at the mound stage and do not ever manage to form the spore or stalk structures. These include the genes identified as being down-regulated by qRT-PCR: ecmA, ecmB, pspA and cotB. Further genes found in these families are also see to be down-regulated, including; cotC, cotA, cotD, pspB and pspD (Table 3). The fourth cAMP receptor to be developmentally expresses; CAR4 is encoded by the gene carD [42]. This particular receptor is involved in the final stages of culmination. In these null mutant cells the expression is seen to be decreased at the time of developmental arrest. Conversely to what was seen in vegetative chdC null cells the pre-spore specific genes 3B1 and 3B2 are down-regulated. These genes have been seen to

increase in expression through development in wild-type cells, yet in these mutants have the opposite expression pattern [120]. All of these genes being down-regulated could be due to a direct affect of knocking out *chdC* but also may result from an indirect knock on effect occurring when the direct targets are down-regulated.

One gene group which may affect the transcription of these genes is the pre spore initiation factor (PSI) family. Several of these genes are down-regulated in the null cells including; psiC, psiR and psiJ. These genes are seen to have maximal expression at the loose mound stage in wild-type cells. They have been reported to control the differentiation of both pre-spore and pre-stalk cells [122].

Another entire gene family that is down-regulated in these cells is the structural maintenance of chromosome family. This family of proteins is involved in the maintenance and dynamic restructuring of chromosomal conformation during the cell cycle. They have been identified as playing roles in sister chromatid cohesion, chromosome condensation, DNA recombination and repair, and gene dosage compensation, reviewed in [130]. They play a major role in both mitotic and meiotic cell division and mis-expression are thought to be involved in a number of human diseases. The decrease in expression of these genes may be a direct effect of the knock out of chdC, however it is also likely that this may a secondary effect of the developmental arrest whereby cell division is no longer required and so machinery involved in this process down-regulates. Further evidence supporting this theory comes from the observation that the gene encoding the proliferating cell nuclear antigen (PCNA); pcna is also transcriptionally reduced at this developmental timepoint. PCNA is responsible for clamping the DNA polymerase complex to the DNA allowing for efficient transcription. Nuclear DNA synthesis has previously been shown to occur during later developmental stages, using a GFP fused PCNA protein

with cells undergoing DNA synthesis in the final stages decreasing to less than 1% [131]. A decrease in pcna expression at 12 hours in the chdC null cells along with the decrease in the smc1-6 gene family indicates that DNA synthesis has been reduced and is in concordance with the idea that these cells have preparing to enter the sporulation stage early, missing out the developmental stages between there and the mound stage.

Whilst there are half as many genes up-regulated as down, there are a large number which play a role in development. Similarly to the *arp8* null mutant a number of the genes involved in the production of ribosomes exhibit increased transcriptional activation over the wild-type.

Interestingly one of the genes with the highest level of increased expression over wild-type is gdcA a GP64 and disintegrin like protein, which in other species falls within the category of the ADAM proteins (A Disintegrin And Melloproteinase). These are a family of secreted and transmembrane proteins that play a significant role in regulating cell migration, adhesion, signaling and proteolysis through their function of "shedding" cell surface molecules [132]. GP64 has been identified in Polysphondilium pallidum where it was shown to be a cell surface receptor that was maximally expressed during vegetative growth this then decreases during development [133]. It is possible that, in vegetative wild-type Dictyostelium, this protein is regulating the production of development specific cell surface proteins. Once development is entered its expression decreases allowing for the correct expression of cell surface receptors and subsequent chemotaxis and adhesion. In the chdC null cells if this protein were up-regulated these cell surface proteins would still be being "shed" and would lead to incorrect development.

Contrary to what is seen during vegetative growth, where proteins associated with the counting factor (CF) complex are down-regulated, the gene *ctnA*, encoding Countin, is over-expressed 12 hours into development. The CF complex in this case could be having a similar effect to treating the cells with recombinant or semi-purified countin where motility is increased but cell-cell adhesion is decreased [134].

Looking through the list of genes mis-expressed in the *chdC* null there are a large number of candidates for those responsible for producing the arrested development phenotype. It is unlikely to be one of these genes in particular that is creating this effect but more a number of them working in concert. Also, it is possible that a large number of them are not directly affected but are an artifact caused through the direct mis-expression of other genes. To address this problem and to identify which genes are directly bound by the CHDC enzyme a ChIP-sequencing experiment was designed.

Time point	Dictybase ID/gene	Fold change down-	Found in ChIP-seq
	name	regulated	data?
12 hours	psiC	25397	+
12 hours	cotC	11736	+
12 hours	cotA	3324	+
12 hours	pspB	2414	+
12 hours	pspD	2348	-
12 hours	cotD	1365	+
12 hours	cotB	1211	+
12 hours	ecmA	673	+
12 hours	psiR	574	+
12 hours	psiJ	258	+
12 hours	ecmB	72	+
12 hours	carD	32	+
12 hours	3B-1 (3B-2)	13	+
12 hours	yelA	8	+
12 hours	smc1	5	+
12 hours	smc2	4	+
12 hours	smc3	7	+
12 hours	smc4	7	+
12 hours	smc5	3	+
12 hours	smc6	3	+
12 hours	pcna	5	+

Table 5.4 development associated genes down-regulated 12 hours into starvation.

Time point	Dictybase ID/gene	Fold change up-	Found in ChIP-seq
	name	regulated	data?
12 hours	rps24	45	-
12 hours	rpl15	38	+
12 hours	rps2	30	+
12 hours	rps17	29	-
12 hours	rpl11	28	-
12 hours	rpl4	28	-
12 hours	rps15	25	+
12 hours	rps7	25	+
12 hours	rpl3	25	-
12 hours	rpl38	21	-
12 hours	gdcA	246	+
12 hours	ctnA	41	+
12 hours	nap l	30	-

Table 5.5 development associated genes up-regulated 12 hours into starvation

### 5.8 ChIP-seq data reveals the pattern of re-modeler binding throughout development.

A ChIP-sequencing investigation was designed to assess the binding of the CHDC re-modeler throughout the first 12 hours of starvation induced development. This would hopefully provide some insight as to the direct interactions of this complex across the genome and development. ChIP experiments were performed as described in Chapter 2 using the anti-CHDC antibody raised against the N-terminal region of the CHDC protein. As this antibody was not seen to bind completely cleanly to CHDC (Fig. 5.3), with a number of other bands sometimes being observed on western blots, the ChIP experiments were also performed on the chdC null mutants for each time point to provide a suitable negative control. We finally ended up sequencing 9 samples: wild-type 0, 4, 8 and 12 hours, plus chdC null 0, 4, 8, and 12 hours and also a no IP input sample. Once ChIP DNA was prepared it was assayed for specificity using PCR with primers designed towards the inol gene. Finally samples were adaptor ligated using the Illumina ChIP-seq adaptor ligation kit following the standard protocol, with minor modifications described in Chapter 2. The samples were sequenced using an Illumina Genome analyser II sequencer, courtesy of Dr. Alan Kimmel at the NIH, the data was output using the 1.6.47.1 pipeline.

Data analysis was performed using the CLC genomics workbench software provided by CLCbio. First the reads are imported into the software, along with the *Dictyostelium discoideum* AX4 reference genome and the reads are then mapped onto this reference genome, once again allowing for up to 3 mismatches during this process. Once aligned the sequence was run through CLC genomics work bench peak finder to identify regions of sequence enrichment and therefore regions where the CHDC re-modeler is likely to be bound. This process incorporates the ability to

supply a negative control method to account for any background reading and for this the alignments for the *chdC null* runs were used. The software produced a list of genes for each of the developmental time points and these were then exported and examined using Microsoft Excel.

Once the gene lists were created for each time point it became apparent that there were a very similar number of genes bound across development, all being in the region of 8000 and varying by less than ~500 genes. This made me think of the possibility that the re-modeling factor stays persistently bound to the same genes and that expression is modulated by other factors binding or modifying the enzyme. To assess this possibility the VLOOKUP function of Excel was utilised. This process simply compares data in one cell to lists found in others, looking to see if that data occurs again within the set. Using this system it is shown that 5743 (approx 75%) of the genes are found in all four of the gene sets across the first 12 hours of development (Fig. 5.7). This is a very high percentage and suggests that a large number of genes are indeed persistently bound by this factor. Further investigations may be made into this in future as to the binding partners of CHDC along the genome. It has been shown in other organisms that CHD8 (homolog of CHDC) associates with the factor CTCF [90] which in turn has been shown to co-localise with cohesion [135]. In a similar report cohesions have been shown to reside at the same locus throughout cell division and also guide transcription by targeting factors such as CTCF and CHD8, it could be possible that a similar system is at work in Dictyostelium.

Using this data it is also possible to identify the genes that were mis-expressed in the RNA-seq data and were directly bound by the CHDC factor. Once again the VLOOKUP process available in Excel was employed to identify these. Once all of the

genes were identified the FIND function was utilised to search for the genes identified earlier as possibly being involved in producing the *chdC* null phenotype.

Fig.s 5.8 - 5.11 graphically represent the number of mis-regulated genes directly bound by the CHDC re-modeler during vegetative growth and at 12 hours into development. A large number of the genes affected by knocking out *chdC* are seen to be directly bound by the factor. The other genes are assumed to be indirectly affected and a knock on affect of the mis-regulation of the directly affected genes. The final column in Tables 5.2 – 5.5 represents whether the gene was also identified in the ChIP-seq data or not.



Fig. 5.7 A large portion of genes are consistently bound throughout development. The Venn diagram describes the number of genes bound by the CHDC re-modeler at each developmental stage investigated. The total number of genes appears to be quite consistent across development, with approximately 75% of the genes being bound at all stages. Values were calculated from ChIP-seq data produced by CLC genomics

workbench and sorted using the VLOOKUP function in Microsoft Excel 2003.

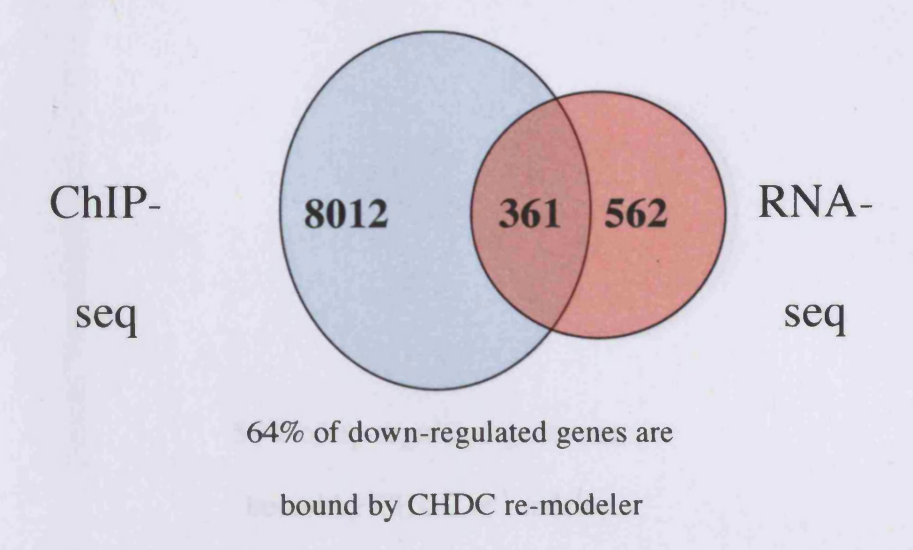


Fig. 5.8 A large percentage of the genes down-regulated during vegetative growth are bound by the CHDC re-modeler

The Venn diagram describes the number of genes down-regulated in the *chdC* null mutant during vegetative growth and that are also bound by the CHDC re-modeler in wild-type cells. Values were calculated from ChIP-seq data produced by CLC genomics workbench, RNA-seq data produced by DNAstar Arraystar and sorted using the VLOOKUP function in Microsoft Excel 2003.

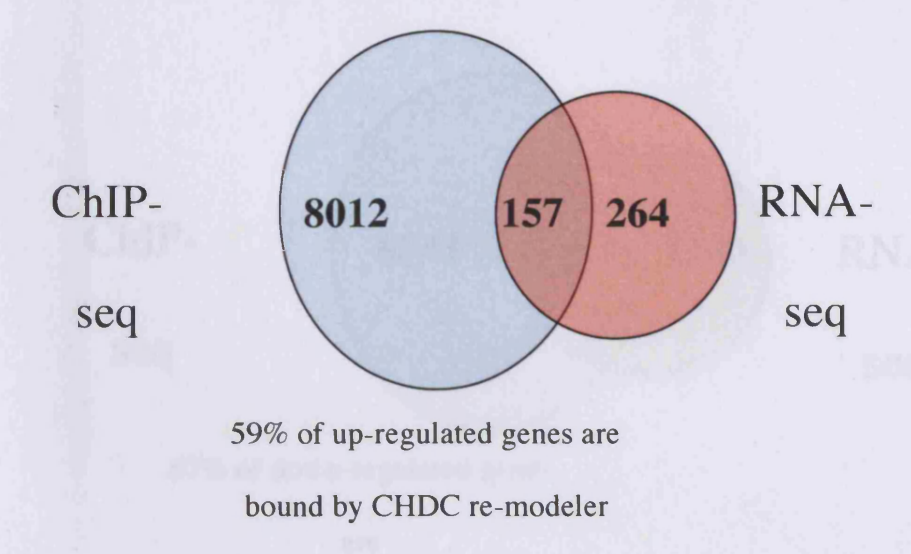


Fig. 5.9 A large percentage of the genes up-regulated during vegetative growth are bound by the CHDC re-modeler

The Venn diagram describes the number of genes up-regulated in the *chdC* null mutant during vegetative growth and that are also bound by the CHDC re-modeler in wild-type cells. Values were calculated from ChIP-seq data produced by CLC genomics workbench, RNA-seq data produced by DNAstar Arraystar and sorted using the VLOOKUP function in Microsoft Excel 2003.

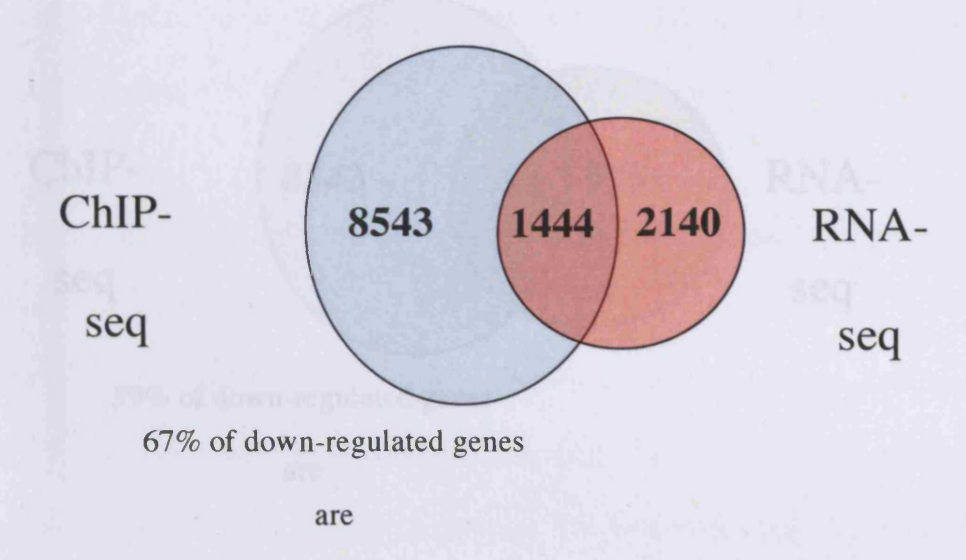


Fig. 5.10 A large percentage of the genes down-regulated after 12 hours of starvation are also bound by the CHDC re-modeler

The Venn diagram describes the number of genes down-regulated in the *chdC* null mutant 12 hours after initiation of development and that are also bound by the CHDC re-modeler in wild-type cells at this time point. Values were calculated from ChIP-seq data produced by CLC genomics workbench, RNA-seq data produced by DNAstar Arraystar and sorted using the VLOOKUP function in Microsoft Excel 2003.

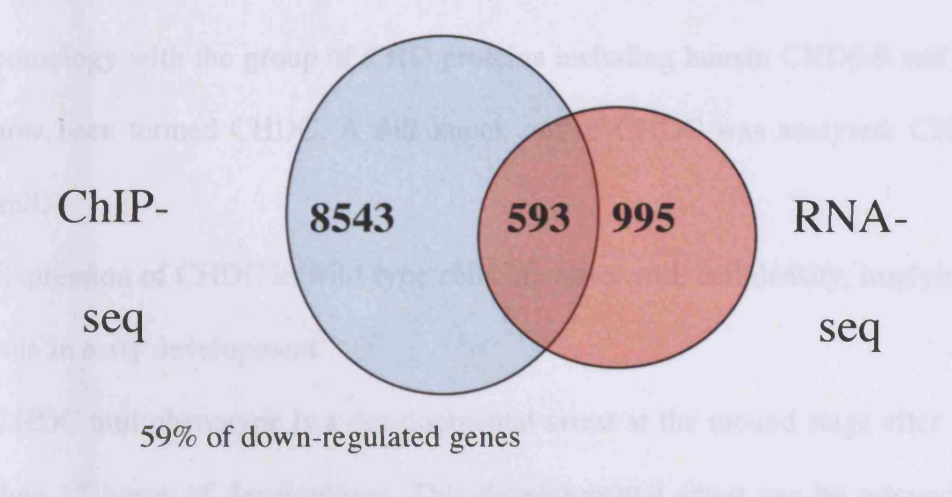


Fig. 5.11 A much lower percentage of the genes up-regulated after 12 hours of starvation are also bound by the CHDC re-modeler

The Venn diagram describes the number of genes up-regulated in the *chdC* null mutant 12 hours after initiation of development and that are also bound by the CHDC re-modeler in wild-type cells at this time point. Values were calculated from ChIP-seq data produced by CLC genomics workbench, RNA-seq data produced by DNAstar Arraystar and sorted using the VLOOKUP function in Microsoft Excel 2003.

#### 5.9 Summary

- Lithium resistant mutant LisG is a CHD family ortholog that shares most homology with the group of CHD proteins including human CHD6-9 and has now been termed CHDC. A full knock out of CHDC was analysed: CHDC null.
- Expression of CHDC in wild-type cells increases with cell density, implying a role in early development.
- CHDC null phenotype is a developmental arrest at the mound stage after less than 12 hours of development. This developmental arrest can be rescued by creating mixed populations with as little as 5% wild-type cells. CHDC null cells exhibit a severe deficiency in cAMP signaling during aggregation.
- CHDC null cells show a decreased expression of both pre-spore and pre-stalk genes suggesting a role in regulating genes involved in differentiation.
- RNA-seq identifies a much larger group of genes that are mis-expressed during development. Several of these, including the gene *yelA* may be directly responsible for the developmental phenotype.
- ChIP\_seq shows that approximately 75% of the genes bound by the factor during development are done so consistently across this period.

### **Chapter 6:**

### CHDC affects lithium sensitivity

Sumary: Starving Dictyostelium cells are capable of chemotaxing towards a cAMP signal. In wild-type cells lithium has been shown to inhibit this process, greatly reducing the cell's ability to follow a cAMP gradient. Here two mutations in the same gene, CHDC result in two allelles each responding in two opposite ways to both a cAMP gradient and to lithium treatment. LisG REMI shows enhanced chemotaxis which is reduced when treated with lithium. CHDC null cells are severely chemotactically impaired and when treated with therapeutic levels of lithium are rescued and chemotaxis is improved.

## 6.1 The LisG REMI exhibits an improved chemotaxis which provides it with lithium resistance.

It has been shown in earlier chapters that novel evidence exists to suggest that Dictyostelium are capable of responding to chemoattractants across a large order of magnitude and are able to attenuate their response to these varying concentrations through changes in gene expression leading to a switch between signaling mechanisms. Here in this brief final chapter another new phenomenom in this field will be introduced and that is for two alleles of the same chromatin re-modeler to have opposing phenotypes and to respond to lithium treatment in converse ways also.

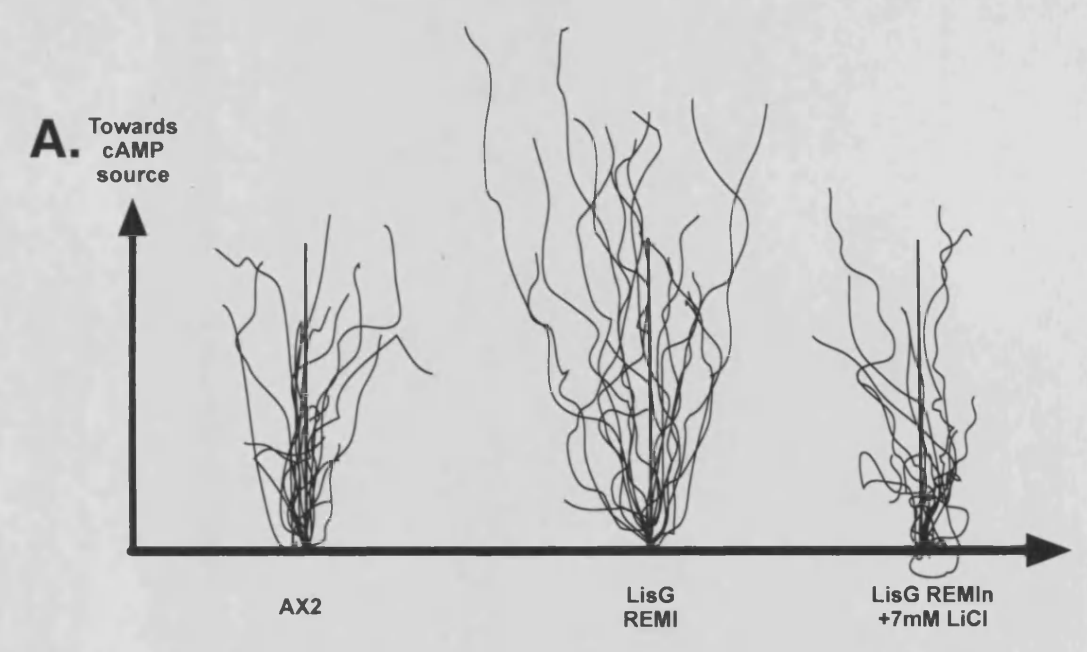
These two alleles are the two CHDC mutants described in the introduction to chapter 5. One has an insert between the first and second open reading frame and produces an almost full length transcript, yet is resistant to lithium and the second is the CHDC null mutant which has had the entire region that contains the CHROMO domains, ATPase domain and the helicase domain genetically ablated.

These experiments were once again carried out in a zigmond chamber with cells that had been pulsed for 5 hours with  $1\mu$ M cAMP to place them in what is considered to be a chemotactically competent state. In this case looking first at the LisG REMI mutant it is seen that they appear to be more chemotactically competent than wild-type cells. They move with a better CI and with a quicker speed towards the cAMP source (Fig. 6.1).

When wild-type cells are treated with 2mM lithium, within the therapeutic dose, they are seen to both inhibit development and disrupted chemotaxis. The affects on chemotaxis are to cause a reduction of speed and directionalty resulting in the cells inability to correctly sense the gradient and therefore not develop properly [1].

Several mutants have been identified which are resistant to this affect of lithium on chemotaxis and these are of express interest to us.

One such mutant is LisG REMI, and when you look at the affects of lithium on chemotaxis it is noticeable that lithium does cause a marked reduction in the cells chemotactic ability (Fig. 6.1). However, it is not a large enough reduction to drop this ability much below that of wild-type cells. This could in principle be explained by the LisG REMI cells having a faster speed and CI already counteracting the effect of lithium on the cells. This would suggest that one of the internal signaling pathways is over stimulated in these cells, which is then reduced along the same mechanisms that cause the defects in wild-type chemotaxis. This would lead to the cells appearing to have a resistance to lithium, when in fact they do not. They actually have acquired a buffer against its effects.



B.

Sample	Chemotactic index (CI)	Directionality	Speed	
AX2	0.9±0.17	0.81±0.17	9.6±4.4	
LisG REMI	0.74±0.52	0.62±0.28	12.65±4.57	
LisG REMI + 7mM LiCl	0.66±0.17	0.56±0.30	6.4±3.07	

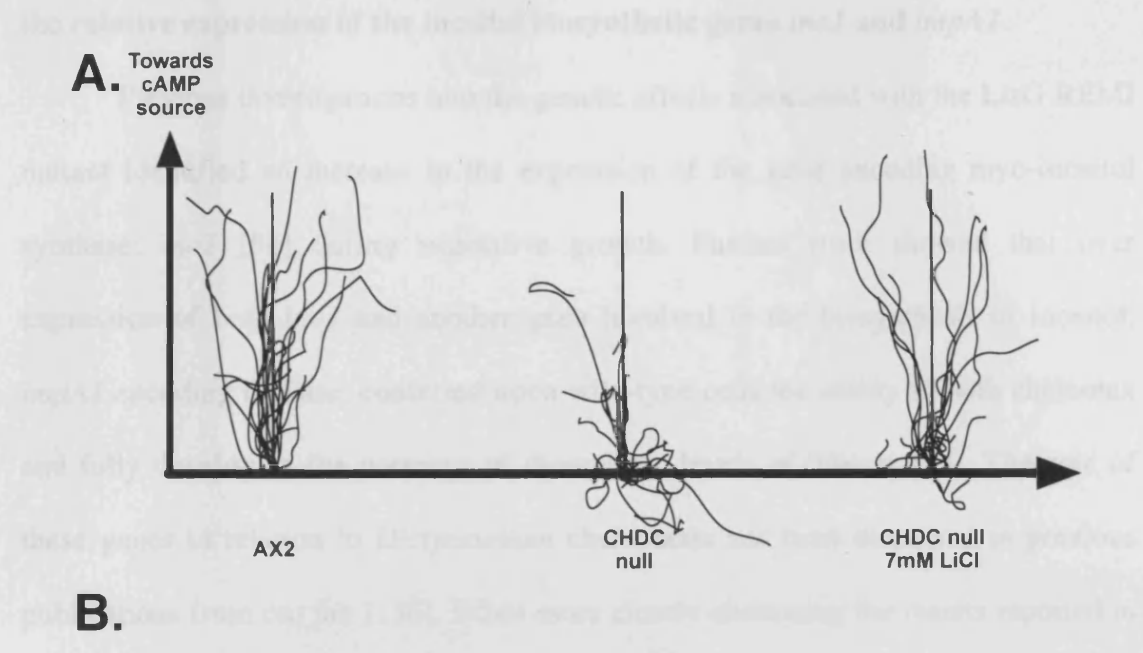
Fig. 6.1 The LisG REMI mutant is protected against the effects of lithium

**A.**) Traces taken from 3D-DIAS software that outline the movement of 20 randomly selected cells taken from a pool collected over 3 days. LisG REMI cells display increased chemotactic speed which is reduced upon addition of lithium. **B.**) The values for CI, directionality and speed as calculated by 3D-DIAS.

## 6.2 The CHDC null mutant shows an opposite response to both chemoattractant and lithium treatment.

Looking at the CHDC null cell traces there is an obvious large difference between the two mutants. The REMI cells are capable of chemotaxing extremely efficiently up the cAMP gradient with comparable directionality and CI to wild-type cells whereas the null cells show a severely decreased ability to move towards the cAMP source. They move erratically with a reduction in speed and almost no ability to sense the gradient whatsoever, randomly changing direction constantly (Fig. 6.2). Both the CI and directionality are reduced significantly. This movement is not like migrating vegetative cells looking for food. It is as if the pathways that trigger development have been activated yet the directional sensing mechanisms have been impaired.

Conversely the CHDC null cells are rescued by treatment with the same dose of lithium as inhibits chemotaxis in wild-type and LisG REMI cells. There is a large improvement in their sensing of the gradient, with increases in directionality, CI and speed. This is in stark contrast to the other allele: LisG REMI. This suggests that in each case there is a different system being affects. In this case it is likely that the loss of the chromatin re-modeler has affected one or more signaling systems resulting in the cells inability to sense the gradient, which is once again improved by inhibiting one of the molecular targets of lithium.



Sample	Chemotactic index (CI)	Directionality	Speed
AX2	0.9±0.17	0.81±0.17	9.6±4.4
CHDC null	0.74±0.52	0.62±0.28	12.65±4.57
CHDC null + 7mM LiCl	0.66±0.17	0.56±0.30	6.4±3.07

Fig. 6.2 The CHDC null mutant shows greatly impaired chemotaxis that is rescued by lithium treatment.

**A.**) Traces taken from 3D-DIAS software that outline the movement of 20 randomly selected cells taken from a pool collected over 3 days. *chdC* nulls display decreased ability to chemotax which is rescued when treated with 7mM LiCl as opposed to the REMI cells. **B.**) The values for CI, directionality and speed as calculated by 3DDIAS.

# 6.3 The chemotactic response to lithium is possibly controlled, at least in part, by the relative expression of the inositol biosynthetic genes *inol* and *impA1*.

Previous investigations into the genetic affects associated with the LisG REMI mutant identified an increase in the expression of the gene encoding myo-inositol synthase; inol [56] during vegetative growth. Further work showed that over expression of both inol and another gene involved in the biosynthesis of inositol, impA1 encoding IMPase, conferred upon wild-type cells the ability to both chemotax and fully develop in the presence of therapeutic levels of lithium [24]. The role of these genes in relation to Dictyostelium chemotaxis has been discussed in previous publications from our lab [136]. When more closely examining the results reported in the King et al paper [24] it is seen that in fact the cells over-expressing inol and impA1 move with a considerable increase in speed, similar to that which is seen with the LisG REMI mutant. As this mutant has been shown to have increased inol expression it seemed that the expression of these genes may play a significant role in the control of Dictyostelium chemotaxis. However, earlier in chapter 4 my work with the arp8 null cells has suggested that over-expressing inol and impAl will inhibit chemotaxis through over production of PIP<sub>3</sub> so there may be another process at work in the case of LisG REMI mutant. It could also be possible that the entire system is up-regulated rather than just these two genes.

Looking at the expression levels of both *ino1* and *impA1* in the CHDC null mutant (Fig. 6.3) it is observed that whilst there is a large increase in the expression of *impa1* during vegetative growth this does then decrease during the first few hours of development staying low for the duration of development. Interestingly the expression of *ino1* is decreased during vegetative growth, the opposite to what was found at this

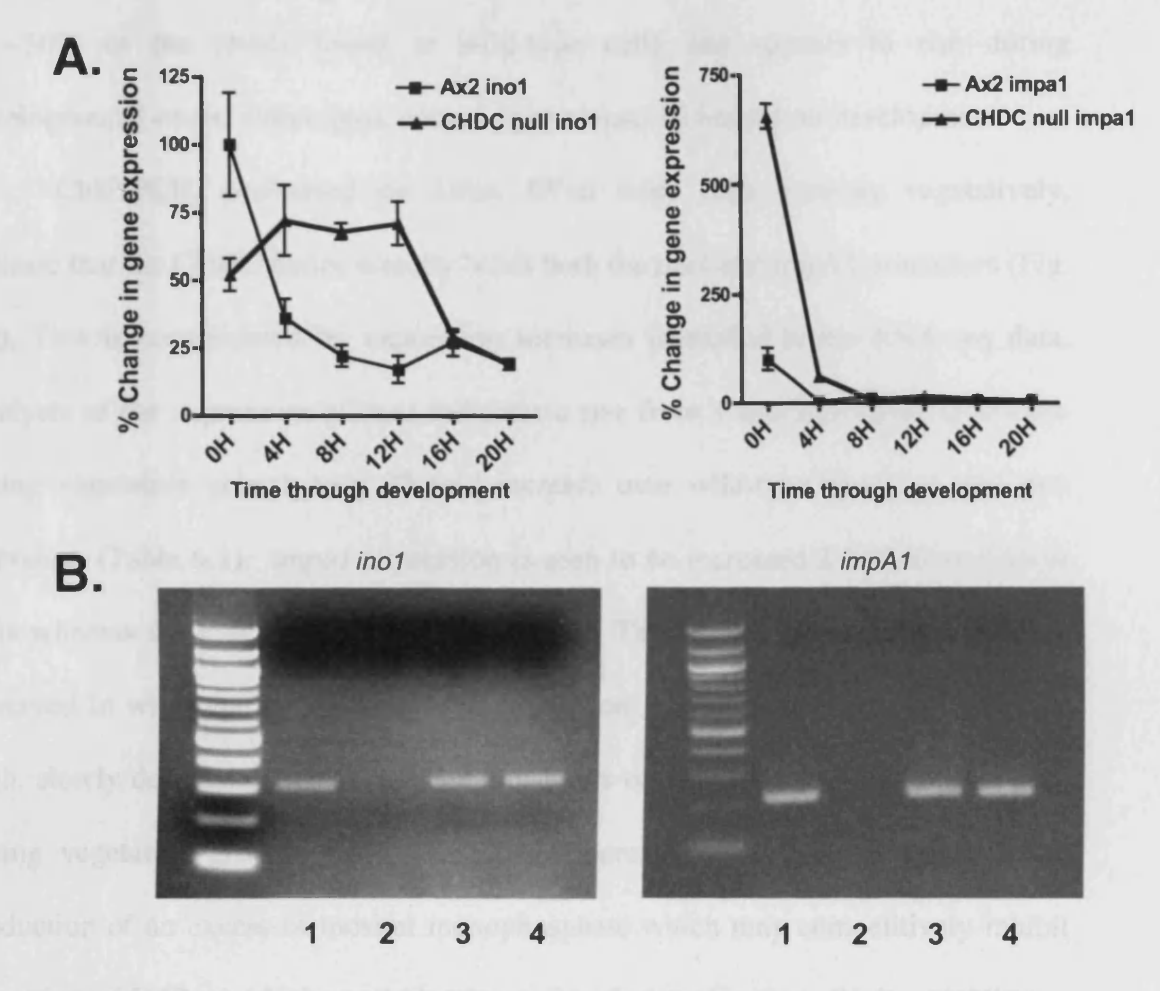


Fig. 6.3 Both *ino1* and *impA1* show different expression patterns in the CHDC null cells

**A.**) Analysis of the mRNA levels present in wild type or CHDC null cells by QRT-PCR. All expression is normalized to AX2 0H which is given a 100% expression value. *impA1* whilst initially higher, shows a similar expression pattern in both wild-type and null cells, dropping off over the early stages of development. Null cell expression of *ino1* is converse to wild-type with expression increasing over the first 12 hours as opposed to dropping. **B.**) ChIP with our anti CHDC antibody indicates that the CHDC chromatin re-modeler directly interacts with both the *ino1* and *impA1* promotors. 1- anti CHDC, 2 - just beads, 3 - anti RNApolII 4 - Genomic DNA control.

stage in the LisG REMI mutant. The expression during vegetative growth is reduced to ~50% of the levels found in wild-type cells and appears to rise during developmental onset, with a peak occurring at around 12 hours into development.

ChIP-PCR, performed on DNA IP'ed from cells growing vegetatively, indicate that the CHDC factor directly binds both the *ino1* and impA1 promotors (Fig. 6.3). This is consolidated by expression increases identified in the RNA-seq data. Analysis of the expression of *ino1* indicates a rise from a non significant difference during vegetative growth to a 27 fold increase over wild-type levels at 12H into starvation (Table 6.1). *impa1* expression is seen to be increased 2 fold in vegetative cells whereas there is no difference at 12 hours. This is in stark contrast to what is observed in wild-type cells where *ino1* expression mirrors that of *impA1* and starts high, slowly decreasing across the first four hours of starvation to ~20% of that seen during vegetative growth. Theoretically this increase in *ino1* could result in the production of an excess of inositol monophosphate which may competitively inhibit the action of IMPase which would be decreasing during this time. Such an inhibition would result in a decrease in PIP<sub>2</sub> production and subsequently a lack of PIP<sub>3</sub> for signaling in response to chemotaxis. This would result in a lack of directional sensing in the cells causing them to move more erratically.

A cell over-producing inositol monophosphate would be more sensitive to the effects of lithium. Lithium, which acts as a non-competitive inhibitor of both IMPase and IPPase [2] could break this cycle prior to IMPase decreasing the free inositol levels, along the same lines as the inositol depletion theory. This would dampen the whole system raising the PIP<sub>2</sub> concentration to near wild-type levels and restoring chemotaxis.

#### 6.4 Genes involved in chemotaxis identified by RNA-sequencing.

The RNA-seq data, produced in Chapter 5, includes a number of genes previously shown to be involved in the control of chemotaxis towards a cAMP source, in both the up- and down-regulated lists. As I mentioned above both *ino1* and *impA1* are mis-expressed in the *chdC* null. Further to these, at 12 hours after starvation, the 5' phosphatase 3 gene *dd5P3* is down-regulated 3 fold. This phosphatase is also involved in the regulation of the inositol phosphates, exerting its de-phosphorylation action at several points in the pathway, specifically at the point of I(1,4,5)P<sub>3</sub> to I(1,4)P<sub>2</sub> [137, 24]. A decrease in the production of this phosphatase would deplete the cellular levels of I(1,4,5)P<sub>3</sub>. Recent data suggests that increased I(1,4,5)P<sub>3</sub> can reduce PTEN expression providing a second feedback loop which would function alongside the up-regulation of *plc* and *ino1* to modulate PIP<sub>3</sub> signaling (personal communication from Regina Teo).

The second down-regulated gene is gcA which encodes the Guanylyl Cyclase that has been reported to play a key role in regulating chemotaxis [138]. Guanylyl cyclase produces the signaling molecule cGMP which has been implicated the correct formation of myosin fibers at the rear of the chemotaxing cell, which are involved in the retraction of the uropod [139]. Knocking out this gene in wild-type cells causes a severe disruption to chemotaxis and its down-regulation in these cells may be contributing to the chemotactic deficiency observed. The defect is characterized by the production of pseudopods over the whole surface of the cell, a behavior also exhibited by the chdC null cells which is clearly seen when watching the supplementary chemotaxis movie chdCnullct.avi. This pathway has not been reported to be a target of lithium and so it is not to be expected that the rescue of the defect by lithium would be due to an affect on this observation.

The largest number of genes identified, that are likely to be involved in the disrupted chemotaxis phenotype are up-regulated at 12 hours into development. It should be noted that most of the cells have finished chemotaxing at this point and these mis-expressions are only being suggested as possibly involved in this process. Further analysis of 4 and 8 hour time points is required to gain true insight into the genes affected during this process.

The first of these genes that has previously been shown to play a role in *Dictyostelium* chemotaxis is *plc*. This produces Phospholipase C which is involved in catalyzing the reaction: PIP<sub>2</sub> to I(1,4,5)P<sub>3</sub> and Diacylglycerol (DAG) when cells receive external stimuli. In the case of this mutant this may also be serving to reduce the free pools of PIP<sub>2</sub> in the cells and having an adverse affect on chemotaxis by reducing PIP<sub>3</sub> mediated signaling. This would also increase the amount of I(1,4,5)P<sub>3</sub> in the cell, possibly necessitating the requirement for more 5' phosphatase 3 to then decrease this. This would also result in a feedback loop producing more inositol (1) phosphate which may, by my earlier theory, inhibit IMPase further.

A second gene involved in PIP<sub>3</sub> related signaling is up-regulated and this is *pkbA*. This is the non-myristolated form of protein kinase B (PKB) is normally found in the cytosol but which translocates to the membrane in a PI3-kinase dependent manner upon stimulation of the cell with cAMP [33] resulting in activation of the TORC2 complex. Once again it is likely that this up-regulation is an indirect affect of the decrease in PIP<sub>2</sub> levels and that more PKB is made available to maximize the affect of what little PIP<sub>3</sub> synthesis may occur.

A number of genes involved in the SCAR/WAVE and Arp2/3 complexes are seen to be up-regulated in these cells. These complexes are both involved in the positive regulation of actin polymerization, with SCAR/WAVE activating Arp2/3.

Both have also been shown to be actively involved in the chemotactic process [140, 141, 142]. The gene *pirA* encodes a member of the SCAR/WAVE complex and Arp3 is produced by *arpC*. Both of these are seen to be up-regulated, along with *arcD* and *arcB*, two actin binding proteins reported to associate with the Arp2/3 complex. Whilst no literature regarding the over-expression of any of these genes was available it could be considered that an increase in the machinery responsible for producing actin polymerization could indeed increase this process and when coupled with the previously reported increase in *gcA* expression lead to an increase in lateral and dorsally produced pseudopods.

Further related to chemotaxis, in particularly cAMP signaling, three genes encoding phosphodiesterases show increased expression in the null cells. These three are pdsA, regA and pde7. The phosphodiesterases are responsible for both the external and internal degradation of cAMP and are key to regulating this important signaling molecule during development. Earlier in this thesis the developmental expression of pdsA was discussed. This is reported to start low, increases over the first 4 hours then decreases sharply after this point to a low peak at 12 hours. This data is unavailable for the other two genes. A key role for these phosphodiesterases was suggested in the initiation of characteristic cAMP signaling patterns [54]. The hypothesis suggests that signaling starts weakly with the cAMP emanating from a signaling center in a tight concentric circle. This pattern of signal release does not allow for a refractory period between the pulses and the cells at the aggregation center are required to keep pulsing for maintenance of the signaling. When the cAMP pulses meet others spreading throughout the population, they become disrupted and produce characteristic spiral waves. This allows time for reduction of cAMP levels by the phosphodiesterases allowing the cells to recover and become responsive to cAMP once again. Along the

lines of this hypothesis if the phosphodiesterases were to be increased then the signal would be reduced too much and cAMP pulsing would become disrupted, much like what is seen with the *chdC* null mutants (Chapter 5, Fig. 5.6, Supplementary movie CHDCcAMPpulse.avi). Therefore, the over-expression of the phosphodiesterases in the null cells may produce the disrupted cAMP signaling observed in the null cells. Looking at the ChIP-seq data to identify whether any of these genes are also directly bound by the CHDC factor the VLOOKUP and FIND functions of Microsoft Excel was once again employed. The final column in Tables 6.1 and 6.2 indicates whether the gene identified was also directly bound by the re-modeler.

Time point	Dictybase ID/gene	Fold change down-	Found in ChIP-seq
	name	regulated	data?
12 hours	dd5P3	3	-
12 hours	gcA	3	+

Table 6.1 Genes down-regulated involved in chemotaxis

A small number of genes previously shown to be involved in *Dictyostelium* chemotaxis are seen to be down-regulated in the *chdC* null cells. In each of these cases there could be a contribution to the chemotactic defect observed in these cells.

Time point	Dictybase ID/gene	Fold change up-	Found in ChIP-seq
	name	regulated	data?
12 hours	ino1	27	+
12 hours	impA1	2	-
12 hours	plc	6	+
12 hours	pkbA	17	-
12 hours	pirA	5	-
12 hours	arpC	4	+
12 hours	arcD	2	+
12 hours	arcB	2	+
12 hours	pdsA	10	-
12 hours	regA	5	+
12 hours	pde7	3	-

Table 6.2 Genes up-regulated involved in chemotaxis

There are a much larger number of genes up-regulated related to chemotaxis. Each of these could play a role in the chemotactic defect observed in the *chdC* null cells.

#### **6.5 Summary**

- We have two mutants for the gene CHDC
- LisG REMI has a stronger chemotactic response than wild-type cells, responding with a faster speed and moving more directly whereas *chdC* null responds extremely poorly to a cAMP stimulus, failing to detect the signal.
- Lithium treatment reduces the response of LisG REMI, but only reduces it down to wild-type response, providing the cells with lithium resistance.
- Treating the *chdC* null cells with lithium rescues the poor response to cAMP stimulus, improving all aspects of chemotaxis.
- chdC null shows over-expressed impA1 levels and reduced ino1 expression.
- Reduced ino1 is the opposite to what has previously been observed in the LisG
   REMI cell line, where ino1 expression is increased.
- The increased chemotactic response of the REMI cells is unlikely to be a result of increased PIP<sub>3</sub> levels as this has previously been shown this to inhibit chemotaxis rather than enhance it in the *arp8* mutants.
- Genes involved in several pathways implicated in Dictyostelium chemotaxis
  and cAMP signaling are seen to be mis-expressed in chdC null cells.

### **Chapter 7:**

#### **Discussion**

Summary: ATP dependent chromatin re-modeling factors are involved in the regulation of key genes required for the correct development of *Dictyostelium discoideum* in response to starvation and also for efficient chemotaxis towards cAMP, the developmental chemoattractant. The primary objectives of this investigation were to identify the roles of two of these ATP dependent chromatin remodeling factors; INO80 and CHDC, during starvation induced development and to characterize their function in the social amoeba; *Dictyostelium discoideum*.

The major findings of this thesis were that both CHDC and INO80 play a significant role in development of these cells, with null strains being defective in this process to differing degrees. Both of these factors are also essential for correct chemotaxis, with both null mutants showing disrupted chemotaxis phenotypes. These defects are seen to occur through different mechanisms, indicating the role of multiple pathways in the regulation of *Dictyostelium* chemotaxis.

#### 7.1 The INO80 complex is involved in regulating *Dictyostelium* development.

Through its interaction with the Arp8 subunit it has been shown that the INO80 chromatin re-modeling complex plays a significant role in the starvation induced development of *Dictyostelum discoideum*. Starvation induced development in *Dictyostelium discoideum* relies on the cells ability to accurately detect and relay the cAMP signal throughout the population. This involves detecting the abundance of nutrients in the environment, the size of the population and the correct temporal expression of the cAMP producing, detecting and regulatory machinery

An arp8 null strain exhibits a delay in the onset of development, with initiation being delayed by a minimum of 4-5 hours. This delay is shown to be related to an inability to produce correct cAMP signals through the population, resulting in a lack of communication that the developmental process and aggregation should begin. Dark field time-lapse movies show an delay in the onset of cAMP pulsing through the population that is on a similar time scale to the delay in onset of aggregation. Several genes responsible for producing the messenger, receptor and regulators of this system are also temporally delayed in their expression and it is hypothesized that this delay in expression of cAMP synthesis is responsible for the delay in initiation of aggregation. These genes are car1, acaA and pdsA encoding the cAMP receptor CAR1, the adenylyl cyclase ACA and the phosphodiesterase PDE respectively. Losing these key factors from the signaling pathway would mean that the positive feedback responsible for initiating this process would be less effective and the developmental process would be delayed.

The correct timing of development and the expression of these genes can all be rescued by mixing in a small amount of wild-type cells into the population, suggesting that the *arp8* null cells are lacking an external secreted factor that signals

entry into development. This was first thought to be cAMP as pulsing the null cells with cAMP rescues the expression of the cAMP biosynthetic genes that are seen to have delayed expression in this mutant. However there is no direct evidence for this as many factors influence the initial release of cAMP that stimulates the positive feedback loop resulting in cAMP pulsing.

Next generation sequencing data provides further evidence to suggest that the null cells are delayed in their ability to enter development through the mis-regulation of several genes involved in initiating this process. A large number of genes involved in a diverse range of processes such as; initiation of development, sensing cell density, cAMP biosynthesis and growth development transition. The most documented of these previously being Discoidin, which is significantly down-regulated, along with the genes involved in the production detection and regulation of the cAMP signal.

It is clear from these results that the INO80 complex is involved in regulating the initiation of development in *Dictyostelium*, particularly in maintaining the correct expression if the cAMP signal and its propagation throughout the population.

# 7.2 Chemotaxing cells respond across a large order of magnitude and alter signaling mechanisms accordingly.

Cells advancing through the aggregation process encounter rising concentrations of cAMP as they approach the mound (aggregation center). The mechanisms by which cells maintain their behavior across concentration changes of several orders of magnitude have previously been unclear. It would seem sensible for a system to have evolved to allow for a modulation of the sensing of external cAMP concentration to be incorporated into the developmental process. Indeed, several

different cAMP receptors are expressed across the developmental time-frame, with each becoming less sensitive the later through development it is expressed [39, 40, 41, 42]. However a more sensitive system could be in place at the onset of development.

The PIP<sub>3</sub> signaling system is a key component of the *Dictyostelium* chemotaxis process. In steep cAMP gradients there is an accumulation of this signaling molecule at the leading edge of the cells, which was previously thought to act as a biological compass directing the cells towards the source. When the INO80 complex is disrupted by knocking out *arp8* there is a severe narrowing of the range over which the starving cells can respond to cAMP, with the majority of cells appearing motionless in high gradients. When the gradient of cAMP is reduced, or when the cAMP is allowed to degrade to a detectable level, the cells begin to chemotax normally.

These data reported in this thesis go some way to suggest that PIP<sub>3</sub> signaling is modulated through the production of the precursor molecule PIP<sub>2</sub>. The inositol biosynthetic genes *inol* and *impAl* have previously been shown to increase PIP<sub>3</sub> signaling through over production of PIP<sub>2</sub> [1]. Elevated levels of PIP<sub>2</sub> result in an increased signal to noise ratio in the cells meaning that they are incapable of detecting the external signal. This results in the cells remaining motionless in steep cAMP gradients.

RNA-sequencing data reveals another set of genes that are possibly linked to the chemotactic phenotype observed in these null cells. Along with *ino1* and *impA1* the PI3-kinase *pikF* is seen to be up-regulated and may also contribute to the increase in PIP<sub>3</sub> signaling through increased production from PIP<sub>2</sub>. The down-regulation of *pldA*, *dpoA*, *dd5P1*, *pikB*, *pikD* would all also serve to modulate the levels of PIP<sub>2</sub> in the cell and thus altering PIP<sub>3</sub> signaling.

The arp8 null cells are also lithium sensitive, responding better to a steep cAMP gradient in the presence of 2mM LiCl. This suggests further that the PIP<sub>3</sub> signal noise ratio is controlled by the inositol biosynthetic genes as IMPase (encoded by impAI) is inhibited by lithium which would therefore reduce the PIP<sub>2</sub> levels in the cell, allowing them to sense the gradient once again.

These results all go some way to showing that chemotaxing *Dictyostelium* cells are able to control the signal to noise ratio within the PIP<sub>3</sub> signaling system, enabling them to maintain the movement towards chemoattractant at high concentrations of cAMP.

# 7.3 The *Dictyostelium* CHD8 homolog CHDC plays a significant role during starvation induced development.

Members of the CHROMO domain helicase DNA binding (CHD) protein family have been shown to modulate transcription of DNA in several model organisms. The family is most characterized by their SWI/SNF like ATPase domain, two CHROMO domains and a DNA binding motif. The lithium resistant mutant LisG was identified as having a mutation in a homolog of the CHD family member which we have now designated CHDC. However the LisG mutant was found to still express a transcript of the gene and so is not considered a null mutant. Full disruption of the CHDC gene resulted in a severe developmental phenotype resulting in developmental arrest at the mound stage after 24 hours.

Developmental arrest of *chdC* null cells suggests that this CHDC re-modeling factor plays an essential role in modulating genes involved in the correct culmination of this process. The cells not only exhibit developmental arrest, but also a non standard aggregation pattern where the cells appear to clump together, rather than

streaming as wild-type do and also the production of several spore heads from the mound structure when left for time in excess of 30 hours. Similarly to the *arp8* null cells, when a small percentage of the population is made up of wild-type cells the developmental arrest can be rescued, with the degree of rescue increasing with wild-type:null cell ratio, resulting in chimeric fruiting bodies. This suggested that the cells were lacking an external signaling molecule which can be replaced by the wild-type cells.

Looking at the expression of several pre-spore and pre-stalk genes these were all observed to be severely reduced and delayed in their expression by up to around 20 hours. This would be consistent with the observation that several spore heads are seen to occur after 24 hours of starvation, yet does not explain the developmental arrest. Dark field time-lapse movies reveal that cAMP signaling occurs incorrectly in these cells, with the nulls showing no cAMP pulses through the population until they enter the loose mound stage, where the pulses resonate throughout this structure. Mixing with wild-type cells does rescue this, once again dependent on the degree of AX2 cells mixed into the population, but never returning to wild-type signaling. An increase in the expression of the genes encoding phosphodiesterases; pdsA, regA and pde7, observed in RNA-seq data, could be responsible for this effect. If the levels of secreted phosphodiesterases are too high they will diminish the secreted cAMP pool, decreasing the cells ability to signal to one another and guide the aggregation process. RNA- and ChIP-sequencing also reveal a large number of genes that may be involved in producing the arrested development phenotype observed in the null cells. The most instantly interesting of these is the down regulation of the gene yelA, which encodes the elongation initiation factor eIF-4. The phenotype associated with this gene almost exactly phenocopies the developmental arrest and associated qualities of the chdC

null cells. It is therefore possible that the mis-regulation of this gene and subsequent down-stream effects results in the phenotype observed when knocking out *chdC*. There are however a number of other candidates all of which could contribute significantly.

These results clearly indicate that CHDC plays a pivotal role in regulating many genes involved in the regulation of the early stages of *Dictyostelium* starvation induced development and also give some insight into the binding of this factor during this time.

## 7.4 The two CHDC mutants respond oppositely to cAMP gradients and to lithium treatment.

Lithium has previously been shown on many occasions to be detrimental to a cells ability to chemotax towards a cAMP source. The LisG null mutant had previously been identified as being resistant to this effect. However upon closer inspection it is revealed that this mutant in fact displays improved chemotaxis characteristic making it more efficient than wild-type cells. This effect has previously also been reported in cells over-expressing both *ino1* and *impA1*, two genes which are also observed to be up-regulated in LisG REMI. This does not explain the phenotype as it has already been indicated that over-expressing these two genes results in an inability to perform chemotaxis. There is a possibility that the entire pathway is up-regulated in this mutant, however further analysis is required to prove this theory.

Conversely to this result the CHDC null mutants behave extremely poorly when placed in a high cAMP gradient, moving erratically and demonstrating a higher number of lateral and dorsal pseudopods. Once again this phenotype appears to be related to the expression of inositol biosynthetic genes *inol* and *impAl*, with a large

increase in the expression of *impA1* during vegetative growth and *ino1* expression appearing opposite to that of wild-type, being low during vegetative growth and then rising as the cells enter development. This increase in inositol monophosphate could flood the IMPase active sites resulting in a decrease in activity due to competitive inhibition of the enzyme. This would then serve to reduce the levels of PIP<sub>2</sub> in the cell leaving the cells insensitive to the cAMP signal and unable to respond effectively. RNA-seq data also reveals an increase in the production of Phospholipase C which would also serve to reduce the PIP<sub>2</sub> in the cells when stimulated with cAMP and a down-regulation of one of the 5' phosphatases which would disrupt recycling of the produced I(1,4,5)P<sub>3</sub>.

Increased pseudopod formation could be a result of the down-regulation of the enzyme producing cGMP: guanylyl cyclase, a signaling molecule which has been implicated in the correct formation of myosin fibres and repression of pseudopod formation at the rear of the cell. Coupled with an increase in the expression of some of the SCAR/WAVE and Arp2/3 complex members, both responsible for actin polymerization, this may explain this aspect of the phenotype.

The *chdC* null cells also show disrupted cAMP pulsing during the aggregation period of development, not producing any pulsing patterns throughout the population indicating that the signal is not being transduced from cell to cell. It has previously been suggested that an increase in phosphodiesterase expression would produce such a phenotype by breaking down too much of the secreted cAMP and disrupting the signal. Three of the major phosphodiesterases are up-regulated in the *chdC* mutant which is likely to produce this effect.

Treating the *chdC* null cells with lithium also has an opposite effect to treating the LisG REMI mutant similarly. These cells are rescued by lithium treatment with an

improvement in cell chemotaxis. Whilst inhibiting IMPase would not alleviate the theorized cause of the chemotactic defects in these mutants, it is possible that lithium is affecting IPPase, an enzyme that acts further up the inositol recycling pathway serving to reduce the levels of inositol monophosphate entering the system and therefore bring the PIP<sub>2</sub> levels back to normal again. This would allow the cells to start chemotaxing more as wild-type.

The results from the CHDC mutants chemotaxing have opened up the idea of what exactly lithium resistance or sensitivity is? It was previously taken as being whereby a population of cells could chemotax or develop in the presence of lithium as a result of *some* form of biological change within the cells. This was generally considered as being a direct action of lithium on one of its targets which resulted in an observable change in behavior. However, in the case of the LisG REMI mutant there is a cell line that is exhibiting a newly described form of lithium resistance which shall be termed lithium protection. The theoretical explanation for this is that the cells aren't actually lithium resistant. They are affected by lithium treatment, most likely by exactly the same mechanism that affects wild-type cells, yet they have an elevated signaling pathway which is then reduced to wild type levels through the action of lithium.

#### 7.5 Final conclusions.

To summarize the findings of my research; roles have been identified for two ATP-dependent chromatin remodeling factors in the *Dictyostelium discoideum* in the starvation induced development process and chemotaxis towards a cAMP signal. This has increased our knowledge of both of these key processes and the roles of these remodeling complexes in this organism, which had to this point yet to be fully investigated.

Both of these processes, development and chemotaxis, are highly regulated by a large number of processes and involve the regulation of a large number of others. Knocking out these re-modelers has resulted in a change in the expression of a very large number of genes, many of which are involved in the developmental process. Experimental evidence has also been introduced for the theory that *Dictyostelium* is responsive to differing concentrations of cAMP with different signaling systems. These systems are switched on and off through the expression of genes regulated by ATP chromatin remodeling. These data, found in this thesis, indicate that when expression of the genes regulating an individual signaling process is removed, the range under which the cells can respond is reduced.

Finally, further evidence has been introduced towards the regulation of chemotaxis by the mood stabilizing drug; lithium. More data is represented to suggest that the drug acts upon the inositol biosynthetic system within the cell effecting the production of the signaling molecules PIP<sub>2</sub> and PIP<sub>3</sub>.

This is the first analysis into the role of chromatin re-modeling in Dictyostelium discoideum. There are several other factors identified in this organism and through a coordinated and combined analysis a pattern of genetic regulation can be elucidated for the full development process

### **Appendicies**

### Appendix A

Gene Ontology (GO) data.

#### A.1 GO analysis of RNA-seq data

The Gene Ontology (GO) project has attempted to provide a unified categorization system to try and end potential confusion that arises when you have extensive descriptive nomenclature. The use of a consistent terminology allows for genes from different species to be analyzed based on their GO annotations. The system initially lists all genes within three major categories; molecular function, biological process and cellular localization and then these are further divided into many other sub-categories describing functions of gene products. The group that was most interesteding and have displayed here is that of biological process.

There are many tools available for analyzing GO data, however, as the capability for GO analysis is available within the Arraystar software that was opted to use this. The genes full gene lists consisting of all genes that have either been up- or down-regulated at either 0H or 8H are highlighted individually and then subject to the Arraystar analysis. This analysis identifies the most significantly affected GO gene groups within the listed genes. The significance is represented by the p-value, which symbolizes the chance that the test results observed could have also happened through random chance. The group that proved most interesting and has been displayed here is that of biological process.

Looking at the vegetative cells the groups that are significantly affected are mainly those involved in cellular process such as metabolism and catabolism which is to be expected in normal growing cells (Table 3.6). The fact that there are no significant results for the up-regulated gene group suggests that Arp8 and the INO80 complex are involved more in activating genes than repressing them at this stage.

	Gene Ontology					
Term	ID	P-Value	Z-Score	Selected	Total	%
metabolic process	8152	0.0000847	4.8884054	160	2611	6.13%
catabolic process	9056	3.37E-12	9.7650458	57	402	14.18%
macromolecule						
catabolic process	9057	1.72E-11	9.5300247	44	275	16.00%
biopolymer						
catabolic process	43285	4.63E-12	10.0816491	43	248	17.34%
protein catabolic						
process	30163	8.3E-12	9.9918798	39	214	18.22%
cellular protein						
catabolic process	44257	3.48E-11	10.8966276	22	72	30.56%
proteolysis						
involved in cellular						
protein catabolic	E4602	3.16E-11	10 9066076	22	72	30.56%
process modification-	51603	3.10E-11	10.8966276	22	12	30.36%
dependent protein						
catabolic process	19941	3.15E-11	10.9981262	22	71	30.99%
ubiquitin-	13341	3.13L-11	10.3301202	22	, ,	30.3370
dependent protein						
catabolic process	6511	4.2E-11	10.9981262	22	71	30.99%
proteolysis	6508	3.8E-11	9.5387576	37	208	17.79%
cellular biopolymer		5.52	0.000.0.0	<b>.</b>		
catabolic process	34962	5.18E-10	9.8630917	23	90	25.56%
cellular .						
macromolecule						
catabolic process	44265	2.31E-08	8.5774174	24	117	20.51%
modification-						
dependent						
macromolecule					_,	
catabolic process	43632	3.6E-11	10.9981262	22	71	30.99%
cellular catabolic	44248	0.000000208	7.4046200	33	232	14.22%
process protein metabolic	44240	0.000000208	7.4046398	33	232	14.2270
process	19538	0.00114	4.4793408	74	1043	7.09%
nucleobase,	19550	0.00114	4.4755466	7-7	1045	7.0570
nucleoside,						
nucleotide and						
nucleic acid						
metabolic process	6139	0.00813	-3.4104801	12	680	1.76%
regulation of						
developmental						
process	50793	0.00687	5.2514246	10	52	19.23%

**Table A.1** GO term enrichment for genes exhibiting a 2-fold decrease in expression in the *arp8* null cell line in comparison to wild type cells during vegetative growth. The P-value cut off was set at 0.01 and the GO data file used was gene\_association.ddb.

Looking at the genes that are significantly affected at the 8 hour developmental stage there are a much larger and varied number of groups identified. Those down-regulated include many involved in starvation induced development, including developmental processes locomotion, regulation of cAMP biosynthesis and several groups involved with the production of spores (Table 3.8). Many of those significant GO groupings that are identified in the up-regulated gene list are involved in protein synthesis, cellular metabolism and energy production plus a large number of other processes you would expect to find in vegetatively growing rather than starving cells (Table 3.9). This includes the ribosomal proteins and translational machinery which were noticed earlier when simply scanning the gene lists for anything that stood out on first inspection. This stands to reason, as if the *arp8* null cells are delayed in their entry to development then they will still be operating under a similar set of processes as if they were growing vegetatively and the switch between the two states has not been fully registered.

	Gene					
Term	Ontology ID	P-Value	Z-Score	Selected	Total	%
binding	5488	3.81E-13	8.030697	678	3235	20.96%
ion binding	43167	1.49E-09	7.064406	213	849	25.09%
cation binding	43169	1.78E-09	7.064406	213	849	25.09%
metal ion binding	46872	8.61E-09	6.730836	202	812	24.88%
transition metal ion	10072	0.012 00	0.70000	202	0.2	21.0070
binding	46914	4.57E-05	4.953982	153	654	23.39%
calcium ion binding	5509	7.18E-05	5.294431	38	108	35.19%
protein binding	5515	2.32E-06	5.596687	201	866	23.21%
adenyl						
ribonucleotide						
binding	32559	9.59E-05	4.696408	171	759	22.53%
ribonucleotide						
binding	32553	0.00014	4.545973	209	967	21.61%
purine ribonucleotide						
binding	32555	0.000134	4.545973	209	967	21.61%
catalytic activity	3824	4.24E-13	8.110028	599	2791	21.46%
hydrolase activity	16787	1.61E-10	7.43908	248	1001	24.78%
peptidase activity	8233	2.51E-09	7.545738	60	155	38.71%
peptidase activity,						
acting on L-amino	70011	4 44 5 00	6 090200	EE	4.46	27 670/
acid peptides endopeptidase	70011	4.41E-08	6.980209	55	146	37.67%
activity	4175	3.46E-07	6.722978	38	89	42.70%
phosphoric ester	4175	3. <del>4</del> 0L-07	0.722970	30	09	42.7070
hydrolase activity	42578	4.13E-05	5.487431	39	109	35.78%
phosphotransferase						
activity, alcohol						
group as acceptor	16773	2.78E-07	6.300819	98	339	28.91%
protein kinase						
activity	4672	2.43E-05	5.327163	81	291	27.84%
kinase activity	16301	4.83E-05	4.997692	113	453	24.94%
enzyme regulator						
activity	30234	4.68E-05	5.234347	60	200	30.00%
structural						
constituent of ribosome	3735	2.96E-06	-4.49436	1	114	0.88%
developmental	3/35	2.900-00	-4.49436		114	0.00%
process	32502	2.38E-11	7.976119	110	342	32.16%
anatomical structure	02002	2.002 11	7.070110	110	042	<b>32</b> . 10 /0
development	48856	4.43E-12	8.493379	85	230	36.96%
culmination during						
sorocarp						
development	31154	1.49E-05	5.896442	22	45	48.89%
reproductive						
structure						
development	48608	1.83E-05	5.399134	44	130	33.85%
spore-bearing organ	75250	0.000048	E 200424	4.4	120	22.050/
development body	75259	0.000018	5.399134	44	130	33.85%
development	30582	1.94E-05	5.399134	44	130	33.85%
fruiting body	JUUJE	1.076-00	J.555 154	<del></del>	130	JJ.UJ 70
development in						
response to						
starvation	55084	1.98E-05	5.399134	44	130	33.85%
sorocarp						
development	30587	2.02E-05	5.399134	44	130	33.85%
aggregation involved	31152	1.92E-05	5.6246	30	74	40.54%

in sorocarp development						
organ development	48513	2.06E-05	5.399134	44	130	33.85%
reproductive						
developmental	3006	0.000019	5.399134	44	130	33.85%
process metabolic process	8152	1.2E-09	6.698719	<del>44</del> 542	2611	20.76%
catabolic process	9056	5.05E-12	8.216212	126	402	31.34%
macromolecule						0.5.050/
catabolic process biopolymer catabolic	9057	3.93E-12	8.540993	97	275	35.27%
process	43285	5.27E-12	8.366368	89	248	35.89%
protein catabolic	20402	0.005.40	0.700004	00	044	20.220/
process cellular protein	30163	3.29E-12	8.729824	82	214	38.32%
catabolic process	44257	5.28E-12	8.997811	40	72	55.56%
proteolysis involved in cellular protein						
in cellular protein catabolic process	51603	5.81E-12	8.997811	40	72	55.56%
modification-				-		
dependent protein catabolic process	19941	5.13E-12	9.113313	40	71	56.34%
ubiquitin-dependent	19941	J. 13L-12	9.113313	40	, ,	30.34 //
protein catabolic	0544			4.0	_,	
process proteolysis	6511 6508	4.4E-12 3.79E-11	9.113313 8.094917	40 77	71 208	56.34% 37.02%
cellular biopolymer	0300	3.78L-11	0.094917	,,	200	37.0270
catabolic process	34962	7.05E-11	8.352761	44	90	48.89%
cellular macromolecule						
catabolic process	44265	7.21E-11	8.229166	52	117	44.44%
modification- dependent						
macromolecule						
catabolic process	43632	6.16E-12	9.113313	40	71	56.34%
cellular catabolic process	44248	1.15E-08	6.967848	77	232	33.19%
primary metabolic	77270	1.132-00	0.307040	,,	202	33.1370
process	44238	7.82E-10	6.812859	467	2189	21.33%
protein metabolic process	19538	6.93E-14	8.702572	271	1043	25.98%
cellular protein						
metabolic process protein modification	44267	6.69E-11	7.460349	226	892	25.34%
process	6464	8E-09	6.748571	151	566	26.68%
post-translational	10007	• 44= •=				
protein modification protein amino acid	43687	2.11E-07	6.177743	110	397	27.71%
phosphorylation	6468	2.44E-06	5.683067	83	290	28.62%
translation	6412	3.5E-07	-4.76686	2	138	1.45%
carbohydrate metabolic process	5975	2.62E-07	6.287168	72	227	31.72%
ncRNA metabolic		2.022 07	0.207 100	'-		01.7270
process	34660	2.03E-05	-4.22315	3	124	2.42%
macromolecule metabolic process	43170	2.14E-06	5.319727	347	1658	20.93%
macromolecule						
biosynthetic process biopolymer	9059	2.64E-06	-4.80857	21	320	6.56%
biosynthetic process	43284	1.68E-06	-4.89108	20	316	6.33%
•						

cellular biopolymer biosynthetic process	34961	2.2E-06	-4.83793	20	313	6.39%
cellular	34901	Z.ZL-00	<del>-4</del> .03733	20	313	0.0070
macromolecule						
biosynthetic process	34645	2.26E-06	-4.83793	20	313	6.39%
biopolymer					1000	00 740/
metabolic process	43283	7.46E-06	5.032121	336	1620	20.74%
biopolymer modification	43412	1.66E-07	6.12141	151	592	25.51%
cellular metabolic	.0112	1.002 01	0.12111			
process	44237	3.36E-05	4.593361	411	2072	19.84%
phosphorus	0700	4.445.00	0.00044	400	050	00.50%
metabolic process phosphate metabolic	6793	1.14E-08	6.80941	106	359	29.53%
process	6796	1.09E-08	6.80941	106	359	29.53%
phosphorylation	16310	3.41E-07	6.119523	88	300	29.33%
response to stimulus	50896	1.49E-08	6.638139	137	505	27.13%
response to external						
stimulus	9605	4.27E-08	6.692874	74	226	32.74%
response to extracellular						
stimulus	9991	3.6E-07	6.355945	53	149	35.57%
response to nutrient		0.02 0.	0.0000			00.0.70
levels	31667	2.85E-07	6.413747	53	148	35.81%
response to	40504	0.67E.0E	E 202627	45	136	33.09%
starvation response to chemical	42594	2.67E-05	5.283637	45	130	33.09%
stimulus	42221	7.51E-06	5.631815	49	146	33.56%
response to stress	6950	1.93E-05	5.137101	94	357	26.33%
cellular process	9987	4.59E-08	6.013901	582	2901	20.06%
biological regulation	65007	1.16E-06	5.578086	209	908	23.02%
regulation of	50789	2.65E-07	5.917622	203	859	23.63%
biological process regulation of cellular	30709	2.03E-07	5.917022	203	059	23.03%
process	50794	2.45E-07	5.949848	196	822	23.84%
regulation of						
nucleobase,						
nucleoside, nucleotide and						
nucleic acid						
metabolic process	19219	8.72E-05	4.775618	70	256	27.34%
regulation of						
nucleotide metabolic	6440	E	E 600246	45	26	E7 C00/
process regulation of	6140	5.58E-05	5.692346	15	26	57.69%
nucleotide						
biosynthetic process	30808	5.49E-05	5.692346	15	26	57.69%
regulation of cyclic						
nucleotide	30802	5.76E-05	E 602246	15	26	E7 C00/
biosynthetic process regulation of cAMP	30602	3.76E-U3	5.692346	15	26	57.69%
biosynthetic process	30817	9.74E-05	5.553515	14	24	58.33%
regulation of cyclic						
nucleotide metabolic	20700	- 07F 07	5.0000.15	4.5	00	F7 060'
process regulation of cAMP	30799	5.67E-05	5.692346	15	26	57.69%
metabolic process	30814	9.89E-05	5.553515	14	24	58.33%
regulation of primary				-		
metabolic process	80090	0.000176	4.556902	73	276	26.45%
positive regulation of	51349	0.000156	5.508729	12	19	63.16%

lyase activity						
positive regulation of						
cyclase activity	31281	0.000158	5.508729	12	19	63.16%
reproductive process	22414	1.87E-05	5.399134	44	130	33.85%
locomotion	40011	4.17E-05	5.222896	39	113	34.51%
cell part	44464	2.16E-07	5.752175	658	3360	19.58%
membrane part	44425	1.05E-06	5.64611	207	894	23.15%
intrinsic to						
membrane	31224	7.5E-08	6.360578	182	732	24.86%
integral to membrane	16021	1.71E-07	6.156684	179	727	24.62%
proteasome core						
complex	5839	3.13E-07	7.349175	14	17	82.35%
proteasome						
regulatory particle	5838	1.36E-06	7.045158	11	12	91.67%
ribosome	5840	3.24E-05	-4.07787	1	96	1.04%
cytosol	5829	6.44E-10	7.876761	57	139	41.01%

**Table A.2** GO term enrichment for genes exhibiting a 2-fold decrease in expression in the *arp8* null cell line in comparison to wild type cells 8H into starvation induced development. The P-value cut off was set at 0.01 and the GO data file used was gene\_association.ddb.

PRODUCTION OF THE PARTY OF THE	Gene	and the latest terms	interestation of	incomes.	OCCUPATION	
	Ontology				_	04
Term	ID	P-Value	Z-Score	Selected	Total	%
molecular_function structural molecule	3674	6E-79 2.08E-	18.59705	748	6797	11.00%
activity structural	5198	71	27.1664	103	175	58.86%
constituent of		2.22E-				
ribosome	3735	78 3.14E-	29.97458	89	114	78.07%
binding	5488	42 5.22E-	14.89447	413	3235	12.77%
nucleoside binding purine nucleoside	1882	15 5.87E-	9.442549	121	795	15.22%
binding adenyl nucleotide	1883	15	9.442549	121	795	15.22%
binding adenyl	30554	4.7E-15	9.442549	121	795	15.22%
ribonucleotide		1.27E-				
binding	32559	12 9.37E-	8.549365	111	759	14.62%
ATP binding	5524	13 5.47E-	8.620696	110	745	14.77%
nucleotide binding purine nucleotide	166	15 1.98E-	9.236232	156	1148	13.59%
binding purine	17076	14	9.045792	141	1014	13.91%
ribonucleotide binding ribonucleotide	32555	1.51E- 12 1.61E-	8.362667	131	967	13.55%
binding	32553	12 1.31E-	8.362667	131	967	13.55%
protein binding cytoskeletal protein	5515	14 3.27E-	9.219148	127	866	14.67%
binding	8092	16 3.82E-	11.44385	47	156	30.13%
actin binding nucleic acid	3779	12 2.52E-	9.845955	34	111	30.63%
binding	3676	08 3.09E-	6.6636	114	924	12.34%
catalytic activity	3824	20 1.33E-	10.26283	317	2791	11.36%
hydrolase activity	16787	08 3.29E-	6.763286	122	1001	12.19%
cellular_component	5575	76 5.57E-	18.80389	661	5566	11.88%
cell part	44464	88 1.27E-	21.68852	511	3360	15.21%
intracellular part	44424	91 7.6E-	23.54145	392	2047	19.15%
cytoplasmic part	44444	102 4.92E-	26.96385	292	1084	26.94%
ribosome	5840	60 6.54E-	25.8988	71	96	73.96%
cytoplasmic vesicle cytoplasmic membrane-	31410	52	20.71994	115	318	36.16%
bounded vesicle	16023	2.2E-52 4.71E-	20.86277	115	315	36.51%
endocytic vesicle	30139	53	21.12468	114	305	37.38%

phagocytic vesicle	45335	1.6E-52 6.21E-	20.99606	113	303	37.29%
ribosomal subunit small ribosomal	33279	15	12.97574	17	22	77.27%
subunit	15935	4.3E-10 3.96E-	10.95008	10	11	90.91%
cytosolic part chaperonin-	44445	08	8.559831	14	30	46.67%
containing T-		8.25E-				
complex	5832	09	10.34829	8	8	100.00%
intracellular		2.69E-				
organelle	43229	75	22.06024	289	1346	21.47%
intracellular non-	.02-0	. •	22.0002	200	10.0	21.1770
membrane-		5.71E-				
bounded organelle	43232	58	21.81274	131	370	35.41%
bounded organiene	43232		21.012/4	131	3/0	33.4176
	5050	3.12E-	0.400440	0.4	405	00 500/
cytoskeleton	5856	11	9.126442	31	105	29.52%
intracellular						
membrane-		1.05E-				
bounded organelle	43231	38	15.39918	198	1075	18.42%
ribonucleoprotein		4.89E-				
complex	30529	38	17.88116	82	219	37.44%
intracellular				-		• • • • • • • • • • • • • • • • • • • •
organelle part	44446	1.3E-22	11.60608	135	786	17.18%
•						
cytoskeletal part	44430	1.3E-18	11.70072	55	196	28.06%
		2.16E-				
cytoplasm	5737	15	10.09797	61	273	22.34%
		5.29E-				
intracellular	5622	32	14.57821	128	582	21.99%
		1.49E-				
cell leading edge	31252	12	10.5869	23	52	44.23%
3		7.73E-			<b>-</b>	
cell projection	42995	09	8.593064	18	46	39.13%
55 p. 6,550	12000	8.91E-	0.000004		40	33.1370
organelle	43226	77	22.32285	292	1351	21.61%
•	43220		22.32203	292	1331	21.01%
non-membrane-	40000	6.43E-	04 04074	404	070	05 4404
bounded organelle	43228	58	21.81274	131	370	35.41%
		1.15E-				
vesicle	31982	52	20.75955	120	341	35.19%
membrane-		9.62E-				
bounded vesicle	31988	51	20.33995	116	331	35.05%
membrane-		1.11E-				
bounded organelle	43227	38	15.39918	198	1075	18.42%
macromolecular		7.83E-				
complex	32991	55	19.25985	199	861	23.11%
oop.ox	0200	9.43E-	10.2000	100	001	23.1170
protein complex	43234	22	11.53808	116	632	10 250/
protein complex	43234		11.55606	110	032	18.35%
annonella nort	44400	1.59E-	44.57040	405		4= 4004
organelle part	44422	22	11.57218	135	788	17.13%
		7.87E-				
biological_process	8150	69	17.72266	688	6137	11.21%
		3.33E-				
cellular process	9987	73	20.19146	447	2901	15.41%
cellular metabolic		1.36E-				
process	44237	49	16.88067	324	2072	15.64%
cellular				J.,	2012	10.0470
biosynthetic		3.51E-				
process	44249	5.51E-	19.71516	169	644	26.240/
cellular	<del>コマ</del> ムサフ	2.44E-	19.11010	103	644	26.24%
	24645		10.64040	400	040	04.0004
macromolecule	34645	46	19.61018	109	313	34.82%

biosynthetic process cellular biopolymer biosynthetic		2.17E-				
process	34961	46 2.28E-	19.61018	109	313	34.82%
translation nucleotide	6412	73	28.38839	94	138	68.12%
biosynthetic process purine nucleotide	9165	1.04E- 11	10.32801	24	58	41.38%
biosynthetic		1.39E-				
process purine	6164	10	10.09519	19	40	47.50%
ribonucleotide biosynthetic		6.37E-				
process ribonucleotide	9152	80	8.756662	14	29	48.28%
biosynthetic process	9260	2.83E- 08	0 007500	15	32	46.88%
cellular	9260	00	8.887592	15	32	40.00%
macromolecule		4.72E-				
metabolic process	44260	26	12.1671	215	1477	14.56%
cellular biopolymer metabolic process cellular protein	34960	5.3E-26 9.68E-	12.16612	212	1448	14.64%
metabolic process cellular nitrogen	44267	32	14.15787	166	892	18.61%
compound	24644	6.78E-	0.400044	50	220	00.040/
metabolic process cellular amine	34641	13 1.64E-	9.489644	52	228	22.81%
metabolic process cellular amino acid	44106	11 4.62E-	9.13975	41	164	25.00%
metabolic process cellular ketone	6520	12 2.53E-	9.489586	40	151	26.49%
metabolic process oxoacid metabolic	42180	11 2.53E-	8.60802	56	282	19.86%
process carboxylic acid	43436	11 2.45E-	8.623713	55	274	20.07%
metabolic process organic acid	19752	11 2.77E-	8.623713	55	274	20.07%
metabolic process heterocycle	6082	11 1.16E-	8.591688	55	275	20.00%
metabolic process purine nucleotide	46483	10 8.84E-	8.93913	34	125	27.20%
metabolic process cellular amino acid	6163	09	8.771992	19	49	38.78%
and derivative		1.83E-				
metabolic process nucleobase,	6519	10	8.533089	41	177	23.16%
nucleoside and nucleotide		8.23E-				
metabolic process nucleoside	55086	12	9.639485	34	114	29.82%
phosphate		6.45E-				
metabolic process nucleotide	6753	10 6.62E-	8.857555	27	87	31.03%
metabolic process	9117	0.02E- 10 7.71E-	8.857555	27	87	31.03%
metabolic process	9259	08	8.528981	15	34	44.12%

		0 E7E				
membrane	16044	8.57E- 11	9.239788	30	98	30.61%
organization	10044	9.22E-	9.239100	30	90	30.01%
membrane	40224		0.040646	25	84	29.76%
invagination	10324	09	8.242616			
endocytosis	6897	1.3E-08	8.208555	24	79	30.38%
vesicle-mediated		5.28E-				
transport	16192	10	8.454261	36	146	24.66%
cytoskeleton		1.32E-				
organization	7010	07	7.306421	28	116	24.14%
		5.93E-				
metabolic process	8152	48	16.21857	371	2611	14.21%
biosynthetic		1.67E-				
process	9058	52	19.46025	172	673	25.56%
macromolecule						
biosynthetic		1.98E-				
process	9059	45	19.29137	109	320	34.06%
biopolymer						
biosynthetic		5.23E-				
process	43284	46	19.4724	109	316	34.49%
primary metabolic		3.37E-				
process	44238	46	16.12814	328	2189	14.98%
protein metabolic		6.51E-				
process	19538	34	14.50192	187	1043	17.93%
macromolecule		1.55E-				
metabolic process	43170	27	12.43778	236	1658	14.23%
biopolymer .		8.89E-				
metabolic process	43283	28	12.52556	233	1620	14.38%
nitrogen compound		1.18E-				
metabolic process	6807	09	7.196168	110	842	13.06%
amine metabolic		4.89E-				
process	9308	10	8.267547	42	190	22.11%
multi-organism		5.43E-				
process	51704	19	13.71022	32	63	50.79%
response to other		3.98E-				
organism	51707	20	14.30793	32	59	54.24%
response to		1.85E-				
bacterium	9617	20	14.60327	31	54	57.41%
response to		8.43E-				
stimulus	50896	15	9.605665	89	505	17.62%
response to biotic		2.13E-				
stimulus	9607	15	11.62638	34	89	38.20%
cellular component	<del></del>			- •		20.2070
organization	16043	2.7E-14	9.556361	78	418	18.66%
g			J. J J J J J J		•	. 5.5575

**Table A.3** GO term enrichment for genes exhibiting a 2-fold increase in expression in the *arp8* null cell line in comparison to wild type cells 8H into starvation induced development. The P-value cut off was set at 0.01 and the GO data file used was gene\_association.ddb.

### A.2 GO analysis of chdC null RNA-seq data

Remember to mention no significant GO data for CHDC 0H 2-fold up!

	Gene Ontology					
Term	ID	P-Value	Z-Score	Selected	Total	%
molecular_function	3674	2.65E-10	7.150595	365	6797	5.37%
catalytic activity	3824	4.65E-07	6.19923	174	2791	6.23%
hydrolase activity	16787	8.51E-09	7.487896	87	1001	8.69%
hydrolase activity,						
acting on glycosyl						
bonds	16798	0.000241	6.56776	15	80	18.75%
hydrolase activity,						
hydrolyzing O-						
glycosyl	4550	0.000000	0.505404	4.4	74	40.700/
compounds	4553	0.000239	6.595434	14	71	19.72%
hydrolase activity, acting on ester						
bonds	16788	0.00596	4.540205	26	271	9.59%
nucleic acid	10700	0.00000	4.540205	20	211	3.5570
binding	3676	0.00459	-3.64643	17	924	1.84%
myosin binding	17022	0.00304	6.161973	9	37	24.32%
structural	16818		10,0416,74	Neg-	387	20.61%
constituent of						
cytoskeleton	5200	0.00384	6.191134	8	30	26.67%
cellular_component	5575	4.37E-06	5.346908	292	5566	5.25%
extracellular region	5576	0.00346	4.989998	12	78	15.38%
membrane part	44425	1.08E-05	5.710192	70	894	7.83%
intrinsic to						
membrane	31224	6.87E-06	6.217431	63	732	8.61%
integral to	10001	0.005.00	0 0000 17	00		0.500/
membrane	16021	6.23E-06	6.086047	62	727	8.53%
vacuole	5773	0.00202	5.340104	12	72	16.67%
lytic vacuole	323	0.000831	6.089317	10	45	22.22%
lysosome	5764	0.000997	6.089317	10	45	22.22%
nucleus	5634	0.00181	-3.54922	7	566	1.24%
biological_process	8150	1.36E-05	5.571043	319	6137	5.20%
cellular						
macromolecule						
biosynthetic process	34645	0.00815	2 42720	1	212	0.220/
cellular biopolymer	34043	0.00615	-3.43728	1 888	313	0.32%
biosynthetic						
process	34961	0.0068	-3.43728	1	313	0.32%
biopolymer						
biosynthetic						
process	43284	0.00904	-3.45684	1	316	0.32%
amine metabolic	Line Co.	A PARTICIO				
process	9308	0.008	4.805305	21	190	11.05%

**Table A.3** GO term enrichment for genes exhibiting a 2-fold decrease in expression in the *chdC* null cell line in comparison to wild type cells during vegetative growth. The P-value cut off was set at 0.01 and the GO data file used was gene\_association.ddb.

	Gene Ontology						
Term	ID	P-Value	Z-Score	Selected	Total	%	
catalytic activity	3824	6.49E-12	7.690488	573	2791	20.53%	
transferase activity	16740	6.82E-06	5.292469	216	996	21.69%	
transferase activity,							
transferring							
phosphorus-							
containing groups	16772	0.00047	4.281115	132	599	22.04%	
kinase activity	16301	0.000021	5.166175	111	453	24.50%	
protein kinase							
activity	4672	0.000968	4.228225	72	291	24.74%	
phosphotransferase							
activity, alcohol							
group as acceptor	16773	0.00186	3.987368	80	339	23.60%	
hydrolase activity	16787	3.71E-05	4.848972	212	1001	21.18%	
hydrolase activity,							
acting on acid							
anhydrides	16817	1.59E-06	5.888855	103	388	26.55%	
hydrolase activity,							
acting on acid							
anhydrides, in							
phosphorus-							
containing							
anhydrides	16818	1.66E-06	5.918574	103	387	26.61%	
pyrophosphatase							
activity	16462	1.51E-06	5.918574	103	387	26.61%	
nucleoside-							
triphosphatase			7.			and have	
activity	17111	2.01E-06	5.813744	101	381	26.51%	
microtubule motor		0.00405	- 1011-				
activity	3777	0.00125	5.124477	10	16	62.50%	
DNA-dependent	0004	4 045 05	0.000005	40	00	50.050/	
ATPase activity	8094	1.24E-05	6.280935	18	32	56.25%	
binding	5488	9.2E-12	7.563505	648	3235	20.03%	
nucleoside binding	1882	8.41E-09	6.754549	193	795	24.28%	
purine nucleoside	4000	0.045.00	0.754540	400	705	0.4.000/	
binding	1883	9.61E-09	6.754549	193	795	24.28%	
adenyl nucleotide binding	20554	1 125 00	6.754540	102	705	0.4.000/	
adenyl ribonucleotide	30554	1.13E-08	6.754549	193	795	24.28%	
binding	32559	7.39E-09	6.871155	187	759	24.64%	
ATP binding	5524	8.67E-09	6.746861	183	745		
						24.56%	
nucleotide binding ribonucleotide	166	0.000121	4.535641	235	1148	20.47%	
binding	32553	0.000018	5.052309	208	967	24 540/	
purine ribonucleotide	32333	0.000018	5.052509	200	907	21.51%	
binding	32555	0.000019	5.052309	208	967	21.51%	
purine nucleotide	32333	0.000019	3.032309	200	307	21.5170	
binding	17076	2.12E-05	4.994488	216	1014	21.30%	
nucleic acid binding	3676	0.000466	4.206077	191	924	20.67%	
DNA binding	3677	4.72E-17	10.12345	126	360		
transcription factor	3077	4.726-17	10.12345	120	300	35.00%	
activity	3700	0.000328	4.873428	34	102	33 330/	
The state of the s						33.33%	
protein binding	5515	0.00078	4.061562	179	866	20.67%	
protein dimerization	16092	0.000424	4 0F7192	24	62	20 740/	
activity	46983	0.000431	4.957182	24	62	38.71%	
ion binding	43167	0.00186	3.777184	173	849	20.38%	
transcription	30528	2.1E-06	5.993845	66	216	30.56%	

regulator activity						
structural constituent						
of ribosome	3735	5.55E-06	-4.38655	1	114	0.88%
metabolic process	8152	4.59E-06	5.403473	503	2611	19.26%
primary metabolic						
process	44238	5.97E-05	4.617783	418	2189	19.10%
carbohydrate	5075	0.705.05	E 0.4070	05	227	20 620/
metabolic process cellular carbohydrate	5975	2.73E-05	5.34679	65	227	28.63%
metabolic process	44262	0.00042	4.699929	36	113	31.86%
polysaccharide	1 1202	0.00012	1.000020			01.0070
metabolic process	5976	0.000722	4.98016	15	31	48.39%
translation	6412	1.58E-05	-4.4108	3	138	2.17%
protein modification						
process	6464	0.000277	4.423709	127	566	22.44%
post-translational	40007	0.000400	4 707400	07	007	0.4.400/
protein modification	43687	0.000106	4.787166	97	397	24.43%
protein amino acid phosphorylation	6468	0.000434	4.423807	73	290	25.17%
DNA metabolic	0400	0.000434	4.423007	73	290	25.1770
process	6259	0.000122	4.906445	60	215	27.91%
DNA strand	0_00	0.000				
elongation	22616	9.22E-06	6.92772	9	9	100.00%
DNA strand						
elongation during						
DNA replication	6271	8.56E-06	6.92772	9	9	100.00%
leading strand	0070	2.055.05	C 50407C	0		400.00%
elongation  DNA replication	6272	3.05E-05	6.531276	8	8	100.00%
initiation	6270	6.81E-05	6.112521	11	15	73.33%
DNA repair	6281	0.000416	4.793218	30	87	34.48%
mismatch repair	6298	4.92E-07	7.867725	14	16	87.50%
ncRNA metabolic	0230	4.52L-01	7.007720	14	10	07.0070
process	34660	0.00106	-3.60894	5	124	4.03%
deoxyribonucleotide						
metabolic process	9262	0.000161	6.01354	8	9	88.89%
cellular metabolic						
process	44237	0.000533	3.96853	388	2072	18.73%
phosphorus	6702	0.055.05	4 990793	00	250	25.079/
metabolic process phosphate metabolic	6793	8.25E-05	4.880783	90	359	25.07%
process	6796	8.51E-05	4.880783	90	359	25.07%
phosphorylation	16310	0.000157	4.738477	77	300	25.67%
macromolecule	.00.0	0.000.07	00	• •		
metabolic process	43170	0.00124	3.740984	314	1658	18.94%
biopolymer metabolic						
process	43283	0.00179	3.633647	306	1620	18.89%
biopolymer	10110			400		0.4 =00/
modification	43412	0.000759	4.086942	129	592	21.79%
cellular component organization	16043	1.97E-05	5.30688	105	418	25.12%
organelle	10043	1.97 =-03	3.30000	105	410	23.1270
organization	6996	3.53E-06	6.117856	74	248	29.84%
chromosome		J. J J _ U	2			
organization	51276	1.09E-06	6.981452	32	69	46.38%
chromatin						
organization	6325	3.81E-05	5.713269	25	58	43.10%
chromatin	40500	0.000057	E 400407	40	20	60.0001
modification	16568	0.000357	5.423437	12	20	60.00%

cellular process	9987	2.79E-05	4.80417	542	2901	18.68%
cell cycle process	22402	3.52E-06	6.786563	23	43	53.49%
microtubule-based						
process	7017	6.77E-05	5.819342	16	29	55.17%
cellular response to						
stimulus	51716	0.000234	4.896568	37	114	32.46%
cellular response to						
stress	33554	0.000653	4.562997	35	111	31.53%
cellular response to						
DNA damage						
stimulus	34984	0.000295	4.868855	33	98	33.67%
cell cycle	7049	0.00108	4.825247	15	32	46.88%
response to stimulus	50896	0.000236	4.502888	116	505	22.97%
•						
response to stress	6950	2.68E-05	5.234637	92	357	25.77%
response to DNA	0074	0.000440	4 7 4 4 4 0 0	0.4	404	00 000/
damage stimulus	6974	0.000416	4.741423	34	104	32.69%
regulation of	40000	4 705 05	5 400007	00	000	00 050/
metabolic process	19222	1.76E-05	5.426367	83	308	26.95%
regulation of						
macromolecule	22255					
metabolic process	60255	4.63E-06	5.919053	76	262	29.01%
regulation of gene	10.100					
expression	10468	3.03E-06	6.078083	74	249	29.72%
regulation of						
transcription	45449	2.76E-06	6.251205	69	223	30.94%
regulation of						
transcription, DNA-						
dependent	6355	1.65E-05	5.620653	59	194	30.41%
regulation of						
macromolecule						
biosynthetic process	10556	5.39E-06	5.884761	72	245	29.39%
regulation of RNA						
metabolic process	51252	1.76E-05	5.575188	59	195	30.26%
regulation of nitrogen						
compound metabolic						
process	51171	6.32E-06	5.8055	76	265	28.68%
regulation of						
nucleobase,						
nucleoside,						
nucleotide and						
nucleic acid						
metabolic process	19219	6.11E-06	5.804665	74	256	28.91%
regulation of						
biosynthetic process	9889	1.87E-05	5.41446	75	271	27.68%
regulation of cellular						
biosynthetic process	31326	1.96E-05	5.41446	75	271	27.68%
regulation of primary						
metabolic process	80090	0.000032	5.234489	75	276	27.17%
regulation of cellular						
metabolic process	31323	4.15E-05	5.143595	77	288	26.74%
cell part	44464	2.31E-06	5.353356	629	3360	18.72%
intracellular part	44424	0.0017	3.590426	378	2047	18.47%
ribonucleoprotein	, <u> </u>	·	2.22 <b>2.23</b>	<del>-</del>		
complex	30529	8.19E-05	-4.22123	12	219	5.48%
ribosome	5840	7.91E-05	-3.97834	1	96	1.04%
intracellular organelle	<del>5570</del>	7.01L-00	-0.97007	•	30	1.07/0
part	44446	0.000315	4.314283	167	786	21.25%
•	44427	2.46E-10	8.407753	38		
chromosomal part nuclear chromosome					74	51.35%
DUCIDAL CHIOMOSOMO	44454	6.06E-06	6.61354	16	25	64.00%

part						
nuclear part	44428	4.47E-05	5.129037	83	317	26.18%
nucleoplasm part	44451	0.000306	4.834849	37	115	32.17%
nucleus	5634	8.34E-08	6.425036	144	566	25.44%
chromosome	5694	0.000468	5.141158	14	27	51.85%
organelle part	44422	0.00033	4.277342	167	788	21.19%
protein complex	43234	0.000382	4.26099	138	632	21.84%

**Table A.4** GO term enrichment for genes exhibiting a 2-fold decrease in expression in the *chdC* null cell line in comparison to wild type cells 8H into starvation induced development. The P-value cut off was set at 0.01 and the GO data file used was gene\_association.ddb.

Term	Gene Ontology ID	P- Value	Z-Score	Selected	Total	%
ICIIII	ID	2.87E-	2-30016	Selected	IOtal	/0
molecular_function structural molecule	3674	81 2.25E-	18.8843	786	6797	11.56%
activity structural	5198	66	25.70577	101	175	57.71%
constituent of		4.77E-				
ribosome	3735	68 6.94E-	27.26351	84	114	73.68%
binding	5488	44 3.05E-	15.16726	434	3235	13.42%
protein binding cytoskeletal protein	5515	21 2.75E-	11.36007	148	866	17.09%
binding	8092	24 6.56E-	14.36524	58	156	37.18%
actin binding	3779	17 9.26E-	11.99881	41	111	36.94%
nucleotide binding purine nucleotide	166	16 6.66E-	9.420643	164	1148	14.29%
binding adenyl nucleotide	17076	15 1.46E-	9.199619	148	1014	14.60%
binding adenyl ribonucleotide	30554	12 4.42E-	8.490918	119	795	14.97%
binding	32559	4.42E- 10 1.47E-	7.481237	108	759	14.23%
ATP binding purine	5524	10	7.695635	108	745	14.50%
ribonucleotide		1.86E-				
binding ribonucleotide	32555	12 1.75E-	8.309626	136	967	14.06%
binding	32553	12 1.25E-	8.309626	136	967	14.06%
nucleoside binding purine nucleoside	1882	12 1.35E-	8.490918	119	795	14.97%
binding	1883	12 9.45E-	8.490918	119	795	14.97%
catalytic activity	3824	21 1.57E-	10.33897	332	2791	11.90%
hydrolase activity	16787	12 2.91E-	8.36748	140	1001	13.99%
biological_process	8150	66 3.3E-	17.47815	715	6137	11.65%
cellular process cellular metabolic	9987	63 5.1E-	18.61598	445	2901	15.34%
process cellular	44237	37	14.34542	309	2072	14.91%
biosynthetic process cellular	44249	1.52E- 33	14.96433	144	644	22.36%
macromolecule biosynthetic		6.73E-				
process cellular biopolymer	34645	38	17.31816	102	313	32.59%
biosynthetic process	34961	5.77E- 38	17.31816	102	313	32.59%
process	34301	30	17.01010	102	313	32.3370

		5.51E-				
translation	6412	60	24.87952	86	138	62.32%
cellular						
macromolecule	44060	3.96E-	44.0500	246	1477	14.62%
metabolic process cellular biopolymer	44260	23 1.81E-	11.3586	216	1477	14.02%
metabolic process	34960	23	11,47191	214	1448	14.78%
cellular protein		4.83E-				
metabolic process	44267	34	14.66908	176	892	19.73%
cellular component movement	6928	3.84E- 19	13.03142	40	95	42.11%
actin filament-	0920	1.26E-	13.03142	40	90	42.11/0
based process	30029	17	12.43076	38	93	40.86%
actin cytoskeleton		1.8E-				
organization	30036	17	12.41729	37	89	41.57%
actin filament organization	7015	5.09E- 13	11.03881	24	50	48.00%
membrane	7010	7.03E-	11.00001			, 0.00,
organization	16044	16	11.58043	37	98	37.76%
membrane	40004	1.49E-	40.0040	25	0.4	44.070/
invagination	10324	16 1.06E-	12.0942	35	84	41.67%
endocytosis	6897	15	11.7626	33	79	41.77%
, , , , , , , , , , , , , , , , , , , ,		1.19E-				
cell division	51301	14	11.05824	35	95	36.84%
outokinopio	910	6.87E- 16	11.86929	33	78	42.31%
cytokinesis vesicle-mediated	910	5.75E-	11.00323	33	70	42.3170
transport	16192	12	9.336917	40	146	27.40%
cytoskeleton		2.03E-				
organization	7010	16	11.60828	41	116	35.34%
cellular component morphogenesis	32989	1.48E- 11	10.53198	20	39	51.28%
morphogeneous	02000	1.45E-	10.00100	20		01.2070
cell morphogenesis	902	11	10.53198	20	39	51.28%
	0450	1.28E-	44.4004	205	0044	40.000/
metabolic process primary metabolic	8152	38 7.05E-	14.4601	365	2611	13.98%
process	44238	41	15.13841	330	2189	15.08%
protein metabolic		8.95E-				
process	19538	37	15.11841	199	1043	19.08%
biosynthetic process	9058	6.38E- 32	14.48354	145	673	21.55%
macromolecule	3030	<b>52</b>	14.40004	140	0,0	21.0070
biosynthetic		4.17E-				
process	9059	37	17.02073	102	320	31.88%
biopolymer biosynthetic		1.33E-				
process	43284	37	17.18963	102	316	32.28%
macromolecule		1.94E-				
metabolic process	43170	25	11.87757	240	1658	14.48%
biopolymer	43283	3.98E- 26	12.07723	238	1620	14.69%
metabolic process cellular component	43203	1.47E-	12.07723	230	1020	14.09%
organization	16043	16	10.33955	85	418	20.33%
response to		2.18E-				
stimulus	50896	14 1 125	9.370221	91	505	18.02%
behavior	7610	1.12E- 10	9.027137	31	101	30.69%
locomotory	7626	1.14E-	9.027137	31	101	30.69%
	<del></del>			-		

behavior		10				
taxis	42330	1.09E- 10	9.027137	31	101	30.69%
chemotaxis response to	6935	5.86E- 10 4.4E-	8.748621	28	89	31.46%
external stimulus response to biotic	9605	10 5.98E-	8.073005	48	226	21.24%
stimulus response to other	9607	10 4.94E-	8.748621	28	89	31.46%
organism response to	51707	13 3.88E-	10.835	26	59	44.07%
bacterium response to	9617	12 1.88E-	10.4701	24	54	44.44%
radiation developmental	9314	10 9.05E-	10.00906	18	35	51.43%
process multi-organism	32502	14 3.74E-	9.420941	70	342	20.47%
process biological	51704	13 1.24E-	10.82875	27	63	42.86%
regulation of	65007	12 5.88E-	8.335921	130	908	14.32%
biological process regulation of	50789	12 3.35E-	8.094288	123	859	14.32%
cellular process	50794	12 1.94E-	8.223512	120	822	14.60%
locomotion	40011	11 4.47E-	9.305255	34	113	30.09%
cellular_component	5575	66 2.43E-	17.54635	671	5566	12.06%
cell part	44464	68 9.69E-	19.00112	496	3360	14.76%
intracellular part	44424	64 4.8E-	19.18339	359	2047	17.54%
cytoplasmic part	44444	82 2.99E-	23.71304	275	1084	25.37%
cytoplasmic vesicle cytoplasmic	31410	50	20.14994	116	318	36.48%
membrane- bounded vesicle	16023	1.1E- 50	20.29153	116	315	36.83%
endocytic vesicle	30139	1.35E- 50 7.16E-	20.3328	114	305	37.38%
phagocytic vesicle	45335	51 4.36E-	20.43097	114	303	37.62%
phagolysosome	32010	10 1.38E-	9.849226	15	26	57.69%
ribosome	5840	49 5.24E-	22.74975	65	96	67.71%
ribosomal subunit	33279	13 4.61E-	11.76381	16	22	72.73%
cell cortex part cortical	44448	10 4.91E-	9.665204	16	30	53.33%
cytoskeleton intracellular	30863	12 7.14E-	11.26463	15	21	71.43%
organelle intracellular non-	43229	66	20.37971	284	1346	21.10%
membrane- bounded organelle	43232	1.78E- 60	22.18836	137	370	37.03%
cytoskeleton	5856	1.1E-	13.62617	44	105	41.90%

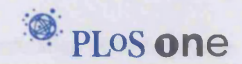
		21 2.21E-				
actin cytoskeleton intracellular	15629	12	10.11507	26	65	40.00%
membrane-		1.6E-				
bounded organelle ribonucleoprotein	43231	32 4.28E-	13.89336	193	1075	17.95%
complex	30529	30	15.38348	75	219	34.25%
intracellular		4.29E-		44-		4=
organelle part	44446	16 3.36E-	9.474691	125	786	15.90%
cytoskeletal part	44430	21	12.57625	60	196	30.61%
actin filament	5884	1.52E- 11	11.09113	14	19	73.68%
actin mament	3004	1.38E-	11.03113	17	19	7 3.00 70
intracellular	5622	29	13.8447	128	582	21.99%
cell leading edge	31252	7.03E- 20	13.94232	30	52	57.69%
cen leading eage	01202	3.52E-	10.04202	30	<b>52</b>	37.0370
cell projection	42995	18	13.37167	27	46	58.70%
pseudopodium	31143	3.58E- 11	10.647	15	23	65.22%
podudopodiam	01140	2.48E-	10.047	10	20	00.2270
phagocytic cup	1891	13	11.52536	19	31	61.29%
organelle	43226	1.54E- 66	20.52558	286	1351	21.17%
non-membrane-	10220	2.04E-	20.02000	200	1001	21.1770
bounded organelle	43228	60	22.18836	137	370	37.03%
vesicle	31982	1.72E- 53	20.8021	124	341	36.36%
membrane-	01002	1.78E-	20.0021	127	541	30.3070
bounded vesicle	31988	52	20.6228	121	331	36.56%
membrane- bounded organelle	43227	1.7E- 32	13.89336	193	1075	17.95%
macromolecular	10221	5.87E-	10.0000	100	1070	11.0070
complex	32991	32	14.00508	167	861	19.40%
organelle part	44422	5.06E- 16	9.442731	125	788	15.86%
organicho part	77766	10	J.772131	120	, 00	10.0070

**Table A.5** GO term enrichment for genes exhibiting a 2-fold increase in expression in the *chdC* null cell line in comparison to wild type cells 8H into starvation induced development. The P-value cut off was set at 0.01 and the GO data file used was gene\_association.ddb.

# **Appendicies**

Appendix B

**Published Papers.** 



# Genetic Control of Lithium Sensitivity and Regulation of Inositol Biosynthetic Genes

Jason King<sup>1</sup><sup>x</sup>, Melanie Keim<sup>1</sup>, Regina Teo<sup>1</sup>, Karin E. Weening<sup>1</sup>, Mridu Kapur<sup>1</sup>, Karina McQuillan<sup>1</sup>, Jonathan Ryves<sup>1</sup>, Ben Rogers<sup>1</sup>, Emma Dalton<sup>1</sup>, Robin S. B. Williams<sup>2</sup>, Adrian J. Harwood<sup>1</sup>\*

1 School of Biosciences, Cardiff University, Cardiff, United Kingdom, 2 School of Biological Sciences, Royal Holloway, University of London, Egham, Surrey, United Kingdom

#### **Abstract**

Lithium (Li<sup>†</sup>) is a common treatment for bipolar mood disorder, a major psychiatric illness with a lifetime prevalence of more than 1%. Risk of bipolar disorder is heavily influenced by genetic predisposition, but is a complex genetic trait and, to date, genetic studies have provided little insight into its molecular origins. An alternative approach is to investigate the genetics of Li<sup>†</sup> sensitivity. Using the social amoeba *Dictyostelium*, we previously identified prolyl oligopeptidase (PO) as a modulator of Li<sup>†</sup> sensitivity. In a link to the clinic, PO enzyme activity is altered in bipolar disorder patients. Further studies demonstrated that PO is a negative regulator of inositol(1,4,5)trisphosphate (IP<sub>3</sub>) synthesis, a Li<sup>†</sup> sensitive intracellular signal. However, it was unclear how PO could influence either Li<sup>†</sup> sensitivity or risk of bipolar disorder. Here we show that in both *Dictyostelium* and cultured human cells PO acts via Multiple Inositol Polyphosphate Phosphatase (Mipp1) to control gene expression. This reveals a novel, gene regulatory network that modulates inositol metabolism and Li<sup>†</sup> sensitivity. Among its targets is the inositol monophosphatase gene IMPA2, which has also been associated with risk of bipolar disorder in some family studies, and our observations offer a cellular signalling pathway in which PO activity and IMPA2 gene expression converge.

Citation: King J, Keim M, Teo R, Weening KE, Kapur M, et al. (2010) Genetic Control of Lithium Sensitivity and Regulation of Inositol Biosynthetic Genes. PLoS ONE 5(6): e11151. doi:10.1371/journal.pone.0011151

Editor: Robert Alan Arkowitz, CNRS UMR6543, Université de Nice, Sophia Antipolis, France

Received January 11, 2010; Accepted March 30, 2010; Published June 17, 2010

Copyright: © 2010 King et al. This is an open-access article distributed under the terms of the Creative Commons Attribution License, which permits unrestricted use, distribution, and reproduction in any medium, provided the original author and source are credited.

Funding: This work was supported by a Wellcome Trust Programme Grant to AJH (74540) and a BBSRC committee studentship to JSK. The funders had no role in study design, data collection and analysis, decision to publish, or preparation of the manuscript.

Competing Interests: The authors have declared that no competing interests exist.

\* E-mail: harwoodaj@cf.ac.uk

© Current address: CR-UK Beatson Institute for Cancer Research, Glasgow, United Kingdom

#### Introduction

Bipolar mood disorder is a common psychiatric disorder, which is treated using mood stabilizer drugs, such as lithium (Li<sup>†</sup>). There is a strong genetic component to risk of developing bipolar disorder, however this is a complex genetic trait and no consensus candidate susceptibility genes have yet emerged from those identified in individual family studies [1]. Genetics is not the only factor affecting risk, and twin studies demonstrate the presence of environmental inputs [2,3]. Environmental risk factors include lifetime events and psychosocial stressors, physical illnesses and hormonal imbalances [4]. Onset of bipolar disorder is most frequent during late adolescence and early adulthood suggesting contributions from developmental and physiological mechanisms. As in the case of genetics, the biological mechanisms underlying environmental risk are also unclear.

An alternative approach is to investigate the therapeutic mechanisms of the mood stabilizer drugs used to treatment bipolar disorder. Li<sup>+</sup> is the most widely used mood stabilizer, taken by 50% of bipolar patients. It is an effective prophylactic agent and good anti-manic, but a weaker anti-depressant treatment [5]. Inositol monophosphatase (IMPase) and Inositol 1-polyphosphatase (IPP) are direct biochemical targets of Li<sup>+</sup> [6,7], and Li<sup>+</sup> treatment leads to reduced inositol synthesis and suppression of inositol phosphate (IP) signalling. Consequently, it has been proposed that the neurological processes underlying bipolar mood

disorder are susceptible to aberrant IP signalling [8]. Consistent with this hypothesis, the structurally unrelated mood stabilizers valproic acid (VPA) and carbamazepine also deplete inositol [9,10], indicating a wider association between mood stabilizers and IP signalling.

To understand why Li<sup>+</sup> is an effective therapy, we undertook a genetic screen for Li<sup>+</sup> resistance in the social amoeba *Dictyostelium*. This identified the serine protease prolyl oligopeptidase (PO) as a modulator of Li<sup>+</sup> sensitivity [11]. Interestingly, reduced PO activity has been associated with bipolar disorder [12,13,14]. We found that ablation of the PO gene or inhibition of PO enzyme activity is accompanied by an increase in inositol(1,4,5)trisphosphate (IP<sub>3</sub>) production. This inhibitory interaction is conserved in mammalian cells as reduced PO activity increases IP<sub>3</sub> in astroglioma and COS-7 kidney cell lines [10,15]. These effects are manifest at the cellular level where PO inhibition both reverses the effects of Li<sup>+</sup>, VPA and carbamazepine on neuronal growth cone morphology and stimulates removal of protein aggregates via macro-autophagy [9,10,16,17].

The mechanism by which PO controls Li<sup>+</sup> sensitivity has not been established. Initial *Dictyostelium* studies showed that PO null mutants had unaltered phospholipase C activity but increased activity of two inositol phosphate phosphatases. One phosphatase activity corresponds to multiple inositol polyphosphate phosphatase (Mipp1), which dephosphorylates IP<sub>6</sub> to IP<sub>3</sub>. The other is an IP<sub>3</sub> 5-phosphatase activity that dephosphorylates IP<sub>3</sub> further to

I(1,4)P<sub>2</sub> [11]. Here, we report that Mipp1 is required to mediate the effects of PO on Li<sup>+</sup> sensitivity. Furthermore, we show that these effects do not arise through direct elevation of IP<sub>3</sub> production as previously assumed, but are due to changes in the expression of genes involved in inositol synthesis and metabolism, including inositol synthase (*ino1*), IMPase (*impA1*) and the *Dictyostelium* IP<sub>3</sub> 5-phosphatase (Dd5P3). Finally, we show that this PO mediated regulation of gene expression is conserved in human cells where among its targets is IMPA2, a gene associated with risk in some bipolar disorder patient family studies. Our observations suggest a signalling pathway that could connect altered PO mediated signalling to aberrant IMPA2 gene regulation.

#### Results

## Dictyostelium PO, dpoA, reduces the effect of Li<sup>+</sup> on chemotaxis

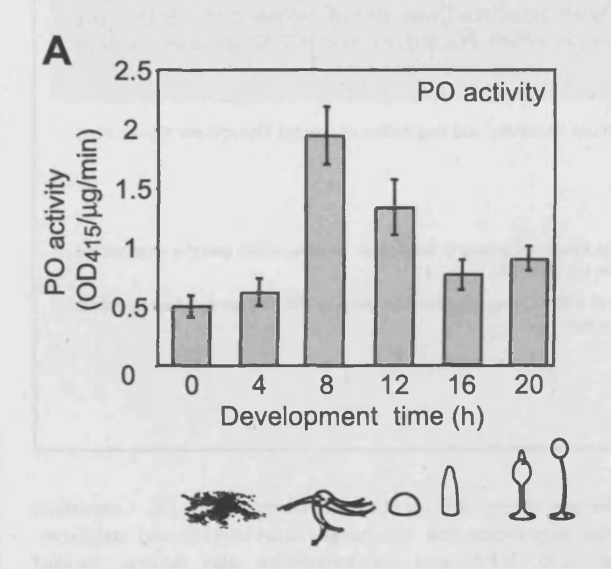
Starved *Dictyostelium* cells aggregate by cAMP-mediated chemotaxis to form a multicellular mass of 100,000 cells, which develops further into a fruiting body of spore and stalk cells [18]. We found

that PO activity is regulated throughout *Dictyostelium* development, peaking during late aggregation and early multicellular stages (Figure 1A), indicative of a regulatory function.

Li<sup>+</sup> treatment of wild type cells has a specific effect on chemotaxis, causing reduced cell speed and Directionality (a measure of the linearity of the cell path) [19]. We found that chemotaxis of *dpoA* mutant cells was less sensitive to Li<sup>+</sup>, with cells exhibiting greater speed and Directionality in the presence of Li<sup>+</sup> than wild type cells (Figure 1B; Table 1). We also noted that *dpoA* mutant cells exhibited increased speed of movement in control conditions, treatment with NaCl, suggesting that DpoA suppresses this aspect of the chemotaxis response.

# Dictyostelium PO acts via Multiple Inositol Polyphosphate Phosphatase (Mipp1)

Previous results indicated that loss of *dpoA* is associated with increased activity of multiple inositol polyphosphate phosphatase (MIPP), an enzyme that dephosphorylates IP<sub>6</sub>, IP<sub>5</sub> and certain IP<sub>4</sub> species to form IP<sub>3</sub> [11]. The *Dictyostelium* genome contains two homologues of the mammalian MIPP, however only one gene,



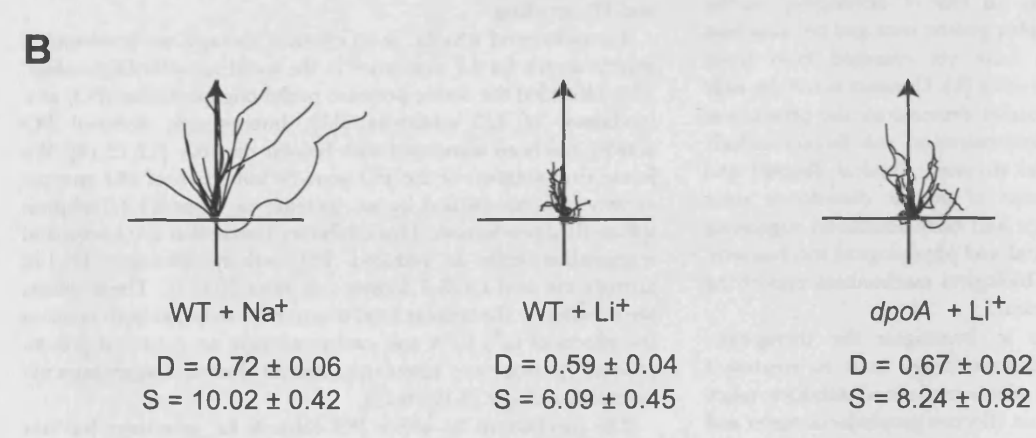


Figure 1. Loss of *dpoA* reduces Li<sup>+</sup> sensitivity. A, PO activity peaks at 8 hours of *Dictyostelium* development, and then declines to levels only slightly higher than in growing cells (0 hours of development). Error Bars: mean ± standard error of 3 independent experiments. Peak activity corresponds to streaming and mound developmental stages. B, Cell tracks of wild type and mutant cells in 7 mM LiCl (or control of 7 mM NaCl) during chemotaxis along a 1 nM/μm cAMP gradient (direction of arrow). D = Directionality, S = cell speed (μm/min). *dpoA* null mutants have a reduced Li<sup>+</sup> sensitivity, showing higher Directionality and speed than wild type in Li<sup>+</sup>. doi:10.1371/journal.pone.0011151.g001

Table 1. Chemotactic analysis of lithium sensitivity.

Strain		Directionality (D)		Relative lithium sensitivity		
			Speed (s) (µm/min)	Directionality	Speed	
Wild type	Na	0.72±0.06	10.02±0.42			
	Li	0.59±0.04 <sup>††</sup>	6.09±0.45 <sup>†††</sup>			
dpoA	Na	0.68 ± 0.02	11.34±0.57 <sup>6</sup>			
	Li	0.67 ± 0.02 ***	8.24±0.82°	++	++	
mipp1	Na	0.69±0.02	9.65±0.19			
	U	0.50±0.06 <sup>†††</sup>	4.69±0.58 <sup>†††</sup>			
mipp1:dpoA	Na	0.73 ± 0.03	9.62±0.27			
	Li	0.51 ± 0.04 <sup>†††</sup>	5.46±0.22 <sup>†††,\$</sup>			
mipp1 <sup>oe</sup>	Na	0.68 ± 0.03	9.02±0.79			
	Li	0.46 ± 0.04 <sup>†††</sup>	2.96±0.12 <sup>†††</sup>		***	
ImpA1 <sup>oe</sup>	Na	0.70±0.06	9.80±0.60			
	Li	0.66 ± 0.05*	7.85±0.43**	++	++	
ImpA1 <sup>oe</sup> :Ino1 <sup>oe</sup>	Na	0.51 ± 0.02	18.89±0.84			
	Li	0.41 ± 0.03	8.48±0.46*		++	
ipkA1 <sup>oe</sup>	Na	0.77±0.05	10.03±0.80			
	Li	0.68±0.03***	10.07±0.65***	++	+++	
ipkB <sup>oe</sup>	Na	0.69±0.01	10.03±0.22			
	Li	0.71±0.03***	9.08±0.95***	+++	++	
mipp1:ipkA1 <sup>oe</sup>	Na	0.65 ± 0.02	8.09±0.59			
	Li	0.36±0.04	4.64±0.60		a specialist	
mipp1:ipkB <sup>oe</sup>	Na	0.62±0.11	8.74±1.79			
No. of Street, Square,	Li	0.40±0.01	5.43 ± 0.54		F	

Cells were treated with 7mM LiCl or NaCl (control treatment) for one hour prior to analysis. Values shown are the mean ± standard error of data from at least three independent experiments. Directionality is defined as the total distance moved divided by the net distance moved. Statistical analysis: two-tailed t-test. tttp<0.001.

This is based on the difference between the numerical values for lithium treatment of wild type and mutant cells, as calculated by (value of mutant in Lithium)/(value for WT in Lithium). For Directionality: (- - -) 60-69% of wild type; (- -) 70-79% of wild type; (- -) 80-89% of wild type; (++) 110-119% of wild type; (+++) 120-129% of wild type. For speed: (- - -) 25-49% of wild type; (- -) 50-74% of wild type; (-) 75-99% of wild type; (++) 125-149% of wild type; (+++) 150-174% of wild type. doi:10.1371/journal.pone.0011151.t001

denoted mipp1, is expressed in growing cells and during development (data not shown). We generated null mutant cell strains, which lack the mipp I gene, and strains that over-expressed Dictyostelium Mipp1. These latter strains were a useful source of Mippl enzyme, which was used to show that Mippl rapidly converts IP<sub>6</sub> to IP<sub>3</sub> (Figure 2A). mipp1 null mutants completely lack Mipp activity and Mippl over-expressors greatly enhanced activity (Figure 2B). However, total mass measurement of all inositol phosphates (IPs) showed that loss of mipp1 had no significant effect on the overall concentrations of IP4, IP5 and IP<sub>6</sub> (data not shown) suggesting that Mipp1 regulates only a small proportion of the cellular IPs. Such robustness in the cellular content of the higher order IPs has been observed previously and means that small changes of the IP species involved in signalling may be masked behind larger non-dynamic IP populations [20].

Chemotaxis of mipp1 null mutants was hypersensitive to Li<sup>+</sup> (Figure 2C), the opposite phenotype of dpoA mutant cells. Double dpoA.mipp1 null mutant cells possess a similar Li<sup>+</sup> hypersensitive phenotype to mipp1 null cells (Figure 2C), indicating that Mipp1

activity is required for PO mediated signalling. Consistent with this we found that elevation of IP3 following PO inhibition was also dependent on Mipp1. The IP3 concentration of wild type cells doubled within 30 minutes of addition of the PO inhibitor Z-pro-L-prolinal (Figure 2D). This increase was transient and IP<sub>3</sub> returned to basal levels after 60 minutes. PO inhibitors were unable to elevate IP3 in mipp1 null mutants (Figure 2D).

To investigate the interaction between PO and Mipp1 at the biochemical level, we pre-incubated Mipp1 extracts with bacterially produced recombinant DpoA protein, and then monitored Mipp1 activity. Incubation with DpoA enzyme caused an approximate twofold decrease in Mipp1 activity, an effect reversed by treatment with PO inhibitor (Figure 2E). However, there was no change in the abundance or size of the Mipp1 protein following PO treatment (Figure 2E), arguing against direct proteolysis. Mipp I is extracted as a membranous particulate fraction and the most likely explanation is that PO acts on a yet unidentified, co-purified intermediate protein or peptide. These results however do indicate a close association between PO activity and Mipp1 regulation.

ttp<0.02, compared to NaCl control treatment.

<sup>\*\*\*</sup>p<0.005,

<sup>\*\*</sup>p<0.05,

p<0.1, compared to LiCI-treated wild-type cells.

<sup>§</sup>p<0.001, compared to NaCl treated wild type cells.

<sup>\$</sup> p<0.05, compared to LiCl treated dpoA null cells.

Relative lithium sensitivity

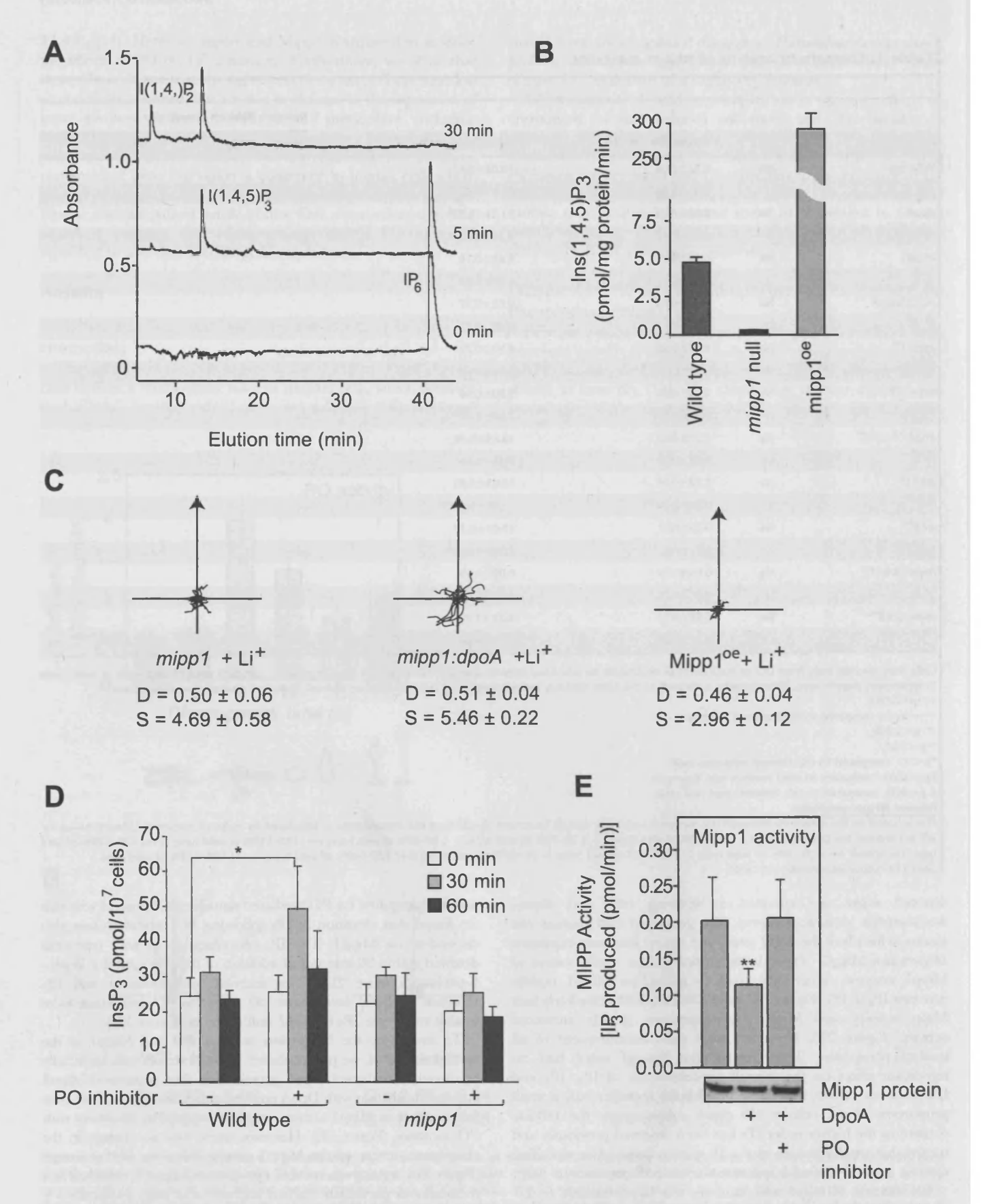


Figure 2. Mipp1 mediates the effects of PO inhibition. A, Mipp1 enzyme prepared from Mipp1 over-expressing cells were incubated with 10 nmoles InsP<sub>6</sub> for the indicated times and analyzed by HPLC-MDD. I(1,4)P<sub>2</sub> was generated by contaminating IP<sub>3</sub> 5-phosphatase activity, and

demonstrates that the product of Mipp1 is I(1,4,5)P<sub>3</sub>. **B**, Mipp1 activity measured as the rate of IP<sub>3</sub> formation in extracts from wild type, *mipp1* null mutant and Mipp1overexpressingcells. **C**, Cell tracks of wild type and *mipp1* mutant cells in 7 mM LiCl (or control of 7 mM NaCl) during chemotaxis. *mipp*, *mipp:dpoA* and Mipp1 over-expressing mutants (Mipp1°) are Li<sup>+</sup> hypersensitive compared to wild type. D = Directionality, S = cell speed (μm/min). **D**, Vegetative wild type and *mipp1* null cells were treated with either 1.2 mM Z-pro-L-prolinal or an equal volume of DMSO carrier as a control. Samples were then removed at the times indicated and IP<sub>3</sub> concentration measured. Values plotted as mean ± standard error of 4 independent experiments. \* P<0.05, paired T-test. **E**, Mipp1 protein extracts were incubated with recombinant DpoA with or without the PO inhibitor Z-pro-L-prolinal. Mipp1 activity is measured by the production of IP<sub>3</sub> from IP<sub>6</sub>. Values plotted as mean ± standard error of 3 independent experiments. \* P<0.01, paired T-test. Samples of Mipp1 protein are shown on Western (underneath). doi:10.1371/journal.pone.0011151.g002

#### Over-expression of Mipp1 causes Li<sup>+</sup> hypersensitivity

A simple hypothesis is that decreased PO activity controls Li<sup>+</sup> sensitivity through Mipp1 mediated changes in IP3 abundance, but a number of observations show this is not the case. First, Mippl over-expression would be expected to increase the IP<sub>3</sub> concentration and reduce Li+ sensitivity, however Mippl overexpressing cells are strongly Li<sup>+</sup> hypersensitive (Figure 2C). Second, in the absence of PO inhibition, we found that neither loss nor over-expression of Mipp1 altered the cellular concentration of IP3, despite both causing Li<sup>+</sup> hypersensitivity (data not shown). This lack of correlation argues against generation of IP3 as a direct mechanism for Li<sup>+</sup> resistance. The same lack of reciprocity also argues against a mechanism involving depletion of the Mipp1 substrate IP<sub>6</sub> or its alternative substrate 2,3-bisphosphoglycerate (2,3-BPG) [21].  $I(1,3,4,5,6)P_5$  and  $I(1,4,5,6)P_4/I(1,3,4,5)P_4$  are intermediates in the dephosphorylation of IP6 to I(1,4,5)P3 by Mippl and both have signalling properties within the cell. Mippl could therefore play a more complex role by regulating the abundance of these molecules through controlling the balance of their synthesis and degradation.

# Over-expression of the IP<sub>3</sub> kinases IpkA1 and IpkB confers Li<sup>+</sup> resistance

In all but one case, it was not possible to observe direct changes in the abundance of IPs in our mutants, however the exception was seen in Mipp1 over-expressing cells, which exhibited a large decrease in the cellular I(1,3,4,5,6)P<sub>5</sub> concentration, in addition to

decreased IP<sub>6</sub> (Figure 3A). As this correlates with a strong Li<sup>+</sup> hypersensitive phenotype, it suggested a positive role of I(1,3,4,5,6)P<sub>5</sub> signalling in establishing Li<sup>+</sup> sensitivity. To pursue this possibility, we over-expressed two structurally distinct IP<sub>3</sub> kinases (IpkA1 and IpkB) each capable of generating I(1,3,4,5,6)P<sub>5</sub> [22,23,24]. In the reverse of that seen for Mipp1 over-expression, chemotaxis of cells over expressing either IpkA1 or IpkB was resistant to Li<sup>+</sup> (Figure 3B). Interestingly, we found that the Li<sup>+</sup> resistant phenotype was lost when the IpkA1 or IpkB were over-expressed in a *mipp1* null mutant background (Figure 3B), arguing that Mipp1 activity may be the key regulator of this signal pathway.

#### DpoA acts via Mipp1-mediated gene regulation

As the yeast homologue of *ipkA1*, Ipk2/Arg82, controls expression of the inositol synthase gene (*ino1*) [25], we investigated potential changes in gene expression mediated by PO and Mipp1. Expression of the *Dictyostelium ino1* gene [9,26] was elevated both in *dpoA* null cells and cells treated with PO inhibitor (Figure 4A,B). Furthermore both conditions gave a 60-100% increase in expression of the genes encoding IMPase (*impA1*), IPP (*ippA* and *ippB*) and Dd5P3, a phosphatase that converts I(1,4,5)P<sub>3</sub> to I(1,4)P<sub>2</sub> (see Table S1). Dd5P3 is homologous to the synaptojanin-like IP<sub>3</sub> 5-phosphatase conserved from yeast to humans [27] and its elevated expression is consistent with the elevated IP<sub>3</sub> 5-phosphatase activity previously observed in *dpoA* null cells [11]. No change was seen for *mipp1*, *dpoA* or *ipkA1* genes (Figure 4B).

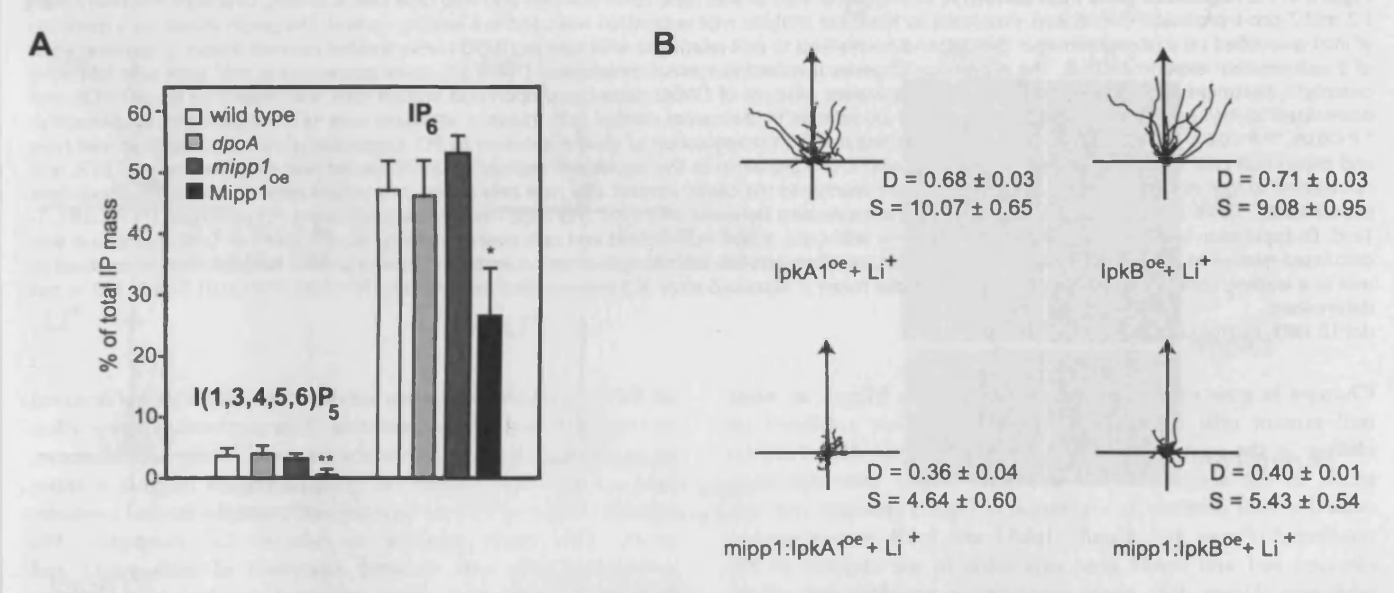


Figure 3. Elevated expression of Mipp1 and IP<sub>3</sub> kinases alter lithium sensitivity. A, Comparison of the I(1,3,4,5,6)P<sub>5</sub> and IP<sub>6</sub> concentration of wild type, dpoA null; mipp1 null and Mipp1 over-expressing cells. Values plotted (means  $\pm$  standard error of 3 independent experiments) as percentage of the total IP content relative to wild type (\*P<0.05, \*\* P<0.01 T-test). B, Cell tracks of wild type and mipp1 null mutant cells over-expressing lpkA1 and lpkB during chemotaxis in 7 mM LiCl. D = Directionality, S = cell speed ( $\mu$ m/min). Over-expression of lpkA1 and lpkB in wild type cells confers Li<sup>+</sup> resistance, whereas Li<sup>+</sup> hypersensitivity is maintained after over-expression in a mipp1 null mutant. doi:10.1371/journal.pone.0011151.g003

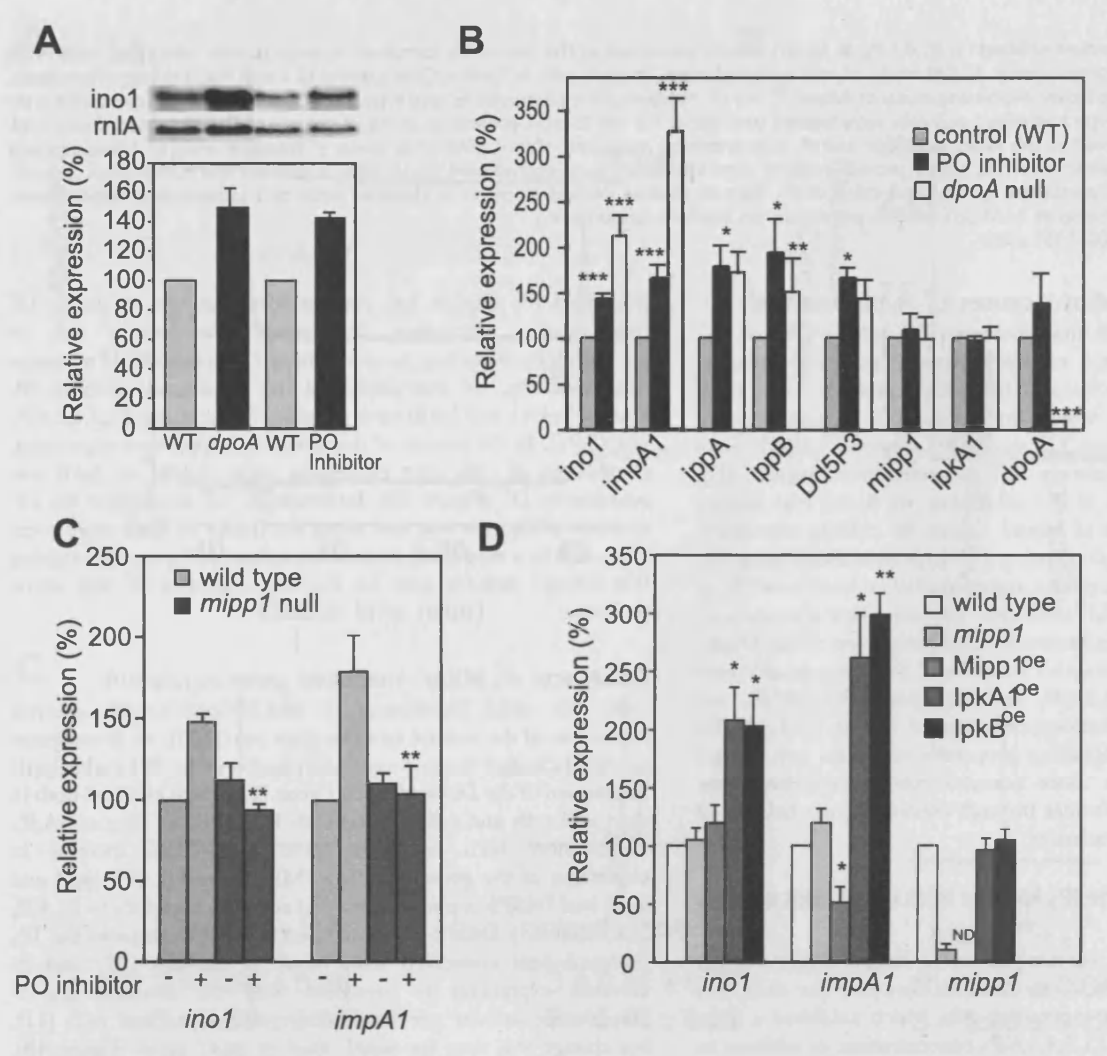


Figure 4. PO regulates gene expression. A, Expression of *ino1* in wild type, *dpoA* null cells and wild type cells following overnight treatment with 1.2 mM Z-pro-L-prolinal (PO inhibitor), measured by Northern analysis. *rnlA* expression was used as a loading control. The graph shows the expression of *ino1* quantified on a phosphoimager (Biorad) and normalised to *rnlA* relative to wild type or DMSO carrier treated controls (mean ± standard error of 3 independent experiments). B, The expression of genes involved in inositol metabolism (Table S1). Gene expression in wild type cells following overnight treatment with Z-pro-L-prolinal or the equivalent amount of DMSO carrier, and *dpoA* null mutant cells was measured by qRT-PCR, and normalised to *rnlA* expression levels. Values plotted are relative to the carrier control cells (mean ± standard error of 3 independent experiments). \*P<0.05, \*\*P<0.01, \*\*\*P<0.05, T-Test. \*C, mipp1 is required for the regulation of gene expression by PO. Expression of *ino1* and *impA1* in wild type and *mipp1* null cells following overnight treatment with Z-pro-L-prolinal or the equivalent amount of DMSO carrier, was measured by qRT-PCR, and normalised to *rnlA* expression levels. Values plotted are relative to the carrier control wild type cells (mean ± standard error of at least 3 independent experiments). There is a significant difference in gene expression between wild type and *mipp1* null mutant following PO inhibition (\*\*P<0.01, T-Test). D, Expression levels of *ino1*, *impA1* and *mipp1* in wild type, *mipp1* null mutant and cells over-expressing Mipp1, lpkA1 or lpkB. Expression was calculated relative to either wild type, or wild type cells transformed with the empty expression vector as appropriate. All samples were normalised to *rnlA* as a loading control and the values plotted are the mean ± standard error of 3 independent experiments (\*P<0.05, \*\*P<0.01 T-test). ND = not determined.

doi:10.1371/journal.pone.0011151.g004

Changes in gene expression were dependent on Mipp1, as mipp1 null mutant cells treated with the PO inhibitor exhibited no change in the expression of ino1 or impA1 (Figure 4C). Furthermore, in the absence of PO inhibitor, Mipp1 over-expression caused a 50% decrease in expression of impA1, although ino1 was unaffected (Figure 4C). Finally, IpkA1 and IpkB over-expression elevated ino1 and impA1 gene expression in the absence of PO inhibition (Figure 4D), again supporting a signalling role of the higher order IPs.

Previously, we demonstrated that elevated expression of *impA1* in *Dictyostelium* cells reverses Li<sup>+</sup> inhibition of chemotaxis [19]. This is consistent with the uncompetitive inhibition mechanism of Li<sup>+</sup>

on IMPase, which unlike other modes of inhibition is only reversed by increased enzyme concentration. This mechanism alone offers an explanation for how PO inhibition could confer Li<sup>+</sup> resistance, however our observations on gene expression suggest a more extensive effect of PO on expression of multiple inositol synthetic genes. This could combine to enhance Li<sup>+</sup> resistance. We investigated cells with elevated expression of both <code>impA1</code> and <code>ino1</code> and found that they appeared to be Li<sup>+</sup> resistant. Quantification showed that in terms of cell speed, <code>impA1:ino1</code> over-expressing cells were Li<sup>+</sup> resistant in comparison to wild type cells. However, we also observed that these cells exhibited higher cell speed compared to wild type cells in the Na<sup>+</sup> control treatment

(Figure 5 A,B). In contrast, Directionality was reduced in both Na<sup>+</sup> control and Li<sup>+</sup> treated cells, effectively making the cells more sensitive than wild type with regard to this parameter. These observations demonstrate that whilst mis-regulation of multiple genes may enhance overall Li<sup>+</sup> resistance, there is likely to be more complexity to the regulation, either involving more genes than *ino1* and *impA1* or perhaps a finer balance in levels of expression.

#### PO and Mipp1 modulate gene expression in HEK293 cells

These results show that PO and Mippl control expression of the Dictyostelium inositol synthetic genes (Figure 6A). A key question is whether a similar modulatory pathway exists in human cells. We therefore examined the effects of PO inhibition on HEK293 cells. PO inhibition caused a strong elevation of expression of the human IMPase genes, IMPA1 and IMPA2 (Figure 6B). siRNA to knockdown human Mippl expression again demonstrated that this increase was dependent on Mippl. Interestingly, basal IMPA1 expression was reduced by mippl siRNA (Figure 6B), suggesting that in these human cells, IMPA1 expression may be more dependent on Mippl function than other co-regulated genes. PO inhibitors also lead to a smaller Mippl-dependent elevation in expression of the human inositol synthase gene ISYNA1.

#### Discussion

These results indicate that PO and Mippl are key components of a gene regulatory network that controls expression of the Dictyostelium inositol synthetic genes (Figure 6A). We suggest that this may act in Dictyostelium during aggregation stage of development to modulate chemotaxis. It has previously been observed that Dictyostelium change their chemotactic response during aggregation in order to accommodate changes in cAMP signalling as cells approach multicellularity [28]. Little is known about the mechanisms that mediate these changes, however we observed elevated PO activity during these later stage of

aggregation, and note that DpoA appears to act as a suppressor of cell speed during chemotaxis, suggesting that the PO/Mipp1 signal pathway could be involved with these developmental changes.

The rapid elevation of IP<sub>3</sub> in response to PO inhibition, suggests a series of direct interactions within this signalling pathway, and consistent with this we see no change in *mipp1* mRNA following PO inhibition. Furthermore, we show that incubation with recombinant PO decreases Mipp1 activity in cell extracts. This *in vitro* effect does not proceed via proteolysis of Mipp1, and therefore is likely to involve an unidentified intermediate peptide or protein.

In addition, we show that although I(1,4,5)P3 is the Mipp1 product, it is not the modulator of Li<sup>+</sup> sensitivity. Instead, we show that this occurs via altered expression of the genes that encode the myo-inositol synthetic and metabolic genes. This fits biochemical observations as Li<sup>+</sup> is an uncompetitive inhibitor of the IMPase and IPP [6,29] and hence targets the enzyme-substrate complex. Uncompetitive inhibitors can only be overcome by increasing the amount of enzyme, and we have previously shown that increased expression of ImpA1 reduces Li<sup>+</sup> sensitivity of Dictyostelium cells undergoing chemotaxis [19]. We also previously found that in the absence of Li<sup>+</sup>, elevated ImpA1 enhances signalling via PIP<sub>3</sub>, an important mediator of the chemotaxis in Dictyostelium and signalling in other cells. We now show that a combined increase in expression of impA1 and ino1genes, as occurs in the dpoA null mutant, enhances the degree of Li<sup>+</sup> resistance with regard to cell speed and also alters the chemotactic response in the absence of Li<sup>+</sup>. A combined up-regulation of gene expression would be expected to have significant effects on PIP3 signalling.

The exact nature of the link between Mipp1 and gene expression requires further study, however genetic evidence implicates signalling via changes in the metabolism of the higher order inositol phosphates,  $I(1,3,4,5,6)P_5$  and  $I(1,4,5,6,)P_4$  [30].  $I(1,3,4,5,6)P_5$  is a good candidate for a signalling and has

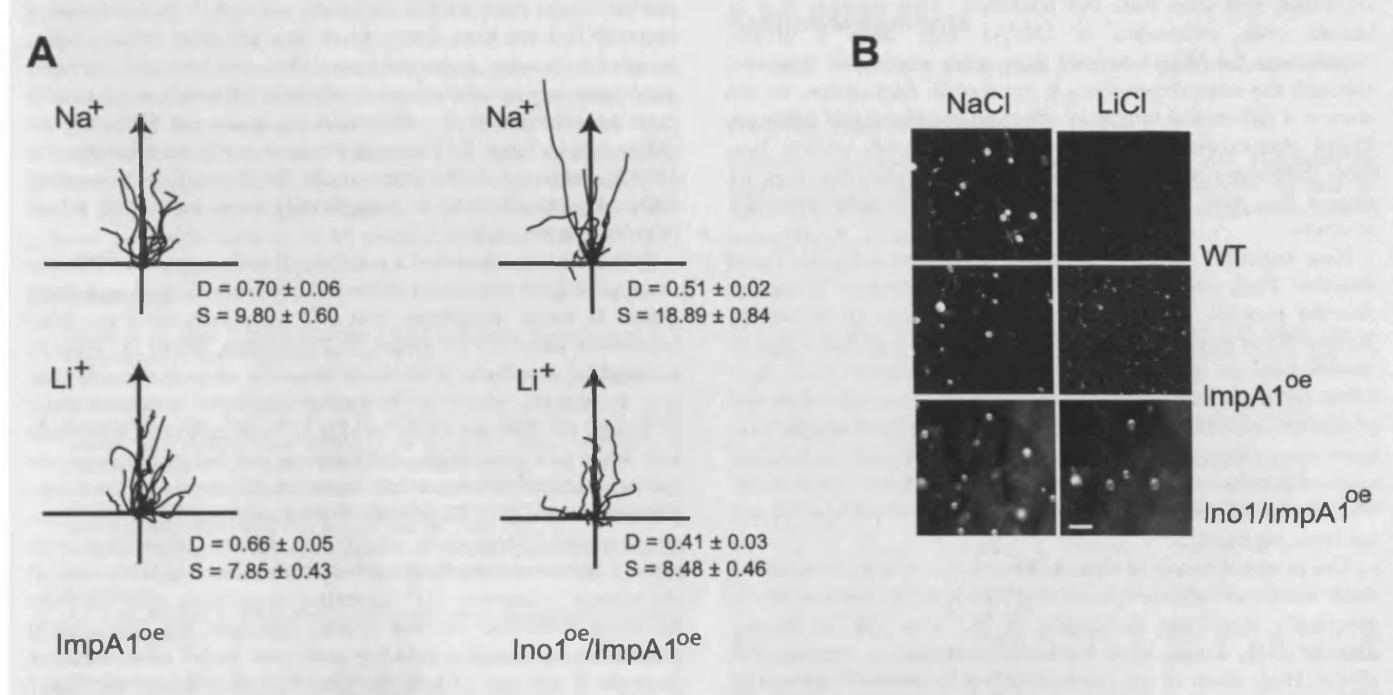


Figure 5. Increased *ino1* and *impA1* gene expression confers Li<sup>+</sup> resistance. A, Cell tracks of wild type cells over-expressing ImpA1 alone or both ImpA1and ino1 undergoing chemotaxis in 7 mM NaCl or LiCl. D = Directionality, S = cell speed (μm/min). B, Cells of wild type cells over-expressing ImpA1 alone or both ImpA1and ino1were developed in the presence of 10 mM LiCl. Images are taken after 24 hours, bar = 5 mm. doi:10.1371/journal.pone.0011151.g005

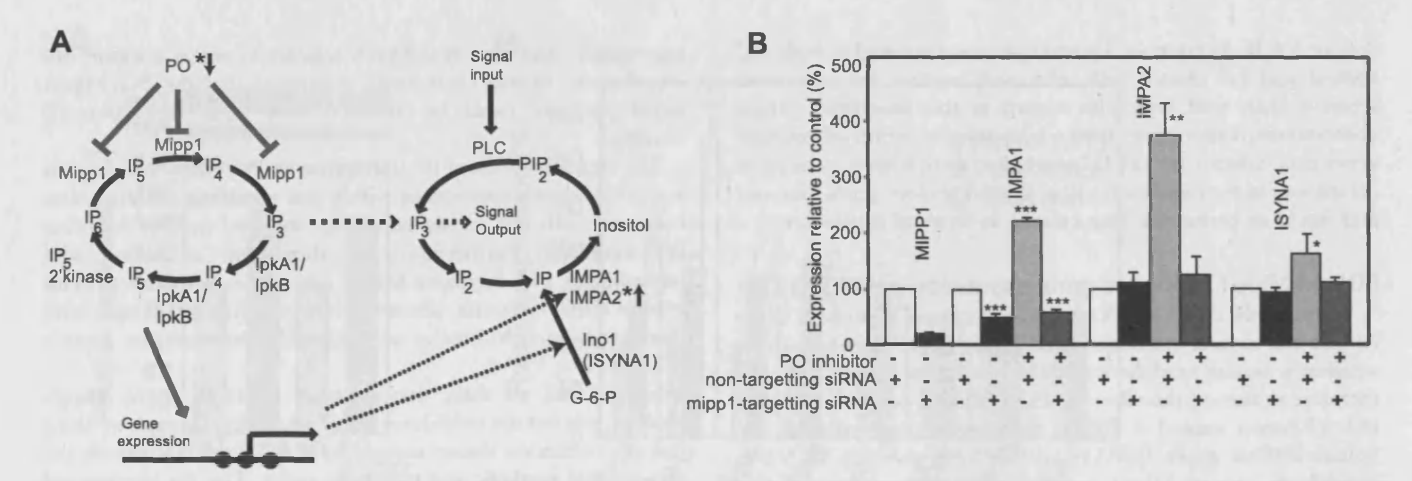


Figure 6. PO regulates expression of human IMPA1, IMPA2 and ISYNA1 genes. A, A diagram to illustrate the gene regulatory network through which PO activity regulates expression of the IMPA1, IMPA2 and ISYNA1 genes. The gene regulatory network is separate from ligand-stimulated regulation of IP3 signalling via phospholipase C (PLC), but interacts via changes in gene expression or interchange of soluble IP3. \* marks genes and enzyme activities associated with bipolar mood disorder. B, HEK293 cells were treated with either mipp1 specific or non-targetting siRNA for 24 hours with or without 130  $\mu$ M Z-pro-L-prolinal (PO inhibitor). Gene expression was quantified by qRT-PCR using expression of B2M as a reference. Expression of IMPA1, IMPA2 and ISYNA1 genes was quantified as percentage relative change compared to control (DMSO carrier treated, non-targetted siRNA samples). \* p<0.05, \*\* p<0.02, \*\*\* p<0.001. doi:10.1371/journal.pone.0011151.g006

previously been observed in the control of *ino1* and *pho* gene expression in yeast [25]. In mammals, recent results indicate the I(1,3,4,5,6)P<sub>5</sub> rapidly accumulates following Wnt3A stimulation [31].

To investigate the effects of PO inhibition in animal cells, we examined PO inhibition and siRNA knock down of Mipplin HEK293 cells. As found in Dictyostelium, expression of inol (ISYNAI), IMPAI and the IMPase paralogue IMPA2 are increased in a Mipp1 dependent manner following treatment with PO inhibitors. Interestingly, basal IMPA1 expression was reduced by Mippl siRNA and no subsequent elevation of expression was seen with PO inhibition. This suggests that in human cells, expression of IMPA1 may have a greater requirement for Mipp1 activity than other genes. We note that although the same dependency is not seen in Dictyostelium, we did observe a differential inhibitory effect on impAland inol following Mippl over-expression (Figure 4D). It is currently unclear how these differences in expression arise between genes, however we suggest that they reside in subtle differences in their promoter structure.

How might PO mediated signalling be relevant to bipolar mood disorder? First, altered PO activity has been observed in bipolar disorder patients. In manic phase patients prior to treatment, plasma PO activity is elevated, but then reduced to below that of control patients following mood stabilizer treatment [13]. In a follow up study, PO activity was shown to be below that of control groups in euthymic patients [14]. Both sets of measurements were made using plasma, however PO is a cytosolic enzyme and plasma levels of activity are 1,000-fold less than intracellular activity [14]. The relationship between intracellular activity and patients has not yet been explored.

The potential causes of altered PO activity are unknown, but as single nucleotide polymorphism (SNP) analysis has failed to find a genetically significant association of PO with risk of bipolar disorder [32], it may arise from environmental or physiological effects. High doses of the cytokine IFN- $\alpha$  in patients undergoing immunotherapy are reported to decrease serum PO activity and be associated with some symptoms of depression [33], and mood disorders in general have previously been associated with an

activation of the inflammatory response. A recent report found bipolar disorder patients have altered expression of a subset of genes that are associated with the pro-inflammatory response, including those involved in cytokine signalling and chemotaxis [34]. Furthermore twin studies showed that these changes arise through a common environmental factor, not a shared genetic component [34]. Altered PO activity may therefore reflect an environmental or physiological component for risk of bipolar disorder.

Second, genetic studies suggest that the presence of a specific set of SNPs within the IMPA2 gene promoter associates with elevated risk for bipolar disorder in some family studies [35,36,37]. Some of these SNPs have been shown to elevate promoter activity when coupled to marker genes and may also associate with elevated expression in post-mortem brain samples, although these studies may be confounded by differences in brain pH [37]. Global differences in brain IMPase activity have not been substantiated [38,39], although differences could be missed by sampling different populations, or if changes only occur in a small subset of cells or brain regions.

Third, we have identified a novel signal pathway, where PO acts to suppress gene expression of the inositol synthetic and metabolic genes. It seems significant that PO suppresses IMPase gene expression, which is a Li+ target. In Dictyostelium, loss of PO leads to reduced Li+ sensitivity. This would seem the opposite case to that seen in patients, where Li<sup>+</sup> treatment suppresses a clinical state. However, the difference may be that Li+ treatment of Dictyostelium cells leads to a quantifiable difference in cell behaviour, whereas no behavioural difference has been observed in human nonpatient controls. Our Dictyostelium experiments can be viewed from an alternative perspective, where our mutant Dictyostelium cells possess aberrant signalling and in some cases exhibit altered chemotaxis behaviour. Li+ treatment suppresses this aberrant signalling behaviour so that it now falls into the behavioural parameters measured in wild type cells prior to Li<sup>+</sup> treatment. For example in the case of both the dpoA null mutant and inol:impal over-expressors we observed differences in chemotactic behaviour that were reversed by Li<sup>+</sup> treatment. Similarly we have previously observed elevated PIP3 signalling in wild type cells over-expressing impa1 in the absence of Li<sup>+</sup>, which is suppressed by Li<sup>+</sup> treatment [19].

We therefore envisage that treatment of patients may fit a general model, where elevated signalling activity is suppressed by mood stabilizer treatment. We propose that altered transcriptional control of inositol synthetic and metabolic genes, particularly IMPA2, could contribute to elevated risk of bipolar disorder. This risk could be heightened through changes in PO activity. In the simplest scenario, a genetic predisposition for elevated IMPA2 expression could be enhanced though an environmentally mediated decrease in PO activity leading to overactive cell signalling. Long-term Li<sup>+</sup> treatment would in turn suppress elevated cell signalling to compensate for elevated gene expression. Although this will be difficult to directly demonstrate in patient studies, further genetic analysis and development of model systems will be useful to probe the clinical relevance of PO-mediated signalling.

#### **Materials and Methods**

#### **Analysis of Cell movement**

All Dictyostelium mutants and over-expressing strains were generated in the AX2 parental background (Materials and Methods S1) and grown using standard methods [40]. Cells were shaken at 10<sup>6</sup> cells/ml for 5 hours in KK2 with 6-minute pulses of 100 nM cAMP every 6 minutes. Lithium was added for the final hour of pulsing. Cells were placed in 1 µM gradient of cAMP[41] and images collected every 10 seconds on a DIC inverted microscope. Data was analysed using DIAS 3.4.1 analytical software (Soll Technologies Inc; [42]). Data sets were analysed for statistical significance using a Mann-Whitney U-test, and based on 200-300 cells per experiment.

**Biochemical analysis.** PO activity was measured as described by Williams et al (1999) [11]. For MIPP activity, cell extracts were prepared as described by Van Dijken et al (1995) [43] and incubated with an equal volume of TEE [20 mM triethanolamine pH 6.5, 5.9 mM EGTA, 0.5 mM EDTA] supplemented with 20 mM CaCl<sub>2</sub>, 50 mM LiCl and 200 μM IP<sub>6</sub>. Production of IP<sub>3</sub> was measured by an isotope dilution assay (Perkin Elmer). For HPLC-MDD analysis, IP were prepared from 10<sup>9</sup> cells and resuspended in 400 μl 0.1 M NaCl, 15 mM NaF, 0.5 mM EDTA pH 6.0, and quantified by hplc analysis using Tricorn Mini Q 4.6/50 PE columns (GE healthcare) with solutions A: (21 μM YCl<sub>3</sub>) and B (0.8 M HCl, 25 μM YCl<sub>3</sub> (Merck). Post-column detection used (2.13 M triethanolamine, 500 μM 4-(2'-

#### References

- Craddock N, Sklar P (2009) Genetics of bipolar disorder: successful start to a long journey. Trends Genet 25: 99-105.
- Taylor L, Faraone SV, Tsuang MT (2002) Family, twin, and adoption studies of bipolar disease. Curr Psychiatry Rep 4: 130–133.
- Padmos RC, Van Baal GC, Vonk R, Wijkhuijs AJ, Kahn RS, et al. (2009)
  Genetic and environmental influences on pro-inflammatory monocytes in
  bipolar disorder: a twin study. Arch Gen Psychiatry 66: 957-965.
- Alloy LB, Abramson LY, Urosevic S, Walshaw PD, Nusslock R, et al. (2005)
   The psychosocial context of bipolar disorder: environmental, cognitive, and developmental risk factors. Clin Psychol Rev 25: 1043 1075.
- Burgess S, Geddes J, Hawton K, Townsend E, Jamison K, et al. (2001) Lithium for maintenance treatment of mood disorders. Cochrane Database Syst Rev CD003013
- Atack JR, Broughton HB, Pollack SJ (1995) Structure and mechanism of inositol monophosphatase. FEBS Lett 361: 1-7.
   Inhorn RC, Majerus PW (1988) Properties of inositol polyphosphate 1-
- Inhorn RC, Majerus PW (1988) Properties of inositol polyphosphate I phosphatase. J Biol Chem 263: 14559-14565.
- Berridge MJ, Downes CP, Hanley MR (1989) Neural and developmental actions of lithium: a unifying hypothesis. Cell 59: 411–419.
- Williams RS, Cheng L, Mudge AW, Harwood AJ (2002) A common mechanism of action for three mood-stabilizing drugs. Nature 417: 292 295.

Pyridylazo)-Resorcinol (PAR) (Merck), pH 9.75) and absorbance [44] at 520 nm [45,46].

#### Analysis of gene expression

Northern blotting was done using standard techniques. For qRT-PCR analysis of *Dictyostelium* samples, total RNA was extracted from growing cells and used as template to generate cDNA using random primers (Roche 1<sup>st</sup> Strand synthesis kit). qRT-PCR was then performed using a SYBR green mastermix kit (Abgene), with 10 ng cDNA template and PCR primers described in Materials and Methods S1. All samples were run in triplicate, with at least three biological replicates. Expression differences were calculated using the  $2^{-\Delta\Delta cT}$  method [47] normalised to *mlA* in *Dictyostelium* and B2M in HEK 293 cells.

#### **Supporting Information**

**Materials and Methods S1** Construction of mutant strains and plasmids; qRT-PCR primers.

Found at: doi:10.1371/journal.pone.0011151.s001 (0.05 MB DOC)

Table S1 Summary of the genes identified and manipulated in this study. mRNA copy number was determined by quantitative RT-PCR, by using a calibration curve generated from plasmid clones of each gene, assuming that 1% of total RNA is mRNA. The activity of genes marked \* is predicted by homology with characterised enzymes from other species. [Williams RS, Eames M, Ryves WJ, Viggars J, Harwood AJ (1999) EMBO J 18: 2734-2745; Fischbach A, Adelt S, Muller A, Vogel G (2006) Biochem J. 397:509 518.; King JS, Teo R, Ryves J, Reddy JV, Peters O, Harwood, AJ. (2009) Dis Model Mech 2: 306-312.; Loovers HM, Veenstra K, Snippe H, Pesesse X, Erneux C, et al. (2003) J Biol Chem 278: 5652-5658].

Found at: doi:10.1371/journal.pone.0011151.s002 (0.08 MB DOC)

#### **Acknowledgments**

We thank Trevor Dale and Stephen Shears for their invaluable critique.

#### **Author Contributions**

Conceived and designed the experiments: JK MK AH. Performed the experiments: JK MK RT KW KM BR ED RW. Analyzed the data: JK MK RT KW KM JR BR ED. Contributed reagents/materials/analysis tools: MK JR. Wrote the paper: AH.

- Sarkar S, Floto RA, Berger Z, Imarisio S, Cordenier A, et al. (2005) Lithium induces autophagy by inhibiting inositol monophosphatase. J Cell Biol 170: 1101-1111.
- 11. Williams RS, Eames M, Ryves WJ, Viggars J, Harwood AJ (1999) Loss of a prolyl oligopeptidase confers resistance to lithium by elevation of inositol (1,4,5) trisphosphate. EMBO J 18: 2734-2745.
- Maes M, De Meester I, Scharpe S, Desnyder R, Ranjan R, et al. (1996)
   Alterations in plasma dipeptidyl peptidase IV enzyme activity in depression and schizophrenia: effects of antidepressants and antipsychotic drugs. Acta Psychiatr Scand 93: 1-8.
- Maes M, Goossens F, Scharpe S, Calabrese J, Desnyder R, et al. (1995) Alterations in plasma prolyl endopeptidase activity in depression, mania, and schizophrenia: effects of antidepressants, mood stabilizers, and antipsychotic drugs. Psychiatry Res 58: 217 225.
- Breen G, Harwood AJ, Gregory K, Sinclair M, Collier D, et al. (2004) Two peptidase activities decrease in treated bipolar disorder not schizophrenic patients. Bipolar Disord 6: 156–161.
- Schulz I, Gerhartz B, Neubauer A, Holloschi A, Heiser U, et al. (2002) Modulation of inositol 1,4,5-triphosphate concentration by prolyl endopeptidase inhibition. Eur J Biochem 269: 5813
   5820.
- Eickholt BJ, Towers GJ, Ryves WJ, Eikel D, Adley K, et al. (2005) Effects of valproic acid derivatives on inositol trisphosphate depletion, teratogenicity,

- glycogen synthase kinase-3beta inhibition, and viral replication: a screening approach for new bipolar disorder drugs derived from the valproic acid core structure. Mol Pharmacol 67: 1426–1433.
- Fornai F, Longone P, Cafaro L, Kastsiuchenka O, Ferrucci M, et al. (2008) Lithium delays progression of amyotrophic lateral sclerosis. Proc Natl Acad Sci U S A 105: 2052–2057.
- Kessin RH (2001) Dictyostelium Evolution, cell biology, and the development of multicellularity. Cambridge, UK: Cambridge Univ. Press xiv + 294.
- King JS, Teo R, Ryves J, Reddy JV, Peters O, et al. (2009) The mood stabiliser lithium suppresses PIP3 signalling in *Dietyostelium* and human cells. Dis Model Mech 2: 306–312.
- Otto JC, Kelly P, Chiou ST, York JD (2007) Alterations in an inositol phosphate code through synergistic activation of a G protein and inositol phosphate kinases. Proc Natl Acad Sci U S A 104: 15653–15658.
- Cho J, King JS, Qian X, Harwood AJ, Shears SB (2008) Dephosphorylation of 2,3-bisphosphoglycerate by MIPP expands the regulatory capacity of the Rapoport-Luebering glycolytic shunt. Proc Natl Acad Sci U S A 105: 598-6003
- 22. Nalaskowski MM, Deschermeier C, Fanick W, Mayr GW (2002) The human homologue of yeast ArgRIII protein is an inositol phosphate multikinase with predominantly nuclear localization. Biochem J 366: 549–556.
- Wilson MP, Majerus PW (1996) Isolation of inositol 1,3,4-trisphosphate 5/6-kinase, cDNA cloning and expression of the recombinant enzyme. J Biol Chem 271: 11904–11910.
- 24. Yang X, Shears SB (2000) Multitasking in signal transduction by a promiscuous human Ins(3,4,5,6)P(4) 1-kinase/Ins(1,3,4)P(3) 5/6-kinase. Biochem J 351 Pt 3: 551-555.
- Steger DJ, Haswell ES, Miller AL, Wente SR, O'Shea EK (2003) Regulation of chromatin remodeling by inositol polyphosphates. Science 299: 114–116.
- Fischbach A, Adelt S, Muller A, Vogel G (2006) Disruption of inositol biosynthesis through targeted mutagenesis in Dictyostelium discoideum - generation and characterisation of inositol-auxotrophic mutants. Biochem J 397: 509-518.
- Loovers HM, Veenstra K, Snippe H, Pesesse X, Erneux C, et al. (2003) A
  diverse family of inositol 5-phosphatases playing a role in growth and
  development in *Dictyostelium discoideum*. J Biol Chem 278: 5652–5658.
- Lax AJ (1979) The evolution of excitable behaviour in *Dictyostelium*. J Cell Sci 36: 311–321.
- Gee NS, Reid GG, Jackson RG, Barnaby RJ, Ragan CI (1988) Purification and properties of inositol-1,4-bisphosphatase from bovine brain. Biochem J 253: 777-782.
- Shen X, Xiao H, Ranallo R, Wu WH, Wu C (2003) Modulation of ATP-dependent chromatin-remodeling complexes by inositol polyphosphates. Science 299: 112–114.
- Gao Y, Wang HY (2007) Inositol pentakisphosphate mediates Wnt/beta-catenin signaling. J Biol Chem 282: 26490–26502.
- 32. Mamdani F, Sequeira A, Alda M, Grof P, Rouleau G, et al. (2007) No association between the PREP gene and lithium responsive bipolar disorder. BMC Psychiatry 7: 9.
- 33. Van Gool AR, Van Ojik HH, Kruit WH, Mulder PG, Fekkes D, et al. (2004) Serum activity of prolyl endopeptidase, but not of dipeptidyl peptidase IV, is

- decreased by immunotherapy with IFN-alpha in high-risk melanoma patients. J Interferon Cytokine Res 24: 411-415.
- Padmos RC, Hillegers MH, Knijff EM, Vonk R, Bouvy A, et al. (2008) A
  discriminating messenger RNA signature for bipolar disorder formed by an
  aberrant expression of inflammatory genes in monocytes. Arch Gen Psychiatry
  65: 395

  –407.
- 35. Sjoholt G, Gulbrandsen AK, Lovlie R, Berle JO, Molven A, et al. (2000) A human myo-inositol monophosphatase gene (IMPA2) localized in a putative susceptibility region for bipolar disorder on chromosome 18p11.2: genomic structure and polymorphism screening in manic-depressive patients. Mol Psychiatry 5: 172-180.
- Sjoholt G, Ebstein RP, Lie RT, Berle JO, Mallet J, et al. (2004) Examination of IMPA1 and IMPA2 genes in manic-depressive patients: association between IMPA2 promoter polymorphisms and bipolar disorder. Mol Psychiatry 9: 621-629.
- 37. Ohnishi T, Yamada K, Ohba H, Iwayama Y, Toyota T, et al. (2007) A promoter haplotype of the inositol monophosphatase 2 gene (IMPA2) at 18p11.2 confers a possible risk for bipolar disorder by enhancing transcription. Neuropsychopharmacology 32: 1727-1737.
- Shaltiel G, Shamir A, Nemanov L, Yaroslavsky Y, Nemets B, et al. (2001) Inositol monophosphatase activity in brain and lymphocyte-derived cell lines of bipolar patients. World J Biol Psychiatry 2: 95–98.
- Agam G, Shaltiel G, Kozlovsky N, Shimon H, Belmaker RH (2003) Lithium inhibitable enzymes in postmortem brain of bipolar patients. J Psychiatr Res 37: 433–442.
- Watts DJ, Ashworth JM (1970) Growth of myxameobae of the cellular slime mould Dictyostelium discoideum in axenic culture. Biochem J 119: 171–174.
- Zigmond SH (1988) Orientation chamber in chemotaxis. Methods Enzymol 162: 65–72.
- Soll DR, Wessels D, Voss E, Johnson O (2001) Computer-assisted systems for the analysis of amoeboid cell motility. Methods Mol Biol 161: 45-58.
- Van Dijken P, De Haas JR, Craxton A, Erneux C, Shears SB, et al. (1995) A novel, phospholipase C-independent pathway of inositol 1, 4,5-trisphosphate formation in *Dictyostelium* and rat liver. J Biol Chem 270: 29724–29731.
- 44. Guse AH, Goldwich A, Weber K, Mayr GW (1995) Non-radioactive, isomer-specific inositol phosphate mass determinations: high-performance liquid chromatography-micro-metal-dye detection strongly improves speed and sensitivity of analyses from cells and micro-enzyme assays. J Chromatogr B Biomed Appl 672: 189–198.
- Casals I, Villar JL, Riera-Codina M (2002) A straightforward method for analysis of highly phosphorylated inositols in blood cells by high-performance liquid chromatography. Anal Biochem 300: 69–76.
- Mayr GW (1988) A novel metal-dye detection system permits picomolar-range h.p.l.c. analysis of inositol polyphosphates from non-radioactively labelled cell or tissue specimens. Biochem J 254: 585–591.
- Livak KJ, Schmittgen TD (2001) Analysis of relative gene expression data using real-time quantitative PCR and the 2(-Delta Delta C(T)) Method. Methods 25: 402-408

# Glycogen Synthase Kinase-3 Is Required for Efficient Dictyostelium Chemotaxis

Regina Teo,\* Kimberley J. Lewis,\* Josephine E. Forde,‡ W. Jonathan Ryves,\* Jonathan V. Reddy,\* Benjamin J. Rogers,\* and Adrian J. Harwood\*

\*Cardiff School of Biosciences, Cardiff University, CF10 3AX Cardiff, United Kingdom; †Cardiff School of Medicine, Cardiff University, CF14 4XW Cardiff, United Kingdom; and †Swansea University, SA2 8PP Swansea, United Kingdom

Submitted October 26, 2009; Revised May 25, 2010; Accepted June 1, 2010

Monitoring Editor: Carole Parent

Glycogen synthase kinase-3 (GSK3) is a highly conserved protein kinase that is involved in several important cell signaling pathways and is associated with a range of medical conditions. Previous studies indicated a major role of the Dictyostelium homologue of GSK3 (gskA) in cell fate determination during morphogenesis of the fruiting body; however, transcriptomic and proteomic studies have suggested that GSK3 regulates gene expression much earlier during Dictyostelium development. To investigate a potential earlier role of GskA, we examined the effects of loss of gskA on cell aggregation. We find that cells lacking gskA exhibit poor chemotaxis toward cAMP and folate. Mutants fail to activate two important regulatory signaling pathways, mediated by phosphatidylinositol 3,4,5-trisphosphate (PIP<sub>3</sub>) and target of rapamycin complex 2 (TORC2), which in combination are required for chemotaxis and cAMP signaling. These results indicate that GskA is required during early stages of Dictyostelium development, in which it is necessary for both chemotaxis and cell signaling.

#### INTRODUCTION

Glycogen synthase kinase-3 (GSK3) is a multifunctional protein kinase that is highly conserved throughout the eukaryotes. In animals, including humans, it is associated with important embryological and physiological signaling processes, such as Wnt and insulin signaling (Cross et al., 1995; Papkoff and Aikawa, 1998). As a consequence it is linked to major clinical conditions, including cancer, diabetes, and Alzheimer's disease. At the cellular level GSK3 mediates processes, such as regulation of gene expression, control of proteolysis, metabolism, and control of the cytoskeleton (Harwood, 2001; Kim et al., 2002). The question of how GSK3 exerts its effects on these multiple processes is important for understanding the integration of cell signaling within the cellular context.

The social amoeba *Dictyostelium* grows and divides in the presence of nutrients in a unicellular form, but when starved it undergoes a developmental program to form a multicellular and differentiated structure, termed the fruiting body (Harwood, 2001). *Dictyostelium* development comprises of two major phases. First, during aggregation phase, cells migrate together by chemotaxis in a process mediated by cAMP pulses. Second, the multicellular aggregate, or mound, undertakes a series of differentiation events and morphogenetic movements to ultimately form a fruiting

This article was published online ahead of print in *MBoC in Press* (http://www.molbiolcell.org/cgi/doi/10.1091/mbc.E09-10-0891) on June 9, 2010.

Address correspondence to: Regina Teo (teor@cardiff.ac.uk).

Abbreviations used: GSK3, glycogen synthase kinase-3; PIP<sub>3</sub>, phosphatidylinositol 3,4,5-trisphosphate; TOR, target of rapamycin; TORC2, target of rapamycin complex 2.

body, which comprises spore cells within a spherical head, supported by a stalk of vacuolated, cellulose encased stalk cells.

Dictyostelium possesses a single homologue of GSK3, gskA (Harwood et al., 1995). It was discovered previously that GskA regulates the processes that control cell fate (Harwood et al., 1995). This initially occurs during early stages of multicellular development, when cells first come together to form a multicellular mound. At this point, cells differentiate into three basic cell types; prespore cells that eventually form spores, and prestalk cells (pst) comprising pstA cells that give rise to the stalk and the majority of its associated structures and pstB cells that form the basal disk that anchors the stalk to the substratum (Williams et al., 1989). In wild-type cells, 80% of the cells form prespore cells and the remainder form pst cells, of which the majority are pstA. However, in a gskA null mutant, the pstB population expands at the expense of the prespore population, so that the final fruiting body of the basal disk is greatly enlarged and the spore head reduced (Harwood et al., 1995). During later stages of fruiting body formation, GskA regulates a second cell fate decision by controlling the differentiation from pstA cells to pstAB cells (Schilde et al., 2004), which progress to form the main structural element of the stalk.

In the mound, activation of GskA is mediated by high concentrations of cAMP via the cAMP receptors carC and carD, which control tyrosine phosphorylation of GskA by the kinase ZakA (Kim *et al.*, 1999) and an unidentified tyrosine phosphatase (Kim *et al.*, 2002). Downstream of GskA lies a  $\beta$ -catenin homologue, Aardvark (Aar; Grimson *et al.*, 2000), and a signal transducer and activator of transcription (STAT) transcription factor, STATa (Ginger *et al.*, 2000), although the full role of these proteins is currently unclear.

Although the phenotypes described for gskA null mutants occur during multicellular stages, GskA expression and ac-

- Kortholt, A., King, J. S., Keizer-Gunnink, I., Harwood, A. J., and Van Haastert, P. J. (2007). Phospholipase C regulation of phosphatidylinositol 3,4,5-trisphosphate-mediated chemotaxis. Mol. Biol. Cell 18, 4772–4779.
- Kumagai, A., Pupillo, M., Gundersen, R., Miake-Lye, R., Devreotes, P. N., and Firtel, R. A. (1989). Regulation and function of G alpha protein subunits in *Dictyostelium*. Cell 57, 265–275.
- Lee, S., Comer, F. I., Sasaki, A., McLeod, I. X., Duong, Y., Okumura, K., Yates, J. R., 3rd, Parent, C. A., and Firtel, R. A. (2005). TOR complex 2 integrates cell movement during chemotaxis and signal relay in *Dictyostelium*. Mol. Biol. Cell 16, 4572–4583.
- Liao, X. H., Buggey, J., and Kimmel, A. R. (2010). Chemotactic activation of Dictyostelium AGC-family kinases AKT and PKBR1 requires separate but coordinated functions of PDK1 and TORC2. J. Cell Sci. 123, 983–992.
- Meili, R., Ellsworth, C., and Firtel, R. A. (2000). A novel Akt/PKB-related kinase is essential for morphogenesis in *Dictyostelium*. Curr. Biol. 10, 708–717.
- Meili, R., Ellsworth, C., Lee, S., Reddy, T. B., Ma, H., and Firtel, R. A. (1999). Chemoattractant-mediated transient activation and membrane localization of Akt/PKB is required for efficient chemotaxis to cAMP in *Dictyostelium*. EMBO J. 18, 2092–2105.
- Morio, T., et al. (1998). The Dictyostelium developmental cDNA project: generation and analysis of expressed sequence tags from the first-finger stage of development. DNA Res. 5, 335–340.
- Pan, P., Hall, E. M., and Bonner, J. T. (1972). Folic acid as second chemotactic substance in the cellular slime moulds. Nat. New Biol. 237, 181–182.
- Pan, P., Hall, E. M., and Bonner, J. T. (1975). Determination of the active portion of the folic acid molecule in cellular slime mold chemotaxis. J. Bacteriol. 122, 185–191.
- Papkoff, J., and Aikawa, M. (1998). WNT-1 and HGF regulate GSK3 beta activity and beta-catenin signaling in mammary epithelial cells. Biochem. Biophys. Res. Commun. 247, 851–858.
- Parent, C. A., Blacklock, B. J., Froehlich, W. M., Murphy, D. B., and Devreotes, P. N. (1998). G protein signaling events are activated at the leading edge of chemotactic cells. Cell *95*, 81–91.
- Plyte, S. E., O'Donovan, E., Woodgett, J. R., and Harwood, A. J. (1999). Glycogen synthase kinase-3 (GSK-3) is regulated during *Dictyostelium* development via the serpentine receptor cAR3. Development 126, 325–333.
- Ryves, W. J., Fryer, L., Dale, T., and Harwood, A. J. (1998). An assay for glycogen synthase kinase 3 (GSK-3) for use in crude cell extracts. Anal. Biochem. 264, 124–127.
- Ryves, W. J., and Harwood, A. J. (2001). Lithium inhibits glycogen synthase kinase-3 by competition for magnesium. Biochem. Biophys. Res. Commun. 280, 720–725.

- Sasaki, A. T., Chun, C., Takeda, K., and Firtel, R. A. (2004). Localized Ras signaling at the leading edge regulates PI3K, cell polarity, and directional cell movement. J. Cell Biol. 167, 505–518.
- Schilde, C., Araki, T., Williams, H., Harwood, A., and Williams, J. G. (2004). GSK3 is a multifunctional regulator of *Dictyostelium* development. Development 131, 4555–4565.
- Snaar-Jagalska, B. E., and Van Haastert, P. J. (1994). G-protein assays in *Dictyostelium*. Methods Enzymol. 237, 387–408.
- Strmecki, L., Bloomfield, G., Araki, T., Dalton, E., Skelton, J., Schilde, C., Harwood, A., Williams, J. G., Ivens, A., and Pears, C. (2007). Proteomic and microarray analyses of the *Dictyostelium* Zak1-GSK-3 signaling pathway reveal a role in early development. Eukaryot. Cell 6, 245–252.
- Sun, T. J., and Devreotes, P. N. (1991). Gene targeting of the aggregation stage cAMP receptor cAR1 in *Dictyostelium*. Genes Dev. 5, 572-582.
- Takeda, K., Sasaki, A. T., Ha, H., Seung, H. A., and Firtel, R. A. (2007). Role of phosphatidylinositol 3-kinases in chemotaxis in *Dictyostelium*. J. Biol. Chem. 282, 11874–11884.
- Tomchik, K. J., and Devreotes, P. N. (1981). Adenosine 3',5'-monophosphate waves in *Dictyostelium discoideum*: a demonstration by isotope dilution-fluorography. Science 212, 443–446.
- Van Dijken, P., Bergsma, J. C., Hiemstra, H. S., De Vries, B., Van Der Kaay, J., and Van Haastert, P. J. (1996). *Dictyostelium discoideum* contains three inositol monophosphatase activities with different substrate specificities and sensitivities to lithium. Biochem. J. 314, 491–495.
- Van Lookeren Campagne, M. M., Erneux, C., Van Eijk, R., and Van Haastert, P. J. (1988). Two dephosphorylation pathways of inositol 1,4,5-trisphosphate in homogenates of the cellular slime mould *Dictyostelium discoideum*. Biochem. J. 254, 343–350.
- Varney, T. R., Casademunt, E., Ho, H. N., Petty, C., Dolman, J., and Blumberg, D. D. (2002). A novel Dictyostelium gene encoding multiple repeats of adhesion inhibitor-like domains has effects on cell-cell and cell-substrate adhesion. Dev. Biol. 243, 226–248.
- Veeranki, S., Kim, B., and Kim, L. (2008). The GPI-anchored superoxide dismutase SodC is essential for regulating basal Ras activity and for chemotaxis of *Dictyostelium discoideum*. J. Cell Sci. 121, 3099–3108.
- Williams, J. G., Duffy, K. T., Lane, D. P., McRobbie, S. J., Harwood, A. J., Traynor, D., Kay, R. R., and Jermyn, K. A. (1989). Origins of the prestalk-prespore pattern in *Dictyostelium* development. Cell *59*, 1157–1163.
- Williams, R. S., Eames, M., Ryves, W. J., Viggars, J., and Harwood, A. J. (1999). Loss of a prolyl oligopeptidase confers resistance to lithium by elevation of inositol (1,4,5) trisphosphate. EMBO J. 18, 2734–2745.

tivity is present throughout *Dictyostelium* development (Plyte *et al.*, 1999). A proteomic and microarray analysis of cells at 5 h of development, several hours before the first multicellular developmental stages, revealed ≈150 genes with altered patterns of expression (Strmecki *et al.*, 2007). Curiously, of those genes identified that had been characterized previously, all are associated with growth and aggregation phase rather than multicellular development. This raises the question of additional roles of GskA during these earlier stages of *Dictyostelium* development.

Here, we report an in-depth investigation of aggregation and chemotaxis of gskA null mutants. We find that gskA null mutant cells have defective chemotaxis toward cAMP and folate, a growth phase chemoattractant. The chemotaxis defect is accompanied by suppression of phosphatidylinositol 3,4,5-trisphosphate (PIP<sub>3</sub>) levels. However, we observe that loss of gskA causes a much greater effect on cAMP-mediated chemotaxis than can be accounted for by loss of PIP3 signaling alone (Lee et al., 2005; Hoeller and Kay, 2007; Takeda et al., 2007). We find that protein kinase B (PKB)R1 is not phosphorylated in gskA mutants, a protein kinase related to PKB but regulated in a PIP<sub>3</sub>-independent manner. Loss of both PIP3 signaling and PKBR1 phosphorylation has a strong effect on chemotaxis. Finally, we show that gskA null mutant cells do not generate cAMP pulses during aggregation, demonstrating that GskA plays a major role in the regulation of chemotaxis and early Dictyostelium development.

#### MATERIALS AND METHODS

#### Chains

The gskA null strain (ID Strain: DBS0236114) was obtained from the Dicty Stock Centre (http://dictybase.org/) and was originally generated in the Dictyostelium discoideum strain AX2 background. The wild-type strain refers to AX2 and is the same strain denoted in Bloomfield et al. (2008). Cells were cultured axenically on plates in HL5 with glucose medium (Formedium HLG0102) before experiment. gskA null mutants were grown in media supplemented with 10  $\mu$ g/ml blasticidin, and gskA null transformants carrying GskA-green fluorescent protein (GFP) (gskA-GSKA) and immobilized metal assay of phosphorylation (IMPA)-GFP (gskA-IMPA) were grown in medium supplemented with 40  $\mu$ g/ml G418 (catalog no. 11811–023; Invitrogen). All cells were maintained at 22°C.

#### **Plasmids**

The GskA-GFP2 rescue protein for gskA was constructed by inserting the coding regions of GskA into pDXA GFP2 at the Kpn1 and Nsi1 restriction sites, such that the fusion protein was expressed under the control of a constitutive Actin15 promoter. By introducing point mutations into the coding region of the pDXA GskA-GFP2, the kinase-dead construct pDXA GskA-GFP2 K85R was made with the QuikChange site-directed mutagenesis kit (Strategene , La Jolla, CA) as per the manufacturer's direction. The coding sequence of the IMPA gene was amplified from the cDNA clone FCBP15, obtained form the Japanese D. discoideum cDNA project (Morio et al., 1998). The insert was subsequently ligated into the pTX-GFP vector.

#### Cell Signaling Assays

cAMP was measured as described previously (Snaar-Jagalska and Van Haastert, 1994) by using isotope dilution assay kits (GE Healthcare, Little Chalfont, Buckinghamnshire, United Kingdom). Cells were starved in KK2 buffer (6.5 mM KH2PO4, 3.8 mM K2HPO4, pH 6.2) for 5 h in shaking culture at a concentration of  $1\times10^7$  cells/ml. To determine cAMP levels, cells were resuspended at  $5\times10^7$  cells/ml, and  $100~\mu l$  of cells was stimulated with 5  $\mu M$  2'-deoxy-cAMP in the presence of 5 mM dithiothreitol. Reactions were terminated by the addition of  $100~\mu l$  of 3.5% (vol/vol) perchloric acid on ice. Samples were neutralized with  $50~\mu l$  of KHCO $_3$  (50% saturated), followed by centrifugation for 2 min at  $14,000\times g$  at  $4^{\circ}C$ . Finally,  $50~\mu l$  of each sample was added to the cyclic AMP  $^3H$  assay system (GE Healthcare).

Wild-type cells transformed with the plasmid WF38 (PHCRAC-GFP; Parent et al., 1998) were pulsed with cAMP for 5 h with an end concentration of 100 nM. Cells were subsequently stimulated by the addition of 1  $\mu$ M cAMP, and protein translocation was recorded by fluorescence videomicroscope with a 60× objective.

#### Time-Lapse Analysis

For chemotaxis to folate, cells were grown axenically to a density of  $1\times10^6$ , and  $4 \times 10^5$ /cm<sup>2</sup> cells were washed twice in 20% media/KK2 and replated in a LabTek coverglass chambered well (Nunc 155379; Nalge Nunc International, Rochester, NY) with 2 ml of 20% media/KK2. Folate (25 mM) was delivered via a Femtotip (5242 952.008; Eppendorf, Hamburg, Germany), and images were recorded for every 20 s under 10× phase objective. For aggregation,  $5 \times 10^6$  cells were washed and plated on KK2 agar. Images were taken every 30 s for cAMP pulse movies under 4× objective for at least 24 h. Postprocessing was carried out with ImageJ (National Institutes of Health, Bethesda, MD). For chemotaxis,  $5 \times 10^7$  cells were shaken in KK2 buffer (Formedium KK29907) for 5 h while being pulsed every 6 min with cAMP to an end concentration of  $10^{-7}$  M. The chemotaxis-competent cells were placed in a Zigmond chamber (Z02; Neuro Probe, Gaithersburg, MD) in a cAMP gradient (source at 10<sup>-6</sup> M cAMP, sink with no cAMP). Differential interference contrast images of cells were captured with a 20× objective at 6-s intervals for 15 min. Cell movement was analyzed using Dynamic Image Analysis System (DIAS), version 3.4.1 (Soll Technologies, Iowa City, IA; Curreli et al., 2001). Statistical analysis was carried out using the nonparametric Kruskal-Wallis test, with a post hoc Dunn's multiple comparison test using Prism 4 (GraphPad Software, San Diego, CA).

#### Phospholipid Radiolabeling and Thin Layer Chromatography (TLC) Analysis

Cells (1  $\times$  10<sup>8</sup>) were starved and pulsed for 4 h with 100 nM cAMP. At the fourth hour, cells were pelleted and resuspended in 600  $\mu$ l of KK2. Radioactive [ $\gamma$ -3<sup>2</sup>P]ATP was added (1.2 MBq), and the cells were pulsed with cAMP for a further hour (100 nM/6 min).

Phospholipids were extracted as described in Konig et al. (2008): cells were added to 750  $\mu$ l of acidified A (chloroform/methanol/HCl (1M) ratio: 40:80:1) and sonicated. A further 250  $\mu$ l of chloroform and 450  $\mu$ l of 1 M HCl were added to the cells, and then the cells were vortexed and spun, and the lower phase was collected. The process was repeated two more times, once with chloroform/methanol/HCl (1M) (ratio: 10:10:4) and the second time with methanol/EDTA (100 mM) (ratio: 1:0.9) and subsequently dried. Samples were then resuspended in chloroform/methanol (ratio: 2:1) and spotted onto a TLC plate (Cole-Parmer Instrument, Vernon Hills, IL). Plates were developed with a chloroform/acetone/methanol/acetic acid/double-distilled  $H_2O$  solvent system (ratio 46:17:15:14:8), and phospholipids were visualized by spraying with molybdenum Blue spray reagent (Sigma Chemical, Poole, Dorset, United Kingdom). Radiolabeled lipid spots were imaged by exposing the plate to Hyperfilm (GE Healthcare) for 3 d. PIP<sub>3</sub> measurements were carried out according to manufacturer's instructions (K-2500s PIP<sub>3</sub> Mass ELISA kit; Echelon Biosciences, Salt Lake City, UT). Anti-phospho protein kinase C (PKC; pan) antibody used for detection of PKBA and PKBR1 was purchased from Cell Signaling Technology (190D10; Danvers, MA) and analyzed as described previously (King et al., 2009).

### Quantitative Reverse Transcription-Polymerase Chain Reaction (qRT-PCR)

Dictyostelium cells were starved and shaken with pulses of 100 nM cAMP for 5 h. Cells (2  $\times$  106) were then harvested and pellets were snap-frozen. RNA was isolated using an illustra RNA spin mini kit (25-0500-72; GE Healthcare), and its integrity was checked on a 1% formaldehyde agarose gel. Genomic DNA contamination was checked by PCR using existing primers for a known gene. cDNA was prepared using the First-Strand cDNA kit (11483188001; Roche Diagnostics, Mannheim, Germany) using 1  $\mu g$  of RNA and random primers. A minus-reverse transcriptase control was also set up. qRT-PCR was carried out on a Chromo4 machine (Bio-Rad laboratories, Hercules, CA) with the Opticon2 detection software. The fluorophore used for detection was SYBR Green. iq SYBR Green master mix (170-8884; Bio-Rad Laboratories) was used for the reactions with 100 µg of cDNA. Housekeeping genes incorporated for quantification were lg7 (www.dictybase.com; ID Strain: DDB\_G0294034), impk1, and impk2. The genes of interest were carA-1 (DDB\_G0273397), acaA (DDB\_G0281545), and pdsA (DDB\_G0285995). Data analysis was carried out using the qbase software Jo VandeSomple and Jan Hellemans (Hellemans et al., 2007). Standard curves were created for all genes by using a 3-point 10-fold dilution series of Ax2 0 h cDNA, and all samples also were normalized to the Ax2 0 h cDNA. Primer sequences are as follows: ig7 forward, TCCAAGAGGAAGAGGAGAACTGC and ig7 reverse, TGGG-GAGGTCGTTACACCATTC; ipmk1 forward, GCAGGTTCAACACCATTCA-AAAAATC and ipmk1 reverse, TCCAACACTATCCATTCCTTACCATC; ipmk2 forward, TGGTAGTTTTTTGAGTGTCAGCCC and ipmk2 reverse, TGAT-GATGTTGTTGTTG TTGTAGTG; carA-1 forward, ATGTTGGGTTGTAT-GGCAGTG and carA-1 reverse, AGGGAAACCACCATTGACAG; acaA forward, CATTCTAGAGGCGGTATTGGC and acaA reverse, GGAGAAAATG-TCTGATTTCGCTT; and pdsA forward, CCATTGGGTACAACTGGTGGA and pdsA reverse, AACTGCCCATGATGGATAGGT.

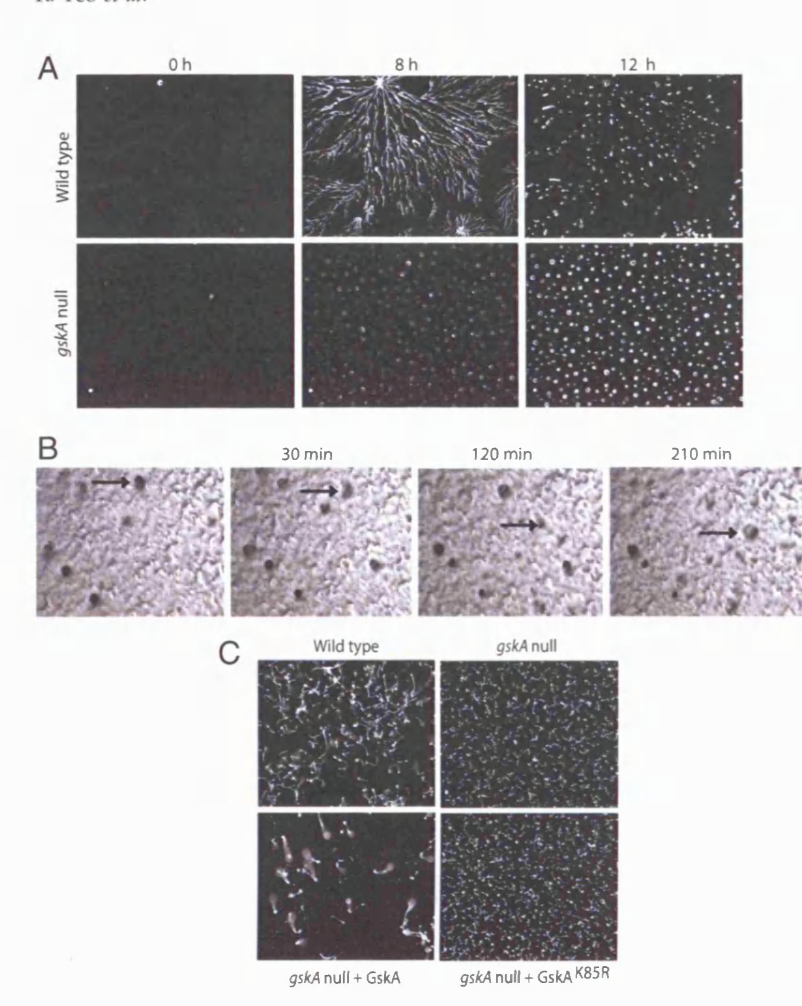


Figure 1. Analysis of *Dictyostelium* development. (A) Wild-type cells form streams  $\sim 8$  h after starvation, but gskA null mutants bypass this stage and form small mounds that are unstable. (B) Mounds of gskA null mutant cells are constantly disaggregating and reaggregating. Arrows indicate mounds exhibiting this process. (C) gskA null mutant cells carrying a rescue plasmid proceed normally through development (bottom left), but a kinase-dead version (GskA<sup>K85R</sup>) in the gskA null mutant had similar development to the original null, indicating a requirement for kinase activity for normal development.

#### RESULTS

#### gskA Null Mutants Have Aberrant Aggregation

We observed previously that gskA null mutant cells had unusual aggregation, forming small mounds  $\sim 2$  h before wild-type strains. This was independent of parental background, being seen in mutants created from both DH1 and AX2 parental wild-type strains (Harwood et~al., 1995; Schilde et~al., 2004). Small mounds also were seen in cells treated with lithium, an inhibitor of GSK3 (Williams et~al., 1999). This prompted a more in depth investigation of gskA null mutants.

To investigate the role of GskA during aggregation, wildtype and gskA null mutant cells were plated for development and recorded using time-lapse videomicroscopy. As seen previously, gskA null mutant cells formed small mounds ≈2 h earlier than wild-type cells (Supplemental Movie 1). These small mounds formed without the multicellular streams seen in wild-type cells (Figure 1A). Furthermore, the small mounds were unstable, and they often disaggregated before reaggregating in different positions on the substratum (Figure 1B). Restoring GskA activity via expression of the wild-type gskA cDNA in gskA null mutants, rescued aggregation to that seen in the wild type (Figure 1C). However, no phenotypic rescue was seen after expression of a mutant gene that lacks kinase activity (GskA<sup>K85R</sup>), indicating a requirement for kinase activity to mediate GskA function (Figure 1C).

#### GSK3 Is Required for Chemotaxis to cAMP and Folate

We tested the ability of gskA null cells to undergo chemotaxis to cAMP. Cells were pulsed with cAMP for 5 h and then placed in a gradient formed from a 1  $\mu$ M cAMP source. gskA null mutant cells had a complete loss of chemotaxis. Cell chemotaxis can be measured as the chemotactic index (CI), where +1 represents maximally accurate chemotaxis toward the cAMP source, -1 represents chemotaxis away from the cAMP source, and 0 is random movement neither toward nor away from the cAMP source. We also have calculated the percentage of cells that respond positively toward cAMP (% cells respond), and this represents the proportion of cells that have CI values of  $\geq 0.7$ , with  $\cos^{-1}(0.7) = 45^{\circ}$  and  $\cos^{-1}(1.0) = 0^{\circ}$ . Hence, cells with CI = 1.0, chemotax in a straight line to cAMP, whereas any cell that deviates 45° on either side of this would exhibit a value of 0.7.

Wild-type cells possessed a mean CI of 0.9, with 88.7% of wild-type cells exhibiting chemotaxis toward cAMP compared with 31.5% of *gskA* mutant cells. This is a slightly higher percentage (25%) than expected from cells when they randomly move. The *gskA* null mutant cells have a strongly decreased mean CI value of 0.18 and in addition exhibited an approximate 50% decrease in cell speed and directionality, a measure of cell turning as they migrate toward the cAMP source. Re-expression of GskA in the *gskA* null mutant restores CI, cell speed, and directionality to that of the

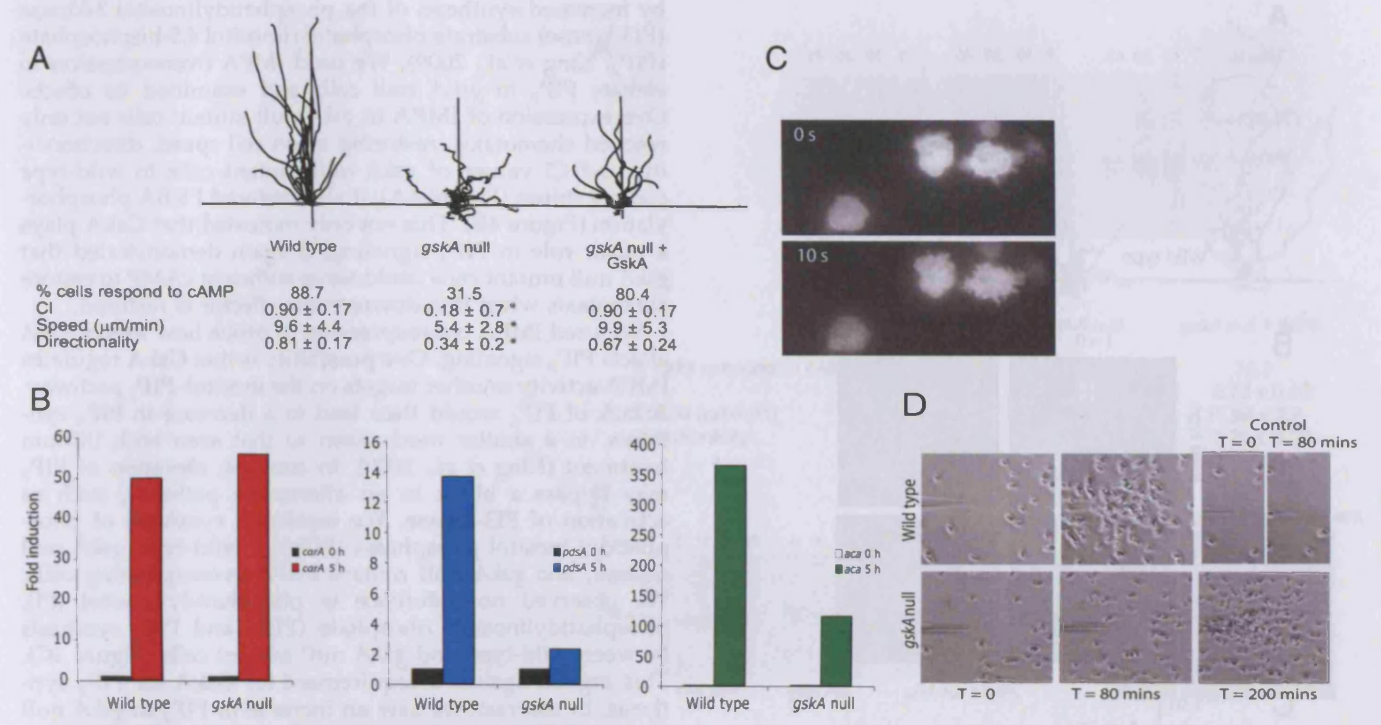


Figure 2. Chemotaxis of gskA null mutant cells. (A) Chemotaxis parameters for wild-type, gskA null mutant, and gskA null cells expressing GskA (gskA-GskA). "% cells respond to cAMP" indicates the proportion of cells that have a CI values of  $\geq 0.7$ , with  $\cos^{-1}(0.7) = 45^{\circ}$  and  $\cos^{-1}(1.0) = 0^{\circ}$ . Values are means and SDs based on at least 140 cells, compiled from three independent experiments. Dunn's multiple comparison's test between wild type and gskA null mutant showed a significant difference at p < 0.001 for all three parameters. (B) qRT-PCR showed gene induction for carA, pdsA, and aca are to similar levels to that observed in the earlier microarray study (Strmecki et al., 2007). The y-axes denote fold induction. (C) gskA null mutant cells are able to cause PTEN-GFP relocalization within 10 s of cAMP stimulation. (D) Chemotaxis to 25 mM folate. Wild-type cells take on average 140 min to show clustering at the micropipette compared with gskA null mutants, taking an average of 270 min. Figures here show a representative of one replicate experiment. Control, buffer used to dissolve folate.

wild-type cells. These results indicate a strong chemotaxis defect toward cAMP in the *gskA* null mutant (Figure 2A).

To exclude the possibility that the cells could not sense cAMP, we examined expression of genes involved in chemotaxis and cell signaling. The earlier microarray was carried out in cells that had been starved for 5 h and matched the developmental state of those used in our chemotaxis experiments (Strmecki et al., 2007). We reexamined the results of the microarray but failed to detect differences in gene expression of the cAMP receptor genes. carA is the major receptor expressed during aggregation (Sun and Devreotes, 1991), and we used qRT-PCR to confirm that there was no difference in carA gene expression between wild-type and gskA null mutant cells (Figure 2B). The microarray showed altered expression of pdsA and pdiA genes, all which play a role in aggregation and we confirmed that induction of pdsA, which encodes a cAMP phosphodiesterase, is indeed substantially reduced in gskA null cells (Figure 2B). Finally, a survey of major genes expressed during aggregation showed that the expression of the adenylyl cyclase acaA gene was induced to only 30% of the wild type. This may have been below the threshold to detect on the microarray (Figure 2B).

To confirm that *gskA* null cells can sense and respond to cAMP, we examined the response of phosphatase and tensin homologue (PTEN) to cAMP stimulation. In wild-type cells, an accumulation of PTEN protein was seen on the cell membrane but was lost to the cytosol within seconds of cAMP accumulation. This relocalization was still present in *gskA* null cells (Figure 2C), demonstrating that the loss of *gskA* did not block cAMP sensing and some downstream events.

To examine chemotaxis in a context independent of cAMP signaling, we investigated the ability of the *gskA* null mutant to chemotax toward folate. This occurs during growth of *Dictyostelium* where cells are attracted to folic acid and pterins (Pan *et al.*, 1972, 1975), substances that are secreted by bacteria, the *Dictyostelium* food source. We recorded the chemotaxis response of growth phase cells to 25 mM folic acid, delivered via a micropipette. We again observed a substantial chemotaxis defect in *gskA* null cells compared with wild type (Figure 2D). Together, these results indicate a requirement of GskA in *Dictyostelium* chemotaxis.

#### GSK3 Is Required for PIP<sub>3</sub> Signaling

To investigate the chemotaxis deficit in gskA null mutant cells during early development, we examined PIP3, a downstream effector of cAMP and mediator of the chemotaxis response. To do this, we monitored phosphorylation of PKBA, the Dictyostelium homologue of PKB. As in its animal homologues, PKBA contains a pleckstrin homology (PH)domain that mediates translocation to the plasma membrane via PIP3 binding, where the protein is subsequently phosphorylated (Kamimura et al., 2008). It therefore is a good monitor for PIP3 synthesis after cAMP stimulation. In wildtype cells, PKBA phosphorylation occurred within seconds of cAMP stimulation, with a peak between 10 and 20 s, and then declined to basal levels by 60 s. No cAMP stimulated elevation of PKBA occurred in gskA null mutant cells (Figure 3A). We can exclude a failure to express the PKBA gene because no difference in expression between mutant and

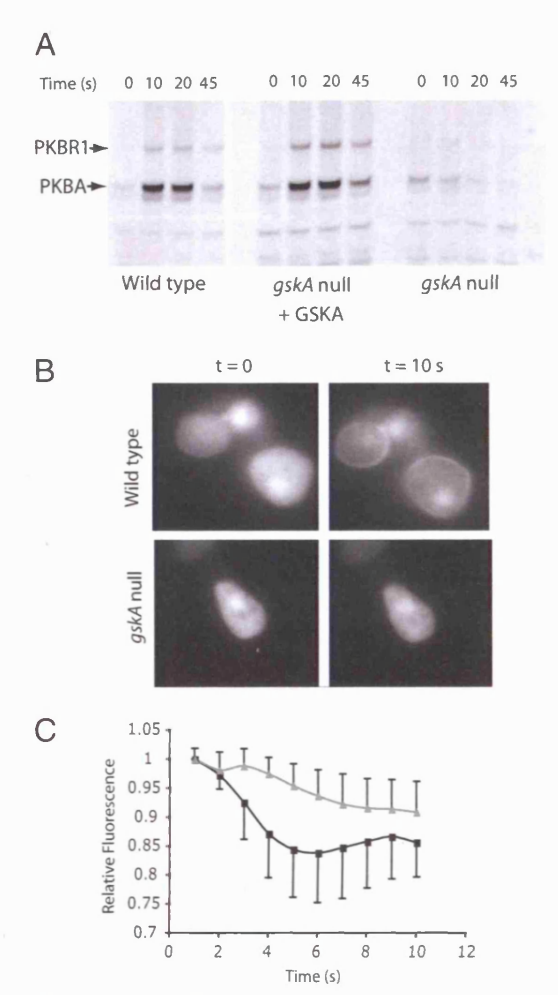


**Figure 3.** PKB phosphorylation is lost in *gskA* null mutant cells. (A) Phosphorylation of PKBA on T278, indicative of PIP<sub>3</sub> synthesis (bottom arrow) peaks at 10 s post cAMP stimulation in the wild type and *gskA*-GskA but not the *gskA* null mutant. Phosphorylation of PKBR1 on T309 (top arrow) showed kinetics similar to that for T278 for both wild type and *gskA*-GskA and again is not observed for the *gskA* null mutant. (B) PH<sub>crac</sub>-GFP translocation to the membrane is not observed in the *gskA* null mutant; however, relative fluorescence profiles post-cAMP stimulation showed small cytosolic fluorescence loss but not to the extent that observed for the wild type (C).

wild-type cells was observed either in the microarray (Strmecki et al., 2007) or by qRT-PCR (data not shown).

To pursue this further, we monitored PIP<sub>3</sub> synthesis in living cells by expression of the PIP<sub>3</sub>-specific binding protein PH<sub>CRAC</sub>-GFP (Parent *et al.*, 1998). When cells are stimulated with a global cAMP signal, PIP<sub>3</sub> is generated on the entire plasma membrane, causing translocation of PH<sub>CRAC</sub>-GFP from the cytosol to the membrane. In wild-type cells, PH<sub>CRAC</sub>-GFP was recruited to the membrane within 10 s of cAMP addition and is subsequently lost after 30 s. No PH<sub>CRAC</sub>-GFP membrane translocation was observed in the *gskA* null cells (Figure 3B) and when levels of fluorescence were quantified, PH<sub>CRAC</sub>-GFP was suppressed to only 10% of that seen in wild-type cells (Figure 3C).

### Increasing $PIP_3$ Levels Rescues Chemotaxis in the gskA Null Mutant

We previously showed that overexpression of the inositol monophosphatase gene IMPA in wild-type cell elevates PIP<sub>3</sub>

by increased synthesis of the phosphatidylinositol 3-kinase (PI3-kinase) substrate phosphatidylinositol 4,5-bisphosphate (PIP<sub>2</sub>; King *et al.*, 2009). We used IMPA overexpression to elevate PIP<sub>3</sub> in *gskA* null cells and examined its effects. Overexpression of IMPA in *gskA* null mutant cells not only rescued chemotaxis, restoring mean cell speed, directionality, and CI values of *gskA* null mutant cells to wild-type control values (Figure 4A), it also restored PKBA phosphorylation (Figure 4B). This not only indicated that GskA plays a major role in PIP<sub>3</sub> signaling, it again demonstrated that *gskA* null mutant cells could sense sufficient cAMP to restore chemotaxis when this downstream effector is restored.

We used IMPA overexpression to probe how loss of gskA affects PIP<sub>3</sub> signaling. One possibility is that GskA regulates IMPA activity or other targets on the inositol-PIP<sub>2</sub> pathway. A lack of PIP2 would then lead to a decrease in PIP3 synthesis, in a similar mechanism to that seen with lithium treatment (King et al., 2009). In contrast, elevation of PIP<sub>3</sub> may bypass a block in an alternative pathway, such as activation of PI3-kinase. We measured synthesis of phosphatidyl inositol phosphates (PIPs) in wild-type, gskA null mutant, and gskA null mutant IMPA-overexpressing cells. We observed no difference in phosphatidylinositol (PI), phosphatidylinositol phosphate (PIP), and PIP<sub>2</sub> synthesis between wild-type and gskA null mutant cells (Figure 4C). This argued against a requirement for GskA for PIP2 synthesis. In contrast, we saw an increase in PIP<sub>2</sub> in gskA null mutant IMPA-overexpressing cells (Figure 4C). This suggested that IMPA overexpression bypasses a deficit in PIP<sub>3</sub> signaling by elevating PIP<sub>2</sub> and hence PIP<sub>3</sub> synthesis.

Finally, we measured PIP<sub>3</sub> directly and found that in response to cAMP, *gskA* null mutant cells did not synthesize PIP<sub>3</sub> but seemed to lose it. This response is the opposite to that observed in either wild-type or *gskA* null mutant IMPA-overexpressing cells (Figure 4D), which rapidly synthesize new PIP<sub>3</sub> under these conditions. Overall, the data showed that very little PIP<sub>3</sub> is formed in *gskA* null mutant cells.

### GskA Is Required for Target of Rapamycin Complex 2 (TORC2)-mediated Signaling

We noted that the cAMP chemotaxis phenotype seen in the gskA null mutant was much stronger than that observed for loss of PIP<sub>3</sub> signaling alone (Hoeller and Kay, 2007; Takeda et al., 2007; King et al., 2009), and sought evidence for a further molecular defect in the gskA null mutant. Previously, it has been found that signaling via the kinase target of rapamycin (TOR) acting in the TORC2 complex was capable of mediating cAMP chemotaxis when PIP3 synthesis was inhibited (Kamimura et al., 2008). This alternative chemotaxis mechanism acts via a second PKB homologue, known as PkgB, or PKBR1 (Meili et al., 2000). This kinase protein is associated with the plasma membrane via myristoylation and not via a PH domain-PIP<sub>3</sub> interaction (Meili et al., 1999) and is activated by phosphorylation from TORC2 (Lee et al., 2005). We examined PKBR1 phosphorylation in gskA null mutant cells after cAMP stimulation, and found that as seen for PKBA, PKBR1 phosphorylation was also lost (Figure 4B). We could detect PKBR1 expression (data not shown), suggesting a signaling failure upstream of PKBR1. In contrast to PKBA phosphorylation, PKBR1 phosphorylation was not restored by overexpression of IMPA (Figure 4B), indicating that this second molecular mechanism is independent of PIP3 signaling. These results indicated that GskA is required for two intracellular signaling processes, explaining why it possesses a very strong chemotaxis defect.

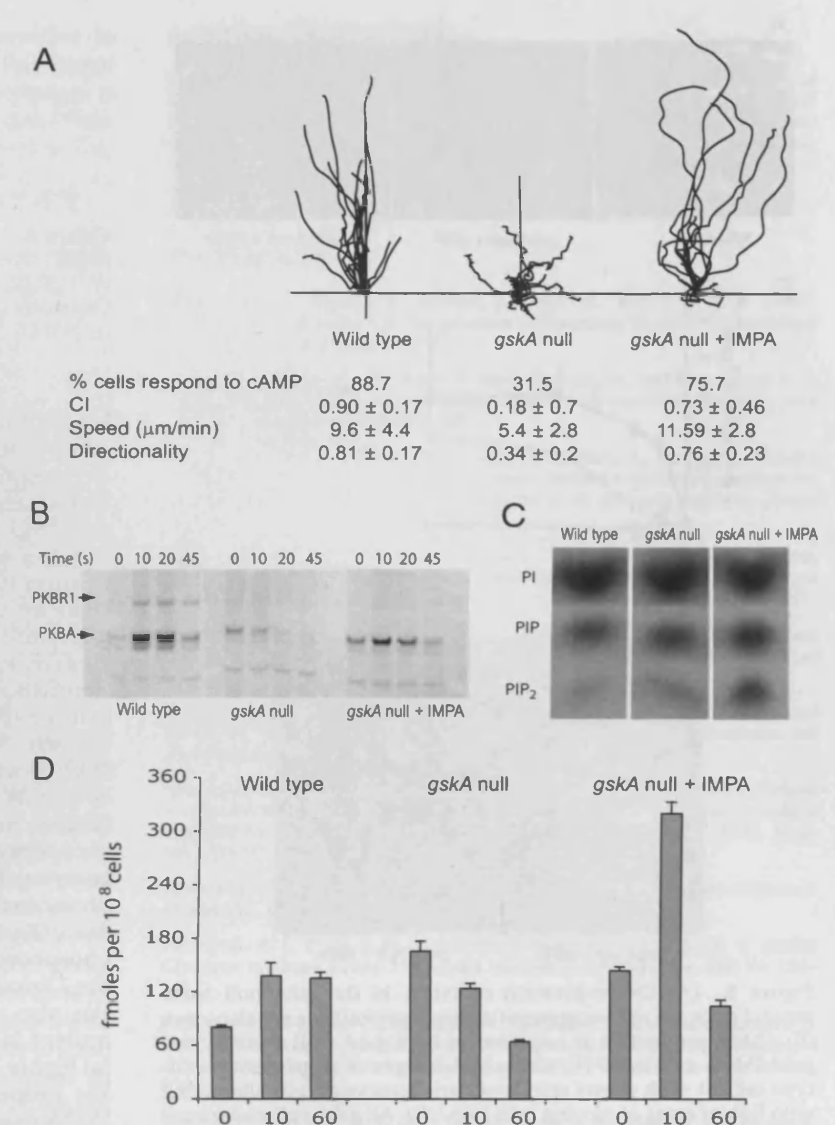


Figure 4. IMPA overexpression restores chemotaxis to gskA null mutant cells. (A) Comparison of wild-type cells and gskA null mutant cells overexpressing IMPA (gskA + IMPA) demonstrates rescued chemotaxis in the gskA-IMPA. (B) gskA-IMPA shows similar PKBA T278 phosphorylation kinetics to that observed in wild-type cells. However, T309 phosphorylation of PKBR1 is still absent after IMPA overexpression. (C) PI, PIP, and PIP<sub>2</sub> synthesis between fourth to fifth hour of early development show gskA mutant cells are still capable of producing phosphoinositides at levels similar to that of the wild type. (D) gskA mutant cells show higher basal PIP<sub>3</sub> levels compared with wild type; however, kinetics of PIP<sub>3</sub> synthesis do not reflect that shown in wild type and gskA-IMPA, post-cAMP stimulation.

#### gskA Null Mutants Have Impaired cAMP Synthesis

Although it restored chemotaxis, IMPA overexpression did not rescue aggregation or any other aspect of morphogenesis (Figure 5A and Supplemental Movie 2). This indicated that the aggregation defect was not a simple consequence of loss of chemotaxis, and may arise from an additional signaling deficiency. To test whether these cells can generate cAMP signals, cells were developed for 5 h in suspension and stimulated with the cAMP analogue 2-deoxyadenosine 3,5-monophosphate (dcAMP), and cAMP synthesis was measured. There was almost undetectable cAMP synthesis in gskA null- and gskA null-expressing IMPA cells (Figure 5B).

Dark-field optics was used to examine the cell signaling activity during aggregation. When viewed under these conditions, changes in cell shape in response to cAMP pulses can be seen as a change in light scattering (Tomchik and Devreotes, 1981). In wild-type cells, waves of light scattering propagate from the center of the aggregation field pass through the developing cell field as spiral waves (Figure 5C and Supplemental Movie 3A). In contrast to wild-type cells, no light scattering waves were observed in *gskA* null mutant cells or *gskA* mutants overexpressing IMPA (Figure 5C and

Supplemental Movie 3B). These observations suggested that although PIP<sub>3</sub> signaling is sufficient to rescue chemotaxis, it was unable to restore cAMP signaling and fully rescue aggregation.

Time (sec)

#### DISCUSSION

Here, we report that loss of GskA has substantial effects on *Dictyostelium* aggregation, causing a major defect in chemotaxis and cAMP signaling. This phenotype correlates with the presence of GskA activity during early stages of development and the results of previous microarray and proteomic analysis (Plyte *et al.*, 1999; Strmecki *et al.*, 2007). These results reveal an unexpectedly strong chemotaxis phenotype, which has been previously missed, and indicates that the terminal developmental phenotype of *Dictyostelium* mutants may not be a good indicator of defective chemotaxis.

Loss of *gskA* has a substantial effect on chemotaxis toward both cAMP and folate. These two chemotactic responses are mediated by different receptors and G proteins (Kumagai *et al.*, 1989; Hadwiger *et al.*, 1994; Kim *et al.*, 1998). Together with the expression of the cAMP receptor *carA* and the

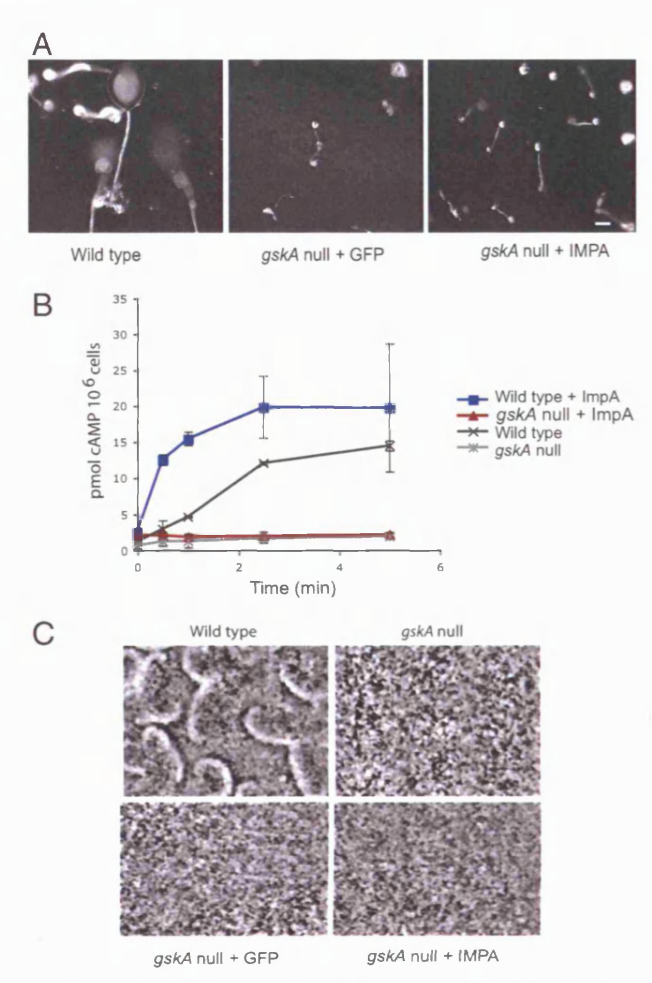
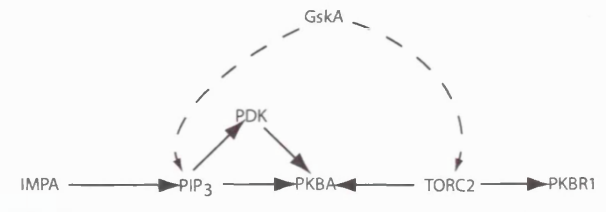


Figure 5. (A) Overexpression of IMPA in the *gskA* null background does not rescue aggregation and multicellular development. (B) cAMP production is impaired in both *gskA* null mutants and *gskA*-IMPA cell lines. (C) Dark-field images of aggregating wild-type cells at  $\approx 3$  h shows spirals of dark, stationary cells alternating with lighter areas of moving cells (top left). All *gskA* null mutant cell lines (null, *gskA*-GFP, and *gskA*-IMPA) do not show such patterning or light scattering waves. Bar, 50  $\mu$ m.

presence of the PTEN response, these observations argue that the requirement for GskA lies at the level of effector activation rather than with signal sensing. We do not know exactly how loss of GskA inhibits folate chemotaxis, and our further conclusions are based on our investigation of the better characterized cAMP chemotaxis response.

We found that loss of gskA caused a major decrease in PIP<sub>3</sub> signaling, which could be bypassed by elevation of PIP<sub>3</sub> after overexpression of IMPA. Previous observations have shown that PIP<sub>3</sub> signaling is able to elicit the chemotaxis response (Kortholt et al., 2007), explaining how this restores chemotaxis to gskA null mutant cells. Although PIP<sub>3</sub> signaling is sufficient for chemotaxis, it is not essential and a simple loss of PIP<sub>3</sub> cannot totally explain the severe chemotaxis phenotype observed for the gskA null mutant cells. Loss or inhibition of PI3K or PIP<sub>3</sub> synthesis reduces speed and directionality in chemotaxing cells; however, it has only a minor effect on the CI value (Hoeller and Kay, 2007; King et al., 2009). In contrast, although we also saw reduced speed and directionality in the gskA null mutant, we also measured a large drop in the CI value. We found that loss of gskA



**Figure 6.** Proposed mechanism of GskA action on both PIP<sub>3</sub> and PKBR1. Phosphorylation of PKBA probably relies on both the action of TORC2 and another kinase, most likely PDK (Kamimura and Devreotes 2010, Liao *et al.*, 2010), whereas GskA also acts upstream of TORC2, hence affecting subsequent phosphorylation of PKBR1.

blocks phosphorylation of PKBR1, a PIP<sub>3</sub>-independent component of a parallel signaling pathway that also mediates chemotaxis to cAMP (Kolsch *et al.*, 2008). We conclude that GskA acts upstream of both PIP<sub>3</sub>- and PKBR1-mediated signaling (Figure 6).

In our experiments, we monitored PKBA and PKBR1 activation through antibodies specific to motifs phosphorylated by the protein kinase PDK-1 (Kamimura and Devreotes, 2010). This in turn is dependent on phosphorylation by TOR kinase as part of the TORC2 complex after cAMP stimulation. These events occur at the plasma membrane so that PKBR1 is dependent solely on TORC2 activation, whereas PKBA phosphorylation requires simultaneous TORC2 activation and PIP<sub>3</sub> synthesis. This presents a paradox: if TORC2 activation is required for both PKBA and PKBR1, how can overexpression of IMPA restore PKBA phosphorylation without an effect on PKBR1? We noted however that a small amount of PKBA phosphorylation occurs in the absence of TORC2. This is evident in the report from (Kamimura et al., 2008; Liao et al., 2010) where PKBA phosphorylation is observed in *pia* mutant cells, which lacks the Dictyostelium homologue of TORC2 component Rictor. We also observed PKBA phosphorylation in a rip3 null mutant, lacking a second component of TORC2 (Supplemental Figure 1, top), but an absence of PKBR1 phosphorylation. We propose that elevation of PIP3, as a consequence of IMPA overexpression, brings more PKBA to the membrane where it is phosphorylated through a TORC2-independent kinase. The identity of this kinase is not known, but a possible candidate could be the PDK1 homologue PdkA (Kamimura and Devreotes, 2010, Liao et al., 2010). Although both PdkA and its paralogue can function in the cytosol, PdkA can translocate to the plasma membrane in response to cAMP through binding to PIP<sub>3</sub> (Kamimura and Devreotes, 2010), and so IMPA overexpression could enhance PKBA phosphorylation by increasing the concentration of both PKBA and PdkA on the membrane. Furthermore, PKBR1 null cells undergo normal chemotaxis (Meili et al., 2000), indicating that PKBA phosphorylation alone is sufficient for chemotaxis.

Further apparent complexity relates to earlier results concerning the effects of lithium on *Dictyostelium* chemotaxis. Lithium inhibits both GSK3 and IMPA (Van Lookeren Campagne *et al.*, 1988; Van Dijken *et al.*, 1996; Ryves *et al.*, 1998; Ryves and Harwood, 2001) and therefore would be expected to produce the strong chemotaxis effect seen in the *gskA* null mutant. However, previously we found that lithium treatment of aggregation competent wild-type cells suppressed PIP<sub>3</sub> signaling, but left PKBR1 phosphorylation and cAMP synthesis unaffected (King *et al.*, 2009). We demonstrated that this result arose from inhibition of IMPA, leading to a decrease in PIP<sub>2</sub> and subsequent PIP<sub>3</sub> synthesis. Arguing

against the possibility that GskA becomes insensitive to lithium, we found that nuclear export of Dd-STATa (Ginger et al., 2000), which is mediated by GskA phosphorylation, is suppressed by lithium in aggregation competent cells (Supplemental Figure 1, bottom left). We therefore propose that these differences arise through the timing of GskA action. Acute inhibition of GskA in aggregation competent cells, practically defined as cells pulsed with cAMP for 4 h before addition of lithium for 1 h, has no effect on chemotaxis or cAMP synthesis. In contrast, loss of GskA activity at the beginning of development or in growth phase cells causes the block to chemotaxis and signaling. In support of this hypothesis, we found that long-term treatment with lithium present from the initiation of cell development caused a substantial suppression of cAMP synthesis (Supplemental Figure 1, bottom right). This suggests that GskA activity acts as a permissive signal to initiate or set up chemotaxis but is not required continuously either as a direct requirement within the chemotaxis response or for maintenance of a chemotactic competent state. How GskA may achieve this is unclear; however, possibilities could range from constitutive phosphorylation of a protein that acts upstream of PIP3 and TORC2 signaling to regulation of gene expression of a component, or components, required for chemotaxis and signaling.

What is clear is that GskA is required in the regulation of some aggregation-specific gene expression. Here, we have shown decreased expression in both pdsA, a cAMP phosphodiesterase, and acaA, the adenylyl cyclase required for generation of cAMP during aggregation. Loss of expression of these genes could account for loss of cAMP signaling during aggregation, but not the GskA requirement for chemotaxis. The earlier proteomic and microarray analysis of gskA null mutant cells (Strmecki et al., 2007) indicates several genes that may contribute to the chemotaxis phenotype. Loss of gskA reduces expression of sodC, a superoxide dismutase, which has been shown to be required for chemotaxis toward cAMP (Veeranki et al., 2008). The sodC mutant causes an increase in RasG activity even in the absence of cAMP stimulation, a known upstream activator of PI3-kinase (Sasaki et al., 2004), and could contribute to the higher basal levels of PKBA phosphorylation before cAMP stimulation (Figure 3). The microarray also showed that expression of the gene alrA is reduced in gskA null mutant cells. The AlrA, protein encodes an aldehyde reductase, which when disrupted also suppresses cell motility, although the mechanism is unclear (Ehrenman et al., 2004). Curiously, both GskA and AlrA have the capacity to alter glucose metabolism within the cell, but the significance of this is not known. In contrast, loss of gskA elevates expression of ampA. The product of this gene is antiadhesion protein that accumulates during aggregation (Varney et al., 2002), and elevated levels of AmpA could explain the instability of the small mounds observed during the aggregation of the gskA null.

Together, this study indicates that GskA is an important regulator of the aggregation process and is essential for cell chemotaxis. Our observations however also indicate that the role of GskA is probably complex, acting through a combination of mechanisms that are required at a minimum for chemotaxis and signaling but that also may include metabolism and cell adhesion. These may integrate to during early development to allow aggregation proceed to the multicellular stage, in which GskA mediates cell fate determination.

#### **ACKNOWLEDGMENTS**

We thank Peter D. Watson for invaluable help in creating the dark-field movies and advice related to microscopy. We also thank Gerry Weeks and Parvin Boulourani for advice regarding the folate experiments and Tsuyoshi Araki and Jeff Williams for the *Dictyostelium* monoclonal antibodies against STATa (D4). This work was funded by a Wellcome Trust Programme grant to A.I.H.

#### REFERENCES

Bloomfield, G., Tanaka, Y., Skelton, J., Ivens, A., and Kay, R. R. (2008). Widespread duplications in the genomes of laboratory stocks of *Dictyostelium discoideum*. Genome Biol. 9, R75.

Cross, D. A., Alessi, D. R., Cohen, P., Andjelkovich, M., and Hemmings, B. A. (1995). Inhibition of glycogen synthase kinase-3 by insulin mediated by protein kinase B. Nature *378*, 785–789.

Curreli, N., Sollai, F., Massa, L., Comandini, O., Rufo, A., Sanjust, E., Rinaldi, A., and Rinaldi, A. C. (2001). Effects of plant-derived naphthoquinones on the growth of *Pleurotus sajor-caju* and degradation of the compounds by fungal cultures. J. Basic Microbiol. 41, 253–259.

Ehrenman, K., Yang, G., Hong, W. P., Gao, T., Jang, W., Brock, D. A., Hatton, R. D., Shoemaker, J. D., and Gomer, R. H. (2004). Disruption of aldehyde reductase increases group size in *Dictyostelium*. J. Biol. Chem. 279, 837–847.

Ginger, R. S., Dalton, E. C., Ryves, W. J., Fukuzawa, M., Williams, J. G., and Harwood, A. J. (2000). Glycogen synthase kinase-3 enhances nuclear export of a *Dictyostelium* STAT protein. EMBO J. 19, 5483–5491.

Grimson, M. J., Coates, J. C., Reynolds, J. P., Shipman, M., Blanton, R. L., and Harwood, A. J. (2000). Adherens junctions and beta-catenin-mediated cell signalling in a non-metazoan organism. Nature 408, 727–731.

Hadwiger, J. A., Lee, S., and Firtel, R. A. (1994). The G alpha subunit G alpha 4 couples to pterin receptors and identifies a signaling pathway that is essential for multicellular development in Dictyostelium. Proc. Natl. Acad. Sci. USA 91. 10566–10570.

Harwood, A. J. (2001). Signal transduction and *Dictyostelium* development. Protist 152, 17–29.

Harwood, A. J., Plyte, S. E., Woodgett, J., Strutt, H., and Kay, R. R. (1995). Glycogen synthase kinase 3 regulates cell fate in *Dictyostelium*. Cell 80, 139–148.

Hellemans, J., Mortier, G., De Paepe, A., Speleman, F., and Vandesompele, J. (2007). dBase relative quantification framework and software for management and automated analysis of real-time quantitative PCR data. Genome Biol. 8, R19.

Hoeller, O., and Kay, R. R. (2007). Chemotaxis in the absence of PIP3 gradients. Curr. Biol. 17, 813–817.

Kamimura, Y., and Devreotes, P. N. (2010). Phosphoinositide-dependent protein kinase (PDK) activity regulates phosphatidylinositol 3,4,5-trisphosphate-dependent and -independent protein kinase B activation and chemotaxis. J. Biol. Chem. 285, 7938–7946.

Kamimura, Y., Xiong, Y., Iglesias, P. A., Hoeller, O., Bolourani, P., and Devreotes, P. N. (2008). PIP3-independent activation of TorC2 and PKB at the cell's leading edge mediates chemotaxis. Curr. Biol. 18, 1034–1043.

Kim, J. Y., Borleis, J. A., and Devreotes, P. N. (1998). Switching of chemoattractant receptors programs development and morphogenesis in *Dictyostelium*: receptor subtypes activate common responses at different agonist concentrations. Dev. Biol. 197, 117–128.

Kim, L., Harwood, A., and Kimmel, A. R. (2002). Receptor-dependent and tyrosine phosphatase-mediated inhibition of GSK3 regulates cell fate choice. Dev. Cell 3, 523–532.

Kim, L., Liu, J., and Kimmel, A. R. (1999). The novel tyrosine kinase ZAK1 activates GSK3 to direct cell fate specification. Cell 99, 399–408.

King, J. S., Teo, R., Ryves, J., Reddy, J. V., Peters, O., Orabi, B., Hoeller, O., Williams, R. S., and Harwood, A. J. (2009). The mood stabiliser lithium suppresses PIP3 signalling in *Dictyostelium* and human cells. Dis. Model Mech. 2, 306–312.

Kolsch, V., Charest, P. G., and Firtel, R. A. (2008). The regulation of cell motility and chemotaxis by phospholipid signaling. J. Cell Sci. 121, 551–559.

Konig, S., Hoffmann, M., Mosblech, A., and Heilmann, I. (2008). Determination of content and fatty acid composition of unlabeled phosphoinositide species by thin-layer chromatography and gas chromatography. Anal. Biochem. 378, 197–201.

- Kortholt, A., King, J. S., Keizer-Gunnink, I., Harwood, A. J., and Van Haastert, P. J. (2007). Phospholipase C regulation of phosphatidylinositol 3,4,5-trisphosphate-mediated chemotaxis. Mol. Biol. Cell 18, 4772–4779.
- Kumagai, A., Pupillo, M., Gundersen, R., Miake-Lye, R., Devreotes, P. N., and Firtel, R. A. (1989). Regulation and function of G alpha protein subunits in *Dictyostelium*. Cell 57, 265–275.
- Lee, S., Comer, F. I., Sasaki, A., McLeod, I. X., Duong, Y., Okumura, K., Yates, J. R., 3rd, Parent, C. A., and Firtel, R. A. (2005). TOR complex 2 integrates cell movement during chemotaxis and signal relay in *Dictyostelium*. Mol. Biol. Cell 16, 4572–4583.
- Liao, X. H., Buggey, J., and Kimmel, A. R. (2010). Chemotactic activation of Dictyostelium AGC-family kinases AKT and PKBR1 requires separate but coordinated functions of PDK1 and TORC2. J. Cell Sci. 123, 983–992.
- Meili, R., Ellsworth, C., and Firtel, R. A. (2000). A novel Akt/PKB-related kinase is essential for morphogenesis in *Dictyostelium*. Curr. Biol. 10, 708–717.
- Meili, R., Ellsworth, C., Lee, S., Reddy, T. B., Ma, H., and Firtel, R. A. (1999). Chemoattractant-mediated transient activation and membrane localization of Akt/PKB is required for efficient chemotaxis to cAMP in *Dictyostelium*. EMBO J. 18, 2092–2105.
- Morio, T., et al. (1998). The Dictyostelium developmental cDNA project: generation and analysis of expressed sequence tags from the first-finger stage of development. DNA Res. 5, 335–340.
- Pan, P., Hall, E. M., and Bonner, J. T. (1972). Folic acid as second chemotactic substance in the cellular slime moulds. Nat. New Biol. 237, 181–182.
- Pan, P., Hall, E. M., and Bonner, J. T. (1975). Determination of the active portion of the folic acid molecule in cellular slime mold chemotaxis. J. Bacteriol. 122, 185–191.
- Papkoff, J., and Aikawa, M. (1998). WNT-1 and HGF regulate GSK3 beta activity and beta-catenin signaling in mammary epithelial cells. Biochem. Biophys. Res. Commun. 247, 851–858.
- Parent, C. A., Blacklock, B. J., Froehlich, W. M., Murphy, D. B., and Devreotes, P. N. (1998). G protein signaling events are activated at the leading edge of chemotactic cells. Cell 95, 81–91.
- Plyte, S. E., O'Donovan, E., Woodgett, J. R., and Harwood, A. J. (1999). Glycogen synthase kinase-3 (GSK-3) is regulated during *Dictyostelium* development via the serpentine receptor cAR3. Development *126*, 325–333.
- Ryves, W. J., Fryer, L., Dale, T., and Harwood, A. J. (1998). An assay for glycogen synthase kinase 3 (GSK-3) for use in crude cell extracts. Anal. Biochem. 264, 124–127.
- Ryves, W. J., and Harwood, A. J. (2001). Lithium inhibits glycogen synthase kinase-3 by competition for magnesium. Biochem. Biophys. Res. Commun. 280, 720–725.

- Sasaki, A. T., Chun, C., Takeda, K., and Firtel, R. A. (2004). Localized Ras signaling at the leading edge regulates PI3K, cell polarity, and directional cell movement. J. Cell Biol. 167, 505–518.
- Schilde, C., Araki, T., Williams, H., Harwood, A., and Williams, J. G. (2004). GSK3 is a multifunctional regulator of *Dictyostelium* development. Development 131, 4555–4565.
- Snaar-Jagalska, B. E., and Van Haastert, P. J. (1994). G-protein assays in *Dictyostelium*. Methods Enzymol. 237, 387–408.
- Strmecki, L., Bloomfield, G., Araki, T., Dalton, E., Skelton, J., Schilde, C., Harwood, A., Williams, J. G., Ivens, A., and Pears, C. (2007). Proteomic and microarray analyses of the *Dictyostelium* Zak1-GSK-3 signaling pathway reveal a role in early development. Eukaryot. Cell *6*, 245–252.
- Sun, T. J., and Devreotes, P. N. (1991). Gene targeting of the aggregation stage cAMP receptor cAR1 in *Dictyostelium*. Genes Dev. 5, 572–582.
- Takeda, K., Sasaki, A. T., Ha, H., Seung, H. A., and Firtel, R. A. (2007). Role of phosphatidylinositol 3-kinases in chemotaxis in *Dictyostelium*. J. Biol. Chem. 282, 11874–11884.
- Tomchik, K. J., and Devreotes, P. N. (1981). Adenosine 3',5'-monophosphate waves in *Dictyostelium discoideum*: a demonstration by isotope dilution-fluorography. Science 212, 443–446.
- Van Dijken, P., Bergsma, J. C., Hiemstra, H. S., De Vries, B., Van Der Kaay, J., and Van Haastert, P. J. (1996). *Dictyostelium discoideum* contains three inositol monophosphatase activities with different substrate specificities and sensitivities to lithium. Biochem. J. 314, 491–495.
- Van Lookeren Campagne, M. M., Erneux, C., Van Eijk, R., and Van Haastert, P. J. (1988). Two dephosphorylation pathways of inositol 1,4,5-trisphosphate in homogenates of the cellular slime mould *Dictyostelium discoideum*. Biochem. J. 254, 343–350.
- Varney, T. R., Casademunt, E., Ho, H. N., Petty, C., Dolman, J., and Blumberg, D. D. (2002). A novel Dictyostelium gene encoding multiple repeats of adhesion inhibitor-like domains has effects on cell-cell and cell-substrate adhesion. Dev. Biol. 243, 226–248.
- Veeranki, S., Kim, B., and Kim, L. (2008). The GPI-anchored superoxide dismutase SodC is essential for regulating basal Ras activity and for chemotaxis of *Dictyostelium discoideum*. J. Cell Sci. 121, 3099–3108.
- Williams, J. G., Duffy, K. T., Lane, D. P., McRobbie, S. J., Harwood, A. J., Traynor, D., Kay, R. R., and Jermyn, K. A. (1989). Origins of the prestalk-prespore pattern in *Dictyostelium* development. Cell 59, 1157–1163.
- Williams, R. S., Eames, M., Ryves, W. J., Viggars, J., and Harwood, A. J. (1999). Loss of a prolyl oligopeptidase confers resistance to lithium by elevation of inositol (1,4,5) trisphosphate. EMBO J. 18, 2734–2745.

- 1. King, J.S., et al., The mood stabiliser lithium suppresses PIP3 signalling in Dictyostelium and human cells. Disease Models & Mechanisms, 2009. 2(5-6): p. 306-312.
- 2. Quiroz, J.A., T.D. Gould, and H.K. Manji, *Molecular effects of lithium*. Mol Interv, 2004. 4(5): p. 259-72.
- 3. Mitchell, P.B., On the 50th anniversary of John Cade's discovery of the antimanic effect of lithium. Aust. N.Z.J. Psychiatry, 1999. 33: p. 623-628.
- 4. Williams RS, H.A., *Lithium metallotherapeutics. Metallotherapeutic drugs and metal-based diagnostic agents: the use of metals in medicine.* Wiley, 2005.
- 5. Hallcher, L.M. and W.R. Sherman, The effects of lithium ion and other agents on the activity of myo-inositol-1-phosphatase from bovine brain. Journal of Biological Chemistry, 1980. 255(22): p. 10896-10901.
- 6. Forde, J.E. and T.C. Dale, Glycogen synthase kinase 3: a key regulator of cellular fate. Cell Mol Life Sci, 2007. 64(15): p. 1930-44.
- 7. Jope, R.a.B., GN, Mood stabilizers, glycogen synthase kinase-3beta and cell survival. Molecular Psychiatry, 2002. 7: p. S35-S45.
- 8. Loewus, M.W., et al., Stereochemistry of the myo-inositol-1-phosphate synthase reaction. J Biol Chem, 1980. 255(24): p. 11710-2.
- 9. Calker, D.v. and R.H. Belmaker, The high affinity inositol transport system implications for the pathophysiology and treatment of bipolar disorder. Bipolar Disorders, 2000. 2(2): p. 102-107.
- 10. Shears, S.B., How versatile are inositol phosphate kinases? Biochem J, 2004. 377(Pt 2): p. 265-80.
- 11. Berridge, M.J., C.P. Downes, and M.R. Hanley, Neural and developmental actions of lithium: A unifying hypothesis. Cell, 1989. 59(3): p. 411-419.
- 12. Allison JH, S.M., Reduced brain inositol in lithium-treated rats. Nat New Biol., 1971. 233(43): p. 267-8.
- 13. Allison JH, B.M., Holland WH, Hipps PP, Sherman WR., *Increased brain myo-inositol 1-phosphate in lithium-treated rats*. Biochem Biophys Res Commun., 1876. **71**(2): p. 664-70.
- 14. Shimon, H., et al., Reduced frontal cortex inositol levels in postmortem brain of suicide victims and patients with bipolar disorder. American Journal of Psychiatry
- Am J Psychiatry, 1997. 154(8): p. 1148-1150.
- 15. Williams, R.S.B., et al., A common mechanism of action for three mood-stabilizing drugs. 2002. 417(6886): p. 292-295.
- 16. Shaltiel, G., et al., Specificity of mood stabilizer action on neuronal growth cones. Bipolar Disorders, 2007. 9(3): p. 281-289.
- 17. Belmaker RH, G.N., Magnetic stimulation of the brain in animal depression models responsive to ECS. J. ECT., 1998. 14(3): p. 194-205.
- 18. Lopez, F., et al., The yeast inositol monophosphatase is a lithium- and sodium-sensitive enzyme encoded by a non-essential gene pair. Mol Microbiol, 1999. 31(4): p. 1255-64.
- 19. Raper, K., Dictyostelium discoideum, a new species of slime mold from decaying
- forest leaves./. J. Agric. Res., 1935. 50: p. 135-47.

- 20. Eichinger, L., et al., The genome of the social amoeba Dictyostelium discoideum. Nature, 2005. 435(7038): p. 43-57.
- 21. Ho, L. and G.R. Crabtree, Chromatin remodelling during development. Nature, 2010. 463(7280): p. 474-484.
- 22. Coates, J.C. and A.J. Harwood, Cell-cell adhesion and signal transduction during Dictyostelium development. J Cell Sci, 2001. 114(Pt 24): p. 4349-58.
- 23. Nagano, S., Modeling the model organism Dictyostelium discoideum. Dev Growth Differ, 2000. 42(6): p. 541-50.
- 24. King, J., et al., Genetic Control of Lithium Sensitivity and Regulation of Inositol Biosynthetic Genes. PLoS ONE, 2010. 5(6): p. e11151.
- 25. Parent, C.A., et al., G Protein Signaling Events Are Activated at the Leading Edge of Chemotactic Cells. Cell, 1998. 95(1): p. 81-91.
- 26. Iijima, M. and P. Devreotes, Tumor Suppressor PTEN Mediates Sensing of Chemoattractant Gradients. Cell, 2002. 109(5): p. 599-610.
- 27. Hoeller, O. and R.R. Kay, Chemotaxis in the absence of PIP3 gradients. Curr Biol, 2007. 17(9): p. 813-7.
- 28. Zigmond, S., Orientation chamber in chemotaxis. Methods Enzymol, 1988. 162: p. 65-72.
- 29. Chen, L., et al., PLA2 and PI3K/PTEN pathways act in parallel to mediate chemotaxis. Dev Cell, 2007. 12(4): p. 603-14.
- 30. van Haastert, P.J., I. Keizer-Gunnink, and A. Kortholt, Essential role of P13-kinase and phospholipase A2 in Dictyostelium discoideum chemotaxis. J Cell Biol, 2007. 177(5): p. 809-16.
- 31. Dormann, D., et al., Visualizing PI3 Kinase-Mediated Cell-Cell Signaling during Dictyostelium Development. Current Biology, 2002. 12(14): p. 1178-1188.
- 32. Bosgraaf, L., I. Keizer-Gunnink, and P.J.M. Van Haastert, P13-kinase signaling contributes to orientation in shallow gradients and enhances speed in steep chemoattractant gradients. Journal of Cell Science
- J Cell Sci, 2008. 121(21): p. 3589-3597.
- 33. Kamimura, Y., et al., PIP3-Independent Activation of TorC2 and PKB at the Cell's Leading Edge Mediates Chemotaxis. Current Biology, 2008. 18(14): p. 1034-1043.
- 34. Van Haastert, P.J. and D.M. Veltman, *Chemotaxis: navigating by multiple signaling pathways.* Sci STKE, 2007. **2007**(396): p. pe40.
- 35. Roelofs, J. and P.J. Van Haastert, Characterization of two unusual guanylyl cyclases from dictyostelium. J Biol Chem, 2002. 277(11): p. 9167-74.
- 36. T M Konijn, J.G.V.D.M., J T Bonner, and D S Barkley, *The acrasin activity of adenosine-3',5'-cyclic phosphate.* Proc Natl Acad Sci U S A., 1967. **58**(3): p. 1152–1154.
- 37. Gerisch, G., *Chemotaxis in Dictyostelium*. Annual Review of Physiology, 1982. 44(1): p. 535-552.
- 38. Newell, P., Attraction and adhesion in the slime mold Dictyostelium. In Fungal Differentiation: A Contemporary Synthesis. Mycology Series, 1983. 43: p. 43-71.
- 39. Saxe, C.L., 3rd, et al., Expression of a cAMP receptor gene of Dictyostelium and evidence for a multigene family. Genes Dev, 1991. 5(1): p. 1-8.
- 40. Saxe, C.L., 3rd, et al., CAR2, a prestalk cAMP receptor required for normal tip formation and late development of Dictyostelium discoideum. Genes Dev, 1993. 7(2): p. 262-72.

- 41. Johnson, R.L., et al., Identification and targeted gene disruption of cAR3, a cAMP receptor subtype expressed during multicellular stages of Dictyostelium development. Genes Dev, 1993. 7(2): p. 273-82.
- 42. Louis, J.M., G.T. Ginsburg, and A.R. Kimmel, The cAMP receptor CAR4 regulates axial patterning and cellular differentiation during late development of Dictyostelium. Genes Dev, 1994. 8(17): p. 2086-96.
- 43. Kim, J.Y., J.A. Borleis, and P.N. Devreotes, Switching of Chemoattractant Receptors Programs Development and Morphogenesis inDictyostelium:Receptor Subtypes Activate Common Responses at Different Agonist Concentrations,. Developmental Biology, 1998. 197(1): p. 117-128.
- 44. Louis, J.M., C.L. Saxe, 3rd, and A.R. Kimmel, Two transmembrane signaling mechanisms control expression of the cAMP receptor gene CAR1 during Dictyostelium development. Proc Natl Acad Sci U S A, 1993. 90(13): p. 5969-73.
- 45. Pitt, G.S., et al., Structurally distinct and stage-specific adenylyl cyclase genes play different roles in Dictyostelium development. Cell, 1992. **69**(2): p. 305-15.
- 46. Comer, F.I. and C.A. Parent, *Phosphoinositide 3-kinase activity controls the chemoattractant-mediated activation and adaptation of adenylyl cyclase*. Mol Biol Cell, 2006. 17(1): p. 357-66.
- 47. Lilly, P.J. and P.N. Devreotes, *Identification of CRAC*, a cytosolic regulator required for guanine nucleotide stimulation of adenylyl cyclase in Dictyostelium. Journal of Biological Chemistry, 1994. **269**(19): p. 14123-14129.
- 48. Kriebel, P. and C. Parent, Adenylyl Cyclase Expression and Regulation During the Differentiation of Dictyostelium Discoideum. IUBMB Life, 2004. 56(9): p. 541-546.
- 49. Anjard, C., F. SAJderbom, and W.F. Loomis, Requirements for the adenylyl cyclases in the development of Dictyostelium. Development, 2001. 128(18): p. 3649-3654.
- 50. van Es, S., et al., Adenylyl Cyclase G, an Osmosensor Controlling Germination of Dictyostelium Spores. Journal of Biological Chemistry, 1996. 271(39): p. 23623-23625.
- 51. Saran, S., et al., *cAMP signaling in Dictyostelium*. Journal of Muscle Research and Cell Motility, 2002. **23**(7): p. 793-802.
- 52. Kessin, R.H.O., S J. Shapiro, R I. and Franke, J, Binding of inhibitor alters kinetic and physical properties of extracellular cyclic AMP phosphodiesterase from Dictyostelium discoideum. Proc Natl Acad Sci U S A, 1979. **76**(11): p. 5450-5454.
- 53. Faure, M., et al., The cyclic nucleotide phosphodiesterase gene of Dictyostelium discoideum contains three promoters specific for growth, aggregation, and late development. Molecular and Cellular Biology
- Mol. Cell. Biol., 1990. 10(5): p. 1921-1930.
- 54. Pálsson, E., et al., Selection for spiral waves in the socialâ≠‰amoebaeâ≠‰Dictyostelium. Proceedings of the National Academy of Sciences of the United States of America, 1997. 94(25): p. 13719-13723.
- Van Haastert, P.J., J.D. Bishop, and R.H. Gomer, *The cell density factor CMF regulates the chemoattractant receptor cAR1 in Dictyostelium*. The Journal of Cell Biology, 1996. 134(6): p. 1543-1549.
- 56. Keim-Reder, M., PhD Thesis, 2006.

- 57. Shen, X., et al., Modulation of ATP-dependent chromatin-remodeling complexes by inositol polyphosphates. Science, 2003. **299**(5603): p. 112-4.
- 58. Campos, E.I. and D. Reinberg, *Histones: annotating chromatin*. Annu Rev Genet, 2009. 43: p. 559-99.
- 59. Luger, K. and J.C. Hansen, *Nucleosome and chromatin fiber dynamics*. Curr Opin Struct Biol, 2005. **15**(2): p. 188-96.
- 60. Muers, M., Epigenetics: An expanding horizon for DNA methylation. 2009. **10**(12): p. 818-819.
- 61. Katoh, M., et al., Developmentally regulated DNA methylation in Dictyostelium discoideum. Eukaryot Cell, 2006. 5(1): p. 18-25.
- 62. Sawarkar, R., et al., Histone deacetylases regulate multicellular development in the social amoeba Dictyostelium discoideum. J Mol Biol, 2009. 391(5): p. 833-48.
- 63. Peterson, C.L. and I. Herskowitz, Characterization of the yeast SWI1, SWI2, and SWI3 genes, which encode a global activator of transcription. Cell, 1992. 68(3): p. 573-583.
- 64. Gangaraju, V.K. and B. Bartholomew, *Mechanisms of ATP dependent chromatin remodeling*. Mutat Res, 2007. **618**(1-2): p. 3-17.
- 65. Wang, W., The SWI/SNF family of ATP-dependent chromatin remodelers: similar mechanisms for diverse functions. Curr Top Microbiol Immunol, 2003. 274: p. 143-69.
- 66. Corona, D.F. and J.W. Tamkun, Multiple roles for ISWI in transcription, chromosome organization and DNA replication. Biochim Biophys Acta, 2004. **1677**(1-3): p. 113-9.
- 67. Marfella, C.G. and A.N. Imbalzano, *The Chd family of chromatin remodelers*. Mutat Res, 2007. **618**(1-2): p. 30-40.
- 68. Bao, Y. and X. Shen, *INO80 subfamily of chromatin remodeling complexes*. Mutat Res, 2007. **618**(1-2): p. 18-29.
- 69. Ebbert, R., A. Birkmann, and H.-J. Schüller, The product of the <i>SNF2/SWI2</i> paralogue <i>INO80</i> of <i>Saccharomyces cerevisiae</i> required for efficient expression of various yeast structural genes is part of a high-molecular-weight protein complex. Molecular Microbiology, 1999. 32(4): p. 741-751.
- 70. Shen, X., et al., A chromatin remodelling complex involved in transcription and DNA processing. Nature, 2000. 406(6795): p. 541-4.
- 71. Cai, Y., et al., Purification and assay of the human INO80 and SRCAP chromatin remodeling complexes. Methods, 2006. 40(4): p. 312-7.
- 72. Klymenko, T., et al., A Polycomb group protein complex with sequencespecific DNA-binding and selective methyl-lysine-binding activities. Genes Dev, 2006. **20**(9): p. 1110-22.
- 73. Joseph, J.M., et al., The actinome of Dictyostelium discoideum in comparison to actins and actin-related proteins from other organisms. PLoS One, 2008. 3(7): p. e2654.
- 74. Muller, J., et al., Sequence and comparative genomic analysis of actin-related proteins. Mol Biol Cell, 2005. 16(12): p. 5736-48.
- 75. Ibarra, N., A. Pollitt, and R.H. Insall, Regulation of actin assembly by SCAR/WAVE proteins. Biochem Soc Trans, 2005. 33(Pt 6): p. 1243-6.
- 76. Szerlong, H., et al., The HSA domain binds nuclear actin-related proteins to regulate chromatin-remodeling ATPases. Nat Struct Mol Biol, 2008. 15(5): p. 469-76.

- 77. Shen, X., et al., Involvement of actin-related proteins in ATP-dependent chromatin remodeling. Mol Cell, 2003. 12(1): p. 147-55.
- 78. Jonsson, Z.O., et al., Rvb1p/Rvb2p recruit Arp5p and assemble a functional Ino80 chromatin remodeling complex. Mol Cell, 2004. 16(3): p. 465-77.
- 79. Conaway, R.C. and J.W. Conaway, *The INO80 chromatin remodeling complex in transcription, replication and repair*. Trends Biochem Sci, 2009. 34(2): p. 71-7.
- 80. Ford, J., O. Odeyale, and C.H. Shen, Activator-dependent recruitment of SWI/SNF and INO80 during INO1 activation. Biochem Biophys Res Commun, 2008. 373(4): p. 602-6.
- 81. Nakamura, T.M., et al., Histone H2A Phosphorylation Controls Crb2
  Recruitment at DNA Breaks, Maintains Checkpoint Arrest, and Influences
  DNA Repair in Fission Yeast. Molecular and Cellular Biology
- Mol. Cell. Biol., 2004. 24(14): p. 6215-6230.
- 82. van Attikum, H., et al., Recruitment of the INO80 complex by H2A phosphorylation links ATP-dependent chromatin remodeling with DNA double-strand break repair. Cell, 2004. 119(6): p. 777-88.
- 83. Paro, R.a.H., DS, The Polycomb protein shares a homologous domain with a heterochromatin-associated protein of Drosophila. Proc Natl Acad Sci U S A, 1991. 88(1): p. 263-267.
- 84. Delmas, V.S., DG and Perry, RP, A mammalian DNA-binding protein that contains a chromodomain and an SNF2/SWI2-like helicase domain. Proc Natl Acad Sci U S A., 1993. 90(6): p. 2414-2418.
- 85. Flanagan, J.F., et al., Molecular Implications of Evolutionary Differences in CHD Double Chromodomains. Journal of Molecular Biology, 2007. 369(2): p. 334-342.
- 86. Flanagan, J.F., et al., Double chromodomains cooperate to recognize the methylated histone H3 tail. Nature, 2005. 438(7071): p. 1181-5.
- 87. Stokes, D.G. and R.P. Perry, *DNA-binding and chromatin localization properties of CHD1*. Mol Cell Biol, 1995. **15**(5): p. 2745-53.
- 88. Daubresse, G., et al., The Drosophila kismet gene is related to chromatinremodeling factors and is required for both segmentation and segment identity. Development, 1999. 126(6): p. 1175-1187.
- 89. Lutz, T., R. Stöger, and A. Nieto, CHD6 is a DNA-dependent ATPase and localizes at nuclear sites of mRNA synthesis. FEBS Letters, 2006. 580(25): p. 5851-5857.
- 90. Ishihara, K., M. Oshimura, and M. Nakao, CTCF-Dependent Chromatin Insulator Is Linked to Epigenetic Remodeling. Molecular Cell, 2006. 23(5): p. 733-742.
- 91. Ho, L. and G.R. Crabtree, Chromatin remodelling during development. Nature. 463(7280): p. 474-84.
- 92. Brunner, H.G. and H. van Bokhoven, Genetic players in esophageal atresia and tracheoesophageal fistula. Curr Opin Genet Dev, 2005. 15(3): p. 341-7.
- 93. Felix, T.M., et al., CHD7 gene and non-syndromic cleft lip and palate. Am J Med Genet A, 2006. 140(19): p. 2110-4.
- 94. Vissers, L.E., et al., Mutations in a new member of the chromodomain gene family cause CHARGE syndrome. Nat Genet, 2004. 36(9): p. 955-7.
- 95. Sanlaville, D. and A. Verloes, *CHARGE syndrome: an update*. Eur J Hum Genet, 2007. **15**(4): p. 389-99.

- 96. Zahir, F., et al., Novel deletions of 14q11.2 associated with developmental delay, cognitive impairment and similar minor anomalies in three children. J Med Genet, 2007. 44(9): p. 556-61.
- 97. Menon, T., J.A. Yates, and D.A. Bochar, Regulation of Androgen-Responsive Transcription by the Chromatin Remodeling Factor CHD8. Mol Endocrinol.
- 98. Yuan, C.C., et al., CHD8 associates with human Staf and contributes to efficient U6 RNA polymerase III transcription. Mol Cell Biol, 2007. 27(24): p. 8729-38.
- 99. Nishiyama, M., et al., CHD8 suppresses p53-mediated apoptosis through histone HI recruitment during early embryogenesis. 2009. 11(2): p. 172-182.
- 100. Clapier, C.R. and B.R. Cairns, *The biology of chromatin remodeling complexes*. Annu Rev Biochem, 2009. **78**: p. 273-304.
- 101. Lee, Y.S., et al., Regulation of a cyclin-CDK-CDK inhibitor complex by inositol pyrophosphates. Science, 2007. 316(5821): p. 109-12.
- 102. Altschul, S.F., et al., Gapped BLAST and PSI-BLAST: a new generation of protein database search programs. Nucleic Acids Res, 1997. 25(17): p. 3389-402.
- 103. Kuspa, A. and W.F. Loomis, Tagging developmental genes in Dictyostelium by restriction enzyme-mediated integration of plasmid DNA. Proceedings of the National Academy of Sciences of the United States of America, 1992. 89(18): p. 8803-8807.
- 104. Keim, M., R. Williams, and A. Harwood, An inverse PCR technique to rapidly isolate the flanking DNA of <i&gt;Dictyostelium&lt;/i&gt; insertion mutants. Molecular Biotechnology, 2004. 26(3): p. 221-224.
- 105. De Lozanne, A. and J.A. Spudich, Disruption of the Dictyostelium myosin heavy chain gene by homologous recombination. Science, 1987. 236(4805): p. 1086-1091.
- 106. Vandesompele, J., et al., Accurate normalization of real-time quantitative RT-PCR data by geometric averaging of multiple internal control genes. Genome Biology, 2002. 3(7): p. research0034.1-research0034.11.
- 107. Hellemans, J., et al., qBase relative quantification framework and software for management and automated analysis of real-time quantitative PCR data.

  Genome Biology, 2007. 8(2): p. R19.
- 108. Livak, K.J. and T.D. Schmittgen, Analysis of Relative Gene Expression Data Using Real-Time Quantitative PCR and the 2-[Delta][Delta]CT Method. Methods, 2001. 25(4): p. 402-408.
- 109. Glockner, G., et al., Sequence and analysis of chromosome 2 of Dictyostelium discoideum. Nature, 2002. 418(6893): p. 79-85.
- 110. Zigmond, S.H., Orientation chamber in chemotaxis. Methods Enzymol, 1988. 162: p. 65-72.
- 111. Sun, T.J. and P.N. Devreotes, Gene targeting of the aggregation stage cAMP receptor cAR1 in Dictyostelium. Genes & Development, 1991. 5(4): p. 572-582.
- 112. Manahan, C.L., et al., CHEMOATTRACTANT SIGNALING IN DICTYOSTELIUM DISCOIDEUM. Annual Review of Cell and Developmental Biology, 2004. 20(1): p. 223-253.
- 113. Blusch R V, A.S.a.N.W., Multiple signal transduction pathways regulate discoidin 1 gene expression in Dictyostelium discoidin. Differentiation, 1995. 58: p. 253-260.

- 114. McPherson, C.E. and C.K. Singleton, V4, a gene required for the transition from growth to development in Dictyostelium discoideum. Developmental Biology, 1992. 150(2): p. 231-242.
- 115. Brock, D.A., et al., A Dictystelium mutant with defective aggregate size determination, in Development. 1996. p. 2569-2578.
- 116. Tang, L., et al., A Cell Number-counting Factor Regulates Group Size inDictyostelium by Differentially Modulating cAMP-induced cAMP and cGMP Pulse Sizes. Journal of Biological Chemistry, 2001. 276(29): p. 27663-27669.
- 117. Okuwa, T., et al., Two cell-counting factors regulate the aggregate size of the cellular slime mold Dictyostelium discoideum. Development, Growth & Differentiation, 2001. 43(6): p. 735-744.
- 118. Zeng, C., et al., Interaction of gdt1 and protein kinase A (PKA) in the growth-differentiation-transition in Dictyostelium. Differentiation, 2001. 67(1-2): p. 25-32.
- 119. Chibalina, M., C. Anjard, and R. Insall, Gdt2 regulates the transition of Dictyostelium cells from growth to differentiation. BMC Developmental Biology, 2004. 4(1): p. 8.
- 120. Stevens, B.A., et al., Control elements of Dictyostelium discoideum prespore specific gene 3B. Differentiation, 2001. 68(2-3): p. 92-105.
- 121. Watanabe, S., et al., Unexpected roles of a Dictyostelium homologue of eukaryotic EF-2 in growth and differentiation. Journal of Cell Science J Cell Sci, 2003. 116(13): p. 2647-2654.
- 122. Yamada Y, M.H., Fukuzawa M, Kawata T, Oohata AA., Prespore cell inducing factor, psi factor, controls both prestalk and prespore gene expression in Dictyostelium development. Development Growth & Differentiation, 2010. 52(4): p. 377-83.
- 123. Early, A., Signalling pathways that direct prestalk and stalk cell differentiation in Dictyostelium. Seminars in Cell & Developmental Biology, 1999. 10(6): p. 587-595.
- 124. Early A E, J.G.W., H E Meyer, S B Por, E Smith, K L Williams, and A A Gooley, Structural characterization of Dictyostelium discoideum presporespecific gene D19 and of its product, cell surface glycoprotein PsA. Molecular Biology of the Cell, 1988. 8(8): p. 3458-3466.
- 125. Fosnaugh KL, L.W., Sequence of the Dictyostelium discoideum spore coat gene SP96. nucleic acids res, 1989. 17(22): p. 9489.
- 126. Ponte, E., et al., Severe developmental defects in Dictyostelium null mutants for actin-binding proteins. Mechanisms of Development, 2000. 91(1-2): p. 153-161.
- 127. Takeda, K., et al., Role of Phosphatidylinositol 3-Kinases in Chemotaxis in Dictyostelium. Journal of Biological Chemistry, 2007. 282(16): p. 11874-11884.
- 128. Urushihara, H. and T. Muramoto, Genes involved in Dictyostelium discoideum sexual reproduction. European Journal of Cell Biology
- A special issue dedicated to Guenter Gerisch on the occasion of his 75th birthday, 2006. **85**(9-10): p. 961-968.
- 129. Osherov, N., N. Wang, and W.F. Loomis, *Precocious sporulation and developmental lethality in yelA null mutants of Dictyostelium*. Developmental Genetics, 1997. **20**(4): p. 307-319.

- 130. Jessberger, R., The many functions of smc proteins in chromosome dynamics. 2002. 3(10): p. 767-778.
- 131. Muramoto, T. and J.R. Chubb, Live imaging of the Dictyostelium cell cycle reveals widespread S phase during development, a G2 bias in spore differentiation and a premitotic checkpoint. Development, 2008. 135(9): p. 1647-1657.
- 132. Edwards, D.R., M.M. Handsley, and C.J. Pennington, *The ADAM metalloproteinases*. Molecular Aspects of Medicine
- Metzincin Metalloproteinases, 2008. 29(5): p. 258-289.
- 133. Manabe, R., et al., Molecular cloning and the COOH-terminal processing of gp64, a putative cell-cell adhesion protein of the cellular slime mold Polysphondylium pallidum. Journal of Biological Chemistry, 1994. 269(1): p. 528-535.
- 134. Gao, T., et al., Cells Respond to and Bind Countin, a Component of a Multisubunit Cell Number Counting Factor. Journal of Biological Chemistry, 2002. 277(36): p. 32596-32605.
- 135. Parelho, V., et al., Cohesins Functionally Associate with CTCF on Mammalian Chromosome Arms. Cell, 2008. 132(3): p. 422-433.
- 136. Teo, R., et al., PtdIns(3,4,5)P3 and inositol depletion as a cellular target of mood stabilizers. Biochemical Society Transactions, 2009. 037(5): p. 1110-1114.
- 137. Loovers, H.t.M., et al., A Diverse Family of Inositol 5-Phosphatases Playing a Role in Growth and Development in Dictyostelium discoideum, Journal of Biological Chemistry, 2003. 278(8): p. 5652-5658.
- 138. Veltman, D.M., I. Keizer-Gunnik, and P.J.M. Van Haastert, Four key signaling pathways mediating chemotaxis in Dictyostelium discoideum. The Journal of Cell Biology, 2008. 180(4): p. 747-753.
- 139. Veltman, D.M. and P.J.M. van Haastert, The role of cGMP and the rear of the cell in Dictyostelium chemotaxis and cell streaming. Journal of Cell Science J Cell Sci, 2008. 121(1): p. 120-127.
- 140. N. Ibarra, A.P.a.R.H.I., Regulation of actin assembly by SCAR/WAVE proteins. Biochemical Society Transactions, 2005. 33: p. 1243-1246.
- 141. Lee, E., K.-m. Pang, and D. Knecht, *The regulation of actin polymerization and cross-linking in Dictyostelium*. Biochimica et Biophysica Acta (BBA) General Subjects, 2001. **1525**(3): p. 217-227.
- 142. Langridge, P.D. and R.R. Kay, Mutants in the Dictyostelium Arp2/3 complex and chemoattractant-induced actin polymerization. Experimental Cell Research, 2007. 313(12): p. 2563-2574.